# Weather and crop dynamics in a complex terrain, the Gamo Highlands – Ethiopia

## Towards a high-resolution and model-observation based approach
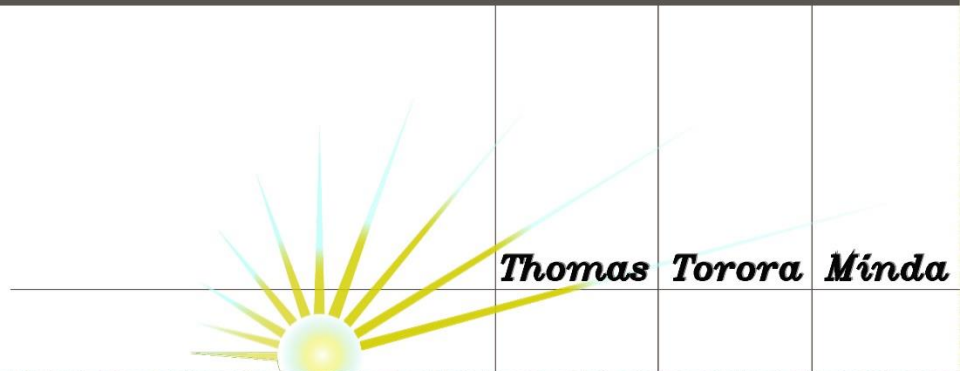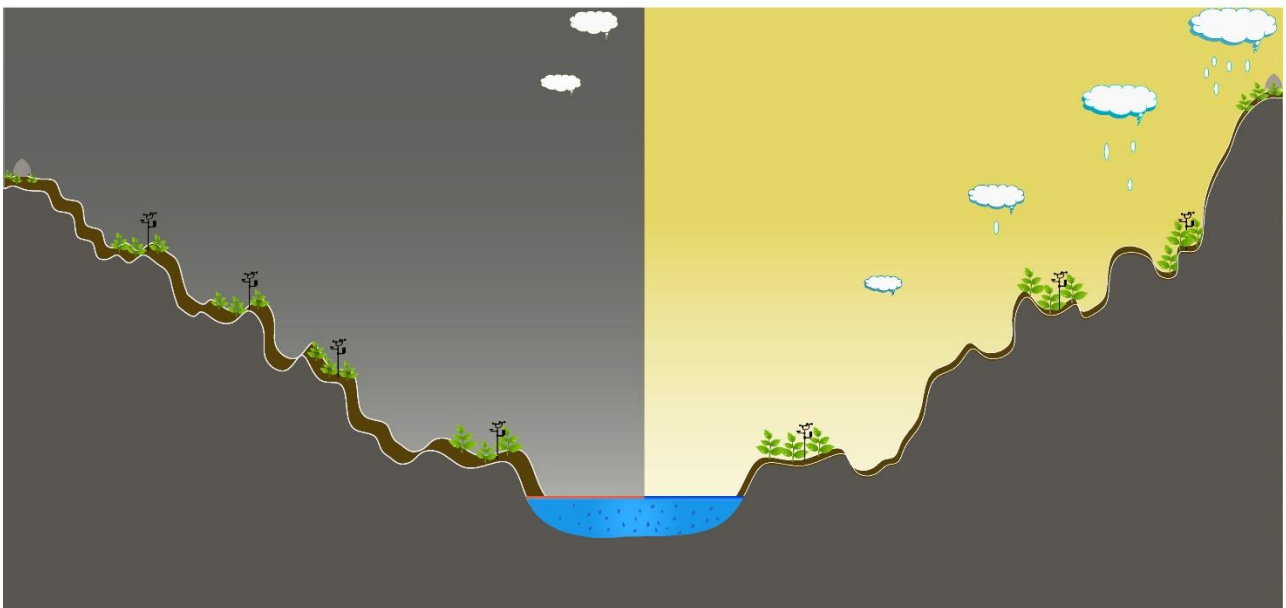


*Thomas Torora Minda*

# Weather and crop dynamics in a complex terrain, the Gamo Highlands – Ethiopia:

**Towards a high-resolution and model-observation based approach**

**Thomas Torora Minda**

**Thesis committee**

**Promotors**
Prof. Dr Jordi Vilà-Guerau de Arellano
Personal Professor of Meteorology and Air Quality Group
Wageningen University & Research

Prof. Dr Paul C. Struik
Professor of Crop Physiology
Wageningen University & Research

**Co-promotor**
Dr Michiel K. van der Molen
Associate Professor, Meteorology and Air Quality Group
Wageningen University & Research

**Other members**
Prof. Dr Fulco Ludwig, Wageningen University & Research
Prof. Dr Andreas Ibrom, Technical University of Denmark
Dr Allard de Wit, Wageningen University & Research
Prof. Dr Stefan Dekker, Utrecht University

This research was conducted under the auspices of the Graduate School for Socio-Economic and Natural Sciences of the Environment (SENSE)

# Weather and crop dynamics in a complex terrain, the Gamo Highlands – Ethiopia:
## Towards a high-resolution and model-observation based approach

**Thomas Torora Minda**

**Thesis**

submitted in fulfilment of the requirements for the degree of doctor
at Wageningen University
by the authority of the Rector Magnificus,
Prof. Dr A.P.J. Mol,
in the presence of the
Thesis Committee appointed by the Academic Board
to be defended in public
on Wednesday 30 October 2019
at 4 p.m. in the Aula.

# Contents

## 4 Observational characterisation of the synoptic and mesoscale circulations in relation to crop dynamics: *Belg* 2017 in the Gamo Highlands, Ethiopia        75

# 1
# Introduction

## 1.1 The Environment-food nexus

The United Nations (UN) designed the Millennium Development Goals (MDGs) to end poverty and hunger by 2015. The Sustainable Development[*] Goals (SDGs) are a continuation of the MDGs and further included the planetary must-haves, *e.g.* tasking our planet to achieve climate stability by 2030 (Griggs *et al.*, 2013). In the 2030 SDG agenda, set by the UN General Assembly in 2015, Goal 2 aimed at achieving sustainable food security[†] (Assembly, 2015). This goal aims to end hunger and to achieve long-term food security, including better nutrition, through sustainable systems of production, distribution and consumption by 2030 (Griggs *et al.*, 2013; UNDP, 2018). The SDGs have been defined as: "development that meets the needs of the present while safeguarding Earth's life-support system, on which the welfare of the current and future generations depends" (Griggs *et al.*, 2013; Kates, 2018; Keeble, 1988). However, humanity is driving global environmental change and has pushed the earth into a new geological epoch – the Anthropocene. This geologic epoch started around the end of the 18th century (Crutzen, 2006; Griggs *et al.*, 2013; Steffen *et al.*, 2011).

The Anthropocene is dominated by mankind and is characterised by exponential growth in a number of global environmental indicators compared to the pre-industrial level (Steffen *et al.*, 2011). The Intergovernmental Panel on Climate Change (IPCC) considers the term "pre-industrial" as a reference and it precedes the period from 1850 to 1900, which marks the onset of large-scale industrial activities around

---

[*] *Sustainable development is defined as development that meets the needs of the present without compromising the ability of future generations to meet their own needs (Kates* et al., *2005).*

[†] *Food security exists when all people, at all times, have physical, social and economic access to sufficient, safe and nutritious food to meet their dietary needs and food preferences for an active and healthy life (Devaux* et al., *2014).*

the world (IPCC, 2018a). Today, the atmospheric concentration of the major greenhouse gas (GHG), carbon dioxide ($CO_2$), has passed 400 parts per million (ppm) by volume, as compared to the pre-industrial level of 280 ppm (Tans and Keeling, 2014). Steffen *et al.* (2011) explained that the planetary upper threshold for atmospheric $CO_2$ concentration is 350 ppm and that above this, the earth's system may shift from a safe operating space to a zone of uncertainty. The pronounced increase in the concentrations of $CO_2$ and other GHGs has induced a 1.5 $W \cdot m^{-2}$ additional radiative forcing to the climate system relative to the pre-industrial level, while a 1.0 $W \cdot m^{-2}$ additional forcing relative to the pre-industrial is considered as a planetary threshold (Adger *et al.*, 2003; Myhre *et al.*, 2013; Steffen *et al.*, 2011). As a result, the global temperature is currently nearly 1.0 °C warmer (with a probable range of 0.8 °C to 1.2 °C) than the pre-industrial level, and will likely pass the 1.5 °C threshold in 2050 (IPCC, 2018b). Developing countries, in which agriculture is the backbone of the economy, are among the more vulnerable members of the global community (Adger *et al.*, 2003; Godfray *et al.*, 2010b). Among the developing countries, countries in the sub-Saharan Africa (SSA) region, including Ethiopia, are the ones most seriously affected by climate change (Met-Office, 2015; Rosenzweig and Parry, 1994).

The challenge facing the international community is to achieve SGD Goal 2 under current climate variability and change conditions. In this introduction, I first review the relationships between weather and food production on different spatial (from global to local) and temporal (from daily, seasonal to decadal) scales. I specifically stress how meteorological crop drivers occurring on different scales (from mesoscale to synoptic scale) influence the *potato* crop, which can play a key role in the food security endeavours of developing nations, including Ethiopia, in the near future. The study further scales down and focuses on the Gamo Highlands in southern Ethiopia.

### 1.1.1    The global scale

The global environmental change and food provision are interwoven topics that are arousing serious concerns, such as how to provide sufficient food for the demands of society, particularly to more vulnerable groups. However, sufficient food provision will create additional pressure on the environment (Tilman *et al.*, 2001). In a feedback loop, this environmental pressure can further increase uncertainties in food production systems (Godfray *et al.*, 2010a; Ingram and Brklacich, 2006). Therefore, the impacts of climate change, the adaptation and mitigation measures and their effects on the food systems are issues that have attracted global attention (Godfray *et al.*, 2010a; Gregory *et al.*, 2005).

Global food production has significantly increased throughout the past half century (Ray *et al.*, 2013). Nevertheless, more than one in seven people today do not

have access to sufficient energy and dietary protein and even more suffer from various types of micronutrient deficiencies (DeFauw *et al.*, 2012; Godfray *et al.*, 2010a), although food supply is abundant in most Western countries. The world population is expected to plateau at nearly 9 billion in 2050, compared to 7.3 billion in 2015 (Godfray *et al.*, 2010a; Godfray *et al.*, 2010b; May, 2018). Studies have shown that to feed the increased population the world will need greater than 85% more food by 2050, relative to the 2013 food supply (Long *et al.*, 2015). Devaux *et al.* (2014) argued that 40% to 60% of global food insecurity could be eliminated if small-holder farmers were supported. In this regard, potato could play a key role in household food security, *e.g.* in SSA, where farmland holdings are small but labour is relatively available. The average farm sizes of land constrained (*e.g.* Nigeria) and land abundant (*e.g.* Ghana) African nations are 1.2 and 3.0 hectares per farmer, respectively (Jayne *et al.*, 2014). If maize, rice, wheat and soybean crops are considered, to meet the rising demand, the world needs a 2.4% yield increase per year in the four crops averaged, whereas the current rates of yield improvement are below 1.5% (Long *et al.*, 2015; Ray *et al.*, 2013). Note that such data are not available for the potato crop.

Recently, the World Meteorological Organization (WMO) estimated that anthropogenic warming has raised the mean global surface temperature by approximately 1.1 °C (1.1±0.1 °C) relative to the pre-industrial level (WMO, 2018) and the rate of increase is ~0.2 °C per decade (Hansen *et al.*, 2006). From 1970 to 2017, the global surface temperature rose by 0.9 °C, which shows that warming has accelerated in recent decades (Brönnimann, 2018). For instance, 2017 ranks as the warmest non-El Niño year on record (Blunden *et al.*, 2018; Sánchez-Lugo *et al.*, 2018). Most remarkable is that 2015 to 2017 were the four warmest consecutive years on record (Sánchez-Lugo *et al.*, 2018; WMO, 2018). Such an increase in the global temperature significantly influences food production (Godfray *et al.*, 2010b). In order to limit the accelerated warming of the climate system, the Paris climate agreement aims to keep anthropogenic warming below 2 °C and even further, to limit the rise in global surface temperature to 1.5 above the pre-industrial level (Rogelj *et al.*, 2016).

Increased anthropogenic radiative forcing has also had an enormous impact on global water bodies (Karl and Trenberth, 2003). The global upper 75 m of the ocean warmed at a rate of 0.11 °C per decade between 1971 and 2010 (Rhein *et al.*, 2013). Near the Equator, the rising sea surface temperature (SST) and ocean heat content weaken the tropical easterly winds, shifting the location of atmospheric convection and changing patterns of global climatic teleconnection (Collins *et al.*, 2010; WMO, 2016). A typical outcome of such a change is the amplification of the El Niño/Southern Oscillation (ENSO): El Niño (warm) and La Niña (cold) episodes (Adger *et al.*, 2003). For example, 2015 showed one of the strongest El Niños since 1950, manifested by either major floods or worst ever droughts in many parts of the world (Blunden and Arndt, 2016). In Ethiopia, it triggered one of the worst droughts for

many years and affected more than 8 million people (Blunden and Arndt, 2016; Lewis, 2017; Tsidu, 2016).

Enhanced warming and changing climate affect aspects of food security such as availability, access, utilisation and food systems (Kanamaru, 2009). A recent estimate of food insecurity categorised the developing world (mainly SSA) as among the regions most vulnerable to food insecurity, relative to other parts of the world (Met-Office, 2015). Furthermore, predictions also show increases in food insecurity in the future in the region (FAO, 2016; Met-Office, 2015; Wheeler and von Braun, 2013). The FAO reported that 36% of the global workforce and two-thirds of the population of SSA make their living from agriculture (FAO, 2008a). The figure even rises to 85% if the Ethiopian situation is considered alone (Kassie, 2014). To quantify the impact, a recently defined global hunger index showed that, in 2015, the SSA region and Ethiopia are indexed 32 (rated 'serious' in severity) and 40 (rated 'alarming'), respectively, whilst the global average was 22 (rated 'serious') (Von Grebmer *et al.*, 2015; Wheeler and von Braun, 2013). Furthermore, equatorial or low-latitude (roughly $30^{\circ}$S – $30^{\circ}$N) regions are compared with temperate regions (high latitudes), the former are at larger risk of suffering food insecurity than the latter (Hijmans, 2003; Hoegh-Guldberg *et al.*, 2018).

Regarding the crop studied for this thesis, Hijmans (2003) projected that the global potential yield of potato will fall by 18 to 32% without adaptation[‡] to climate change in the 2050s and by 9 to 18% with adaptation between 2040 and 2069. Similarly, from 2050 to 2069, FAO estimated that potato yields will fall by from 10 to 19% due to climate change (FAO, 2016). Regionally, warmer temperatures could have a severe negative impact on potato farming at low latitudes as compared with high-latitude regions (Haverkort and Struik, 2015; Hijmans, 2003).

As mentioned above, the Anthropocene is characterised by an unprecedented population increase and by the fact that humanity influences the environment with a number of global food security concerns. A useful way to quantify our needs is by defining crop yield. Crop yield can be defined at various levels: potential yield, experimental yield, attainable yield, aspired yield and actual yield (Haverkort, 1986, 2018; Haverkort and Struik, 2015). Potential yield is *the theoretical yield that can be modelled without any limiting factor being present* (Haverkort and Struik, 2015). Actual yield is a yield that *a farmer harvested, which can be reduced by pests, weeds and sub-optimal farm inputs* (Haverkort, 2018). The yield gap is defined as *the difference between potential and actual yield* in a certain agro-ecological environment (Godfray *et al.*, 2010a; Haverkort and Struik, 2015).

The global, African and Ethiopian actual potato yields are estimated to be 20 t·ha$^{-1}$, 15 t·ha$^{-1}$ and 12.3 t·ha$^{-1}$, respectively (George *et al.*, 2018; Haverkort, 2018; Tafesse

---

[‡] *Adaptation is defined as an adjustment in natural or human systems in response to actual or expected climatic stimuli or their effects, which moderates harm or exploits beneficial opportunities (Parry* et al., *2007).*

*et al.*, 2018). In a review, Tadele (2017) concluded that some regions of the world have nearly reached their maximum attainable crop yield, whereas other regions such as Africa showed considerable yield gaps. For instance, in Ethiopia, potato yields of more than 65 t·ha$^{-1}$ in research stations and 50 t·ha$^{-1}$ in farms have been achieved (Tafesse *et al.*, 2018). This shows that there is a huge potential to improve productivity, *e.g.* by improving cultivars and crop management practices (Tadele, 2017). Furthermore, environmental variables such as differences in $CO_2$ concentrations, altering planting dates/seasons/years/variations in latitude and altitude influence the potential yield (Haverkort and Struik, 2015). Godfray *et al.* (2010a) and Jovanovic *et al.* (2018) suggested closing the yield gap as one of the most important potential strategies to feed the world while maintaining the emphasis on sustainability. Table 1.1 presents potential and actual yields and yield gap from around the world.

**Table 1.1 | The potential and actual yields and yield gaps of countries in Asia, South America, Europe and Africa (including Ethiopia in all potato-growing seasons). Note that the largest (blue) and lowest (red) values are highlighted and for the yield gap column, the red text shows the largest and the blue shows the smallest yield gaps. Data obtained from Haverkort (2018), Jovanovic *et al.* (2018) and Svubure *et al.* (2015). Note that according to the National Meteorological Agency, the Ethiopian climate is classified in *belg* (FMAM), *kirmet* (JJAS) and *bega* (ONDJ).**

| Country | Country/ city | Production (season, irrigated) | Potential yield (t·ha$^{-1}$) | Actual yield (t·ha$^{-1}$) | Actual : potential (ratio) | Yield gap (%) |
|---|---|---|---|---|---|---|
| China | Hei-longjiang | Summer | 64 | 32 | 0.50 | 50 |
|  | Ningxia | Summer | 66 | 25 | 0.38 | 62 |
| India | Gurjarat | Winter | 63 | 41 | 0.65 | 35 |
|  | Punjab | Winter | 29 | 22 | 0.76 | 24 |
| Bangladesh | Bangladesh | Irrigated winter | 61 | 35 | 0.57 | 43 |
| Indonesia | Bandung | Rain-fed | 32 | 17 | 0.53 | 47 |
|  | Bandung | Irrigated | 33 | 16 | 0.48 | 52 |
| Vietnam | Vietnam | Winter, river delta | 28 | 11 | 0.39 | 61 |
|  |  | Highland | 52 | 20 | 0.38 | 62 |
| Myanmar | Myanmar | Rainy season, highland | 35 | 13 | 0.37 | 63 |
|  | Myanmar | Irrigated, winter highland | 45 | 15 | 0.33 | 67 |
| Argentina | Argentina | Spring-summer | 95 | 55 | 0.58 | 42 |
| Netherlands | Netherlands | Summer, consumption | 96 | 63 | 0.66 | 34 |
|  | Netherlands | Summer, starch | 96 | 47 | 0.49 | 51 |
| Algeria | Algeria | Autumn | 35 | 25 | 0.71 | 29 |
|  | Algeria | Spring | 43 | 30 | 0.70 | 30 |
| Tunisia | Jendouba | Winter | 41.1 | 21 | 0.51 | 49 |
| Zimbabwe | Zimbabwe | 2011-'14 | 88 - 96 | 8 - 34 | 0.08 - 0.35 | 65 - 92 |
| Ethiopia | Debre Zeit | *Belg* | 75 | 13 | 0.17 | 83 |
|  |  | *Meher* | 60 | 10 | 0.17 | 83 |
|  |  | *Bega* | 55 | 15 | 0.27 | 63 |

Typical numbers shown in Table 1.1 indicate that potential yields range between 28 t·ha⁻¹ in Vietnam to 96 t·ha⁻¹ in the Netherlands and Zimbabwe. The actual yield ranges from 8 t·ha⁻¹ in Zimbabwe to 63 t·ha⁻¹ in the Netherlands. The East African region has a high potential yield (> 60 t·ha⁻¹), but the yield gap is more than 65%. Ethiopia produces potato throughout the year: in *belg* and *meher* with rainfall and in *bega* if irrigated (Tufa, 2013) with potential yields of 75 t·ha⁻¹, 60 t·ha⁻¹ and 55 t·ha⁻¹, respectively. The yield gaps are pronounced and estimated to be 83% in *belg* and in *meher* and 63% in *bega*.

The strategy of "closing the yield gap" could raise sustainability issues related to impacts on the environment and potential feedbacks in future food production (Godfray *et al.*, 2010a; Ingram and Brklacich, 2006). However, with a number of environmental intervention approaches and activities (*e.g.* soil and water conservation), which can potentially improve microclimates, the yield gaps can be closed (Godfray *et al.*, 2010a).

Potato is ranked fourth in production on the global scale (Haverkort, 2018; Haverkort and Struik, 2015). In 2014, global production, area planted and productivity are estimated to be 383 million tonnes, 19 million hectares of land and 20.2 tonnes per hectare, respectively (George *et al.*, 2018). Since 1990, in Eastern Africa, data have shown that yield did not show much improvement but the area under cultivation has significantly increased (Haverkort and Struik, 2015).

The potato crop is mainly adapted to the temperate climate (Haverkort and Struik, 2015). The crop is also grown in tropical mountainous regions all over the world (Haverkort, 2018; Haverkort and Struik, 2015). Recently, potatoes are becoming popular and are considered as a key crop to improve food security, especially in the developing countries (FAO, 2008b; Lutaladio and Castaldi, 2009; Struik *et al.*, 2014; Tadesse *et al.*, 2018). Potato is considered as a 'hunger breaker' because of its short crop cycle (Struik *et al.*, 2014; Tadesse *et al.*, 2018) and it can give yield in situations in which other crops might fail (Lutaladio and Castaldi, 2009). The crop has a number of advantages over cereals: harvest index of greater than 75% (as compared with 40% to 60% for cereals) (DeFauw *et al.*, 2012; Haverkort, 2018; Haverkort and Struik, 2015); relatively low water requirements (George *et al.*, 2018; Haverkort and Struik, 2015; Pandey *et al.*, 2012); mostly consumed by local to national markets (Lutaladio and Castaldi, 2009; Tadesse *et al.*, 2018); improving small-holder farmers' economy (DeFauw *et al.*, 2012) and high nutritional values but a healthy diet with low fat content (Lutaladio and Castaldi, 2009; Oerke and Dehne, 2004; Tufa, 2013). Much of our understanding of environment and potato crop relations comes from temperate climate regions (Haverkort *et al.*, 2015; Khan *et al.*, 2013; Kooman, 1995; Struik, 2007). However, potato production in the developed world has shown a slight falling trend, while in the developing countries production has increased al-

most four fold (Devaux *et al.*, 2014; Haverkort and Struik, 2015). Hence, studies focusing on weather-crop interactions can help to improve crop productivity in realising food security improvements in the third world (Devaux *et al.*, 2014).

### 1.1.2 From the Eastern Africa to Ethiopia

The population of Africa is projected to be 2.5 billion by 2050 (~28% of the global population) (Tadele, 2017). Because of anthropogenic warming, the African continent is also exposed to and affected by extreme weather and climate change. From the climate change related impact perspective, a region can be more vulnerable[§] (*i.e.* increased exposure and sensitivity and with less adaptive capacity) than others and thus at increased risk of suffering the impacts of climate change (Adger *et al.*, 2003; Parry *et al.*, 2007; WMO, 2018). To quantify the vulnerability, the effect of a 1 $^{\circ}$C increase in temperature on real per capita output showed that the African continent is rated the most negatively affected (rated < -0.95 on a scale between -2.25 to 4.5) region in the world (WMO, 2018).

The Representative Concentration Pathways, presented in the IPCC Fifth Assessment Report and a number of Global Climate Models (GCMs) showed that the temperature in the African continent is projected to rise faster than the global average during the century (James and Washington, 2013; Niang *et al.*, 2014). During March to May in 2017, Tsidu (2018) indicated that East Africa (also referred to as the Greater Horn of Africa, GHA, which is located between 20$^{\circ}$-50$^{\circ}$E and 15$^{\circ}$S-20$^{\circ}$N and includes Ethiopia, see Figure 1.1a) showed nearly 3 $^{\circ}$C increase in temperature as compared to 1981-2010 ERA-Interim temperature climatology. Despite the fact that the observed precipitation in the region showed a falling trend since 1980 (Rowell *et al.*, 2015), while a number of GCM projections indicated a rising trend (up to nearly 20%) for March to May precipitation (James and Washington, 2013; Kerandi *et al.*, 2018; Van Oldenborgh *et al.*, 2013). The lack of reliable long-term weather measurements makes it more difficult to quantify the temperature and precipitation mismatches.

A number of global circulation features and teleconnections influence Eastern Africa, in particular Ethiopia. In addition, heterogeneous landscape with complex terrain and proximity of the region to large water bodies (such as the Indian Ocean, Red Sea and a number of lakes) play significant roles in modulating the spatial and temporal variability of weather and climate of the GHA (Cattani *et al.*, 2016; Haile *et al.*, 2009; Pierre *et al.*, 2018). The elevation of Ethiopia ranges from 125 m below sea level at the Danakil depression to 4620 m a.s.l. at the summit of Mount Ras Dashen. To mention just a few of the atmospheric and oceanic systems involved: the seasonal oscillation (between 15$^{\textbf{o}}$S and 15$^{\textbf{o}}$N) of the Intertropical Convergence Zone (ITCZ) (see Figure 1.1a) (Diro *et al.*, 2008; Nicholson, 2011); the tropical easterly jet (Diro *et*

---

[§] *The IPCC defines vulnerability as the degree to which a system is susceptible to and unable to cope with, adverse effects of climate change, including climate variability and extremes (Parry* et al.*, 2007).*

*al.*, 2011a; Segele *et al.*, 2015); East African low level and the subtropical westerly jets; Azores and Arabian high; humidity anomalies over the Red Sea and Gulf of Guinea; low level wind anomalies from Indian and Atlantic oceans; and ENSO (Diro *et al.*, 2011a; Gissila *et al.*, 2004; WMO, 2018). Deviations from the mean state of these climatic features influence the weather and climate dynamics of the country. Ultimately, such anomalies affect crop growth and yield in the region. In this thesis, I attempt to relate and quantify how key synoptic features like ICTZ influence a relevant agricultural region in Ethiopia, the Gamo Highlands, which is characterised by its complex topography and landscape heterogeneity.

In SSA, crop production and productivity are categorised as among the world's most vulnerable sectors because (1) the agriculture is rainfed and sensitive to weather/climate variations (Awulachew *et al.*, 2010); (2) climate variability has intensified in recent decades (Lobell and Field, 2007; Lobell and Gourdji, 2012; Niang *et al.*, 2014); and (3) as a result, recurrent floods and droughts occurred (Lesk *et al.*, 2016). For example, the Ethiopian Gross Domestic Product (GDP) growth trend is highly correlated with precipitation, which shows that livelihoods are highly sensitive to weather/climate anomalies (Diro *et al.*, 2011a; Kassie, 2014). In the country, agriculture is the source of 85% of family income, accounts for 50% of GDP and contributes >80% to the foreign exchange earnings (Kassie, 2014). However, in an agricultural perspective, potato is a relatively recent crop in Ethiopia, but is already becoming an important staple food that improves both food security and the financial situation of the small-land holder rural farmer (FAO, 2019). The potato can thus be a means out of poverty that will contribute attaining the MDGs in Eastern Africa (Bradshaw and Bonierbale, 2010; Schulte-Geldermann, 2013). Because of its short growing cycle and low water requirements (compared to cereals) (Lutaladio and Castaldi, 2009), the crop can still be grown despite the generally falling trend in precipitation in the GHA (Rowell *et al.*, 2015). In this circumstance, potato cultivation can be regarded as an adaptation to climate change. Potato is also nutritionally rich and simple to cultivate in most of the year by small landholding farmers (Bradshaw and Bonierbale, 2010; Haverkort *et al.*, 2012). Furthermore, in the GHA, potato is widely cultivated and its production has been almost exponentially increasing since 1990 (Haverkort and Struik, 2015; Scott *et al.*, 2000; Struik *et al.*, 2014).

### 1.1.3 The Gamo Highlands, southern Ethiopia

Atmospheric and oceanic phenomena occurring at different spatiotemporal scales in the tropical and extratropical regions influence the weather/climate dynamics in southern Ethiopia, as shown in Figure 1.1a (Diro *et al.*, 2011a). A few of the relevant synoptic (thousands of kilometers spatial scale) and mesoscale (up to 3 kilometers) phenomena were explained by Stull (2000). These are investigated in this study and are key features that control the temperature and precipitation regimes, which are the meteorological crop growth drivers, as explained in Figure 1.1.

Recent studies have shown that the rainbelt lies ~6° to the south of the ITCZ during the rainy season in April (note that the ITCZ oscillates between the red line in January and blue line in July (Figure 1.1a)) (Nicholson, 2009; Nicholson, 2018). In short, the minimum surface pressure over the Gamo Highlands (southern Ethiopia) is observed around mid-March (March was also the warmest month during *belg*-2017); however, the maximum precipitation occurred during May in 2017 (in the same month, the ITCZ over-head the northern part of Ethiopia) (ACMAD, 2017; NOAA, 2017).
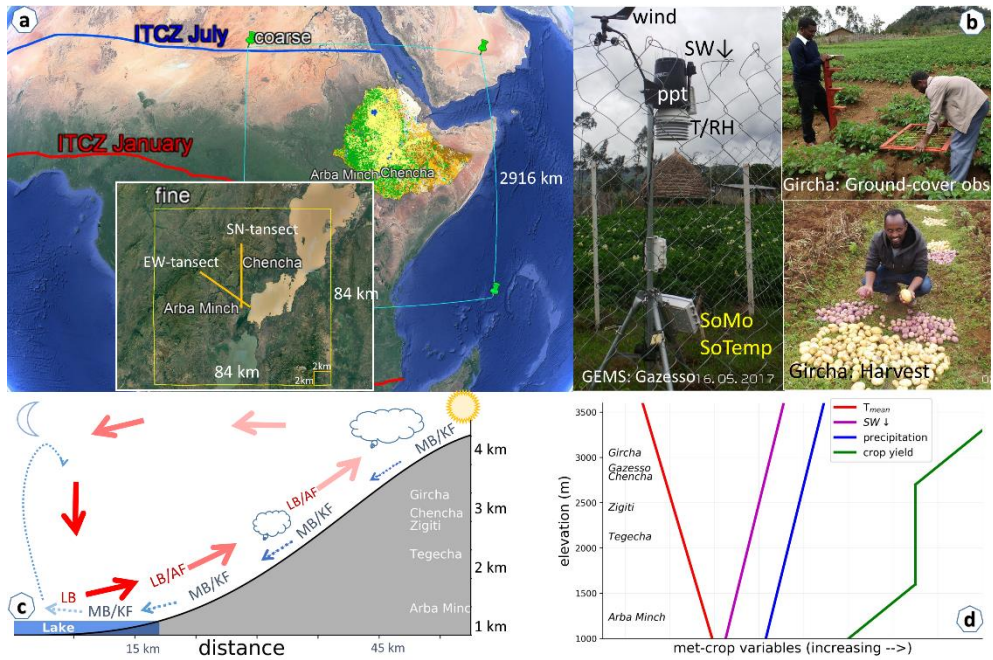
**Figure 1.1 | The main topics raised in this thesis (moving clockwise from top left):**

**(a) Map of Africa showing the land-use land-cover map of Ethiopia. The lower red and the upper blue lines show the approximate latitudinal location of the ITCZ in January and July, respectively. The Weather Research Forecasting model's coarse (54 × 54 km² resolution in an area of 2916 × 2916 km²) model domain (green pins and with lines). Inset is a map showing the WRF model's fine domain (2 × 2 km² resolution in an area of 84 × 48 km²) centered the Gamo Highlands (Chapter 3). Superimposed on this fine domain, the Gamo Ethiopian Meteorological Stations (GEMS) network's south - north (SN) and east - west (EW) transects (Chapter 4).**

**(b) (i) GEMS-Gazesso station with the main sensors (16 May 2017); (ii) shows Gircha farm with field assistants gathering canopy cover data using a grid technique (04 May 2017); and (iii) potato harvest in Gircha (02 August 2017) (Chapters 4 and 5).**

**(c) The most dominant mesoscale flows during daytime (LB - lake-breeze and AF - anabatic flows in combination with valley flow circulations) and night (MB – mountain breeze flows and KF - katabatic circulations) are shown. The relative elevations of the GEMS network are also indicated (Chapter 4).**

**(d) The major meteorological crop drivers (temperature, the SW↓ and PPT) (Hoogenboom, 2000) related to crop yield vary as function of elevation in the Gamo Highlands (Chapters 3, 4 and 5).**

Numerous studies have associated the bimodal precipitation regime around equatorial Africa (from central Tanzania to southern Ethiopia) with the seasonal and meridional excursion of the ITCZ (Gleixner *et al.*, 2017; Korecha and Sorteberg, 2013; Segele and Lamb, 2005). The other atmospheric-oceanic large-scale feature affecting southern Ethiopia is ENSO. Literature showed that the equatorial Pacific SST variability is strongly correlated (50%) with precipitation anomalies in Ethiopia (Gleixner *et al.*, 2017). Interestingly, the impact of ENSO differs among regions and seasons in the country (Gleixner *et al.*, 2017; WMO, 2018). For northern Ethiopia, El Niño/La

Niña conditions are correlated with less/more *kirmet* precipitation, respectively (Korecha and Sorteberg, 2013; WMO, 2016), whereas the opposite trend is observed in southern Ethiopia during ENSO events (Nicholson, 1996; Tsidu, 2016; WMO, 2016). These large features of atmospheric motions are important as they influence weather and climate in several spatiotemporal scales and consequently affect crop growth.

Moving to finer spatiotemporal scales, Figure 1.1 shows the complexity of topography in the Gamo Highlands in southern Ethiopia. The landscape is composed of lakes, forests and agricultural land. The elevation ranges between 1000 m a.s.l. in the valleys and 3600 m a.s.l. in the highlands (Daye and Healey, 2015). The complex topography and heterogeneous landscape not only influence large-scale circulations but also the local meteorological (*e.g.* mesoscale dynamics) conditions of the region (Jury, 2019).

The mesoscale meteorology displays seasonality and plays a key role in the crop dynamics of the Gamo Highlands. In the season of study, *belg*, the mesoscale flows vary in time and space in the area. A general diurnal pattern of anabatic flows during the day and katabatic flows at night is depicted (Figure 1.1c). The diurnal variations in mesoscale dynamics also showed prominent differences between the beginning (February) and the end (May) of the *belg* season. In February, variations in the day- and night-time flows are much more pronounced and the lake and mountain flows are more prominent than the large-scale features. Before the onset of the *belg* precipitation, strong easterly to south-easterly lake breezes can be observed during the day, with weak and localised flows at night. On the other hand, during the peak rainy month, the synoptic features prevailed and differences between day and night flows were less pronounced. In this period, the southerly flows to the highlands prevailed. The presence of lakes and the complex topography influenced how major roles played out during the dry month of the *belg,* whereas synoptic features such as ITCZ played key roles during the wettest month of *belg* season (Gebremariam, 2007).

Jury (2019) indicated that during the *kirmet* season in 2015, in the morning (0300 to 0900 Local Standard Time, LST), the Ethiopian highlands are dominated by divergent katabatic flows from the mountains to the lowlands. Upslope flows are initiated from 0900 LST and become stronger from 1500 to 2100 LST. During the evening (before midnight), surplus precipitation spreads at 7 m·s$^{-1}$ westwards from the highest mountains almost at 38°E and 14°N to 36.5°E. Jury (2019) remarked that solar heating initiated surface heat fluxes that generated moisture convergence in the late afternoon and precipitates in the evening. Rientjes *et al.* (2013), in the Lake Tana basin, showed a late afternoon (mostly), midnight and early morning precipitation diurnal maxima depending on the location around the basin. In the mountainous area in eastern Africa, Geerts and Dejene (2005), using TRMM satellite data showed an afternoon to evening (peak occurs during 1500 to 1800 LST) precipitation maximum in the *kirmet* season. Elevation and aspect angle (by influencing the large-scale flows)

and Lake Tana played key roles in modulating the diurnal precipitation cycle (Haile *et al.*, 2009; Rientjes *et al.*, 2013).

### 1.1.4 Scaling down: From global to the smallholder farmer's land

#### a) *Meteorology*

Forty-two percent (471 thousand km²) of Ethiopian land is categorised as mountainous area, in which 55% of the population dwells (Huddleston *et al.*, 2003). In the country, the average farm size is estimated to be 0.96 hectare per farmer (Headey *et al.*, 2014). In such complex topography with diverse climatology (Diro *et al.*, 2009) and a system of fragmented landholdings, a downscaling approach (from global to local/field-scale) can be appropriate to implement weather/climate related decisions (Takle *et al.*, 2014). For such relevant farm-scale agricultural decisions, outputs from fine resolution weather-crop models/observations are crucial.

Agro-meteorological models involve plant physiological (*e.g.* carbon allocation in plant parts) or physical (*e.g.* crop growth) processes, on the basis of which the models calculate relationships between the plant functions as influenced by environmental variables such as weather and edaphic variables and crop management interventions (Hoogenboom, 2000; MacKerron, 2007). Crop growth models use weather elements as model input (Klemm and McPherson, 2017). Their applications are twofold: (1) to enhance our knowledge of crops and relevant crop processes; (2) to predict the impacts of manipulations in cropping systems (Khan *et al.*, 2014; Motha, 2007; Van Ittersum and Donatelli, 2003). Several methodological options with different spatial and temporal resolutions can be employed here to understand historical and to predict future weather/climate, which can be used as inputs for agro-meteorological models. These are weather station networks (or interpolated and generated data) (*e.g.* (Boogaard *et al.*, 2002; Carbone, 1993; Ceglar *et al.*, 2016; Van Keulen and Stol, 1995)); weather reanalysis products (*e.g.* (De Wit *et al.*, 2010; Elliott *et al.*, 2015)); remotely sensed datasets (*e.g.* (Jin *et al.*, 2018; Ma *et al.*, 2013)) and statistically or dynamically (with numerical weather prediction models) downscaled products (*e.g.* (Marletto *et al.*, 2007; Raposo *et al.*, 1993)). It is important to stress that these data streams are quite different in source and have different values for crop modelling. In this thesis, I used dynamically downscaled weather model data at both fine (representing mesoscale processes) and coarse (GCM scale) resolutions and a dense network of stations as input for a crop growth model. Outputs such as seasonal to inter-annual climate (temperature and precipitation) forecast products with lead-times of a month to a year or more are of enormous benefit for agricultural productivity (Ash *et al.*, 2007; Garbrecht and Schneider, 2007; Motha, 2007; Takle *et al.*, 2014). Examples of such outputs are future climate change scenarios, predicted by GCMs (*e.g.* (Hijmans, 2003; Tubiello *et al.*, 2002)); and climate variability and ocean/atmosphere teleconnections such as ENSO predictions (*e.g.* (Ash *et al.*, 2007;

Cane *et al.*, 1994; Jury, 2012; Maracchi *et al.*, 2005; Motha, 2007)) can be regarded as weather input for crop models for predicting the future crop growth and yield.

In order to understand how weather and climate variations influence potato growth, it is essential to design a research methodology that integrates scales, resolves processes and captures the main spatiotemporal details in weather dynamics (Hunink *et al.*, 2014; Motha, 2007; Otieno *et al.*, 2018). The global climate forecasts with coarser horizontal resolutions (approximately 50 km) need to be downscaled (smaller spatiotemporal scales) for both regional and farm-specific interpretations are presented (see coarse and fine model domains in Figure 1.1a). To scale down global weather/climate products, dynamical and statistical-empirical downscaling and a combination of the two methodologies are in use today (Garbrecht and Schneider, 2007).

### b) *The potato crop dynamics*

On farm level, crop models can be used as decision-support systems (DSS) to assist the farmer's decision-making (Haverkort, 2018; Hoogenboom, 2000). There are three types of DSS management decisions: (1) strategic (decisions prior to farming potato crop based on climate suitability, resources availability and efficiency, *e.g.* agro-ecological zoning (Haverkort *et al.*, 2013; Van Evert *et al.*, 2013)); (2) tactical (decisions prior to planting but following strategic decisions, *e.g.* fertilizer rating (Gayler *et al.*, 2002)); and (3) operational/forecasting (decisions taken in the course of a cropping season, *e.g.* yield predictions (Haverkort *et al.*, 2015; Khan *et al.*, 2014)).

Agro-meteorological models mainly use meteorological crop drivers to assist farming decisions (Frisvold and Murugesan, 2013; Klemm and McPherson, 2017). The major meteorological crop drivers are temperature (T), precipitation (PPT) and incoming shortwave radiation (SW↓) (see Figure 1.1d). Temperature data are relevant for decisions on planting, disease outbreaks, pest management and harvesting in agricultural activities. Precipitation data are needed for planting, fertilizer applications, irrigation, spraying, cultivation, disease outbreak and harvesting (Frisvold and Murugesan, 2013; Klemm and McPherson, 2017; Pasteris *et al.*, 2004). Similarly, the SW↓ data is required for planting, potential evaporation estimates and harvesting (Pasteris *et al.*, 2004).

Today, a number of potato crop models are applied in the DSS in the farming system. The Daisy model (Abrahamsen and Hansen, 2000; Heidmann *et al.*, 2008); the water-driven FAO crop model – AquaCrop (Raes *et al.*, 2009; Steduto *et al.*, 2009); the decision-support system for agrotechnology transfer – DSSAT model (Jones *et al.*, 2003); the Agricultural Production Systems Simulator – APSIM-Potato model (Brown *et al.*, 2011; Keating *et al.*, 2003; McCown *et al.*, 1996); and yet other models are listed by Raymundo *et al.* (2014). The pioneering work of C.T. de Wit of Wageningen University and Research has played a leading role in crop model development and application all over the world (Van Ittersum *et al.*, 2003). The Wageningen

production situations are based on potential and water-limited (SUCROS in Van Laar *et al.* (1992)); potential, water-limited and N-limited (NPOTATO in Seligman (1987), LINTUL-POTATO in Kooman and Haverkort (1995a) and GECROS in Yin and van Laar (2005)); potential, water-limited and NPK-limited (WOFOST in Boogaard *et al.* (1998) and De Wit *et al.* (2019)) and other models mentioned in Van Ittersum *et al.* (2003). In the wake of the Wageningen models, this study employed the GECROS (Genotype-by-Environment interaction on CROp growth Simulator) model. This model is discussed in some detail in Chapters 2 and 3. For details regarding the model framework, the reader is referred to Yin and van Laar (2005) and regarding model applications in potato modelling to Khan (2012).

## 1.2    Research strategy

The aim of this thesis is to appraise how weather and crop growth vary in a complex terrain and heterogeneous landscape. The study is based on a combination of high-resolution weather and crop models, in which datasets from our dense network of weather stations are used, as well as data from field crop trials at several different elevations and during two *belg* cropping seasons. In order to meet the aim of the thesis, I drew up three research questions:

1) *How do complex topography and heterogeneous landscapes affect weather and crop dynamics on different spatiotemporal scales?*

2) *What can we learn from a dense network of meteorological-soil observations network with respect to the crop growth variables (e.g. length of growing season and attainable yield)?*

3) *How do variations in the observed environmental variables correlate with crop growth and yield on sub-seasonal, seasonal and interseasonal scales in the Gamo Highlands? Can we identify periods in which the meteorological crop drivers have a different influence on potato growth characteristics?*

To support the model evaluation and interpretation, I combined fine resolution model outputs with observations from our dense automatic weather stations network. These datasets have also been correlated with several field crop experiments in the highlands. In other words, this thesis can be regarded as a pilot project to assess the need of this combined approach (modelling/observations) in remote region characterised by a highly complex topography and heterogeneous landscapes with the long-term goal to develop and apply a weather-food forecasting system.

To this end, I performed a coarse ($54 \times 54$ km$^2$) and fine ($2 \times 2$ km$^2$) spatial resolution weather model experiment (Figure 1.1a). To ensure that the synoptic situations are well reproduced (Jiménez *et al.*, 2016), I utilised the ERA-Interim reanalysis data (Dee *et al.*, 2011). My model integration covered a 10-year period following the modelling strategy described by Jiménez *et al.*, (2010; 2011b). This approach is fundamental, since the detailed topographic maps can explicitly resolve the orographic

features as described in Figure 1.1c. Such a detailed weather model simulation enabled us to obtain a first quantification of the impact of the weather variation on the potato growth and yield. The mountain area (>300 m a.s.l.) in Ethiopia, for instance, is much better represented by a 2 km resolution model than a typical GCM model output with a horizontal grid resolution of 50 km. Mass *et al.* (2002) showed that fine resolution models with a horizontal grid less than 10 to 15 km generally improve the realism of the models' outputs but do not necessarily significantly enhance their accuracy. By applying this methodology, I aimed to represent dynamical features related to the complex topography and the small (0.96 hectare average landholdings) farms of rural Ethiopia (Headey *et al.*, 2014). The weather model output was validated by means of observations from the lowlands (Arba Minch) and highlands (Chencha) as depicted in Figure 1.1a.

As mentioned above, the WRF model (Skamarock *et al.*, 2005) output is (one-way) coupled to the advanced and versatile eco-physiological crop model GECROS (Haverkort and Struik, 2015; Khan *et al.*, 2014; Yin and van Laar, 2005). The six weather model outputs were: maximum and minimum temperatures ($T_{max}$, $T_{min}$), PPT, SW↓, vapour pressure deficit (VPD) and wind speed (Yin and van Laar, 2005). The meteorological data were utilised as inputs to the crop model GECROS, in which the same spatial resolution model run was performed. The soil type and soil moisture data were supplied to the crop model from the fine resolution ISRIC soil database (Leenaars *et al.*, 2014).

Modelled precipitation driven by the ERA-Interim reanalysis is reasonable in simulating the observed trends in weather elements. However, the model overestimated precipitation in the highlands and underestimated in the lowland regions of Ethiopia (Van Vooren *et al.*, 2018). One of the reasons for the mismatches between modelled and observed precipitation was the poor quality of the observational datasets (Araya, 2011; Diro *et al.*, 2009). The density of weather stations' network is also poor in the SSA (Menne *et al.*, 2012). Consequently, and as part of our research strategy, the Gamo Ethiopian Meteorological Stations (GEMS) network was systematically installed along two transects in the Gamo Highlands (see inset in Figure 1.1a). The GEMS network was designed to quantify meteorological variability (lowland, midland and highland). These data are also utilised to simulate potato growth and yield at farm level in the Gamo Highlands. GEMS is a dense network (currently eight operational automatic weather stations) within a radius of nearly 50 km. The stations measure meteorological (temperature, SW↓, PPT, relative humidity (RH), wind, etc.), soil moisture and temperature (at 5, 10, 20 and 40 cm soil depths) and leaf-wetness (two sensors per station) with sub-hourly temporal resolutions (Figure 1.1b).

Close to the GEMS network, potato crop field experiments were performed during the two *belg* seasons in 2017 and 2018. Note that potato in Ethiopia is cultivated

during *belg*, *kirmet* and *bega* (if irrigated) seasons. However, the *belg* is the most suitable season for both meteorological (moisture availability) and agronomic (with less disease pressure) reasons (CSA, 2002; Haverkort *et al.*, 2012; Tufa, 2013). The field trials were carried out at five farms in *belg*-2017 and six farms in *belg*-2018. Two widely available local and six improved cultivars were planted in both seasons. The GECROS model was employed to simulate the observed canopy growth, yield and yield traits. The GEMS observations were used as the model input and model sensitivity experiments. I also analysed weather and crop datasets to explain the observed crop growth and yield in terms of meteorology and elevation as shown in Figure 1.1c,d.

## 1.3 Thesis outline

To answer the research questions set out in Section 1.2, I have structured the remainder of this thesis into the following chapters: a general method (Chapter 2), three research chapters (Chapters 3-5), followed by a general discussion and statement of perspectives (Chapter 6) and conclusions (Chapter 7). **Chapter 2** explains and describes the methods used, both the modelling tools and the design of the new GEMS observational network. The main climatological and weather factors are also discussed in the region under study during the period 2001-2010.

**Chapter 3** presents a 10-year study on meteorology and the impacts on potato growth and yield. The study investigated the role of complex terrain and landscapes modulating weather and crop dynamics in the Gamo Highlands (see research question 1) and covered spatial and temporal (*belg* seasons and interannual) variations in weather and crop growth; and sensitivity of crop growth to the meteorological perturbations. **Chapter 4** introduces and discusses the first observations from the dense network of weather observations with sub-hourly resolution data recording: the GEMS network. In this chapter, I introduced the GEMS (six automatic weather stations) network in two transects in the Gamo Highlands. Nearby, the network of stations was used to monitor the *belg*-2017 potato field trials. The objective of this chapter is to describe how landscape heterogeneity in a mountainous region influences both local and large-scale weather systems and crop growth (see research question 2). **Chapter 5** deals with how weather changes (sub-seasonal, seasonal and interseasonal) affect crop growth, yield and yield traits under different environmental conditions in the Gamo Highlands (see research question 2). This research project was based on the GEMS network and crop experiments in *belg*-2017 and *belg*-2018.

**Chapter 6** provides a general discussion; putting the results into perspective; synthesising the main findings of the thesis within the existing literature; presents outlooks and research gaps identified for future work. **Chapter 7** concludes by the key findings of Chapters 3 to 6 in line with the research questions described in this chapter. Finally, summary of the thesis presented.

<span style="float: right; font-size: 3em; color: gray;">2</span>

# Research strategy to study weather, climate and crop dynamics in the Gamo Highlands

This chapter presents the research strategy we applied in this thesis. The chapter also shows some preliminary findings of the PhD study. The strategy follows a combined approach of the implementation of models and observations. The area of study is a complex topographic region southwest Ethiopia, the Gamo Highlands. Models in the field of weather and crop science are implemented to generate high spatiotemporal resolution data. We also used datasets from our newly installed weather stations' network in combination with data from our potato crop field experiments in the highlands. Here, we show some preliminary model outputs related to the temporal and spatial variations in *belg* seasonal climate and crop yield during 2001 to 2010. Findings related to the future climate change are also analysed and some adaptation mechanisms are discussed. The findings in the chapter relate to the follow-up chapters presented in the thesis.

## 2.1 Motivation and strategy

Globally, mountains account for 25% of the Earth's land surface and hills and plateaus contribute 19% (Meyers and Steenburgh, 2013). In the Greater Horn of Africa (GHA), the Ethiopian Highlands are known by their complex topography and heterogeneous landscape (Viviroli *et al.*, 2003). Specifically, this region is characterised by a range of elevation between 125 m below sea level and 4620 m above sea level (a.s.l.). The lowest elevation is at the Danakil depression in the north-east. And the highest elevated area is at the summit of Mount Ras Dashen in the northern Ethiopia (Kassie, 2014). The GHA also includes the 5500 km long Great East African rift system. The rift system ranges from the Red Sea towards Lake Victoria in the GHA (Cattani *et al.*, 2016). The dominant land cover types of the region include lakes, deserts, savannah, woodlands and closed forests (Cunningham *et al.*, 2008). The Ethiopian Highlands are also close to large global waterbodies such as the Indian Ocean

and the Red Sea. In Ethiopia, the Gamo Highlands are characterised by rugged terrain (from 1000 m a.s.l. to 3600 m a.s.l.) and heterogeneous landscape including Lake Abaya and Lake Chamo. They are situated in southern Ethiopia and west of the Great Rift valley plain (Assefa and Bork, 2014). These versatile land cover features add complexity to the weather/climate dynamics of the region (Abdelwares *et al.*, 2018; Dinku *et al.*, 2011; Lehner and Rotach, 2018; Meyers and Steenburgh, 2013).

In complex terrain regions with varied landscape characteristics, weather and climate significantly vary in space and in time (Dinku *et al.*, 2011; Pohl *et al.*, 2011). Spatially, mountains influence synoptic** circulations and produce planetary waves, generate mesoscale** features and produce microscale** surface and boundary layer turbulent motions. Temporally, mountains modulate the weather systems ranging from seconds to a few days (Serafin *et al.*, 2018). These detailed spatiotemporal variations in land cover and meteorological phenomenon in mountainous region cannot be well represented by Global Circulation Models (GCMs) (Kendon *et al.*, 2012). Typically, GCMs have horizontal resolution of tens of kilometers in which topographic variation is poorly represented and sub-grid processes that control clouds and precipitation are only parametrised†† (Abdelwares *et al.*, 2018; Salathé *et al.*, 2008). On the other hand, fine resolution Mesoscale Atmosphere Model can better represent orography, more explicit which resolve weather dynamical features in mountainous regions. This results in accurate outputs of meteorological variables as compared to the *in situ* data (Abdelwares *et al.*, 2018; Torma *et al.*, 2015).

Weather model products simulated by GCMs can be applied to global scale studies but have limited importance for impact assessments such as food security issues particularly in the complex topography region of the GHA (Abdelwares *et al.*, 2018), a region in which smallholder farmers reside (Headey *et al.*, 2014; Holden and Yohannes, 2002). Pohl *et al.* (2011) discussed that downscaling coarse GCMs to regional and local scales is crucial mainly in the GHA as a result of the complex topography and land heterogeneity of the region. Model outputs from the fine resolution RCMs can be used for understanding the weather/climate dynamics in regions with complex terrain. Furthermore, the outputs also can be coupled with crop models used for regional investigation of crop growth and yield.

In this thesis, we used the state-of-the-art numerical weather prediction model called Weather Research and Forecasting (WRF) model (Skamarock *et al.*, 2005). The model's outputs are compared with observations at different elevations. The WRF model output is also deployed to an advanced process-based crop model, GECROS (Yin and van Laar, 2005). Both weather and crop observations are limited in Ethiopia, specifically in remote mountainous regions. To this end, we deployed the Gamo

---

** *Weather system occurring from ~1000 km to 4000 km scale is synoptic, ~3 km to 300 km scale is mesoscale, and 3 mm to 300 m is microscale (Stull, 2000).*

†† *Parameterization is a simplified physical or statistical representation of atmospheric processes occurring at sub-grid scale and/or too complex and hence computationally costly.*

Ethiopian Meteorological Stations (GEMS) network (8 automatic weather stations). The stations' network has been operational since April 2016. In combination, field experiments are conducted nearby the GEMS network.

## 2.2 The new research approach: weather-crop dynamics in a complex terrain

To address the research questions posed in Chapter 1, we designed a methodology that combines the use of models and observations. Figure 2.1 shows the research strategies we designed and their connections.
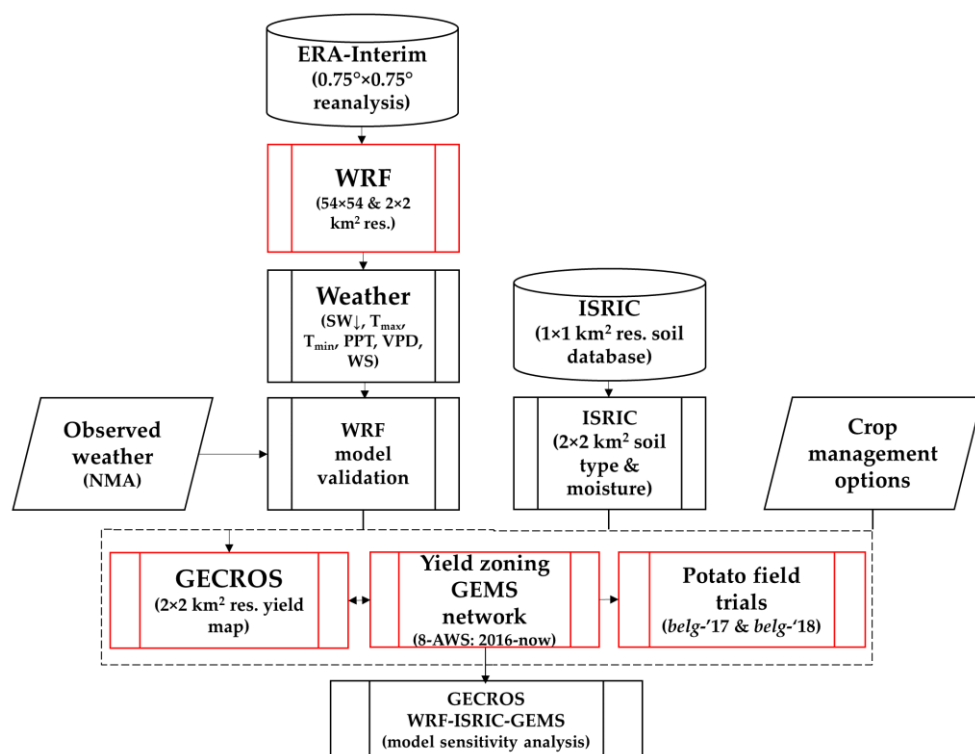


**Figure 2.1 | Research design, connections among the different methods and tools used in this study.** Acronyms: WRF – Weather Research and Forecasting, SW↓ – incoming shortwave radiation (MJ·m$^{-2}$·d$^{-1}$), T$_{max}$ and T$_{min}$ – maximum and minimum temperatures (°C), PPT – precipitation (mm·d$^{-1}$), VPD – vapour pressure deficit (kPa), WS – wind speed (m·s$^{-1}$), ISRIC – International Soil Reference and Information Center, NMA – National Meteorology Agency, Ethiopia, GECROS – Genotype-by-Environment interaction on CROp growth Simulator, AWS – Automatic Weather Station, GEMS – Gamo Ethiopian Meteorological Stations, *belg* – (February to May), seasonal climate classification in Ethiopia, according to NMA. Note that the red boxes indicate methods developed in this thesis.

We followed a model-observation combined approach. The modelling and observational datasets deployed in this thesis and presented in Figure 2.1 are discussed below.

### 2.2.1 The modelling research strategy

*a) The weather model*

We used an advanced Mesoscale Atmosphere Model namely the Weather Research and Forecasting (WRF) model version 3.4.1 for weather simulations (Skamarock *et al.*, 2005). The model's initial and boundary conditions are prescribed by the ERA-Interim reanalysis with a horizontal resolution of 0.75° × 0.75° as shown in Figure 2.1 (Dee *et al.*, 2011). WRF is configured in four model domains in order to resolve the more important weather scales: synoptic, mesoscale and local scales. The mother domain is centred at Arba Minch and has a 54 km × 54 km horizontal resolution and covered the East African countries, the north-west Indian Ocean and the Arabian Peninsula (see Figure 3.2 in Chapter 3). The inner nested domains are interacting in two ways with a 3-to-1 spatial refinement to successively attain a 2 km × 2 km horizontal resolution. The model's physical representations are summarised in Table S2 (Follow the link: https://www.sciencedirect.com/science/article/pii/S0168192318302302#sec0095). To carry out the 10-year continuous model run, we followed the modelling design by Jiménez *et al.* (2011a; 2013; 2016; 2011b). This 10-year datasets are composed of 48 h spanned short model runs. Each model run is initialised at 0 UTC and model results are recorded every hour for 48 h. The first 24 h of the data are the model spin-up and those data are discarded. The period 24 h to 48 h are retained for analysis for that day. This process is repeated for each day in the period from 2001 to 2010.

The high horizontal spatial (2 km × 2 km) and temporal (hourly outputs integrated for the period of 10-year) resolution datasets enabled us, for the first time in Ethiopia, to study the complex interplay between weather and crop dynamics in the steep topographic region of the Gamo Highlands (Chapter 3). The WRF output was compared with the *in situ* data at different elevations. We identified the major atmospheric crop drivers (minimum and maximum temperatures – $T_{min}$ and $T_{max}$, precipitation – PPT and the incoming shortwave radiation – SW↓. We selected the *belg* (February to May) crop season and statistically identified the normal and anomalous years during the 10-year. The *belg* season is relevant in terms of meteorology (*i.e.* the weather is favourable for crop growth) and agronomy (*i.e.* it has less disease pressure compared to the *meher* [June to September] agronomic season) (CSA, 2014; Tufa, 2013). Weather outputs from the WRF model are supplied to the genotype-by-environment interaction crop model – GECROS (Yin and van Laar, 2005).

*b)* *The crop model*

GECROS by Yin and van Laar (2005) is the state-of-the-art crop model categorised within the Wageningen 'School of de Wit, Bouman *et al.* (1996)' models (Adam, 2010; Ingwersen *et al.*, 2018). We used version 1.0 of the crop model with the model's surface energy budget improvements as implemented in Combe *et al.* (2015). Six meteorological variables ($T_{min}$ and $T_{max}$ (°C), PPT (mm·d$^{-1}$), SW↓ (MJ·m$^{-2}$·d$^{-1}$), vapour pressure deficit – VPD (kPa) and wind speed (m·s$^{-1}$)) are used as model's weather input. As Figure 2.1 showed, the crop model considers the weather variables on a daily basis and the variables are calculated either from the WRF model (hourly temporal resolution data) (implemented in Chapter 3) or our stations observational datasets (15-min recorded datasets presented in Chapter 4). The crop model also needs soil data and crop management options as presented in Figure 2.1. The GECROS model is compared with observations from our field experiments. The crop model output is used for yield zoning as a function of elevation.

A number of model sensitivity experiments are conducted (Figure 2.1). The model sensitivity experiments results are presented in Chapters 3 and 4. Variations in modelled data are used as model sensitivity experiment. These were weather data (*e.g.* PPT), edaphic variables (*e.g.* percent clay), crop parameters (*e.g.* seed weight), crop management options (*e.g.* shifting potato-planting dates) and climate change assumptions (*e.g.* atmospheric $CO_2$ concentration) following the Intergovernmental Panel on Climate Change – IPCC future scenarios (Stocker *et al.*, 2013; Van Oldenborgh *et al.*, 2013). We also analysed the sensitivity of the GECROS model for variations in the observed weather and shifts in the *belg* precipitation in the Gamo Highlands (Chapter 4). The first experiment design was altering one variable (*e.g.* PPT, feeding a constant daily value, *i.e.* an average precipitation during the growing season) at a time and maintaining the other five variables as observed. The model experiment with the shifted PPT simulates an early *belg* onset (it exchanges the maximum PPT observed in May with the PPT in March), a normal *belg* PPT onset (it exchanges the maximum PPT observed in May with the PPT in April) and a late *belg* PPT onset (it exchanges the maximum PPT observed in May with the PPT in June).

### 2.2.2  High spatial resolution environmental and crop datasets

*a)* *ISRIC soil database*

The soil module in the GECROS model requires soil data as model input (Chapter 3 and as shown in Figure 2.1). These input data include percent clay, total organic matter, minimum soil water content, soil water content at field capacity and maximum water holding capacity of the soil. These data are obtained from the Africa soil information project International Soil Reference and Information Center (ISRIC) database (Leenaars *et al.*, 2014). Weighted (0-5 cm, 5-10 cm, 15-30 cm and 30-60 cm

depths) averages of the top 60 cm soil depths data are considered. These data are with 1 km × 1 km resolution. We interpolated and re-gridded the data to fit the WRF model's 2 km × 2 km resolution domain. To this end, the weather model output and the ISRIC soil data are run using the GECROS model grid-by-grid-wise (Figure 2.1).

*b)   Station observations*

Figure 2.1 showed the observational datasets utilised in this thesis. Two meteor-ological datasets are used: (1) from the National Meteorology Agency (NMA) – Ethi-opia, which are manually operated stations; (2) the GEMS network. To validate the performance of the WRF model, we used data from the NMA. The stations are equipped with gauged instruments and located in Arba Minch at 1200 m a.s.l. and in Chencha at 2700 m a.s.l. These locations are representative of the lowland and highland areas. In Chapter 3, we discussed the evaluation of modelled and observed weather. In short, WRF underestimated/overestimated precipitation at low-lands/highlands, respectively. The modelled temperature was, in general, cooler than the observed. Few of the potential reasons for the model-observation mis-matches are the low quality of weather information and limited availability of sta-tions in a region where weather significantly varies over short distances (Dinku *et al.*, 2014; Van Vooren *et al.*, 2018). To fill the gap and to better understand the weather dynamics in the complex topographic region of the Gamo Highlands, we installed a network of automatic weather stations – the GEMS, operational from April 2016 to date.

*c)   The GEMS network*

The GEMS is a network of eight automatic weather stations (AWSs) installed at different elevations in the Gamo Highlands. We installed the stations according to the elevation-based yield zoning following GECROS modelled yield patterns pre-sented in Chapter 3 (see Figure 2.1). These yield zones are: yield Zone-I (from 1100 m a.s.l. to 1500 m a.s.l.), yield Zone-II (1600 m a.s.l. to 2650 m a.s.l.) and yield Zone-III (from 2950 m a.s.l. to 3600 m a.s.l.) (see Table 2.1 and Figure 3.7). The stations are aligned along two transects to represent the south and east facing slopes of the high-lands. By doing so and in combination with stations installed around the shores of Lake Abaya and Lake Chamo, we are able to study mountain-lake driven circula-tions and their roles in crop growth. The AWS models are Davis Vantage Pro2 + (DVP2) and Campbell Scientific (CS) with CR200X series data-logger. Both of the stations' models have been widely used globally and tested for robustness (Bell *et al.*, 2015; Lagouvardos *et al.*, 2017; Steeneveld *et al.*, 2014). The stations record weather (temperature, PPT, SW↓, wind, relative humidity, sea-level-pressure, etc.); soil moisture and temperature at 5 cm, 10 cm, 20 cm and 40 cm depths; leaf-wetness

in east and west directions of each station. The sensors sample data at intervals between 2.5 and 90 seconds, after which the 15-minute averages of the samples are recorded. The data generated by the GEMS are used to study both mesoscale to synoptic scale weather and crop dynamics (with crop modelling and analysing weather-crop relations) in the Gamo Highlands (see Chapters 4 and 5).

**Table 2.1 | Descriptions of weather stations (farms), geographical locations and field experiments** (crop yield zone as classified in Chapter 3, the number of cultivars planted during *belg*-2017 and *belg*-2018). Acronyms: Lon – Longitude (°), Lat – Latitude (°), Elv – Elevation (m), Var. – Variables, DVP2 – Davis Vantage Pro2 +, NMA – National Meteorology Agency, Ethiopia, CS – Campbell Scientific, W·S·L – Weather (*e.g.* PPT and SW↓)-Soil (moisture and temperature)-Leaf-wetness, W – Weather, S – Soil, L – Lake, EW – East-West, SN – South-North and NS – Not Suitable location for potato farming because of the warmer climate.

| Station (farm) | Location | | | Automatic Weather Station (AWS) | | | | Potato field experiment | | |
| --- | --- | --- | --- | --- | --- | --- | --- | --- | --- | --- |
| | Lon (°) | Lat (°) | Elv (m) | Model | Var. | Since | Tran-sect | Yield zone | Culti-vars '17 | Culti-vars '18 |
| Sille | 37.483 | 5.869 | 1120 | DVP2 | W·S·L | Apr-18 | L. Chamo | I | NS | NS |
| Arba Minch | 37.568 | 6.067 | 1200 | DVP2 | W·S·L | Apr-16 | Ref. | I | NS | NS |
| Alge | 37.795 | 6.286 | 1220 | DVP2 | W·S·L | Apr-18 | L. Abaya | I | NS | NS |
| Derashe | 37.368 | 5.637 | 2120 | | | | | II | 8 | 8 |
| Tegecha | 37.573 | 6.161 | 2143 | DVP2 | W·S·L | Apr-16 | EW | II | 8 | |
| Geresse | 37.310 | 5.929 | 2298 | NMA | W | | EW | II | 8 | 8 |
| Zigiti | 37.459 | 6.073 | 2420 | DVP2 | W·S·L | Apr-16 | EW | II | | |
| Zozo | 37.605 | 6.265 | 2695 | | | | | II | | 2 |
| Chencha | 37.572 | 6.254 | 2738 | CS | W | Jun-13 | SN | II | | 2 |
| Gazesso | 37.337 | 6.130 | 2840 | DVP2 | W·S·L | Apr-16 | EW | II | 8 | 8 |
| Gircha | 37.563 | 6.302 | 3015 | DVP2 | W·S·L | Apr-16 | SN | III | 8 | 2 |

*d) Crop field experiments during belg seasons: 2017 and 2018*

To validate the performance and sensitivity of the GECROS crop model and study weather-crop relations, we designed a set of field experiments at different elevations in the Gamo Highlands (Table 2.1). The GECROS modelled length of the growing season (LGS) and maximum plant height (MPH) outputs are compared with our observations from field experiments. The research methodology is discussed in detail in Chapter 4 to answer the research question (2) posed in Chapter 1. The farm experiments nearby the GEMS network allowed us to better investigate the GEMS data both for crop modelling (Chapter 4) as well as to associate weather data to crop growth (Chapter 5). We collected potato seed tubers from three research centres in Ethiopia for improved cultivars and local cultivars are purchased from local markets. For *belg*-2018, we collected seed tubers from Gircha and Gazesso farm

and stored the seed tubers in the diffused light storage (DLS) facility located at Gircha. The DLS allows free ventilation, to slow down sprout ageing and to supress sprout elongation (Hirpa *et al.*, 2010). The improved cultivars with their year of release are the following: *Horro* (2015), *Belete* (2009), *Gudene* (2006), *Hunde* (2006), *Ararasa* (2006) and *Jalene* (2002). The local cultivars are *Suthalo* (unknown) and *Kalsa* (unknown) (Table 2.1) (Baye and Gebremedhin, 2012; Gebreselassie *et al.*, 2016; MOANR, 2016).

We applied the randomised complete block design with experiments in triplicates (Gomez *et al.*, 1984). Each plot had 3 m × 3 m dimension with four rows. The planting pattern was 0.75 m (between rows) × 0.30 m (between plants within a row). Spacing between replications and plots were 1.5 m and 1.0 m, respectively. The farm management was the same for all farms and seasons. The inorganic fertilizers were: urea (144 kg·ha$^{-1}$), NPS (236 kg·ha$^{-1}$) and murate of potash (125 kg·ha$^{-1}$) were added at planting, but the urea was split into two dressings, in which the first half was added at planting and the remaining half was applied at the start of the flowering stage.

Crop data were taken from the central two rows to avoid boarder effects (Yactayo *et al.*, 2013). Plant height (cm) and canopy cover (%) data were taken on a daily basis during *belg*-2017 and three times per week during *belg*-2018 for selected farms and cultivars (improved and local). Yield traits (*e.g.* tuber number and weight per plant) and yield per plot at the end of the growing season were also collected. Yield and crop growth (*e.g.* maximum plant height) data were used for the GECROS model validation as discussed in Chapter 4. In Chapter 5, the crop growth data collected at high temporal resolution were correlated to temperature sum (the sum of the daily average temperature minus the base temperature–$T_b$ [0 °C ≤ $T_b$ ≤ 5°C] (Haverkort, 2018; Khan, 2012)). In addition, environmental (weather and edaphic) data were used for correlational analysis between environment and crop variables.

## 2.3  *Belg* climatology: a 10-year perspective

To complete the scales and processes investigated in this thesis, here we provide a 10-year perspective on the climate and crop yield variations during 2001 to 2010. The objective here is to get insights on the interannual variability represented by the observations and modelled by WRF.

### a)  *Temporal variability*

The major meteorological crop drivers modelled for the years from 2001 to 2010 enabled us to identify the years close to the average *belg* climate during the 10-year period and the ones that were characterised by anomalous *belg* seasons, mainly related to heat ($T_{max}$ and $T_{min}$) or drought (precipitation). We focused on meteorological variables that play a key role on the crop growth dynamics such as $T_{max}$, $T_{min}$, PPT

and SW↓. We selected the fine resolution domain of our weather model (see Figure 2.1) as it was better in representing the temporal (using statistical model validation measures) and spatial variations than the coarse resolution output. Figure 2.2 shows the interannual anomalies (deviations from the 10-year mean for both modelled and observed data) of the main meteorological crop drivers.
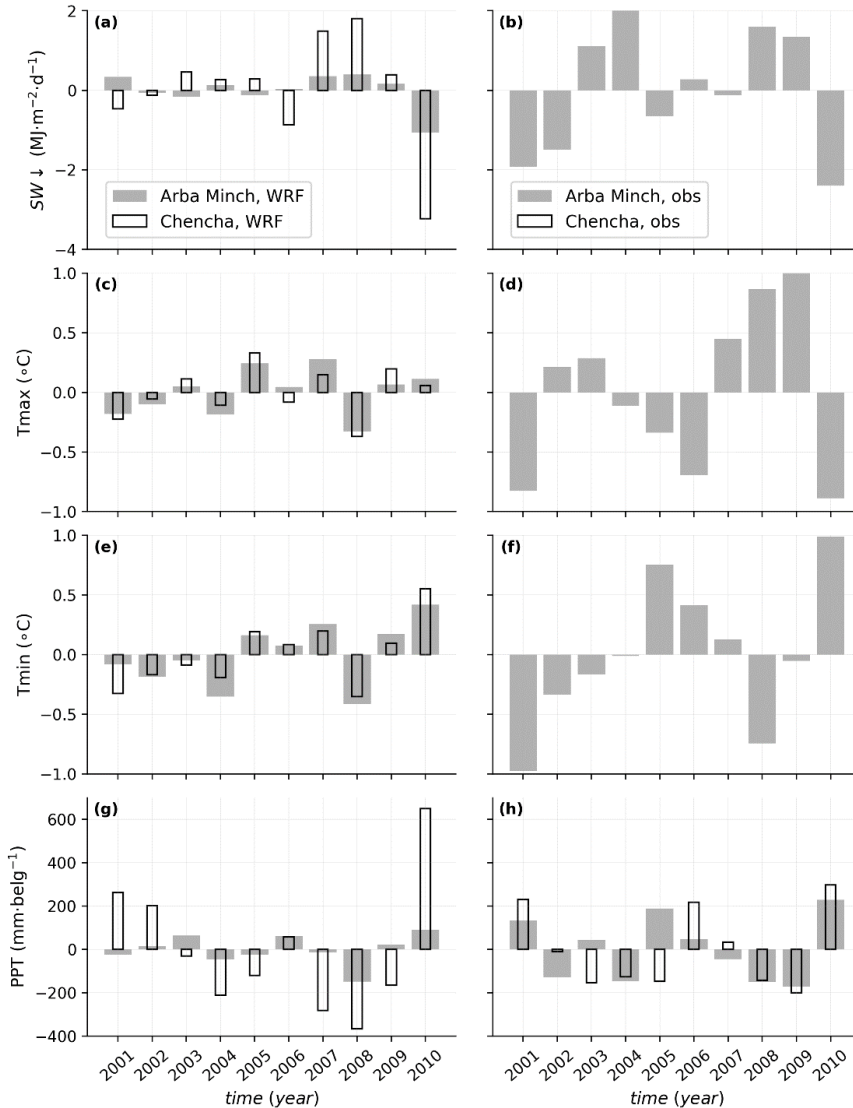


**Figure 2.2 | Interannual *belg* season weather anomalies (deviation from the 10-year *belg* mean) of the WRF model fine resolution (2 × 2 km²) output (left-panel) and observed (right-panel) data for the major meteorological crop growth drivers during 2001-2010: SW↓ (MJ·m⁻²·d⁻¹) (a and b), Tmax/Tmin (°C) (c – f) and PPT (mm·*belg*⁻¹) (g and h). The filled and box bar plots indicate Arba Minch and Chencha stations, respectively.**

Variability in the modelled SW↓ during the 10-year *belg* seasons was underestimated (±0.42 MJ·m$^{-2}$·d$^{-1}$, explained in terms of standard deviation) for Arba Minch as compared to the observed variation (±1.59 MJ·m$^{-2}$·d$^{-1}$) as shown in Figure 2.2a and b. Although WRF satisfactorily predicts the pattern of the annual cycle, the model largely overestimated SW↓ in Arba Minch (Mean Bias Error–MBE of +4.5 MJ·m$^{-2}$·d$^{-1}$, where the average modelled and observed SW↓ were 25.2 MJ·m$^{-2}$·d$^{-1}$ and 20.1 MJ·m$^{-2}$·d$^{-1}$, respectively). For the Chencha station, the variation in the modelled SW↓ was nearly three times larger than that of Arba Minch (we do not have observation to compare). The annual (2001 to 2010) mean modelled SW↓ for Arba Minch and Chencha were nearly 26 MJ·m$^{-2}$·d$^{-1}$ and 17 MJ·m$^{-2}$·d$^{-1}$, respectively. This can be a reason why the model underestimated PPT in Arba Minch while it overestimated PPT in Chencha. The simulated cloud fraction near Arba Minch and Chencha were ~1.2% and ~4.5%, respectively (analysis not shown here). Tariku and Gan (2018) also discussed that increased SW↓ is associated with decreased cloud cover, which results in less PPT and vice versa. The mismatch between the model and observations can be related to (1) the model underestimated the expected cloud cover around Arba Minch that the modelled SW↓ increased significantly and (2) we calculated the SW↓ from the sunshine hours duration observations as suggested by Garg and Garg (1983), in which the sunshine hour measurements data can have errors.

The variations in T$_{max}$ and T$_{min}$ during the 10-year *belg* seasons were smaller (from 0.20 to 0.27 °C) for the WRF model as compared to the observed (nearly 0.64 °C) for Arba Minch (Figure 2.2c and f). It is also underlined that the model was cooler during the day and somewhat warmer at night than observed (MBE in T$_{max}$ was -3.2 °C and MBE in T$_{min}$ was +0.5 °C). This result also agrees with Tariku and Gan (2018) findings, who modelled weather for the Nile River Basin. There are a number of possible causes for the mismatches: (1) The model bias in representing elevation (*e.g.* the elevation Arba Minch in the model is represented 62 m above the true elevation); (2) an increased SW↓ shows a lower amount of clouds, which ultimately decrease the longwave radiations and finally causes a cooler condition.

The modelled PPT variation was lower (68.4 mm·*belg*$^{-1}$) for Arba Minch as compared to the observed (149.6 mm·*belg*$^{-1}$) during the 10-year (Figure 2.2g and h). However, for Chencha, variation in the modelled precipitation was much higher (304.6 mm·*belg*$^{-1}$) than observed (186.2 mm·*belg*$^{-1}$). The WRF model had a warm bias for lowlands and a moist bias for elevated areas (MBE of -1.3 mm·d$^{-1}$ and +3.7 mm·d$^{-1}$ for Arba Minch and Chencha, respectively) (see Chapter 3).

In temperate climates, temperature can be a limiting factor for crop growth. However, in the tropical environment, like the Gamo Highlands, soil moisture driven by PPT is the limiting factor for crop production (Tadele, 2017). Here, we further focus on the modelled annual and seasonal PPT variation. This also helps us to define potato-planting dates using GECROS. Table 2.2 shows descriptive statistics on WRF modelled PPT using the fine resolution domain during 2001 to 2010.

**Table 2.2 | Statistics of WRF modelled yearly and *belg* precipitation for the year 2001 – 2010 for Chencha station using the WRF model's fine resolution. Note that the bold values indicate the highest or latest and the underlined values indicate the lowest or earliest precipitation onsets during the 10-year period in Chencha.**

| Year | Annual summary | | Summary of the *belg* season | | | | | | | |
|---|---|---|---|---|---|---|---|---|---|---|
| | mm· yr$^{-1}$ | mm· d$^{-1}$ | mm· *belg*$^{-1}$ | mm· d$^{-1}$ | % *belg* | std dev. | #days ≥0.85 mm | #days ≥5 mm | #days ≥10 mm | PPT onset |
| 2001 | **3483** | **9.5** | 1368 | 11.4 | 39 | 15 | 80 | 59 | 47 | <u>5-Feb</u> |
| 2002 | 2554 | 7.0 | 1307 | 10.9 | 51 | 16 | 73 | 51 | 39 | 2-Mar |
| 2003 | 2421 | 6.6 | 1075 | 9.0 | 44 | 15 | 65 | 40 | 29 | 11-Apr |
| 2004 | <u>2147</u> | <u>5.9</u> | 894 | 7.4 | 42 | 12 | 71 | 43 | 29 | 12-Mar |
| 2005 | 2238 | 6.1 | 986 | 8.2 | 44 | 13 | 72 | 47 | 32 | 27-Feb |
| 2006 | 2603 | 7.1 | 1162 | 9.7 | 45 | 14 | 75 | 49 | 34 | 21-Feb |
| 2007 | 2578 | 7.1 | 825 | 6.9 | 32 | 13 | <u>59</u> | 35 | 25 | 19-Mar |
| 2008 | 2316 | 6.3 | <u>740</u> | <u>6.1</u> | <u>32</u> | <u>11</u> | 60 | <u>34</u> | <u>23</u> | 27-Mar |
| 2009 | 2533 | 6.9 | 941 | 7.8 | 37 | 12 | 70 | 46 | 29 | 27-Mar |
| 2010 | 3421 | 9.4 | **1755** | **14.6** | **51** | **16** | **86** | **70** | **61** | **11-Apr** |

Table 2.2 shows that the year 2001 was the wettest (9.5 mm·d$^{-1}$) and 2004 was the driest (5.9 mm·d$^{-1}$). Because of the favourable meteorological and agronomic conditions during the *belg* season (moisture availability due to both large and local scale weather phenomenon; moisture availability to grow potato with less disease pressure), we focussed on the *belg* season's seasonal climate. The Chencha station was selected as the representative site for the potato-growing region in the Gamo Highlands. Considering the *belg* season during the 10-year period, *belg*-2010 was the wettest (with 14.6 mm·d$^{-1}$), which is also observed in station dataset. Of the annual total PPT, more than 50% was received during the *belg* season and with the highest number of days with ≥ 0.85 mm (86 days), ≥ 5 mm (70 days) and ≥ 10 mm (61 days) although with high variability amongst the days during the season (standard deviation of 16 mm). The onset of the *belg* PPT in 2010 was 11 April. In contrast, the *belg*-2008 was the driest (6.1 mm·d$^{-1}$). The highest/lowest *belg* season's PPT during the 10-year period can be associated with the lowest/highest SW↓ (~3.5 MJ·m$^{-2}$·d$^{-1}$ in 2010 compared to ~2 MJ·m$^{-2}$·d$^{-1}$ in 2008) simulated for Chencha (Figure 2.2a). Large-scale weather systems such as anomalies over the Pacific Sea Surface Temperature (SST) related to the El Niño Southern Oscillation (ENSO) influence weather systems in Ethiopia. For instance, the warm phase of ENSO (El Niño) and it's cold phase (La Liña) are associated with wetter and drier than the normal *belg* precipitation for the southern Ethiopia, respectively (Tsidu, 2016; WMO, 2016). It is also noted that the *belg*-2008 was driest while *belg*-2010 was wettest (Table 2.2). The 2008 and 2010 years

were during La Liña and El Niño episodes, respectively (follow https://www.esrl.noaa.gov/psd/enso/past_events.html). Climatological speaking, *belg*-2006 received nearly an average PPT and we considered the season as climatologically *normal* during the 10-years period.

The amount of water available to plants strongly depends on the onset, length, temporal distribution and cessation of precipitation (Ngetich *et al.,* 2014). We calculated the onset day of *belg* PPT during the 10-year period (Table 2.2). These days were considered as potato planting dates in the GECROS model. The average *belg* precipitation onset date was 14th of March during the 10-year period, with nearly 2-months range of variation (between 5 February and 11 April). Overall, the WRF model overestimated the SW↓ observed; had a cool bias in terms of temperature; and underestimated PPT in the lowlands (*e.g.* Arba Minch); and had a wet bias compared with the gauged datasets for the elevated areas in the Gamo Highlands (*e.g.* Chencha) as discussed in Chapter 3.

*b)* *Spatial variability*

To complete the interannual variability analysis, we investigated the spatial variations of meteorological crop drivers ($T_{max}$, $T_{min}$, SW↓ and PPT) for the climatological and anomalous *belg* seasons as presented in Figure 2.3 and Figure 2.4. Again, we focus on the fine model domain. Figure 2.3 shows the spatial (2 km × 2 km) resolution model output for the daily maximum and minimum temperatures.

A spatial range of $T_{max}$ from 10 °C to 30 °C is modelled averaged over the 10-year period *belg* seasons during daytime (Figure 2.3a). In the figure, the valley around Lake Abaya and Chamo is the warmest (~30 °C) and the Gamo mountain range around the summit of mount Guge is the coolest locations with mean temperatures near ~10 °C in $T_{max}$. During the night, however, the mean atmospheric temperature ($T_{min}$) drops between 8 °C (on the mountains) to 20 °C (in the valley around the lakes) as compared to the daytime (Figure 2.3b). Interestingly, the WRF model satisfactorily simulated the ~5 °C warmer and ~5 °C cooler air temperature near the lake surroundings than the lake surface temperature during daytime and night-time, respectively (Figure 2.3c-f). This difference (*i.e.* ~5 °C) in lake-land temperature generates lake-breeze circulations during daytime and mountain-breeze flows during night-time as discussed in detail in Chapter 4. The *belg*-2008 is identified as having the coolest by ~0.3 °C in $T_{max}$ and ~0.6 °C in $T_{min}$ from the 10-year (Figure 2.3c and d). In this season, an enhanced warming is simulated for lakes and mountains. We also discussed that *belg*-2008 was the driest of the entire 10-year period (Figure 2.2g and Table 2.2). In contrast, the *belg* seasons of the year 2005 and 2010 are identified as having the highest $T_{max}$ and $T_{min}$, respectively (Figure 2.3e and f).
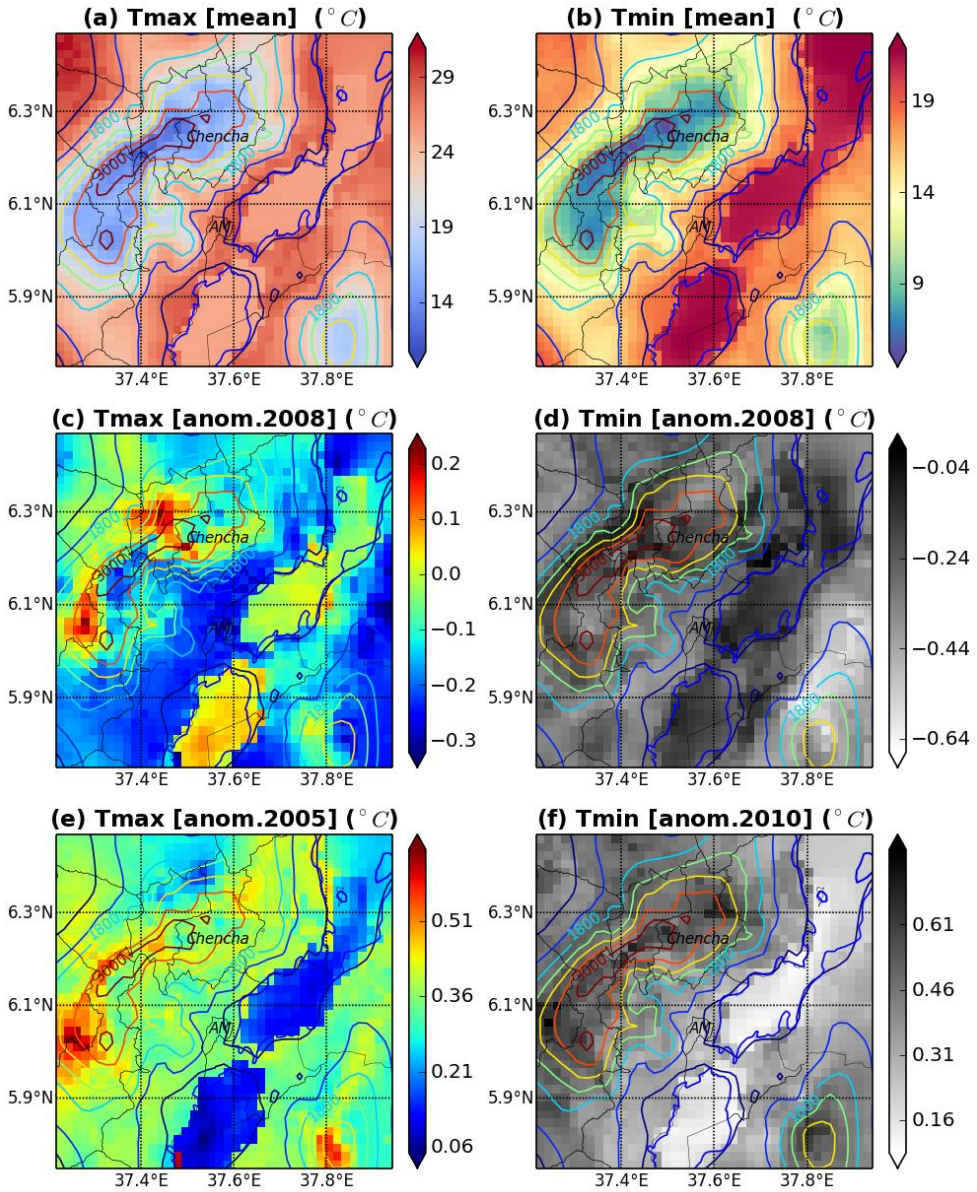
**Figure 2.3 | 10-year** *belg* **season Tmax (left panel) and Tmin (right panel) as simulated by the fine-resolution WRF model during 2001 – 2010. The upper row shows the mean; the middle row shows the coolest; and the lower row shows the warmest in Tmax and Tmin during the 10-year period.**

Figure 2.4 shows the spatial variations of SW↓ (left panel) and precipitation (right panel) for *belg* season during the 10-year. The upper panel show (means of 10-year period), middle panel (the lowest in SW↓ during *belg*-2010 and the driest condition

during *belg*-2008) and bottom panel (the highest in SW↓ during *belg*-2008 and the wettest seasonal weather during *belg*-2010).
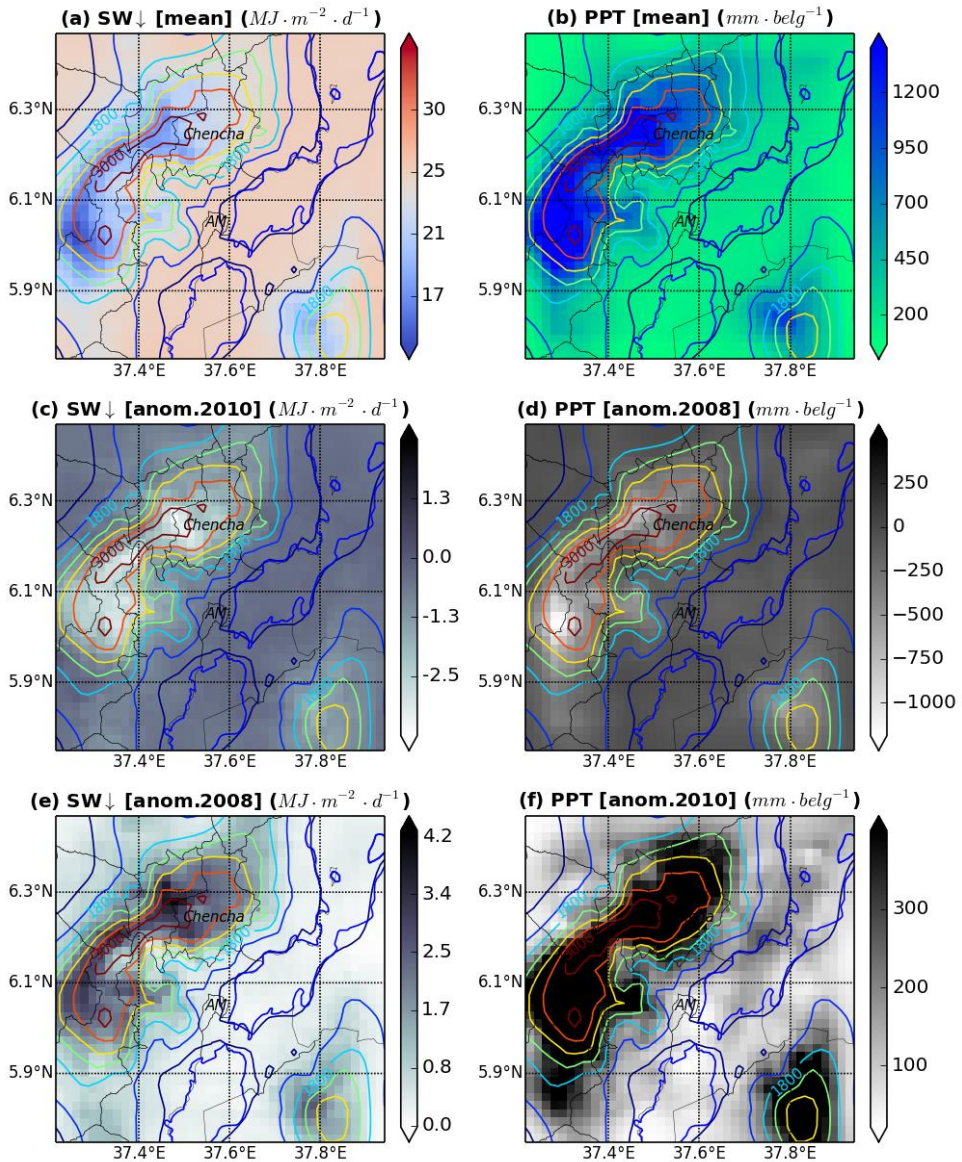


**Figure 2.4 | WRF modelled (2 km × 2 km horizontal resolution) plots of *belg* season SW↓ (MJ·m⁻²·d⁻¹)** (left panel) and precipitation (mm·*belg*⁻¹) (right panel). Plots (a) and (b) show means of SW↓ and means of the total *belg* precipitation during 2001 – 2010. Plots (c) and (d) show anomalies (from the 10-year) for lowest in SW↓ and driest in precipitation during the year 2008. Plots (e) and (f) show anomalies for highest in SW↓ and wettest in precipitation during 2010.

The modelled average SW↓ ranges from 17 MJ·m$^{-2}$·d$^{-1}$ at the summit of Mount Guge to 30 MJ·m$^{-2}$·d$^{-1}$ in the valley around the lakes (Figure 2.4a). During the dry *belg* season (2008), an increase in SW↓ was modelled (up to 3.5 MJ·m$^{-2}$·d$^{-1}$). The highest increase (0.9 MJ·m$^{-2}$·d$^{-1}$ to 3.5 MJ·m$^{-2}$·d$^{-1}$) in the SW↓ was simulated for the mountainous areas compared to other locations in the Gamo Highlands (Figure 2.4e). During *belg*-2010, however, the SW↓ was below (from mean to ~3.5 MJ·m$^{-2}$·d$^{-1}$) the mean. The decrease in SW↓ for the Guge mountain range was significant (2.5 to 3.5 MJ·m$^{-2}$·d$^{-1}$).

Figure 2.4b showed that the average PPT increased from ~200 mm·*belg*$^{-1}$ in the lowland around the lakes to ~1000 mm·*belg*$^{-1}$ at the summit of Mount Guge as calculated from the 10-year period modelled PPT. The GEMS data during *belg*-2017 showed significant PPT spatial variation: 293 mm·*belg*$^{-1}$ in Arba Minch (1200 m a.s.l.), 459 mm·*belg*$^{-1}$ in Tegecha (2143 m a.s.l.) and 540 mm·*belg*$^{-1}$ in Chencha (2738 m a.s.l.). As compared to this data, the WRF modelled PPT was too low for Arba Minch and too high for Chencha.

During *belg*-2008, PPT was significantly decreased from the normal around the lowlands to ~ -750 mm·*belg*$^{-1}$ on the Guge mountain range. During *belg*-2010, nevertheless, PPT was 400 mm·*belg*$^{-1}$ higher than the 10-year period climatology. It is underlined that increased SW↓ during *belg*-2008 was associated with decreased PPT and cooler temperature (Figure 2.3c and d). On the other hand, below normal values for SW↓ during *belg*-2010 were associated with above normal PPT in that year. Here, total cloud amount above the surface played a key role in modulating both the SW↓ and outgoing longwave radiation, in which both determined the atmospheric temperature and PPT regimes of the region. For anomalous *belg* seasons (in years 2008 and 2010), the elevated areas showed increased sensitivity for both SW↓ (enhanced increase/decrease in SW↓ during dry/wet season as compared to other locations in the highlands) and PPT (drier/wetter in dry/wet *belg* seasons).

## 2.4 Spatial variability of crop yield

In Section 2.3, we showed that weather dynamics in the Gamo Highlands was influenced by topography. In this section, we describe how the crop growth and yield respond to interannual seasonal weather variations. Figure 2.5 presents maps relating yield and precipitation in the selected years: (a) climatologically normal *belg* season (2006), (b) the driest *belg* season (2008) and (c) the wettest *belg* season (2010). The modelled attainable yield (t·ha$^{-1}$) was simulated using the GECROS model make use of the WRF model's meteorological output as the crop model's input (see Figure 2.1 and Section 2.2.1). Here, we modelled attainable yield. The attainable yield is a yield limited by water and nutrients (Tadele, 2017), as we applied rainfed agriculture with a recommended fertilizer dose as discussed in Chapter 3.
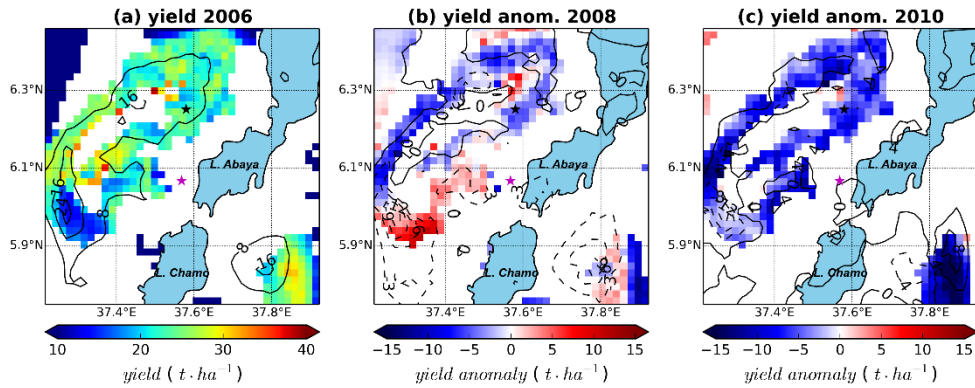
**Figure 2.5 | GECROS modelled attainable fresh tuber yield (t·ha⁻¹) for** *belg*-**2006 season (a). (b) shows** *belg*-**2008 yield anomaly (difference between 2008 and 2006 yields), which was the driest and coolest** *belg* **season of the year 2008. (c) presents** *belg*-**2010 yield anomaly (difference between 2010 and 2006 yields), which was the wettest and warmest day-time of the year 2010. Note that** *belg*-**2006 was climatologically normal (average) in the period 2001 to 2010. The maps show the WRF's fine domain (2 × 2 km² horizontal resolution covering 42 × 42 km² area). The coloured regions indicate the locations in which the LGS was between 70 and 195 days. The contour lines in (a) show the 2006 PPT (mm·d⁻¹) during the growing season. The contour lines show PPT anomaly (mm·d⁻¹) of 2008 (b) and the 2010 (c) growing season from the** *belg*-**2006. The contour lines in (a) increase from 4 to 24 (in the center). In (b) and (c), the solid and dashed contours lines indicate positive and negative anomalies, respectively. The black and pink star symbols show the locations of Chencha and Arba Minch, respectively. Lake Abaya and Chamo are also indicated.**

The simulated attainable yield ranged from 10 to 35 t·ha⁻¹ as elevation increased to the ones of yield Zone II as presented in Section 2.2.2c (Figure 2.5a). Modelled crop yield near the lakes (in valley) was too low (< 12 t·ha⁻¹) with too low length of the growing season (LGS < 70 days). This is due to the warm ($T_{max}$ > 22 °C and $T_{min}$ > 15 °C), dry (PPT < 4 mm·d⁻¹), with high SW↓ (> 25 MJ·m⁻²·d⁻¹) weather conditions in the lowlands (see Figure 2.3 and Figure 2.4). These weather conditions are not optimal to grow potato (see Chapter 5) (FAO, 2008b; Haverkort and Verhagen, 2008). As explained in Chapter 3, the meteorological conditions are unfavourable for potato growth since crop matures unrealistically too early with a leaf area index less than 1.0 m⁻²·m⁻². In turn, as it is mapped in Figure 2.5, near the top of the mountains, the growing season lasts longer than 195 days. In this region, the weather is much cooler ($T_{max}$ < 15 °C and $T_{min}$ < 7 °C), wetter (PPT > 15 mm·d⁻¹) and the incoming shortwave radiation is lower (SW↓ < 15 MJ·m⁻²·d⁻¹). In the region, meteorological conditions are favourable for potato. However, the calculated LGS was too high (LGS > 150 days) hence unrealistic as explained in FAO (2008b). Growing seasons this long can induce yield losses due to increased risks for pests and crop diseases (Hijmans, 2003). In this thesis, we considered the acceptable range in LGS to be between 70 and 195 days. Below and above these values, the conditions are not suitable for potato growth. The areas where the conditions are not met, are shown as a white mask in Figure 2.5a (FAO, 2008b). Relatively high yields (20 t·ha⁻¹ to 35 t·ha⁻¹) were obtained in regions

where the mean precipitation is from 6 mm·d$^{-1}$ to 12 mm·d$^{-1}$. When mean PPT was greater than 16 mm·d$^{-1}$, yield became lower (10 t·ha$^{-1}$ to 15 t·ha$^{-1}$) as mapped in the southwest area (Figure 2.5a). Increased PPT increased loss of nutrients to deep soil layers due to nutrient leaching (see Figure 3.8) (Yin and van Laar, 2005). This results in decreased yield.

In Figure 2.5b, corresponding to the driest *belg* season, the patches with 6 to 12 mm·d$^{-1}$ less PPT (during *belg*-2008) showed ~10 t.ha$^{-1}$ more yield as compared to the *belg*-2006. The northwest facing slopes around 37.3°E and 6.2°N showed a lesser yield nearly 2.5 to 10 t·ha$^{-1}$ than *belg*-2006. However, but as shown in the figure, the PPT is nearly comparable with the normal *belg* season. Thus, the yield decline in those spots can be related to an increase in the SW↓ (from 1.5 to 3.5 MJ·m$^{-2}$·d$^{-1}$) and increase in T$_{max}$ (up to 0.2 °C). This has been discussed in the model sensitivity experiments in Chapter 3 (Figure 3.3 and Table 3.3). The experiments explained that yield declined by 36% for SW↓ and 24% for T$_{max}$ increases as compared to the control run for the climatologically normal *belg* season during 2006. For the wettest *belg*-2010 (Figure 2.5c) a decreased yield was modelled (nearly up to 10 t·ha$^{-1}$ less as compared to *belg*-2006). In most locations, the PPT during the growing season exceeded that of *belg*-2006 up to 8 mm·d$^{-1}$. Still, there were a few locations (southwest corner) with lower PPT as compared to other regions. Besides, the increased PPT, *belg*-2010 was also the warmest of the entire 10-year period (up to ~0.6 °C for T$_{min}$). The warmer weather declined crop yield. With increased PPT, yield declined as the crop lost soil nutrients because of the increased leaching to the deep soil layer (see Figure 3.8) (Yin and van Laar, 2005).

Figure 2.5 showed that the simulated yields for the anomalous *belg* seasons of the years 2008 and 2010 were predominantly lower than those of the normal *belg* season during 2006. The decrease in yield in those years ranged from 5 to 10 t·ha$^{-1}$. This finding is remarkable because the weather anomalies during the two crop-growing years were in opposite directions. That is, drier and cooler in 2008 vs wetter and warmer in 2010 as compared to the average seasonal climate. Apparently, *belg*-2006 was climatologically normal and the simulated crop yield was optimal. This implies any weather anomaly results in a lower yield. The model experiments suggest that with the ongoing global climate change, potato crop productivity may decline in the Gamo Highlands. In agreement with our findings, Hijmans (2003) projected a decrease in global potato yield with a warming future climate as discussed below.

## 2.5 Potato crop yield – future prospects

Figure 2.6 shows the sensitivity of crop yield (black lines) and LGS (blue lines), simulated by the GECROS model. Figure 2.6a presents variation in atmospheric CO$_2$ concentrations [CO$_2$] as a function of yield. This model experiment can be considered as an indicator of how the future crop productivity can be influenced because of

mainly the increase of this greenhouse gas (Cramer *et al.*, 2001). The model experiment design follows the IPCC climate projection assumption (*e.g.* in Representative Concentration Pathways - RCP6 future scenario, [$CO_2$] is projected to increase up to ~700 ppm at the end of the century (Meinshausen *et al.*, 2011)). Figure 2.6b shows potato planting dates influence on modelled yield. This model experiment can be taken as crop management option (*e.g.* a strategy for climate change adaptation mechanism in the changing climate) as explained in Figure 2.1 (Haverkort and Verhagen, 2008).
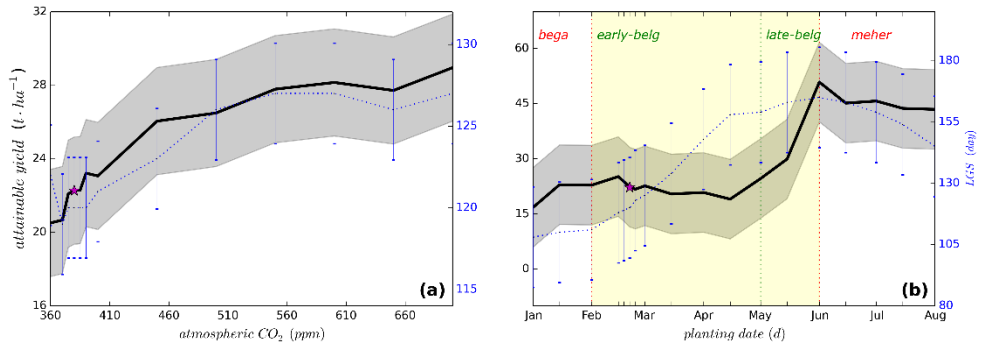


**Figure 2.6 | GECROS model sensitivity analysis for attainable potato fresh tuber yield (t·ha⁻¹) (left-axis – solid-line) and LGS (d) (right-axis – dotted line). Variations in the $CO_2$ concentration (ppm) (a) and planting dates (day) for Chencha station during the *belg*-2006 (climatologically average *belg*) season (b). The shaded/line error bars show the standard deviations of yield/LGS. The asterisks denote yield for the control run. The vertical dotted lines and the yellow highlighted region separate the seasons three seasons (*bega*, *belg* and *meher*). The *belg* season is further classified into early-*belg* and late-*belg*. Note that the scales between panels on the left and those on the right are different.**

Figure 2.6a describes that yield significantly increased from 20 t·ha⁻¹ to 28 t·ha⁻¹ (~40% increase) as the [$CO_2$] increased from 360 ppm to 700 ppm (~95% increase). It is also noted that increased [$CO_2$] slightly increased the LGS (up to 8 days). Haverkort and Struik (2015) discussed that potato yield increases by 36% when [$CO_2$] increases from 280 ppm to 550 ppm. Van de Geijn and Dijkstra (1995) explained that crops exposed to an elevated [$CO_2$] generally respond with positive but variable increases in yield. Nevertheless, the rate of increase in yield was small after 700 ppm, probably due to limiting factors such as soil nutrient and moisture as discussed in Haverkort and Struik (2015) and Oren *et al.* (2001). Hijmans (2003) predicted temperature increase (weighted for potato-weighted-area only) from 1.0 °C to 1.4 °C for the period between 2040 to 2069. With this warming, potato yield is projected to decline by 18% to 32% (with no climate change adaptation option) and 9% to 18% (with climate change adaptation activities). The major potato crop disease known as late blight, caused by *Phytophthora infestans*, is expected to increase due to increased warming caused by global warming (Luck *et al.*, 2011).

Figure 2.6b quantified the effect of variations in planting dates from the late *bega* and early *meher*. For the figure, detailed crop and weather variables variations during the growing season are tabulated as presented in Table 2.3 below.

**Table 2.3 | Further explanation of the modelled attainable yield plotted in Figure 2.6b. Additional model outputs (weather and crop growth variables) are considered for the explanation. Average crop yield, yield increase and weather during the part of the growing season are shown in the table. The statistical analysis is related to the planting date experiment. The experiment covered from *bega*, *belg* (early-*belg* and late-*belg*) and *meher* seasons.**

| Crop/weather variables | Unit | Average/change in the average crop/weather variable | | | |
|---|---|---|---|---|---|
| | | *bega* | *early-belg* | *late-belg* | *meher* |
| Average yield | t·ha$^{-1}$ | 20 | 22 | 35 | 44 |
| Increase in average yield | t·ha$^{-1}$ | 6 | 0 | 11 | -2 |
| LGS | d | 109 | 128 | 162 | 155 |
| $T_{max}$ | °C | 17.1 | 16.5 | 15.3 | 15.6 |
| $T_{min}$ | °C | 8.9 | 9.1 | 8.5 | 8.5 |
| SW↓ | MJ·m$^{-2}$·d$^{-1}$ | 22.5 | 18.6 | 16.4 | 18.2 |
| PPT | mm·d$^{-1}$ | 7.0 | 9.8 | 7.2 | 7.1 |

Table 2.3 shows that the simulated attainable crop yield was increased from 20 t·ha$^{-1}$ during *bega* to 44 t·ha$^{-1}$ during *meher* season (see also Figure 2.6b). A significant increase (11 t·ha$^{-1}$) in yield was simulated during late-*belg*. The changes in yield are related to two factors: (1) crop variable – LGS and (2) weather variables – temperature, SW↓ and PPT. The LGS influence yield positively, *i.e.* the longer the growing season (*e.g.* LGS was 109 d and 155 d during *bega* and *meher* seasons, respectively), the more the crop invests in the tuber. This will be also discussed in Chapter 3. Model sensitivity experiment conducted with variation in PPT did not show change in the LGS (see Chapter 3, Figure 3.3b). Therefore, the change in the LGS is governed by meteorology: $T_{max}$, $T_{min}$ and SW↓. For instance, during *bega*, the average yield was the lowest (20 t·ha$^{-1}$). This was related to weather conditions with the highest temperature ($\Delta T_{max}$ > 1.5 °C, relative to other seasons) and the highest incoming shortwave radiation (SW↓ > 4.5 MJ·m$^{-2}$·d$^{-1}$ on average as compared to the other seasons). In contrast, yield was the highest during late-*belg* and *meher*. The causes are PPT was minimal (~7 mm·d$^{-1}$), low SW↓ and cooler weather (Table 2.3). As a result, the LGS was larger than 155 d. Haverkort and Struik (2015) also discussed that longer growing seasons increase potato yield. Our result is consistent with Hirpa *et al.* (2010) findings which showed the potential yield for *meher* was higher than for the *belg* farming in Ethiopia. However, field experience and literature indicate that there is more crop disease pressure during *meher* than *belg* cropping (Hirpa *et al.*, 2010). This crop disease outbreak might be related to the favourable weather conditions (cooler and cloudy weather) during *kirmet* season (Pérombelon, 2002). Note that diseases are not accounted for in the current GECROS model.

Haverkort and Verhagen (2008) discussed that with increasing global temperature and atmospheric [$CO_2$], in the temperate climate, for example, potato yield may be increased due to increased LGS and [$CO_2$] – provided that irrigable water is available as the current amount. Mountains will become warmer than the present (Elsen and Tingley, 2015), in which shifts in potato growing zone can be expected. The yield zone I (which is not suitable for potato agronomy) will expand into yield zone II (the major potato yield zone). Moreover, yield zone II may shift to upslope into yield zone III. Besides, yield zone III is steeper and less suitable for agriculture. Climate change negatively affects potato yield at least in two aspects: (1) increased warming results in decreased yield (Figure 3.3c and d), (2) decrease in acreage. Therefore, climate change can have negative impact on potato agronomy in the Gamo Highlands. The IPCC climate projection to the East African region showed up to 10% to 18% increases for the March to May precipitation (Rowell *et al.*, 2015; Stocker *et al.*, 2013). Such an increase in PPT decreases potato yield in the Gamo Highlands (Figure 3.3b). On the other hand, observed data since 1980 showed a declining trend (up to 20%) for PPT for the region. This implies that data showed no agreement between modelled and observed PPT.

Figure 2.6a showed a simple model experiment that increasing atmospheric [$CO_2$] increased crop yield. With the increases in $CO_2$ emissions in the changing climate, this can improve the future food security. In line with our findings, both model experiments and field experiments (*e.g.* Free-air concentration enrichment – FACE) showed increases in [$CO_2$] increase crop yield (Bazzaz, 1990; Long *et al.*, 2006). However, increases in the atmospheric temperature and reduced soil moisture due to climate change will have negative impact on crop yield (Lobell and Field, 2007; Long *et al.*, 2006). With increased $CO_2$ concentration, the plant needs more resources (*e.g.* nutrient and water) to compensate the increased photosynthesis (Bazzaz, 1990). Crop management options such as shifting planting dates and scheduling available water (see Chapter 4) can be considered as climate change adaptation options to improve food security in Ethiopia (Hijmans, 2003). The model experiments conducted in Figure 2.6 and Figure 3.3 are based on varying an atmospheric variable (*e.g.* $T_{max}$, SW↓ and PPT) without coupling the meteorological variables to the crop dynamics. However, future climate projections using the EC-Earth model (Hazeleger *et al.*, (2010; 2012)), for example, can give more robust quantification of the future crop yield in the changing climate in regions characterised by complex topography. A similar research strategy as we followed in Chapter 3 can be applied using the EC-Earth climate model.

# The combined effect of elevation and meteorology on potato crop dynamics: A 10-year study in the Gamo Highlands, Ethiopia

*Potato (Solanum tuberosum L.) is an important crop in the Gamo Highlands in Ethiopia. The region is characterised by a complex topography with large inter-annual weather variations, where potatoes grow in a range of altitudes between 1600 and 3200 m above sea level (a.s.l.). Traditional large-scale crop modelling studies only crudely represent the effect of complex topography, misrepresenting spatial variability in meteorology and potato growth in the region. Here, we investigate how weather influenced by topography affects crop growth. We used the Weather Research and Forecasting (WRF) model to simulate weather in relation to topography in coarse (54 × 54 km²) and fine (2 × 2 km²) resolution domains. The first has a resolution similar to those used by large-scale crop modelling studies that only crudely resolve the horizontal and vertical spatial effects of topography. The second realistically represents the most important topographical variations. The weather variables modelled in both the coarse and fine resolution domains are given as input to the GECROS model (Genotype-by-Environment interaction on CROp growth Simulator) to simulate the potato growth. We modelled potato growth from 2001 to 2010 and studied its inter-annual variability. This enabled us to determine for the first time in Ethiopia how variations in weather are linked to crop dynamics as a function of elevation at a fine resolution. We found that due to its finer representation of topography, weather and crop growth spatio-temporal variations were better represented in the fine than in the coarse resolution domain. The magnitude of crop growth variables such as Leaf Area Index (LAI) and Length of the Growing Season (LGS) obtained with weather from the coarse resolution domain were unrealistically low, hence unacceptable. Nevertheless, the resulting potato yields in the coarse resolution domain were comparable with the yields from the fine resolution domain. We explain this paradoxical finding in terms of a compensating effect, as the opposite effects of temperature and precipitation on yield compensated for each other along the major potato growing transect in the Gamo Highlands. These offsetting effects were also dependent on the correct estimations of the LGS, LAI. We conclude that a well-resolved representation of complex topography is crucial to realistically model meteorology and crop physiology in tropical mountainous areas.*

## 3.1 Introduction

Potato is one of the most rapidly expanding crops in Eastern Africa (Haverkort and Struik, 2015) and is a strategic crop for improving food security in Ethiopia (Abebe *et al.*, 2013; FAO, 2008b; Hirpa *et al.*, 2012). Ethiopia has the greatest potential for potato production in Africa (FAO, 2008b). In Ethiopia, potato is grown during the *belg** (February – May) and *kirmet* (June – September) seasons, as well as off-season under irrigation. The *belg* crop is the most important one (from the total area cropped with potato, 77% is during the *belg* season) (Tufa, 2013), but the potato yield is significantly dependent on annual weather variations and local weather and soil conditions. Although meteorological conditions are also favourable for potato production during the *kirmet* (*meher* harvest) season, diseases - mainly late blight - are more prevalent than during the *belg* season (Haverkort *et al.*, 2012; Tufa, 2013).

Ethiopia has a complex topography. In southwest Ethiopia, the Gamo Highlands rise up from the lowlands at the bottom of the Great Rift Valley at 1100 m a.s.l. around Lake Chamo to above 3500 m a.s.l. at the summit of Mount Guge, a distance of less than 50 km. Potato is cultivated there between 1500 and 3200 m a.s.l., where the climate is mild and not too wet. As a result of the complex terrain, large contrasts in weather and climate can be observed (Jury, 2014b). These generate variations in potato growth from the relatively unsuitable lowlands to the highly productive highlands, due to different combinations of adiabatic cooling, orographic lifting and mountain/valley wind conditions. Because crop dynamics and ultimately yield are highly influenced by weather and climate (Samberg *et al.*, 2010), we hypothesise that the modelling of potato crop dynamics is very sensitive to crucial meteorological crop drivers such as short-wave radiation (SW↓), precipitation and temperature and their variations along steep elevation gradients.

Current operational crop models such as the EU MARS (Monitoring Agriculture with Remote Sensing) system are driven by coarse resolution data from global weather models and/or interpolated station data (*e.g.* 0.5° × 0.5°) (Boogaard *et al.*, 2002; De Wit *et al.*, 2010; Hijmans, 2003). In such models, for example, the Gamo Highlands are represented by a smoothed topography, which suggests drier and warmer weather characterised by less variability than in models with fine resolution domains (Section 3.3.1). However, recent studies have shown that numerical weather models require sufficiently high resolution to resolve atmospheric phenomena such as spatial variability in temperature and precipitation driven by complex topography (Hunink *et al.*, 2014; Yarleque *et al.*, 2016; Zhao *et al.*, 2015). Our study furthers these recent efforts, as we investigate the impact of weather model resolution on crop dynamics too in a region characterised by complex orography. While

---

* *See seasonal classification in Ethiopia in Table S1 (follow https://doi.org/10.1016/j.agrformet.2018.07.009)*

we focus on the Gamo Highlands, our objectives and methods are applicable to other mountainous areas in tropical regions.

This study models the impact of key meteorological crop growth drivers on potato growth at high resolution over the Gamo Highlands. To this end, we combine meteorological and crop dynamics models, which exist in a one-way coupled causal relationship. First, we use the Weather Research and Forecasting (WRF) model (Skamarock *et al.*, 2005) to simulate weather during a 10-year period in different resolution domains: a coarse one (54 km × 54 km) covering the Greater Horn of Africa including part of the western Indian Ocean (2808 km × 2808 km) and a fine one (2 km × 2 km), covering the Gamo Highlands, an area of 84 km × 84 km (Figure 3.2). Second, we systematically analyse the impact of these meteorological inputs on the crop dynamics simulated by the Genotype-by-Environment interaction on CROp growth Simulator (or GECROS model, (Yin and van Laar, 2005), hereafter YL05). Using this method, we attempt to answer the following questions:

1) *How do weather and climate vary as a function of local topography and how does it affect potato crop growth variables and yield?*

2) *Does elevation enhance or lower the magnitude of key crop variables such as the length of the growing season (LGS), carbon allocation to different parts of the plant, leaf area index and yield and their interactions?*

Our strategy is first to analyse the inter-annual SW↓, precipitation and temperature patterns during 2001 – 2010. We identify climatologically normal, dry and wet *belg* seasons using anomaly calculations and the Standardised Precipitation Index (SPI) (Raja *et al.*, 2014). This enables us to analyse the sensitivity of key crop metrics (LGS, LAI, the carbon stored in the various crop organs and the crop yield) to weather variations, soil characteristics and crop management options. Finally, we evaluate the performance of our weather model with currently available meteorological observations at low-elevation and high-elevation stations and compare our results with the available literature for the crop model (IPC, 2009; Mazengia *et al.*, 2015; Tufa, 2013). To the best of our knowledge, this is the first study of the influence of weather on a crop in a tropical highland region with such a long integration time and fine spatial resolution.

## 3.2 Methods

### 3.2.1 Weather model

The numerical atmospheric model experiment employed the WRF model, version 3.4.1 (Skamarock *et al.*, 2005). The model is configured in domains with different horizontal grid resolutions: one coarse resolution domain and three consecutively nested domains with increasingly finer resolutions. In this study, we only use the

outer domain with the coarse resolution and the inner domain with the finer resolution. A summary of the numerical settings and physical parameterisation schemes applied is provided in Table S2[†]. The model initialization was as follows: independent 48-hour (data recorded every hour) WRF runs were performed for the period 2001 - 2010. The model's initial and lateral boundary conditions were prescribed from the ECMWF ERA-interim reanalysis data (Dee *et al.*, 2011). The first 24 hours were discarded as a model spin-up for the physical processes that were parameterised. The meteorological output for the second day (interval 24-48 hours) was considered for that day. This modelling strategy was suggested by Jiménez *et al.*, (2010; 2011b) as a way to obtain an appropriate balance between an accurate representation of the complex orography and land-use characteristics (local/regional conditions) without departing from the synoptic dynamical features (Jiménez *et al.*, 2016). By combining high resolution (2 km × 2 km) with long model runs (10-year), we attempt to represent the spatial variability and obtain robust statistics.

### 3.2.2   The crop model

The GECROS crop systems dynamic model requires six weather variables, namely incoming shortwave radiation (SW↓), precipitation, maximum temperature ($T_{max}$), minimum temperature ($T_{min}$), vapour pressure deficit (VPD) and wind speed, all on a daily basis. The model runs with a time step of one day with a diurnal variation estimates in the environmental inputs (YL05). These variables are indicated in Table S3[†] and are calculated by the WRF model. The GECROS model was designed to study the responses of biomass and dry matter production in arable crops to both environmental and genotypic characteristics (Khan, 2012; Yin and van Laar, 2005). The model has been tested and widely used to simulate crop growth (Combe *et al.*, 2015; Gu *et al.*, 2014; Yin and Struik, 2010) and potato in particular (Khan *et al.*, 2014). Since the representation of evaporation is crucial here, we follow the improvements suggested by Combe *et al.* (2015) to obtain more reliable surface energy budget estimates. Parameter/variable values considered from the literature other than those mentioned in YL05 (Table S3[†]). Detailed GECROS model settings for the control run are presented in Table S4 to Table S13[†], where the control run represents the GECROS model run with the best available model setting.

### 3.2.3   Weather observations

Since 1974, weather conditions have been recorded in Arba Minch in the lowlands (1200 m a.s.l.) (Ayana, 2011). The Arba Minch weather station was re-located and re-established in 1987 by the Ethiopian National Meteorological Agency (NMA). It is a WMO 1st class synoptic weather station located at 6.05° N and 37.55° E.

---

Weather variables such as temperatures, relative humidity, precipitation, winds, hours of sunshine, atmospheric pressure, clouds, visibility, evapotranspiration, etc. are recorded/observed on a three-hourly/daily basis (during daytime hours) manually (NMA, 2018).

We also used weather observations collected in Chencha, in the Gamo Highlands (2632 m a.s.l.). This station is a WMO 4th class station category, from which we used the precipitation data only (NMA, 2018). We collected additional data from our recently (2013) established automatic weather station in Chencha. A more detailed description of the observation data used in this article is provided in Table S12[†].

### 3.2.4  Soil data

The GECROS crop model is coupled with a process based soil model (YL05). In agreement with the high topographic resolution prescribed to obtain reliable spatiotemporal meteorological variables, we used high-resolution soil information. Soil parameters such percentage of clay in the soil, soil water content at maximum holding capacity, soil water content at field capacity, minimum soil water content and total organic carbon in the soil (TOC) are required as model input. These parameters were calculated from the International Soil Reference and Information Centre (ISRIC), world soil information, Africa Soil Information Service (AfSIS) project database (Leenaars *et al.*, 2014). 1 km × 1 km resolution data in the top 60 cm were aggregated and interpolated to fit the fine resolution domain.

### 3.2.5  Validation of the meteorological model

WRF meteorological results were validated against observations collected at the two stations described in Section 3.2.3. Our validation of weather will focus on the variables SW↓, precipitation, $T_{max}$ and $T_{min}$. We selected these weather variables because they are the key atmospheric variables that have the strongest influence on crop growth. The SW↓ affects the light-use efficiency of crops. Precipitation is highly correlated with SW↓ by clouds. The amount, frequency and location of precipitation are key factors; since crop stress and yield depend on soil moisture. Temperature strongly influences physiological and biophysical characteristics such as net photosynthesis, canopy development, dry matter accumulation and partitioning and absolute tuber growth rate of potatoes (Ewing, 1981; Hammes and De Jager, 1990; Khan, 2012; Van Dam *et al.*, 1996).

Since our aim was to determine how domain resolution affects the representation of elevation and the resulting weather simulations, we compare the observed weather variables with the modelled weather variables from both the coarse and fine resolution domains. We compare the 10-year mean modelled weather variables of the 840 grid cells in the fine resolution domain together with the four overlapping grid cells in the coarse resolution domain. We also show the elevational gradients of

SW↓, precipitation, $T_{max}$ and $T_{min}$. Finally, we express the performance of the WRF model using statistical metrics such as the Root-Mean-Square Error (RMSE), the Mean Bias Error (MBE) and the coefficient of determination ($r^2$) (Willmott, 1982).

### 3.2.6 Strategy for the crop model sensitivity study

To compensate for the lack of potato yield data during the 10-years period, we investigated how simulated crop growth in GECROS model responds to weather (SW↓, $T_{max}$, $T_{min}$, VPD, precipitation and [$CO_2$]), edaphic variables (soil type, soil moisture content and TOC), crop parameters and crop management options.

The model sensitivity experimental strategy was as follows. We varied the meteorological and other variables over a range representing the uncertainties of the weather model inspired by the model uncertainties discussed in the previous section. The selected range covers the change in meteorological variables under future climate scenarios and is aimed at understanding how the crop dynamics processes respond to the change in climate. The IPCC climate projections for eastern Africa show increased precipitation (up to ~ 18%) in the warming climate (Stocker *et al.*, 2013; Van Oldenborgh *et al.*, 2013). Our edaphic model sensitivity experiments are indicative of how the attainable crop yield, LGS and LAI respond to variations in soil fertility, soil type and moisture content. Attainable yield is defined here are 80% of the potential yield, which in turn is defined as '*the theoretical yield that can be calculated or modelled for a certain cultivar grown in a certain environment without any limiting or reducing factor being present*' (Haverkort and Struik, 2015). Similarly, the crop parameter model experiments tell us how the crop yield variables differ with potato variety.

We based the sensitivity experiment on the weather during the 2006 *belg* season, which is representative of a climatologically normal year and the Chencha location, in the potato-growing zone. The SW↓ was varied within the range of 19.5 ± 4.2 MJ·m$^{-2}$·d$^{-1}$, with a ± 1% simulation resolution interval from the mean. We varied the temperature around the average of 17 °C within a range of 15 °C to 19 °C, with 0.5 °C model run range, as suggested in Van Oldenborgh *et al.* (2013). This analysis was conducted with the assumption that the relative humidity remains constant (Stocker *et al.*, 2013), as the absolute humidity rises with rising temperature (Rieck *et al.*, 2012). We varied precipitation in the range of 10.6 ± 2.2 mm·d$^{-1}$ with ± 5% model run resolution. We took a similar approach for the other atmospheric variables. For the soil, crop variables/parameters and crop management options, we employed a realistic range around the selected inputs. For each value in the ranges thus created, the GECROS model was run separately in order to study the sensitivity of crop growth to the individual input variable.

**3**

## 3.3  Model evaluation and parameter sensitivity analysis

This section presents the results of the weather model evaluation as described in Section 3.2.5 and the crop model sensitivity analysis as described in Section 3.2.6.

### 3.3.1   Weather model evaluation

Figure 3.1 shows the results of the weather model validation. The SW↓ decreased with elevation that was related to an increase in cloudiness at higher altitudes. At the same elevation, SW↓ displayed different patterns in the coarse and fine resolution domains: for the coarse resolution domain, it was underestimated and for the fine resolution domain, it was overestimated. The order of magnitude of these deviations with respect to the observations was similar: ~ 60 W·m$^{-2}$ less in the coarse resolution domain and 50 W·m$^{-2}$ more in the fine resolution domain at the lowland station. At the highland station, the bias became slightly less, but it was still significant. We attribute these differences to the representation of convection in WRF in the coarse and fine resolution domains. Note that for the coarse resolution domain, convection was approximated or parameterised whereas at the domain with finer resolution it was explicitly calculated (Table S2[†]). It is important to stress that the different results due to the differences in the calculations of convection affect not only the SW↓ but also the precipitation, $T_{max}$ and $T_{min}$ results. These findings emphasise the critical role played by clouds and aerosols in the calculation of the SW↓, a key variable in the crop dynamics model.
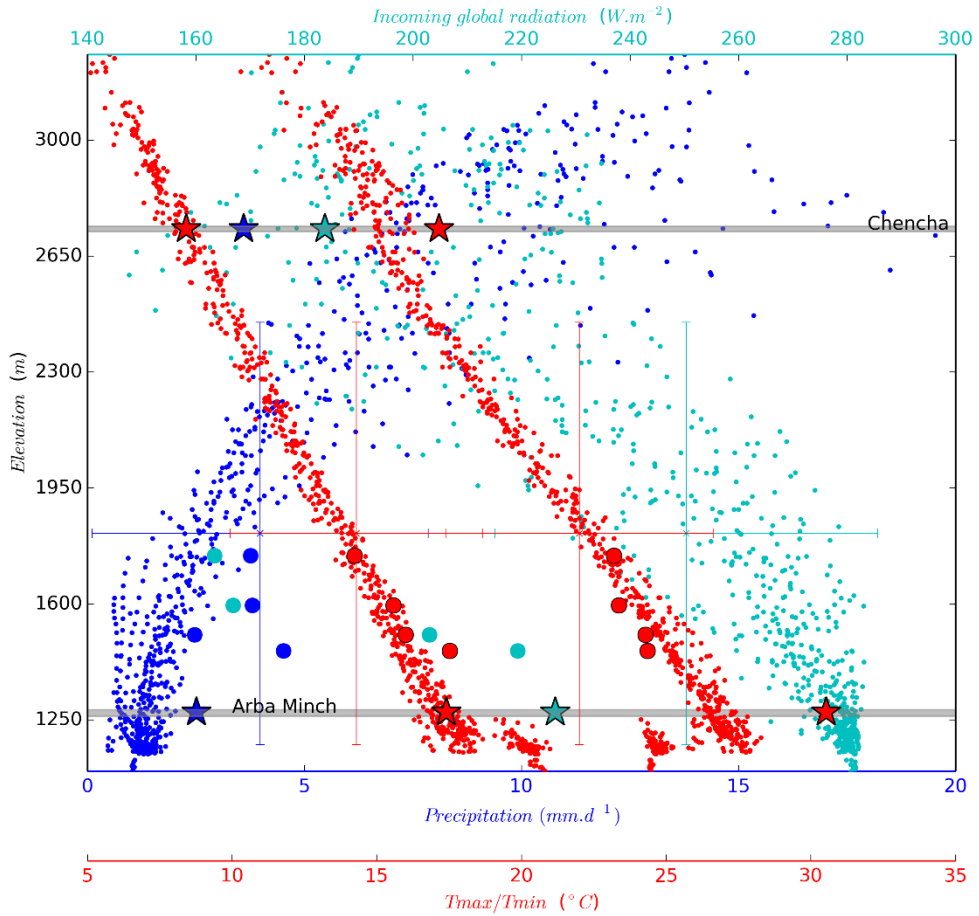
**Figure 3.1 | The relationships between incoming global radiation (W·m⁻²) (cyan dots), precipitation (mm·d⁻¹) (blue dots) and Tₘₐₓ and Tₘᵢₙ (°C) (red dots) and with elevation (m). The small dots represent 840 individual grid cells in the fine resolution domain. The filled circles represent the four individual grid cells in the coarse resolution domain that overlap with the fine resolution domain. The WRF analysis covers the averages of the daily means during 10-years. The observational data covers climatological period. The stars designate observed climatology for Arba Minch and Chencha (corrected for elevation of the stations). The error bars indicate variability in the fine resolution domain. The crosshairs show the mean values of the given weather variables/elevation.**

Precipitation increased exponentially with altitude (Figure 3.1). There was a satisfactory agreement with the modelled precipitation in the coarse resolution domain at both lowland (almost no bias) and highland (bias ~+1.0 mm·d⁻¹) locations. However, we found both a dry (~1.5 mm·d⁻¹) and a large wet (~3.5 mm·d⁻¹) bias in both Arba Minch and Chencha in the fine resolution domain. This large rainfall bias occurred in spite of a better description of the elevation and presumably better model physics in the finer resolution domain. The reason for this large bias is uncertain and our evaluation will need to be continued in the near future, particularly by using

better measurements of rainfall make use of a dense network of stations across elevation gradients (Section 3.5).

We found that $T_{max}$ and $T_{min}$ declined linearly with elevation (Figure 3.1). At Arba Minch $T_{max}$ was negatively biased by ~ -7 and -3 °C in the coarse and fine resolution domains, respectively. At Chencha $T_{max}$ was positively biased in the coarse resolution domain and negatively biased in the fine resolutions (by ~ +8 °C and ~ -1 °C respectively). $T_{min}$ was well represented at Arba Minch in both resolution domains. It was in good agreement in the fine resolution domain and largely positively biased (~ +7 °C) in the coarse resolution domain at Chencha. We conducted a statistical analysis to test the performance of the weather model at both locations.

Table 3.1 shows how the WRF model performed compared to the observed weather for Arba Minch and Chencha using daily averages. We validated the WRF model at the grid points at which the Arba Minch and Chencha stations are located. Our approach was to use the data with a daily temporal scale since here we were interested in studying the impact of fine spatiotemporal scales on meteorology and crop dynamics during the 10-year period. For Chencha, only precipitation observations were available for between 2001 and 2010. The model elevation of the Arba Minch and Chencha sites were modelled to be 62 and 100 m respectively above their actual elevation in the fine resolution domain. In the coarse resolution domain, Arba Minch and Chencha were modelled at 360 and 1050 m respectively above and below their actual elevations. We corrected the modelled temperature for elevation bias using the international standard atmosphere (-0.65 °C/100 m) (Kunz *et al.*, 2007).

**Table 3.1 | Statistical WRF model validation using daily weather station observations for Arba Minch and Chencha for the coarse and fine resolution domains. The analysis was carried out on daily data.**

| Station | Weather variable | Obs. mean | WRF mean | | MBE | | RMSE | | $r^2$ | |
|---|---|---|---|---|---|---|---|---|---|---|
| | | | coarse | fine | coarse | fine | coarse | fine | coarse | fine |
| Arba Minch | $T_{max}$ (°C) | 30.5 | 17.8 | 27.3 | -12.7 | -3.2 | 12.9 | 3.9 | 0.26 | 0.26 |
| | $T_{min}$ (°C) | 17.4 | 9.5 | 17.9 | -7.7 | 0.5 | 8.0 | 1.9 | 0.12 | 0.19 |
| | PPT (mm·d⁻¹) | 2.5 | 2.5 | 1.2 | -0.1 | -1.3 | 7.2 | 7.7 | 0.05 | 0.01 |
| Chencha | $T_{max}$ (°C) | | 17.9 | 16.8 | | | | | | |
| | $T_{min}$ (°C) | | 11.0 | 9.1 | | | | | | |
| | PPT (mm·d⁻¹) | 3.5 | 4.5 | 7.2 | 1.0 | 3.7 | 8.8 | 13.0 | 0.05 | 0.05 |

The first finding was that there was no general improvement in the domain with finer elevation and resolution for the variables under study. Our results showed that the model was negatively biased in terms of $T_{max}$ (12.7 and 3.2 °C) for both coarse and fine resolution domains. Possible explanations for the underestimates are: (i) the initial and boundary conditions provided by the ECMWF ERA-interim reanalysis data may give a cold temperature bias for the tropical and mountainous region (Jury, 2014a) and (ii) WRF has a cold temperature bias (Steeneveld *et al.*, 2008). Similarly, $T_{min}$ was underestimated (7.7 °C) in the coarse resolution domain, despite the fact that $T_{min}$ was well represented in the fine resolution domain with values for MBE and RMSE of 0.5 and 1.9 °C, respectively. Comparing the two model resolutions, the fine resolution domain was closer to the measurements. This was primarily attributable to the direct relationship between temperature and elevation and a better representation of topography in the fine compared to the coarse resolution domain (Section 3.4.1).

Precipitation was underestimated in the lowlands (*i.e.* in Arba Minch) by 0.1 and 1.3 mm·d$^{-1}$ in the coarse and fine resolution domains, respectively. However, in the highlands (*i.e.* in Chencha), our comparison deteriorated, with a tendency towards more rain in the model (+1.0 and +3.7 mm·d$^{-1}$ for the fine and coarse resolution domains, respectively) compared to the observations. We hypothesise that the better representation of topography in the fine resolution domain could trigger more convection than in the coarse resolution domain. There may also be uncertainty in the precipitation measurements because the rain gauges are manually operated and the treatment of the missing data by the National Meteorological Agency – Ethiopia (NMA) could also lead to bias.

A number of authors have shown that the precipitation modelled using the ECMWF ERA-interim reanalysis data has a large wet bias over the Ethiopian Highlands and dry bias over the lowlands (Diro *et al.*, 2011b; Dutra *et al.*, 2013; Jury, 2014a; Tsidu, 2012), which agrees with our finding. For example, Diro *et al.* (2011b) has indicated that the ECMWF ERA-interim (1989 – 2001) reanalysis data underestimated the south and south-eastern lowland regions precipitation by nearly 30 mm·month$^{-1}$ during the *belg* season, as compared to the gauged stations. This result is consistent with our findings at the Arba Minch station. Also, note the opposite behaviour between SW↓ and precipitation, as the first exponentially increases while the latter decreases with elevation (Figure 3.1).

It is also interesting to discuss our validation using different averaging periods, in particular monthly and yearly ones for precipitation. The monthly averages indicate a significant fit and comparable performance between the coarse and fine resolution domains ($r^2$ is respectively 0.68 and 0.66 for the coarse and fine resolution domains in Arba Minch; 0.61 and 0.60 for the coarse and fine resolution domains in Chencha). Although the annual precipitation modelled, in Arba Minch, by the finer resolution domain has a better fit ($r^2 = 0.94$) than with the coarse resolution domain ($r^2 = 0.89$), the opposite is true for the daily precipitation, as the one modelled in the coarse resolution domain results in an $r^2 = 0.05$, compare to $r^2 = 0.01$ in the fine resolution domain. We can attribute these opposite outcomes to (a) the smoothing of the complex terrain (which modifies the modelled precipitation rates); (b) the actual displacement of the site elevation in the model (inherent to the assumed model resolution) and (c) the WRF model physics representation (Kerandi *et al.*, 2018; Riddle and Cook, 2008). For instance, the Arba Minch station is represented by WRF to be at 1574 m a.s.l. in the coarse resolution domain and 1274 m a.s.l. in the fine resolution domain, but is located at 1212 m a.s.l.

### 3.3.2 Sensitivity of crop variables to the weather variability

In the absence of time series of crop yield observations during 2001 to 2010 to validate our results, we first show the strong relation between meteorology and potato yield observed in 2000 and the role played by elevation. In Figure 3.2, we combined the observed potato yield (t·ha⁻¹) and the area of production for Ethiopia during the year 2000, as illustrated by the International Potato Centre (IPC, 2009) and related to the precipitation modelled with WRF. The inset shows the precipitation results obtained by WRF using the finer resolution domain. Each dot in the plot in the larger plot represents potato yield (t·ha⁻¹). The background shaded region (with topographical contours) shows 10-year-average modelled precipitation (mm·d⁻¹). The figure indicates that the most productive potato growing regions in Ethiopia are the mid-elevations (from 2000 to 2400 m a.s.l., which have moderate annual precipitation: ~ 6 – 9 mm·d⁻¹ and produce annual yields > 10 t·ha⁻¹), the Rift-Valley system and the northern and eastern escarpments along the valley. The region represented by the broken line indicates the fine resolution domain, which is also indicated by the overlaid map at the right lower side of the figure. Note that the region (the Gamo Highlands) has one of the lowest potato yields in the country (< 7 t·ha⁻¹) (Dersseh *et al.*, 2016; Mazengia *et al.*, 2015). However, due to its suitable weather and agro-ecology, it has large production potential in the future.
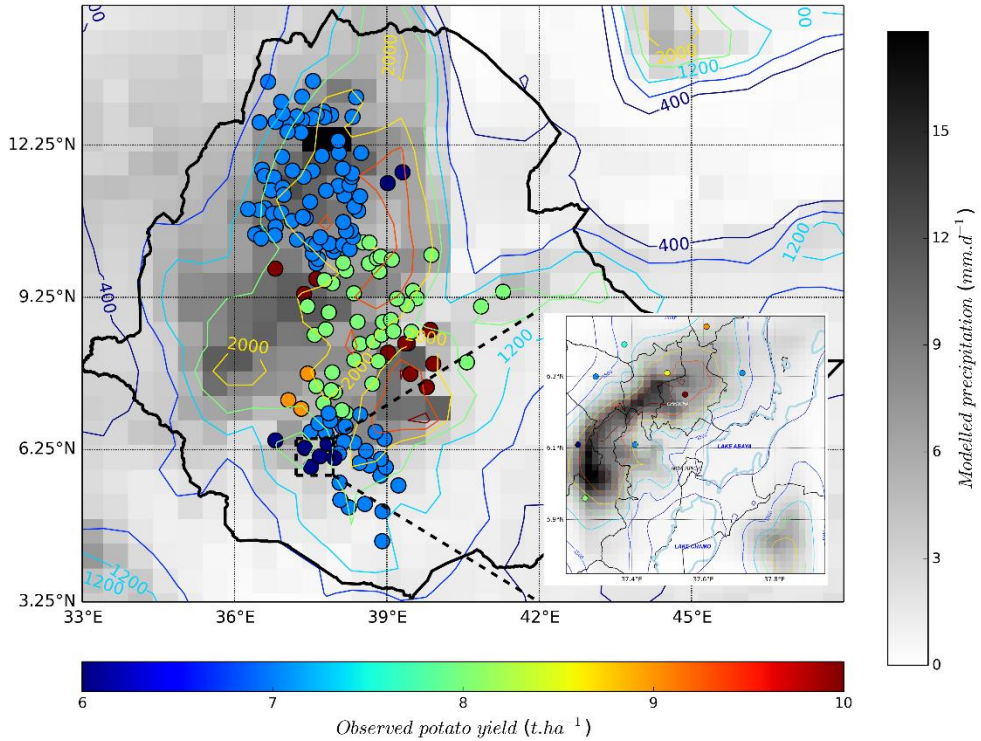
**Figure 3.2 | 10-year mean of WRF modelled precipitation (mm·d⁻¹) – shaded region, topography – contour lines (m) and the observed potato yield – scattered dots in (t·ha⁻¹). The larger plot shows Ethiopia (part of the coarse resolution domain) with spatial resolution of 54 km × 54 km. The dashed square in the figure represents the fine resolution domain, which is magnified and indicated in the right corner. The resolution of the finer resolution domain is 2 km × 2 km and covers 84 km × 84 km area, located in the Gamo Highlands. Each dot represents potato yield per 1000 hectares in the coarser resolution domain. The colour bar scales are applicable to both domains. The potato yield and production observation data are taken from the (IPC, 2009).**

Based on the strategy designed for the crop model sensitivity experiment in Section 3.2.6, the variations introduced in weather and summary of the main results are presented in detail in Table 3.2.

**Table 3.2 | Design of the model sensitivity analysis for crop outputs on atmospheric, edaphic and crop variables and crop management options. The table shows the range of the model sensitivity experiment, the difference between the highest and lowest LGS (day) amongst experiments, the difference between the average LGS of experiments of a variable/parameter and the LGS of the control run and related literature/assumptions.**

| Experiment category | Variable/ parameter | Unit | Range | ΔLGS[‡] (d) | ΔLGS[§] (d) | References/ Assumptions |
|---|---|---|---|---|---|---|
| Atmospheric variables | SW↓ | MJ·m$^{-2}$·d$^{-1}$ | 15 - 23.5 | 28 | 4 | (Haverkort, 1990; Haverkort and Harris, 1986, 1987) |
| | $T_{max}$ | °C | 15 – 21 | 63 | 2 | (Van Oldenborgh et al., 2013) |
| | $T_{min}$ | °C | 7 – 13 | 66 | -2 | (Van Oldenborgh et al., 2013) |
| | VPD | kPa | 0.05 – 0.38 | 10 | 1 | (Kiniry et al., 1998) |
| | PPT | mm·d$^{-1}$ | 8 – 12.25 | 0 | 0 | (Stocker et al., 2013) |
| | [$CO_2$] | ppm | 350-750 | 8 | 3 | (Meinshausen et al., 2011) |
| Edaphic variables | TOC | kg C.m$^{-2}$ | 0 – 20 | 1 | 0 | Model experiment |
| | Soil microbial & humified organic matter | kg C·m$^{-2}$ | 0 – 10 | 3 | 1 | Model experiment |
| | Percent clay | % | 0 – 50 | 0 | 0 | Model experiment |
| | Soil water content at maximum holding capacity | m$^3$·m$^{-3}$ | 0 – 1 | 22 | -8 | Model experiment |
| | Soil water content at field capacity | m$^3$·m$^{-3}$ | 0 – 1 | 4 | 0 | Model experiment |
| | Minimum soil water content | m$^3$·m$^{-3}$ | 0 – 1 | 22 | -9 | Model experiment |
| Crop parameters | Efficiency of germination | g·g$^{-1}$ | 0.1 -0.95 | 12 | 4 | (YL05) |
| | Seed weight | g·seed$^{-1}$ | 20 - 30 | 4 | 1 | (YL05) |
| | Maximum crop nitrogen uptake | g N·m$^{-2}$·d$^{-1}$ | 0.34 – 0.46 | 0 | 0 | (YL05) |
| | Maximum plant height | m | 0.6 – 1.5 | 5 | 1 | (YL05) |
| | Stem dry weight per plant height | g·m$^{-2}$·m$^{-1}$ | 145 - 195 | 2 | 0 | (YL05) |
| Crop management options | Fertilizer dose applied | g·m$^{-2}$·season$^{-1}$ | 0 – 40 | 12 | 0 | Model experiment |
| | Planting date variations | d | Jan 1 – Aug 1 | 57 | 18 | (Wang et al., 2015) |

[‡] *The difference between the shortest and longest LGS (day) amongst the sensitivity experiments for the variable.*

[§] *The deviation of the averages LGS in the sensitivity experiments from the 2006 belg run LGS (i.e. 120 d).*

Figure 3.3 shows how the attainable yield (black – left axis) and LGS (blue – right axis) responded to variations in atmospheric variables and crop management options. The relationship between the meteorology and the crop variables was as follows: variations in the SW↓ controlled by clouds affected the major meteorological crop drivers and these in turn all affected crop growth (a); precipitation, which affected soil moisture and impacted the crop water requirement (b); and $T_{max}$ and $T_{min}$ were associated with extreme meteorological conditions such as heat waves or cold night events and influence crop growth (c and d).
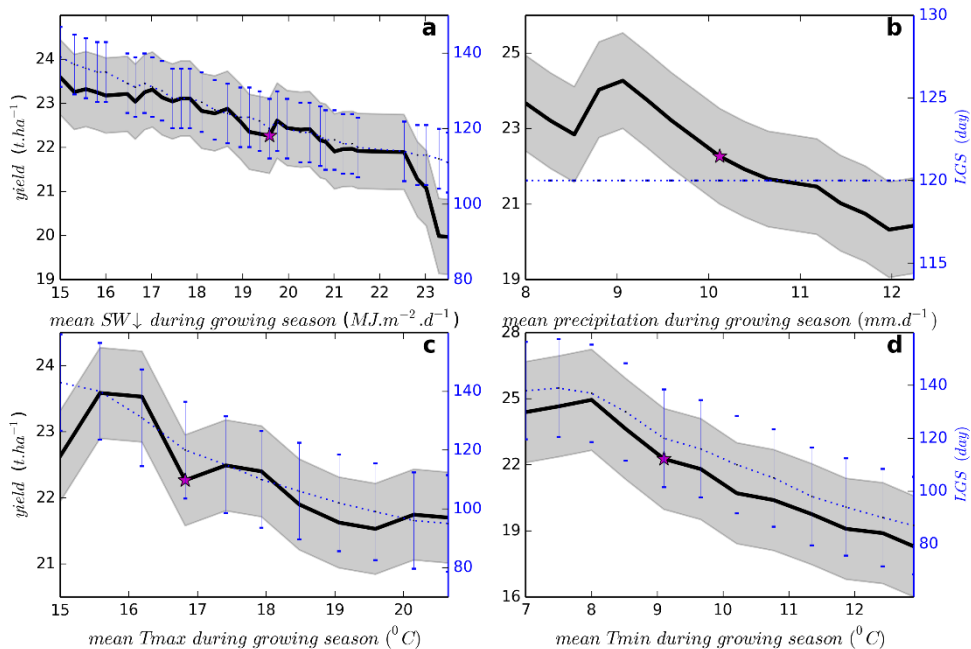


**Figure 3.3 | GECROS model sensitivity analysis for attainable potato fresh tuber yield (t·ha⁻¹) (left-axis – solid-line) and LGS (d) (right-axis – dot line). Variations in the means in atmospheric variables: SW↓ (MJ·m⁻²·d⁻¹) (a), precipitation (mm·d⁻¹) (b), $T_{max}$ and $T_{min}$ (°C) (c and d) with the corresponding LGS (d) (left-axis) for Chencha during the 2006 *belg* season. In all the figures, the LGS variation is included. The shaded/line error bars show the standard deviations of yield/LGS. The stars denote yield for the control run. The scales between panels on the left and those on the right are different.**

Figure 3.3a shows an almost linear decline in yield (23.5 to 20.0 t·ha⁻¹) as SW↓ increases from 15.0 to 23.5 MJ·m⁻²·d⁻¹. This finding is counterintuitive, but our explanation is as follows: by increasing the SW↓, $T_{max}$ and $T_{min}$, LGS and LAI are also varying and diminishing, as shown in Figure 3.3. These lead to the crop having a shorter growing season during which to accumulate additional carbon with the decreased light interception (which limits the amount of photosynthesis performed by the plant) due to the reduced LAI. The LGS and LAI can be considered as an integral

metric that embeds the meteorological dependencies and have a direct impact on the crop yield.

Our sensitivity analysis also indicated that the attainable yield declined non-linearly by ~17% when precipitation increased from 8.0 – 12.5 mm·d$^{-1}$, whereas the LGS remained constant (Figure 3.3b). This counterintuitive result may be explained as follows: the soil model in GECROS is mainly driven by the amount of precipitation and fertilization. Increasing precipitation in the sensitivity study enhances the soil moisture content, which facilitates drainage and leaching of nutrients such as nitrate-nitrogen to the ground water reservoir (YL05). The reduction in nitrate-nitrogen reduces its availability to the plants, as discussed in Waddell *et al.* (2000). Note that climate models project increased precipitation (up to ~ 18%) for Eastern Africa by the end of this century (Stocker *et al.*, 2013), which is likely to reduce future potato productivity.

Figure 3.3c and d show that increases in $T_{max}$ and $T_{min}$ reduced yield by 7 and 13%, respectively, which agrees with the findings of Resop *et al.* (2014). Haverkort and Struik (2015) suggested that the potential global yield of potato would fall by 18 – 32% as a consequence of a global temperature rise of +2.5 °C in 2069. The temperature increase in the future climate significantly shortens the LGS, as discussed in Van de Geijn and Dijkstra (1995), emphasising the need for climate change adaptations for such global change (Haverkort and Struik, 2015). Although yield increases at lower temperatures, crop development is slower. This can increase the risk of damaging night frosts in the highlands, as discussed in (Haverkort and Verhagen, 2008). Forecasting this phenomenon requires the use of detailed elevation maps and high model resolution, as is presented here. Additional model sensitivity experiment results and discussion are included in Fig. S1 to Fig. S3[†].

Most model sensitivity experiments showed variations in the LGS (within runs of a variable and/or as relative to the control run) (Figure 3.3). This was because the variable under study influenced the crop growth rate; in consequence the LGS and the weather to which the crop was exposed during its growth. However, overall the imposed variation dominated over the secondary variations in weather conditions during the growing season. In general, an increase in LGS tended to enhance yield. However, the larger LGS probably increased exposure to biological risks such as pests and diseases, even though these were not accounted for in the model (Haverkort and Struik, 2015; Haverkort *et al.*, 2012; Tufa, 2013) and meteorological stresses (*e.g.* droughts, heat waves, frosts) (Haverkort and Struik, 2015; Haverkort and Verhagen, 2008).

To conclude the model evaluation and parameter sensitivity section, a further quantification was performed to determine the most sensitive variable/parameters to crop yield. To do so, we calculated the relative sensitivities of the variable/parameter by normalizing the experiments, using equation (3.1).

$$S_R = \partial(Y_{expt}/Y_{cont})/\partial(P_{expt}/P_{cont}) \qquad (3.1)$$

Where $Y_{expt}$ represents the yield in the sensitivity experiment, $Y_{cont}$ yield in the control run, $P_{expt}$ the parameter value in the sensitivity experiment and $P_{cont}$ the parameter value in the control run, respectively.

Table 3.3 shows the normalised values (%), which are categorised as increasing or decreasing the yields realised by variables/parameters in the four (atmospheric, edaphic, crop parameter and management) categories. The highest increases and decreases in yield in response to atmospheric variables corresponded to $[CO_2]$ and precipitation, respectively. In the crop parameters category, seed weight and plant height were the most important yield parameters, respectively. Crop management options such as fertiliser dose and differences in planting dates correlated positively with attainable yield. Of the four categories, the edaphic variables such as Biomass Humified Soil (BHC) and TOC were the most important yield-increasing and -decreasing variables, respectively.

**Table 3.3 | The relative sensitivities of atmospheric, edaphic, crop variables and crop management options. The GECROS model values are numerically normalised and calculated using the equation (3.1). The variables/parameters are ordered from high sensitivity to low.**

| Categories | Yield improving | $S_R$ (%) | Yield-reducing | $S_R$ (%) |
|---|---|---|---|---|
| Atmospheric variables | $[CO_2]$ | 31.9 | Precipitation | -37.9 |
| | VPD | 2.1 | $T_{min}$ | -37.7 |
| | | | SW↓ | -35.9 |
| | | | $T_{max}$ | -24.1 |
| Edaphic variables | BHC | 70.3 | TOC | -74.4 |
| | | | Percent clay | -47.1 |
| | Soil water content at field capacity | 14.2 | Soil water content at minimum holding capacity | -12.4 |
| | | | Soil water content at maximum holding capacity | -1.2 |
| Crop parameters | Seed weight | 60.5 | Plant height | -3.6 |
| | Efficiency of germination | 37.0 | Stem dry weight per unit of plant height | -0.3 |
| Crop management options | Fertilizer dose | 51.7 | | |
| | Planting date | 9.2 | | |

## 3.4  Results

### 3.4.1  Representation of topographical variability: the need for high-resolution modelling

The topography of the region under study was highly variable: in a radius of ~ 50 kilometers, there were differences of up to 2500 m in elevation. Meteorological conditions changed with elevation at the Gamo Highlands, influenced by a combination of synoptic and local circulations that led to high variability in the patterns of temperature, clouds and precipitation (Figure 3.1).

Our first analysis focused on how topography influenced the meteorological crop drivers. In particular, SW↓, precipitation, $T_{max}$ and $T_{min}$ influenced the various crop variables related to potato growth and yield. To this end, we show first in Figure 3.4 the relative topographic variations: the 'green', 'blue' and 'yellow' shaded regions indicate variations in elevation of the entire coarse and fine resolution domains that are prescribed in the WRF numerical experiments and the grid points that the coarse and fine resolution domains share.
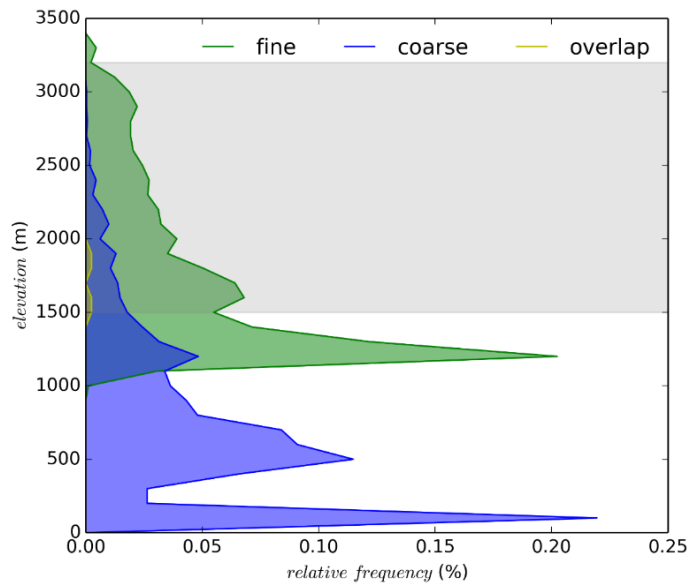


**Figure 3.4 | The distribution of topography in the coarse and fine resolution domains. The grey shaded area marks the elevation zone where potato can be grown in the current climate (Tufa, 2013). In the coarse resolution domain, 8% of the grid points are within the potato growing area, in the fine resolution domain 51%, showing that the coarse resolution domain has more grid points with low elevation and the finer resolution domain has more locations with intermediate elevations. The green, blue shaded areas show the frequency distributions of the elevations in the coarse and fine resolution domain. The coarse resolution domain covers a larger area than the fine resolution domain. The yellow shaded region indicates the elevation range of the four grid points in the coarse resolution domain that includes the same area of the fine resolution domain.**

The topography imposed at the coarser resolution domain showed an elevation that ranges from 0 to 3000 m a.s.l. (marked by the blue area in Figure 3.4). It is relevant to our study that the East-African Highlands including the Gamo Highlands (west of Abaya and Chamo Lakes, roughly 100 km long and 30 km wide) (Freeman, 2002) are highly smoothed and hence the mountain peaks in the coarse resolution domain were shown hundreds of meters lower than in reality. Two representative examples in our study used in the model validation are the weather stations in Arba Minch, which were located 400 m higher than in reality, *i.e.* 1200 m a.s.l. and that of Chencha 1100 m lower than in reality, *i.e.* 2632 m a.s.l. The figure also indicates that only 8% of the grid cells were in the potato-growing range as defined by (Tufa, 2013). In the fine resolution domain, the elevation range from Lake Chamo, the lowest point in the domain (~ 1000 m a.s.l.) to the top of Guge Mountain, the highest point in the domain (~ 3500 m a.s.l.) was well represented (see green area in Figure 3.4). Note that there are only four grid points in the coarse resolution domain that are within the bounds of the fine resolution domain (see yellow area in Figure 3.4). This analysis shows that the topography resolution modelled by the coarse resolution domain smoothed the topography and therefore could affect the potato-growing region of the Gamo Highlands.

We therefore expect that smoothing of the elevation will affect the WRF simulation of meteorological variables. More specifically, when we analysed the results for the coarse resolution domain, which could be considered as a representative domain resolution as used in current weather-crop models and compared them with those by the high-resolution domain, we found a better agreement for $T_{max}$ and $T_{min}$ compared to the observations. This was quantified in terms of MBE, RMSE and $r^2$ between modelled and observed weather variables, as shown in Figure 3.1 and Table 3.1. Furthermore, on a seasonal scale, which is important for crop growth, we found a strong correlation ($r^2 > 0.89$) between modelled and gauged stations and better statistics for the fine resolution than the coarse resolution domain.

### 3.4.2   Relating the resolution of elevation to crop yield

In order to determine the sensitivity of the influence of the prescribed topography on meteorological crop drivers and thus on simulated crop growth, we focused on the following matrices: the LGS and LAI. These crop variables connect the meteorological variables to the potato crop dynamics, mainly the allocated carbon in tubers, or the attainable yield.

Figure 3.5 shows GECROS simulated allocated carbon in tubers and LAI as a function of the LGS during 2006 at Chencha, where the weather station is situated. In order to present the results in a systematic manner, we first studied the meteorological and crop variables in *belg* 2006 and then analysed the variability of these variables in the *belg* seasons through the 10-year period of the study. We identified the

*belg* season of 2006 as a normal climatological year based on the average precipitation of 9.7 mm·d⁻¹ as opposed to the driest year of 2008 (6.1 mm·d⁻¹) and the wettest year, 2010 (14.6 mm·d⁻¹). The year's *belg* season was also climatologically normal in terms of mean temperature (27.7 °C) as compared to the coolest, 2008 (27.0 °C) and the warmest, 2010 (28.3 °C).
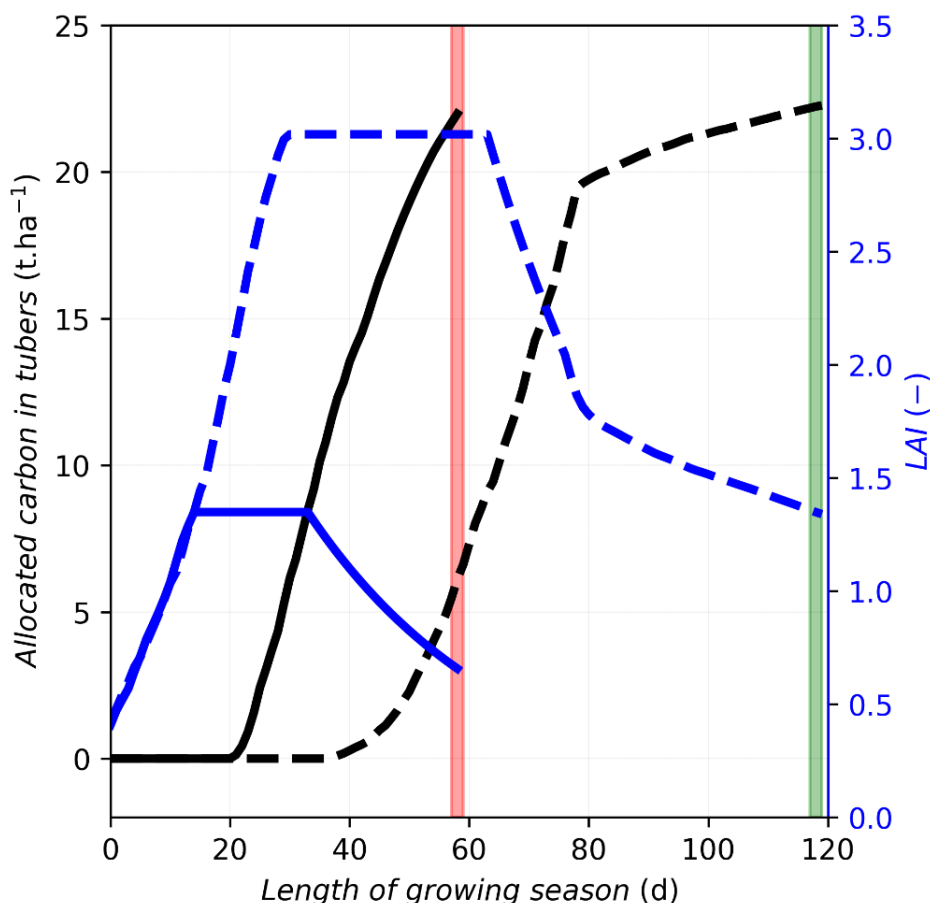


**Figure 3.5 | GECROS modelled allocated carbon in tubers (t·ha⁻¹) (left-axis, black lines) and LAI (-) (right-axis, blue lines) as a function of the LGS during the 2006 *belg* harvest season. The solid lines show model output using the coarse resolution domain's weather input and dotted lines represent output using the fine resolution domain's weather input. The red and green lines show the harvest days of the coarse and fine resolution domains, respectively. The analysis covers the entire length of the growing season (d) at the grid point that represent Chencha station in both model domains.**

The calculated LGS was 59 days in the coarse resolution domain, shorter than the more realistic LGS of 90 to 150 days (FAO, 2008). The maximum LAI was also underestimated at the given value of 1.35, much lower than the optimal maximum LAI of a potato crop: 3.0 − 5.4 (Harper, 1963). In contrast, using the data calculated with

the finer resolution domain, the LGS and the LAI were 120 days and 3.02, respectively (Figure 3.5). As mentioned above, in the coarse resolution model the elevation of Chencha was ~1100 m below the actual elevation. As a result, the averaged *belg* season was 8.5 °C warmer and 4.3 mm·d$^{-1}$ drier than in the fine resolution domain. This caused the crop to mature too early, with a low maximum value for the LAI. Despite significant differences in modelled weather and crop growth calculated in the coarse and fine resolution domains, Figure 3.5 shows that the yields were very similar in both domains during the 2006 *belg* season. This finding is discussed in detail and in context, below and in Section 3.5.

Figure 3.6 shows how GECROS modelled attainable potato yield (a) and LGS (b) for the Chencha station for the 10-year period during the *belg* growing seasons using the modelled coarse and fine resolution domains weather inputs. To complete the figure, we add an observed reference potato yield for 2001 – 2010 in the southern Ethiopia to be < 8 t·ha$^{-1}$ as indicated in Figure 3.2 and by (Hirpa *et al.*, 2010; Mazengia *et al.*, 2015). Other experts have estimated the potential fresh tuber yield in Chencha district in the *belg* season to be about 30 t·ha$^{-1}$, although the actual yield is much lower (*i.e.* ~8 t·ha$^{-1}$) (Haverkort *et al.*, 2012).
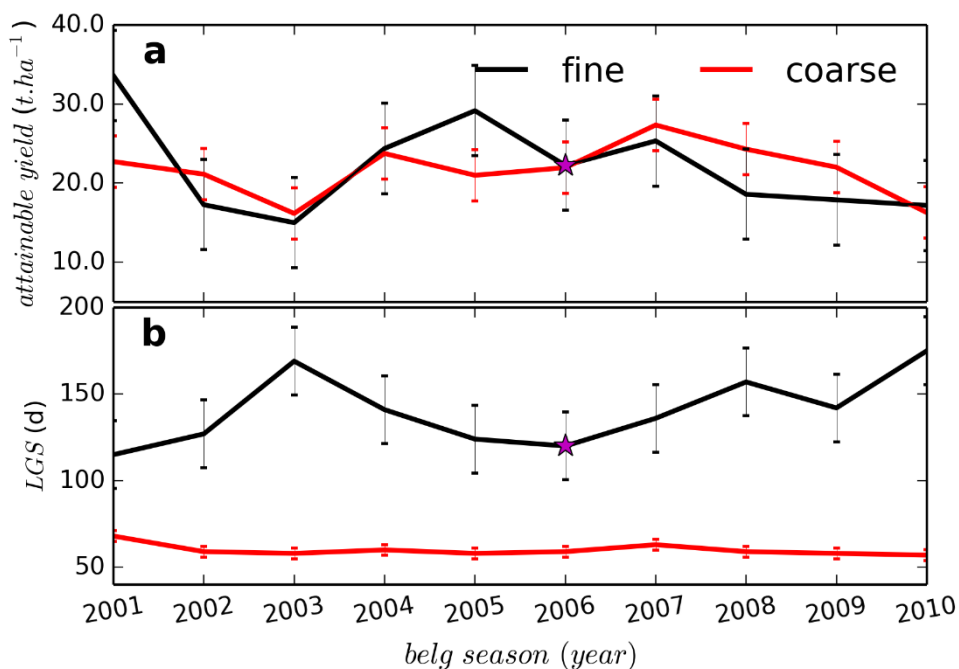


**Figure 3.6 | Inter-annual variability in attainable fresh-matter yield (t·ha$^{-1}$) (a) and LGS (b) modelled by GECROS using the meteorological input from the coarse and fine resolution domain at the grid point that represents Chencha station for *belg* season in 2001 - 2010. The stars denote the control run (*i.e.* yield or LGS during the 2006 *belg* season). The error bars indicate the mean ± standard deviations of the 10-year yields.**

The pattern in inter-annual variability in potato yield was very similar in both domains (Figure 3.5a). The average attainable yields calculated were in the range of 21.7 ± 3.2 and 22.1 ± 5.7 t·ha⁻¹ using the weather modelled in the coarse and fine resolution domains, respectively. The yields were comparable with the modelled yield during the 2006 *belg* season (Figure 3.5). Moreover, the yield modelled for the fine resolution domain was almost constant over the range of elevations in the Gamo Highlands (Figure 3.7). However, and as in 2006, the simulated LGS for both domains was very different. We calculated 60 ± 3 and 141 ± 20 LGS (d) for the coarse and fine resolution domains, respectively (Figure 3.5b)[**]. It is therefore of interest to further study how the LGS and the potato yield change as a function of elevation.
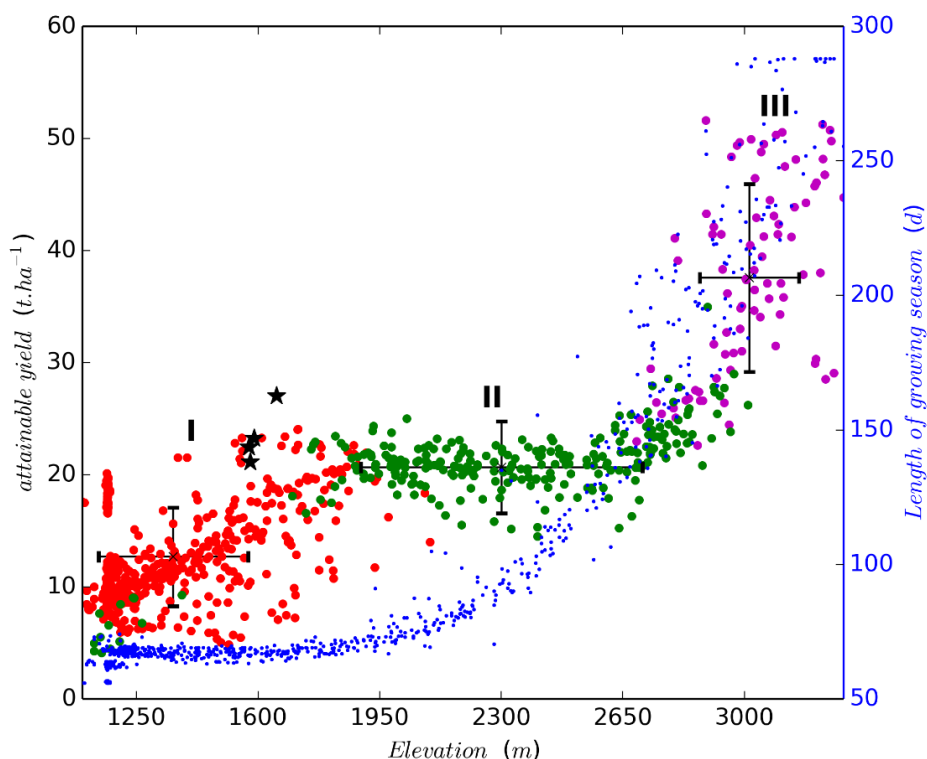


**Figure 3.7 | Relationship between attainable yield (left-axis) and elevation, showing that the yield is fairly constant in the altitude range where potato mostly grows in the Gamo Highlands. The scattered dots indicate fine resolution domain grid cells that spatially overlap with the coarse resolution domain (black star) averaged during the 10 years of *belg* harvests. The error bars (mean ± standard deviations) are calculated for grid points with LGS < 70 (red dots – region-I), between 70 to 195 (green dots – region-II) and > 195 (pink dots – region-III) days, respectively. The blue dots with the corresponding y-axis (right side) indicate the LGS.**

---

[**] *Additional differences in the outputs of the coarse and fine resolutions are presented in Table S13 (follow https://doi.org/10.1016/j.agrformet.2018.07.009).*

Figure 3.7 shows the potato yield and length of growing season for (i) four grid cells in the coarse resolution domain (black stars) that share their spatial location with the fine resolution domain; (ii) 840 grid cells in the fine resolution domain (all dots). As the most representative variable, we show the attainable yield (red, green and purple dots and left y-axis) and the LGS (fine blue dots and right y-axis). The coarse resolution domain led to a yield of 23.4 ± 2.9 t·ha$^{-1}$. For the fine resolution domain, we found that potato grew in the optimal elevation range (1600 m – 2700 m a.s.l.) with an attainable yield range of 20.7 ± 4.1 t·ha$^{-1}$. This optimal region was further corroborated by the calculated values of LGS between 70 to 195 days that once again were in the range of the expected values for the potato growing cycle. GECROS also calculates yield for LGS outside this range, but its estimates are not realistic in terms of potato growth characteristics (FAO, 2008b; Harper, 1963). For LGS < 70 days, the calculated yield was 12.7 ± 4.4 t·ha$^{-1}$, which corresponded to 1150 to 1550 m a.s.l. On the other hand, for LGS > 195 days, the attainable yield was much larger (37.6 ± 8.4 t·ha$^{-1}$), with a narrow elevation range: 2850 to 3200 m a.s.l. Consequently, these calculated values falling outside the optimum LGS range thus represented conditions that were not realistic for potato growth variables.

In spite of the range of elevations in the region and its consequences for weather and crop variables LGS and LAI, the modelled potato yield was rather insensitive across a wide range of elevations (1600 m – 2700 m a.s.l.) and with high topography model resolution. This raises the question whether high-resolution modelling is actually required to model potato yield and related variables reliably. This is discussed in the following section.

### 3.4.3 Compensating effect: the role of length of growing season and LAI

The sensitivity analysis performed in Section 3.3 shows that temperature and precipitation had opposing behaviour to the elevational changes. Our results indicated that at higher elevations the lower temperature led to higher yields, while the increased precipitation decreased yield. Excess precipitation above the maximum moisture holding capacity of the soil was directly proportional to the soil nutrient leached (YL05). The opposing impacts of temperature and precipitation on yield thus compensated each other. In order to further quantify and explain this behaviour, we studied whether the opposing and non-linear effects of the meteorological variables offset each other in the crop growth simulation (Figure 3.3 and Figure 3.7) by performing the following experiment:

1)  *We took the weather data calculated in the fine resolution domain for the Chencha site in 2006, taking the climatologically normal belg season as reference case (control).*

*2)*   *We substituted a weather variable (i.e. $T_{min}$, $T_{max}$, Precp (precipitation), SW↓ or VPD) or pair of weather variables (i.e. $T_{min}$ and $T_{max}$, $T_{min}$ and SW↓, $T_{min}$ and VPD, $T_{max}$ and Precp, $T_{max}$ and SW↓, $T_{max}$ and VPD, SW↓ and VPD, Precp and $T_{max}$, Precp and VPD or Precp and SW↓) in the fine resolution domain for its counterpart in the coarse resolution domain and modelled a new potato yield, combining the substituted weather variable(s) with the ones in the fine resolution domain. See more descriptions in TableS14[†].*

Table 3.4 summarises the yield difference between the control run and the sensitivity experiment. The first row/column (values in brackets) shows the difference between the average weather variable in the coarse resolution domain and that of the fine resolution domain during the growing season. The remainder of the cells indicate the change in yield (*i.e.* yield driven by the new weather combination minus the control run value in the fine resolution domain).

**Table 3.4 | Weather variable (diagonal cells) or a combination of two variables (row × column) of the coarse resolution domain that replaced the corresponding variable(s) in the fine resolution domain (control). The values in the brackets show the difference in the average weather conditions between the variable in the coarse resolution domain and the control conditions during 2006 *belg* growing season. The numbers in the cells indicate the difference in yield calculated between a sensitivity experiment the control run in t·ha⁻¹. The compensating effect experiment matrix shows 15 model experiments for the Chencha station during *belg* 2006.**

| Variables from coarse resolution domain that replaced those in the fine resolution domain | $T_{min}$ (+9.0 °C) | $T_{max}$ (+8.5 °C) | Precip (-4.3 mm·d⁻¹) | SW↓ (+0.9 MJ·m⁻²·d⁻¹) | VPD (+0.5 kPa) |
|---|---|---|---|---|---|
| $T_{min}$ (+9.0 °C) | -7.3 | -7.9 | -5.0 | -7.3 | -6.0 |
| $T_{max}$ (+8.5 °C) | | -4.8 | 6.2 | -3.8 | -2.2 |
| Precip (-4.3 mm·d⁻¹) | | | 12.1 | 12.0 | 11.9 |
| SW↓ (+0.9 MJ·m⁻²·d⁻¹) | | | | 0.9 | 0.9 |
| VPD (+0.5 kPa) | | | | | 0.7 |

Our analysis demonstrated that the yield decreased by 7.3 t·ha⁻¹ when $T_{min}$ in the fine resolution domain was replaced by the 9.0 °C warmer $T_{min}$ in the coarse resolution domain. Similarly, the yield decreased by 4.8 t·ha⁻¹ when $T_{max}$ was warmer by 8.5 °C than the fine resolution domain combined with the fine resolution domain's other weather variables. When $T_{min}$ was simultaneously varied with precipitation or any other variable, the decrease in yield was also significant (5.0 to 7.9 t·ha⁻¹). In contrast, the yield increased by 12.1 t·ha⁻¹ when precipitation that was lower by 4.3 mm·d⁻¹ than the fine resolution domain was substituted. We hypothesise that this yield increase was due to the relationship between precipitation and nutrient leaching included in the GECROS model.

In the case where precipitation was combined with SW↓ or VPD, yield increased by ~ 12.0 t·ha$^{-1}$. The sensitivity experiments indicated that precipitation (+12.1 t·ha$^{-1}$) was the variable that had the largest influence on potato yield, followed by $T_{min}$ (-7.3 t·ha$^{-1}$) and $T_{max}$ (-4.8 t·ha$^{-1}$).

Regarding how the key meteorological actors offset each other in calculations of yield, we found that the increase in yield due to decreased precipitation was mainly offset by the simultaneous decline in yield because of increased $T_{max}$ and $T_{min}$ in the coarse resolution domain. Since this compensation occurred in both domains (with coarse and fine resolution), the potato yield modelled turned out to be comparable. However, in analysing the results for other key variables, we found that LGS and LAI in the fine resolution domain were 120 days and 3.02, respectively, whereas the values at the coarse resolution domain were LGS and LAI 59 days and 1.35, respectively. At the highest locations, the lower SW↓ and the temperatures (because of the increased cloudiness) induced a longer LGS, which explains why the yield was significantly greater at these locations. The sensitivity experiment on SW↓ showed that the potato yield and LGS decreased as the SW↓ increased (Figure 3.3). As a remark, increases in SW↓, $T_{max}$ and $T_{min}$ decreased the LGS and LAI, which also offset yield. Our findings showed that, although we obtained similar results for the potato yield independent of the resolution of topography, there were important differences in the meteorological variables and in the key crop variables related to the calculation of the potato yield. These are discussed in the following section.

## 3.5  Discussion

Based on our findings, Figure 3.8 integrates and summarises the influence of the meteorological variables (as function of elevation) on simulated crop yield and related variables. In general, variations in the meteorological variables with elevation led to an increase in potato yield from 12.7 t·ha$^{-1}$ in the lowlands to 37.6 t·ha$^{-1}$ in the highlands as averaged over 10 *belg* seasons. However, the impact of elevation on the meteorological variables acted differently on the crop integrators (namely LGS and LAI) and on their direct impact on crop yield. As a result, and in the specific region under study, whose elevation ranged from 1600 to 2700 m a.s.l. the crop yield was almost constant with height, with a calculated attainable yield of 20.7 ± 4.1 t·ha$^{-1}$ (Figure 3.7).

The sensitivity analysis discussed in the previous section showed that there was a strong compensation effect in what determined calculated yield. Yield increases due to one meteorological variable were offset by decreases by another variable. The weather variables (SW↓, $T_{max}$ and $T_{min}$) and yield were all interrelated by the crop integrators as shown in Figure 3.8, based on the results obtained in the fine resolution domain (Figure 3.3 and Figure 3.7).

A representative example is that an increase of temperature by 8.8 °C (as compared to the fine resolution domain) in the coarse resolution domain during the growing season led to a reduction in yield of up to 35% (of 22.3 t·ha⁻¹ in the fine resolution domain) at the Chencha station during the 2006 *belg*. This reduction was associated with a 51% decrease in the LGS and a 58% decrease in the LAI. The opposite behaviour was found for precipitation, which was 4.3 mm·d⁻¹ less than in the fine resolution domain and led to an increase in the attainable yield of 54% (relative to the fine resolution domain). This increase may be associated with more nutrients becoming available to the plant, since there was less leaching due to the reduction in precipitation (YL05). Compared to the other meteorological variables, the crop integrators were independent of changes in precipitation. This contrasting meteorological effect resulted in almost constant crop yield along the Gamo Highlands transect (region-II) in Figure 3.7. Our results indicated that in the region, the yield enhancement was the result of a longer growing season and larger LAI driven by the lower temperature and possibly by more nutrient leaching due to higher the level of precipitation at greater elevation. In the lowlands (region-I) and in the most elevated zone (region-III), yield increases were mainly explained in terms of lower temperatures along the mountain transect.
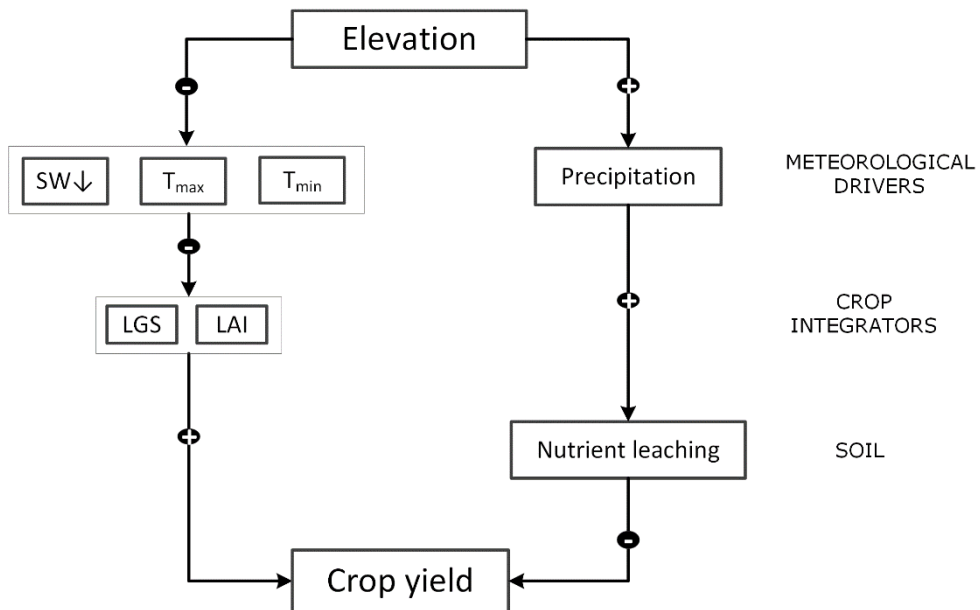


**Figure 3.8 | The role of elevation and meteorological crop drivers in the attainable crop yield in region-II of Figure 3.7. The key integrating matrices such as LGS and LAI relate the SW↓, T$_{max}$ and T$_{min}$. Precipitation may influence the soil model by nutrient leaching. The crop integrators and nutrient leaching connect meteorological crop drivers and crop yield. The positive sign indicates a positive correlation whereas the negative sign shows a negative correlation.**

Our results indicated that the prescribed topography had a major impact on the meteorological crop drivers. Although the results obtained with the finer resolution domain showed an improvement of the model results for key crop driver variables like $T_{max}$ and $T_{min}$, there was no direct improvement for the individual meteorological variables. This was particularly relevant to the daily precipitation, for which the results from the coarse resolution domain matched the available observations better than those of the fine resolution domain, although the topography was very smooth in the coarse resolution domain. Our findings corroborate other studies that show that the WRF model is not very successful in correctly predicting the frequency and location of precipitation (Lunde *et al.*, 2013) around Arba Minch. Improving the accuracy of forecasting daily precipitation, more specifically, the onset and duration of rainfall during the growing season, is therefore a priority. This will require a complete analysis of the sensitivity of the model results to the representation of physical processes in this tropical, mountainous region. To be capable of determining the best combination of physical parameterization, the model validation will require more measurements of the spatiotemporal variability of the meteorological and crop *in situ* data and may benefit from adding remote-sensing observations. The wide range of elevations and the strong diurnal cycles in weather require meteorological observations to be taken hourly and at shorter spatial interval (~ 3 – 5 km).

It is also important to analyse the connections between the meteorological crop drivers and the LGS and LAI. As Figure 3.8 shows, the decrease with elevation of the variables SW↓, $T_{max}$ and $T_{min}$ led to a longer LGS period, as pointed out by (Peiris *et al.*, 1996; Van de Geijn and Dijkstra, 1995) and higher LAI, whereas precipitation has no effect on these two crop variables (Figure 3.3). An accurate calculation of LGS related to the onset of precipitation is crucial to obtaining realistic values for potato yield and related variables (FAO, 2008b; Harper, 1963).

The counteracting effects of temperature and precipitation in yield calculation demonstrate the need to prescribe soil moisture and elevation in fine resolution domains. Our findings show that doing so enables us to provide the best estimates of meteorological and crop variables. For the two crop integrators shown in Figure 3.8, the LGS and LAI values calculated in the fine resolution domain are 120 days and 3.02 m²/m². These are more realistic values than those calculated using the coarser resolution domain: 59 days for LGS and 1.35 m²/m² for LAI. This improved consistency in the calculation using the finer resolution domain is also found for carbon allocation at harvest (attainable yield average over 10 *belg* periods): tuber yield (22.3 t·ha⁻¹ in the fine resolution domain versus 22.3 t·ha⁻¹), stem mass (20.0 versus 4.5 t·ha⁻¹), leaf mass (4.4 versus 2.0 t·ha⁻¹) and root mass (2.7 versus 4.1 t·ha⁻¹).

Considering the sensitivity of meteorological and crop dynamics to elevation and the domain resolution, it is also necessary to perform projections of crop growth and yield for different scenarios of future climate. Haverkort and Struik (2015) suggested that potato production will be shifted to northern latitudes all over the world. On the one hand, in tropical highlands like the one under study here, global warming will reduce yield and could force potato production areas to move to more elevated locations where less arable land is available. On the other hand, a rise in precipitation in the future may reduce yields and shift the potato-growing zone to lower elevations, but this will require a detailed analysis of the relationship between nutrient leaching and precipitation. This makes crop growth difficult to predict in a changing climate. Furthermore, scenarios that include greater amounts of precipitation, $T_{max}$ and $T_{min}$, in the future could increase cloudiness, atmospheric and soil moisture, which could result in a greater loss of potato production due to increases in insects and other pests (Tufa, 2013).

## 3.6 Conclusions

We investigated the effect of representation of elevation on the meteorological variables that drive the dynamics of potato growth. The region area studied is the Gamo Highlands in Ethiopia, which is situated in a tropical region characterised by a complex topography and consequently high spatial variability in meteorology. To this end, we applied a modelling framework that integrates meteorology and crop dynamics. We used high-resolution weather data to feed an advanced crop model and modelled potato growth over 10 years (2001-2010) and employed observations from two weather stations in the Gamo Highlands (located at 1212 and 2632 m a.s.l.) to validate the weather variables modelled.

Our numerical experiment used two domains with different horizontal resolution, both centred around Arba Minch using the Weather Research and Forecasting model (Skamarock *et al.*, 2005). The first has a coarse resolution domain, *i.e.* 54 km × 54 km; the second has a much finer spatial resolution, *i.e.* 2 km × 2 km. In the fine resolution domain, an altitudinal difference of nearly 2500 m is much better is much better resolved. In order to be consistent with the fine spatial resolution meteorological model domain, we also used high-resolution (1 km × 1 km) soil properties from the ISRIC database (Leenaars *et al.*, 2014). A key aspect of our methodology is thus consistency in using high-resolution and hourly weather data as the main inputs to the state-of-the-art, eco-physiological crop model GECROS (Genotype-by-Environment interaction on CROp growth Simulator) over the complex terrain (Yin and van Laar, 2005). We performed a systematic sensitivity analysis on how weather variables influence crop dynamics. The 10-year study can be regarded as covering a sub-climatological period that enabled us to obtain robust and representative statistics.

Our first question was: *how do weather and climate vary as a function of local topography and how does it affect potato crop growth variables and yield?* The major atmospheric crop drivers, the incoming short-wave radiation, precipitation, maximum and minimum temperatures displayed a wide range of spatial variability. The SW↓ exhibited a non-linear reduction with height due to enhanced cloudiness. Precipitation increased exponentially across elevation, whereas temperature dropped linearly with ~ 6 °C per kilometer. Combined together, these atmospheric crop drivers influenced potato crop growth and led to an increase in LGS, LAI and the attainable potato yield as elevation increased. In analysing the 10-year modelled *belg* season weather data, we found large inter-annual variations in both observations and the modelled data. When we compared the results obtained by the coarse and the fine resolution domains, we also found large differences associated with cloud formation and its intensity. For SW↓ and precipitation in particular, the fine resolution domain was on average 22.7 W·m$^{-2}$ larger and 2.7 mm·d$^{-1}$ wetter than the coarse resolution domain over the 10-year period.

In spite of the differences due to different elevation and domain resolutions, the simulated attainable potato yield during the 10-year was comparable for the coarse and fine resolution domains (21.7 ± 3.2 and 22.1 ± 5.7 t·ha$^{-1}$ respectively) at the location of the Chencha station. However, the results were different when we analysed other representative crop variables. Our findings revealed that the fine resolution domain had more realistic values of LGS (90 – 150 days) as suggested by FAO (FAO, 2008b) and LAI (3.0 – 5.4) as indicated in (Harper, 1963) as compared to the much lower values obtained using the coarse resolution domain.

Our second question was: *does elevation enhance or lower the magnitude of key crop variables such as the length of the growing season (LGS), canopy development, carbon allocation to different parts of the plant, leaf area index and yield and their interactions?* The accurate representation of elevation in the finer resolution domain enabled us to identify the following relationship between elevation and attainable yield: a linear increase (region-I) between 1100 to 1500 m a.s.l., a steady-state (region-II) between 1600 to 2650 m a.s.l. and again a linear increase (region-III) between 2950 to 3200 m a.s.l. in yield. From the perspective of potato growth, region-I is not suitable for potato, as it is too warm and dry; region-II is the major potato production belt in the Gamo Highlands and region-III is used for potato cropping although it requires a much longer LGS than region-II.

We have discussed two of the above findings in depth: (a) the similarity in potato yield calculated using both the coarse and fine resolution domains (question 1) and (b) the existence of a region (region-II) with almost constant yield in spite of the wide elevation range (question 2)

In both cases, our analysis revealed that there was a *compensating effect* in the meteorological variables in the yield calculations that depended on the sensitivity of yield to meteorological variables. More specifically, the reduction in SW↓ and temperature with elevation had a positive effect on yield (Resop *et al.*, 2014), unlike an increase in precipitation, which may have had an indirect negative effect on yield because increased precipitation led to an increased nutrient leaching (Yin and van Laar, 2005). Superimposed on these offsetting effects, but playing a key role, the dependence of LGS and LAI on meteorological variables that vary strongly with elevation needs to be taken into account. In view of the interrelationships between the meteorological and potato crop growth variables in regions of complex terrain, we recommend the use of meteorological model data with high spatial (~2 km) and temporal (sub-daily) resolutions, which represent differences in elevation well, in order to adequately simulate not only crop yield but also intermediate crop dynamical processes.

**Appendix: Supplementary material**

A supplementary material to this article is found in https://www.sciencedirect.com/science/article/pii/S0168192318302302#sec0095.

# 4

# Observational characterisation of the synoptic and mesoscale circulations in relation to crop dynamics: *Belg* 2017 in the Gamo Highlands, Ethiopia

*The Gamo Highlands in Ethiopia are characterised by complex topography and lakes. These modulate the mesoscale and synoptic scale weather systems. In this study, we analysed the temporal and spatial variations in weather as function of topography and season and their impact on potato crop growth. To determine how crop growth varies with elevation, we installed a network of six automatic weather stations along two transects. It covers a 30-km radius and 1800-m elevation difference. We conducted a potato field experiment near the weather stations. We used the weather observations as input for a crop model, GECROS. Data analysis showed large differences between weather in February and May. February is more dominated by mesoscale circulations. The averaged February diurnal patter shows a strong east to southeast lake breezes and, at night, weak localised flows driven by mountain density flows. In contrast, in May, the synoptic flow dominates, interacting with the mesoscale flows. The GECROS model satisfactorily predicted the elevational gradient in crop yield. Model sensitivity experiments showed that belg-averaged precipitation distribution gave the highest yield, followed by exchanging May weather observations with April.*

## 4.1 Introduction

Potato (*Solanum tuberosum* L.) is becoming an important crop in Ethiopia (Minda *et al.*, 2018b; Tadesse *et al.*, 2018). The optimal climatological conditions for potato crop growth are 15 to 25 °C mean daily temperature (FAO, 2008b; Khan, 2012; Streck *et al.*, 2007; Tsegaw, 2005). Higher temperatures inhibit tuberisation, promote foliage growth, and reduce allocation of carbon and nitrogen to the tubers (Tsegaw, 2005). Potato requires more than 600 mm of annual total precipitation (MOANR, 2016; Tsegaw, 2005). The crop consumes 500 to 700 mm of water, while inadequate availability of soil water during the growing season results in reduced yield (FAO, 2008b). These climatic conditions generally occur in the Gamo Highlands at elevations >1600 m above sea level (a.s.l.) (Gebreselassie *et al.*, 2016). The crop mainly grows during the *belg* (February to May) cropping season, because this is the season when precipitation provides the moisture for the seed tubers to sprout (Minda *et al.*, 2018b; Tufa, 2013). The season shows lower risk of crop diseases such as late blight than in other seasons (Tufa, 2013). Note that the Ethiopian climate, according to the National Meteorology Agency (NMA), is classified in three regimes namely *belg* (Feb to May), *kirmet* (Jun to Sep) and *bega* (Oct to Jan) (Degefu, 1987; Minda *et al.*, 2018b). The majority of this staple food in Ethiopia is produced by rain-fed agriculture. Only 4–5% of the agricultural land is irrigated in the country (Awulachew *et al.*, 2010). Consequently, potato growth strongly depends on weather and its interaction with elevation.

Here, we study the interplay among weather, potato crop growth and elevation in the Gamo Highlands in southern Ethiopia in the *belg* growing season. This region is characterised by a diverse landscape and complex topography with altitudes ranging from 1100 to 3600 m a.s.l. It is part of the Great East African Rift Valley system, which is over 5500 km long, extending from the Red Sea junction, through Ethiopia, Kenya and Mozambique to Lake Victoria (Cattani *et al.*, 2016). The Gamo Highlands contain two large lakes, namely Lake Abaya (covering 1162 km$^2$) and Lake Chamo with 317 km$^2$, farmlands, settlements, wooded land, grasslands and forests (Daye and Healey, 2015). The steep elevation variation with the water bodies play a role in modulating weather on diurnal to seasonal time scales, as well as the climate of the region. Obviously, these factors influence crop growth across the elevations (Minda *et al.*, 2018b).

Weather in East African regions, just north of the Equator, shows a bimodal precipitation regime following the north–south displacement of the Intertropical Convergence Zone (ITCZ) (Diro *et al.*, 2008). The ITCZ oscillates between 10° south (S) and 20° north (N) in the African continent and strongly influences the annual precipitation cycle of the region (Diro *et al.*, 2008; Nicholson, 2009; Nicholson, 2011). However, weather in the Gamo Highlands is not only controlled by the position of the ITCZ, but also by atmospheric flows driven by complex topography and land

heterogeneity (Pierre *et al.*, 2018). These atmospheric phenomena interact differently during the early and later stages of the *belg* season, inducing a pronounced precipitation seasonality with elevation.

Generally, in tropical mountainous regions like the Gamo Highlands, orographic and thermally driven circulations play important roles in determining the local weather/climate dynamics of the region (Camberlin, 2009; Fraedrich, 1972; Haile *et al.*, 2009; Pierre *et al.*, 2018). These dynamics depend on the orographic spatial orientation defined by the terrain altitude, slope and aspect angle. The terrain orientation affects wind patterns, potentially affecting convergence, convection and precipitation (Haile *et al.*, 2009). The contrast between the large water bodies and land may also play an important role (Haile *et al.*, 2009). Lake breezes can be superimposed on orographic flows and on the development of boundary layers (Camberlin, 2009; Haile *et al.*, 2013; Haile *et al.*, 2009). Haile *et al.* (2009) and Rientjes *et al.* (2013) showed that Lake Tana in Ethiopia modulates the mesoscale circulations trend of its surroundings. For example, the diurnal precipitation of a location in the Lake Tana basin is correlated with the distance to the lake (Haile *et al.*, 2009). This finding, in line of our main goal, shows the role of the lake in influencing the local weather and climate. In addition, Pierre *et al.* (2018) and Rientjes *et al.* (2013) showed that Lake Tana also influences the diurnal distribution of the local weather around the basin. During daytime, lake breezes diverge from the lakes to the warmer surroundings and, during nighttime, land breeze flows converge to the warmer lake.

At the beginning of the *belg* season, in February, the ITCZ is positioned around 15° S and marches to the north. During this period, north-easterly, dry winds from the Arabian Peninsula reach the Gamo Highlands in southern Ethiopia (Barry and Chorley, 2009; Nicholson, 2018). In the subsequent wetter months of April and May, the ITCZ moves overhead toward northern Ethiopia. Consequently, south to south-easterly synoptic winds with high moisture content from the Indian Ocean reach the southern part of Ethiopia (Nicholson, 2018).

Simultaneous to this synoptic variability, during daytime, heating of the slopes induces valley winds, which draw air upward to converge at the mountain top (Houze, 2012). The lake breezes can reinforce these flows. During the nighttime, however, cooling over the higher terrain induces downslope flows. These nocturnal mountain winds normally have a smaller vertical dimension than the daytime valley winds and are more influenced by local topography. The heating/cooling over the high elevation may trigger dynamic flows such as gravity waves and drag (Houze, 2012). These topography-triggered circulations may facilitate/suppress convective precipitation while converging/diverging with large-scale flows, and thus, influence precipitation formation.

Due to the relevance of large and small spatiotemporal scales, predictions of key weather variables become challenging. For example, global climate models predict

an increasing trend in precipitation (up to 18% in East Africa at the end of the century) (Kerandi *et al.*, 2018; Stocker *et al.*, 2013; Van Oldenborgh *et al.*, 2013). However, observations (gauged observations with merged satellite data) show a decreasing trend (Rowell *et al.*, 2015). These opposing trends of precipitation in models and observations were coined the "East African Climate Paradox" (Rowell *et al.*, 2015).

The current crop models used for monitoring crop growth and yield predictions use a coarse-resolution model input for weather variables: models (Schlenker and Roberts, 2009), re-analysis (Rosenzweig *et al.*, 2014), or interpolated station observations (Liu *et al.*, 2007; Portmann *et al.*, 2010). The typical model resolution is tens of kilometers (Liu *et al.*, 2007; Portmann *et al.*, 2010; Rosenzweig *et al.*, 2014). If the models employ observations, they are normally few or unevenly distributed (Portmann *et al.*, 2010). In complex topographic regions such as the Gamo Highlands, coarse-resolution weather products smooth out topography, which lead to an increase the uncertainty of the weather variables. In this circumstance, the average topography is often below the potato-growing zone, which results in crop yield underestimation (Minda *et al.*, 2018b). This is because the weather could be warmer, less cloudy and drier than the anticipated. Our aim in designing and implementing the Gamo Ethiopian Meteorological Stations (GEMS) network is to provide reliable meteorological information to be used in monitoring meteorological conditions in complex topographic regions. These observations can be further employed for the evaluation of fine-resolution weather and crop models.

Minda *et al.* (2018b) applied crop a high-resolution (2 km × 2 km) weather model to represent the spatial meteorological variables during the years 2001 to 2010 in the Gamo Highlands. The analysis showed that precipitation increases and temperature decreases upward into the mountains as expected, creating an elevation zone between 1700 and 3000 m where potato grows optimally. The analysis also showed that the model was dry-biased in the valley and wet-biased in elevated areas. This underlines that high-resolution modelling is necessary, but not sufficient in topographically complex regions. Ground-truthing, quantified by continuous and high-quality measurements, remains essential for understanding and verification (Dee *et al.*, 2016; Lorenz, 1963).

In sub-Saharan countries, weather station networks are typically sparse, unevenly distributed (they are mostly installed along main roads, in cities and towns away from agricultural land) and often with data gaps (Araya, 2011; Dinku *et al.*, 2014; Diro *et al.*, 2009). In Ethiopia, a country covering an area of 1.104 million km$^2$, there are only 22 synoptic stations (NMA, 2018). Moreover, there are few networks focusing at sub-daily temporal resolution (Haile *et al.*, 2009; Pierre *et al.*, 2018). Haile *et al.* (2009) used a network of ten rain gauge stations collecting data on an hourly basis in the Lake Tana basin. Still, a reliable, sub-hourly meteorological information across elevation gradients is crucial to explain crop growth (Minda *et al.*, 2018b).

Given the geographical location of the Gamo Highlands and the complex topography, the major meteorological crop drivers exhibit large spatial and temporal variabilities, in which the impact on crop growth is significant.

Therefore, to complement our model strategy and filling the gap of current observations, we deployed a relatively dense weather stations network, for Eastern African standards, to measure the spatial and temporal variations of weather and crop growth: the GEMS network. The network was established as a continuous operational weather monitoring station in the Gamo Highlands. It was designed along two mountain transects, to better monitor the local circulations and installed at representative altitudes to study the role of meteorology on potato crop growth in the region. The GEMS network measures weather plus soil moisture/temperature and leaf wetness at 15-min intervals of data recorded continuously since April 2016. To our knowledge, this is the first high-spatial-resolution network of weather stations with sub-hourly measurements of all major weather variables including soil/leaf wetness observations in Ethiopia. Recently, we extended the meteorological measurements in the GEMS network with crop measurements at potato experimental farm trials, *e.g.* plant height, canopy cover, yield and the length of the growing season (LGS) (Minda *et al.*, 2018b). The GEMS network allows us, for the first time in Ethiopia, to study the synergy between synoptic and mesoscale weather dynamics and crop growth in the Gamo Highlands.

The objective of this study was, therefore, to study the temporal and spatial variations in weather as a function of topography and their impact on potato crop growth during the *belg* season of 2017. The specific research questions were as follows:

1)  *How does the topography and presence of lakes induce mesoscale circulations in the Gamo Highlands during the belg season?*

2)  *How do the mesoscale circulations interact with the synoptic circulation driven by the ITCZ?*

3)  *How do the weather variations resulting from this interaction affect crop growth?*

As such, we used the datasets from our new GEMS network in the Gamo Highlands. Our analysis was based on almost entirely on observations. Only to determine the impact of meteorology, we employed a potato growth model (Minda *et al.*, 2018b; Yin and van Laar, 2005) using the newly GEMS observed weather information as input. In doing so, we improved our understanding about crop dynamics as affected by elevation and meteorology.

The paper is structured as follows: Section 4.2 presents the GEMS network, field experiments in potato crop and the plan to use the network for weather and crop dynamics study. Section 4.3 shows results from the GEMS datasets in explaining the mesoscale and synoptic dynamics with crop growth modelling. The discussion and conclusions are provided in Sections 4.4 and 4.5.

## 4.2 Methods

### 4.2.1 Description of the GEMS network datasets

In April 2016, we installed a network of six automatic weather stations along two transects in the Gamo Highlands, Ethiopia. These highlands include complex terrain with elevation ranging from 1100 to 3600 m a.s.l., covered by a mixture of forests, bare and agricultural lands and two large lakes (~10 km × 100 km). The Arba Minch station, close to the Lake Abaya and Arba Minch University main campus, was used as a reference station with which we compared the results of all the highland stations. Except for Arba Minch and Zigiti, all the stations are located on the terrain of experimental potato farms. All the station sites are not irrigated and covered by short grasses. Details about the locations of the stations in the GEMS network are shown in Table 4.1 and Figure 4.1.

**Table 4.1 | Gamo Ethiopian Meteorological Stations (GEMS) and potato crop field experiment site descriptions. Key: Lon—longitude; Lat—latitude; Elv—elevation; LULC—land use land cover; N, E, S, W—north, east, south, west.**

| Station | Transect | Location Lon (°E) | Lat (°N) | Elv (m) | Location Description | Soil [a] (LULC [b]) Description | Potato Planting Dates |
|---|---|---|---|---|---|---|---|
| Arba Minch | Ref. | 37.568 | 6.067 | 1200 | A plain farm | Vertisols (crop) | |
| Tegecha | SN | 37.573 | 6.161 | 2091 | Near forest (S), valley (W) & mountain (N) | Nitisols (crop, forest) | 5 April 2017 |
| Chencha | SN | 37.571 | 6.254 | 2753 | Rural town | Andosols (crop, rural settlement) | 25 March 2017 |
| Gircha | SN | 37.564 | 6.302 | 3015 | Open grazing land | Andosols (crop, grazing land) | 7 March 2017 |
| Zigiti | EW | 37.459 | 6.073 | 2414 | Near mountain (N) | Nitisols (crop, rural settlement) | |
| Gazesso | EW | 37.337 | 6.130 | 2847 | Rural town, near mountain | Andosols (crop, rural settlement) | 2 March 2017 |

[a]*Data were obtained from the International Soil Reference and Information Centre (ISRIC) soil grids (https://www.soilgrids.org/#!/?layer=TAXNWRB_250m&vector=1);* [b] *The Ethiopian Sentinel-2 land-use land-cover (LULC) 2016 data were obtained from the Regional Centre for Mapping of Resources for Development (RCMRD) GeoPortal (http://geoportal.rcmrd.org/layers/servir%3Aethiopia_sentinel2_lulc2016).*

Figure 4.1 shows the location of the stations and potato crop field trial farms related to the topography in the digital elevation model (DEM) (accessed from Reference Ramapriyan and Murphy (2017)). The DEM has a horizontal resolution of 30 m. It is relevant to mention that, in designing the GEMS network, we defined a south–north (SN) transect, composed of the stations Arba Minch, Tegecha, Chencha and Gircha; an east–west (EW) transect, composed of the stations Arba Minch, Zigiti and Gazesso. The SN transect starts in the non-potato growing zone near Arba Minch and Lake Abaya; moves into the higher-elevation potato growing areas around Tegecha, Chencha and Gircha. This transect is a south-facing slope. Potato is the major crop along this transect during the *belg* season, while farmers also grow enset (*Ensete ventricosum*, known as Ethiopian banana), wheat, barley, vegetables and apple (Mazengia *et al.*, 2015). Gircha is nearly at the top of the mountains and represents locations which are somewhat higher than the main potato-growing elevation range. The EW transect also starts in Arba Minch. The east-facing slope to Zigiti is very steep. Zigiti is in a diverse, small-scale agricultural landscape where local farmers mainly grow wheat and barley, followed by enset and potato during the *belg* cropping season. Moving from Zigiti, the transect enters into the next valley, where the Gazesso station is located on an east-facing slope. Its exposure to the lake breezes will probably be different. In the EW transect, potato is grown starting from the Zigiti station. The GEMS network set-up in two transects allows us to study how the locations are influenced by the mesoscale (*e.g.* lake breezes and mountain flows) and large-scale weather systems such as the ITCZ and their roles in potato crop dynamics in the highlands.
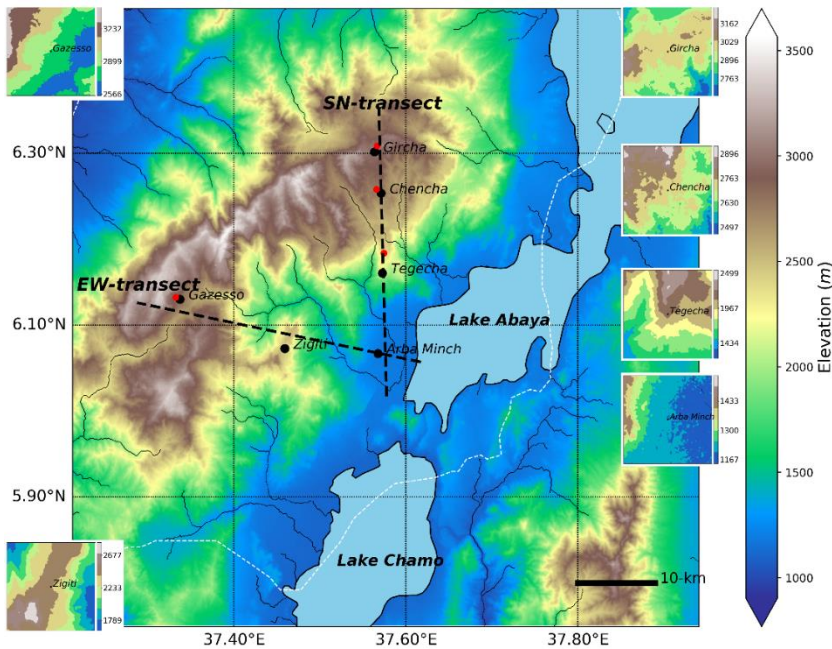
**Figure 4.1 | Six GEMS stations network (black dots) and potato experimental farms (red dots). The large digital elevation model covers an area of 80 × 80 km² and the insets cover 5 × 5 km² area. The dashed black lines show the south–north (SN) and east–west (EW) transects of the network. The dashed white line represents the approximate southeast (SE) boundary of the Gamo Highlands.**

The GEMS network measures (1) meteorological variables, (2) soil moisture tension and soil temperature at four depths (5, 10, 20 and 40 cm) and (3) leaf wetness (an artificial-leaf electrical-resistance type that indicates whether the surface of a foliage in the area is wet or dry by indicating how wet the surface of the sensor is) facing east and west directions (Table 4.2) (Instruments, 2006b). These environmental variables were measured at the data update interval shown in Table 4.2 for each sensor in which 15-min statistics were recorded. Five of the six GEMS are Davis Vantage Pro2 + (DVP2) automatic weather stations and the other (in Chencha) is a Campbell instrument model (Campbell Scientific (CS) CR200X series data-logger, CS Africa, South Africa). Both weather stations are widely used globally (Bell *et al.*, 2015; Lagouvardos *et al.*, 2017; Steeneveld *et al.*, 2014). These stations showed the best agreement compared with a professional meteorological monitoring system for air temperature, relative humidity, dew point and precipitation measurements in a systematic comparison (Bell *et al.*, 2015). Station maintenance, cleaning of sensors, temperature/relative humidity sensor radiation shields and precipitation buckets were done on a weekly basis for the Arba Minch station and a two-weekly basis for the other ones, which are off-road and remote stations. Although we installed GEMS network starting April 2016, in this study, we selected the *belg* of 2017, because of its relevance to potato growth (Minda *et al.*, 2018b).

**Table 4.2 | The automatic weather stations types, weather variables measured, sensor type, measurement resolution, sensors' measurement accuracy, and data update interval of the sensors [47]. Key: AWS – automatic weather station; SLP – sea-level pressure.**

| AWS | Variables Measured | Sensor Type | Resolution | Accuracy (±) | Update Interval |
|---|---|---|---|---|---|
| | Incoming shortwave radiation (SW↓) | Silicon photodiode | 1 W·m⁻² | 2% of full scale | 50 s to 1-min |
| | Temperature ($T$) | P–N junction silicone diode | 1 °C/ | 0.5 °C/ | 10 s |
| | Relative humidity (RH) | Film capacitor element | 1% | 2% | 50 s |
| | Precipitation (PPT) | Tipping bucket with magnetic switch | 0.2 mm | greater of 4% or 1 tip | 20 s |
| **Davis Vantage Pro2 + (DVP2)** | 2 m wind speed ($u$) | Solid state magnetic sensor | 0.1 m·s⁻¹ | 1 m·s⁻¹ | 2.5 s |
| | 2 m wind direction ($\varphi$) | Wind vane potentiometer | 22.5 on compass rose | 3° | 2.5 s |
| | Barometric pressure (SLP) | Davis Instruments 6322 | 0.1 hPa | 1.0 hPa | 1-min |
| | Soil moisture tension ($\psi$) | Watermark | 1 kPa | | 77–90 s |
| | Soil temperature ($T_{soil}$) | Precision thermistor | 1 °C | 0.5 °C | 77–90 s |
| | Leaf wetness (LW) | Artificial leaf electrical resistance | 1 (0 to 15 range) | 0.5 | 1-min |
| | SW↓ | LI-COR 200 r pyranometer | | <1% over 360° | |
| **Campbell Scientific (CS)** | $T$/RH | CS215-L | | 0.10 °C/2.0% | |
| | PPT | Pronamics professional rain gauge | 0.1 mm | 2.0% | |
| | $u$/$\varphi$ | 03001 Wind Sentry Anemometer/Vane | | 0.5 m·s⁻¹/5° | |

**4**

### 4.2.2 ITCZ progression

To determine the synoptic circulations, we used the GEMS network sea-level pressure (SLP) data and related it to the ITCZ data obtained from the NOAA Climate Prediction Center (NOAA-CPC) and the African Center for Meteorological Application for Development (ACMAD) (ACMAD, 2017; NOAA, 2017). The NOAA-CPC calculates the ITCZ latitudinal variation from the daily analysis of two key weather properties: (i) the location where the surface dew point temperature is closest to the 15-degree isodrosotherm; (ii) the region where the lower-level (925 hPa) wind streamlines delineate the axes of zonal convergence. These 10-daily averaged data are available for 15° west (W) to 35° east (E) from April to October. We considered the ITCZ latitudinal variation at 35° E. Note that the Gamo Highlands are located at ~37° E.

### 4.2.3 Analysis of the GEMS datasets

Southern Ethiopia shows a bimodal precipitation regime, in which the main precipitation is during the *belg* season with rainfall maxima in April (Diro *et al.*, 2008). The year 2017 is characterised by a weak La Niña condition in the central and eastern Pacific Ocean (Blunden *et al.*, 2018). As a result, southern Ethiopia showed a 1–2 °C warmer and drier (30%–50% less precipitation) season as compared to the 1981–2010 ERA-Interim data (Tsidu, 2018) during three months (March to May) of the *belg* 2017.

The GEMS network is planned as a long-term (more than five years) meteorological monitoring stations' network. These data will be combined with crop growth monitoring field experiments to understand how certain varieties adjust to this meteorology depending on elevation. We selected the *belg* season during 2017 because of its meteorological (moisture availability) and agronomical suitability to grow potato (Tufa, 2013). From the *belg* season, we further selected the months of February and May because of their contrasting circulation regimes. February (dry) is predominantly driven by mesoscale regimes whereas large-scale circulation features mainly influence May (wet). For February, we focused on the temporal and spatial variabilities of mesoscale dynamics (*e.g.* wind and the conserved variables such as potential temperature ($\theta$; K) and specific humidity ($q$; g·kg$^{-1}$)). For May, we analysed precipitation, which is predominantly driven by large-scale circulation features such as the ITCZ and further pronounced by elevation. We analysed the May precipitation data along the SN transect (for Arba Minch, Tegecha and Chencha), because the data were more complete than the EW transect.

Our criteria for distinguishing between day and night were as follows: we considered incoming shortwave radiation (SW↓) >20 W·m$^{-2}$ as day conditions and SW↓ = 0 W·m$^{-2}$ as night conditions. To calculate $\theta$ and $q$, we needed pressure at stations' locations. Note that the DVP2 stations calculate the necessary correction factor to

consistently translate atmospheric pressure to SLP to standardise pressure measurements at different altitudes (Instruments, 2006a). The stations' atmospheric pressure is calculated (with the sea-level temperature being estimated from the projected temperature of the GEMS network measurements) for a column of air between sea level and a station's elevation using the hypsometric equation (Stull, 2000). We also calculated tendencies (time-derivatives of θ and q; ∂θ/∂t and ∂q/∂t) to investigate lake-breeze and mountain-breeze flow development during the prominent mesoscale-driven month. DVP2 stations measure soil moisture tension of the soil on a scale of 0 kPa (wettest soil) to 200 kPa (driest soil). The Watermark soil moisture sensor measures an electrical resistance that is related to soil water tension (Table 4.2) (Davis-Instruments, 2018).

### 4.2.4  Potato crop field experiment trials

Potato field experiments at the plot scale were conducted in the vicinities of the weather stations (Tegecha, Chencha, Gircha and Gazesso) during the *belg* farming season in 2017, as shown in Figure 4.1. We planted improved (*Gudenie* and *Belete*) (MOANR, 2016; Woldegiorgis, 2013) and local (*Suthalo*) varieties. In this study, we considered cultivar *Belete* as the data on this cultivar were complete for different elevations. We applied the randomised complete block (RCB) design (Gomez *et al.*, 1984) with three replications. This design is recommended for experimental areas with a predictable fertility gradient and is one of the most widely applied field experimental designs in agricultural research (Gomez *et al.*, 1984). The planting pattern was 0.75 m × 0.30 m, the plot size was 3 m × 3 m, the plant density was 4.4 plants·m$^{-2}$, the fertilizer doses were 236 kg·ha$^{-1}$ of nitrogen/phosphorus/sulfur (NPS: 19N, 38P$_2$O$_5$, 0K$_2$O and 7S), 125 kg·ha$^{-1}$ of muriate of potash (MOP: KCl (95–99.5%)) and 144 kg·ha$^{-1}$ of urea (CO(NH$_2$)$_2$). Fertilizers were added upon planting, but urea was split into two additions (half upon planting, half during flowering stages). Data on the crop growth variables (*e.g.* the plant height) were measured on a daily basis (at Gircha and Gazesso farms) and yield parameters were collected. Data were taken from the middle two rows to minimise border effect. From the two rows, five plants were randomly selected and continuously monitored for plant height; the averages of the three plots were reported. In addition, the farm management practices such as tillage were documented. The Arba Minch station (1200 m) does not have a suitable climate for growing potato crop, because the temperature is too high there (Khan, 2012).

### 4.2.5  Simulating crop growth variation along mountain slope using the GECROS model

The GEMS network data were analyzed and used as input on a daily basis to the "Genotype-by-Environment interaction on CROp growth Simulator" (GECROS)

crop model (Yin and van Laar, 2005). The model is the state-of-the-art crop model, which is widely applied for modelling of crop dynamics of the world's major crops. More specifically, it was used for potato crop growth modelling (Khan *et al.*, 2014) and also applied in the Gamo Highlands (Minda *et al.*, 2018b). GECROS is "an eco-physiological model that predicts crop growth and development as affected by genetic characteristics, climatic and edaphic environmental variables" (Khan *et al.*, 2014). The model can be used for examining responses of biomass and protein production in arable crops to both genotypic and environmental characteristics (Yin and van Laar, 2005).

The crop model uses environmental variables and biophysical inputs such as seed weight. The weather variable inputs are SW↓ ($MJ·m^{-2}·d^{-1}$), $T_{min}$ (°C), $T_{max}$ (°C), vapor pressure deficit (VPD; kPa), $u$ ($m·s^{-1}$) and PPT ($mm·d^{-1}$) input at a given latitude on day (d) basis. Model inputs such as crop management options, crop/genotype-specific parameters, soil type/moisture and model constants were taken from Minda *et al.* (2018b).

The crop growth model was coupled with a process-based soil model. The soil data (percent clay in the soil, the total organic carbon in the soil, soil water content at maximum holding capacity, soil water content at field capacity and minimum soil water content) were taken from the ISRIC database (Leenaars *et al.*, 2014) following statistical analysis explained in Minda *et al.* (2018b). For further model details, the reader is referred to Yin and van Laar (2005). Here, we used the tailored model parameters as listed in Minda *et al.* (2018b)[†]. Our main objectives of applying the GECROS model: using the GEMS network data, were to study the sensitivity of crop growth variables and yield to (1) elevation and (2) modifications in the stations' weather observations.

### 4.2.6 Model's sensitivity to changes in the observed GEMS network datasets

GECROS enabled us to perform sensitivity analyses of potato growth to weather variations. Therefore, we conducted the model sensitivity experiments by exchanging the weather in the peak rain *belg* month (May) with March (early *belg* rain onset assumption), with April (climatologically normal *belg* assumption) and with June (late *belg* assumption), while maintaining the data of the other periods as observed. To determine the role of the meteorological variability, we also conducted experiments with average weather input data, *i.e.* where GECROS was run each day with the same diurnal cycle based on the average SW↓, $T_{min}$, $T_{max}$, PPT and VPD over the *belg* season. Table 4.3 presents the detailed design of the sensitivity experiments.

The control run consisted of the one presented and it was compared with crop observations. In this run, all the observed meteorological variables were the input for the model. Sensitivity experiments 1–5 ($SW↓_{avg}$, $T_{min, avg}$, $T_{max, avg}$, $PPT_{avg}$ and $VPD_{avg}$) were with the same meteorological inputs, except that one variable was averaged over the *belg* season. Experiments 6–8 (Early *belg*, Normal *belg* and Late *belg*)

were again with the original meteorological data, but now the May data were exchanged either with March, April, or June data to simulate an early (max PPT in March), normal (max PPT in April) and late (max PPT in June) *belg* precipitation onsets, respectively. Other model input parameters and variables are identical to the experiment set-up in Minda *et al.* (2018b). All the experiments were done for each station mentioned.

**Table 4.3 | GECROS model sensitivity experiment design. PPT—precipitation; VPD—vapor pressure deficit.**

| No. | Experiment | Experiment Name | Description of Input of Meteorological Variables |
|---|---|---|---|
| 0 | Control | Control | 6 variables as observed |
| 1 | SW↓ | SW↓, avg | 5 variables as observed + *belg*-averaged SW↓ |
| 2 | $T_{min}$ | $T_{min, avg}$ | 5 variables as observed + *belg*-averaged $T_{min}$ |
| 3 | $T_{max}$ | $T_{max, avg}$ | 5 variables as observed + *belg*-averaged $T_{max}$ |
| 4 | PPT | $PPT_{avg}$ | 5 variables as observed + *belg*-averaged precipitation |
| 5 | VPD | $VPD_{avg}$ | 5 variables as observed + *belg*-averaged VPD |
| 6 | early-*belg* | Early *belg* | exchanging May and March observation + other periods as observed |
| 7 | normal-*belg* | Normal *belg* | exchanging May and April observation + other periods as observed |
| 8 | *belg*-in-*kirmet* | Late *belg* | exchanging May and June observation + other periods as observed |

## 4.3 Results

### 4.3.1 Monthly variability: The role of large-scale weather dynamics in the Gamo Highlands

Figure 4.2 shows the SLP observations at Arba Minch (1200 m a.s.l.). Here, we considered low SLP as a proxy for the proximity of the ITCZ. The Ethiopian precipitation climatology is mainly determined by the seasonal variation in the latitudinal position of the ITCZ relative to area of interest (Korecha and Barnston, 2007). The ITCZ is one of the main large scale processes that influences the *belg* precipitation in Ethiopia (Berhane and Zaitchik, 2014). Figure 4.2 also shows the SLP (hPa) and the temporal latitudinal movement of the ITCZ climatological (2003–2013) and during *belg* 2017 data. In the figure, the 15-min resolution SLP observations were averaged and reported as daily values. For additional explanation of Figure 4.2, the reader is referred to the map of Ethiopia in Minda *et al.* (2018b) and seasonal latitudinal variation of the ITCZ over the African continent shown in Nicholson (2018).
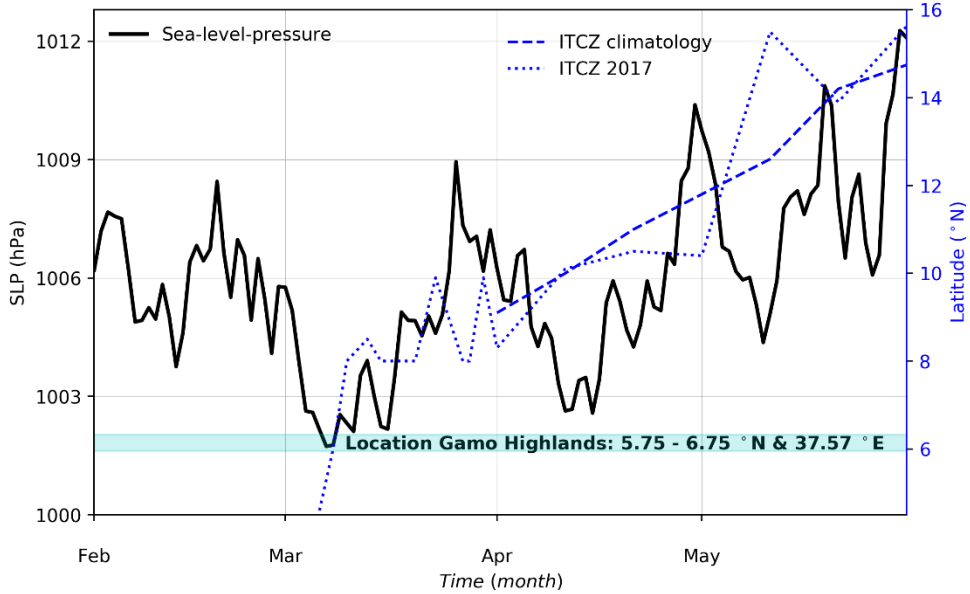
**Figure 4.2 | The daily mean observed SLP at Arba Minch station during the *belg* season of 2017. The SLP (black line with scale on the left y-axis); latitudinal variation of the ITCZ climatology (15-year data following Section 4.2.2) and in 2017 (blue lines with blue right-side y-axis). There are no ITCZ location data before March. The cyan-colored horizontal bar shows the latitude range of the Gamo Highlands.**

Figure 4.3 shows the daily variations in mean temperature and the monthly variations in precipitation during *belg* 2017 for the Arba Minch and Gircha stations, as the weather variables are the major atmospheric crop growth derivers. The 15-min interval observations were calculated and averaged to daily mean temperature and monthly total precipitation. The 30-year climatological (1987–2016) average temperature and precipitation daily observations during *belg* season for the Arba Minch station are also depicted for comparison.

**Figure 4.3** | **Observed temperature (left axis) and total monthly precipitation (right axis) during** *belg* **2017 and following the 1987–2016 climatology. The green-colored bars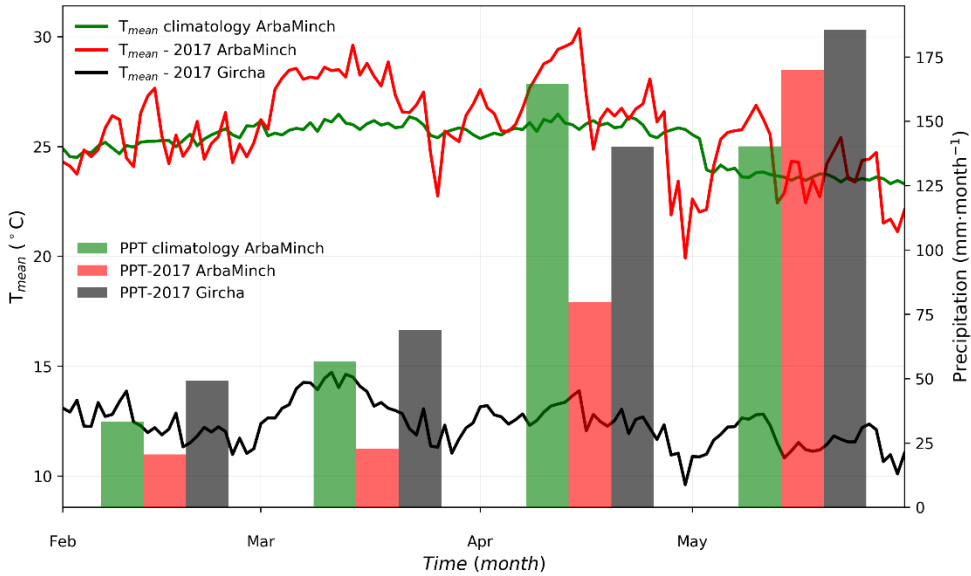 show the climatological** *belg* **data from Arba Minch station (data obtained from the NMA, Ethiopia), the red- and black-colored bars show the 2017** *belg* **season as observed by the GEMS network. The GEMS data were averaged/summed to daily/monthly values.**

Based on Figure 4.2 and Figure 4.3, in February, the ITCZ is located far south of the Gamo Highlands (*i.e.* ~10–15° S) and the Gamo Highlands were at higher pressure relative to the ITCZ. The SLP decreases slowly by ~3 hPa at the end of the month as the ITCZ approaches the Gamo Highlands (Figure 4.2). In this month, the highlands are less influenced by the ITCZ. As a result, the northeasterly winds transport dry air from the Arabian Peninsula. In March, the ITCZ passes the Gamo Highlands (5.75–6.75° N) and the observed SLP was at its minimum (1002 hPa). Still, there is hardly precipitation in this period (Figure 4.3). In turn, from March until the end of May, the ITCZ moved toward northern Ethiopia. In this period, the highlands experienced a higher-pressure system again (SLP increased by ~10 hPa from the minimum in March). Most precipitation fell in the Gamo Highlands after the passage of the backward tilted slope of the ITCZ front, *i.e.* when the front was located between 10 and 14° N. The position of the ITCZ northward of the Gamo Highlands favours southeasterly winds and moisture transport from the Indian Ocean (Berhane and Zaitchik, 2014; Diro *et al.*, 2011a). The Gamo Highlands received >80% of the *belg* precipitation in April and May (Figure 4.3).

The 2017 *belg* season occurred during La Niña year (Blunden *et al.*, 2018), which is characterised by lower than normal and delayed precipitation in the Gamo Highlands (102 mm less and one-month delayed). Less and delayed *belg* precipitation (peak precipitation shift from April to May) as occurred in 2017 are typical La Niña

impacts to our region (Diro *et al.*, 2011a). In 2017, Arba Minch and Gircha received 293 and 443 mm of precipitation, respectively, during the *belg* season, which was ~43% of the annual total. *Belg* 2017 was also characterised by warmer weather (+1.0 °C) as compared to the *belg* climatology in Arba Minch. The average daily *belg* temperature was 25.8 °C for Arba Minch and 12.4 °C for Gircha, with a daily temperature variability of ±4.0 °C and ±2.3 °C at Arba Minch and Gircha, respectively, and in terms of standard deviation. Tsidu (2018) also showed that southern Ethiopia during *belg* 2017 was warmer than the 1981–2010 mean climatology by 1–2 °C (based on the ERA-Interim reanalysis data).

February, the first month of *belg* 2017, was somewhat cooler (0.6 °C and 0.1 °C for Arba Minch and Gircha, respectively) than the other *belg* 2017 months. In this month, the ITCZ was located in the southern hemisphere and the GEMS network measured a relatively higher pressure (Figure 4.2). March was the warmest (+1.5 °C and +0.7 °C compared to the mean 2017 *belg* for Arba Minch and Gircha) and the ITCZ was directly overhead the Gamo Highlands (Figure 4.2). In spite of having the ITCZ overhead, cooler and wetter weather did not yet occur in the highlands in 2017. The warmer period continued until half of April and the Gamo Highlands did not receive the expected precipitation. Ultimately, May was the coolest (−1.9 and −0.8 °C less than *belg* 2017 for Arba Minch and Gircha) and wettest month of the *belg* season.

It is interesting to relate these findings to the diurnal variations in the various months in our study. To this end, we calculated the diurnal evolution of wind direction at the Arba Minch and Chencha stations (Figure 4.4), where Arba Minch is representative of the lowlands and Chencha of the highlands. This diurnal evolution was calculated as an average during the entire month. The standard deviation is also presented to show the variability in the observations. For February, we found that during daytime (0600–1800 local standard time (LST)), easterly flows occur in Arba Minch and southerly flows in Chencha. Note that time is reported in LST (coordinated universal time (UTC) +3). The wind direction in the months of March and April is similar to that in February. In contrast, for May, the wind direction was mainly southerly to southeasterly, indicating a pronounced role of large-scale circulations in relation to the ITCZ (see Figure 4.2). Figure 4.4 shows a daily pattern dominated by the mesoscale wind circulations, caused by the topography and the presence of the two lakes. In May, the synoptic scale was predominant than the mesoscale flows. Then, in particular, for Chencha, the southeasterly component of the large-scale wind is well aligned with the lake breezes and the anabatic winds during the day, causing strong upslope flow. These features are discussed in the following section.
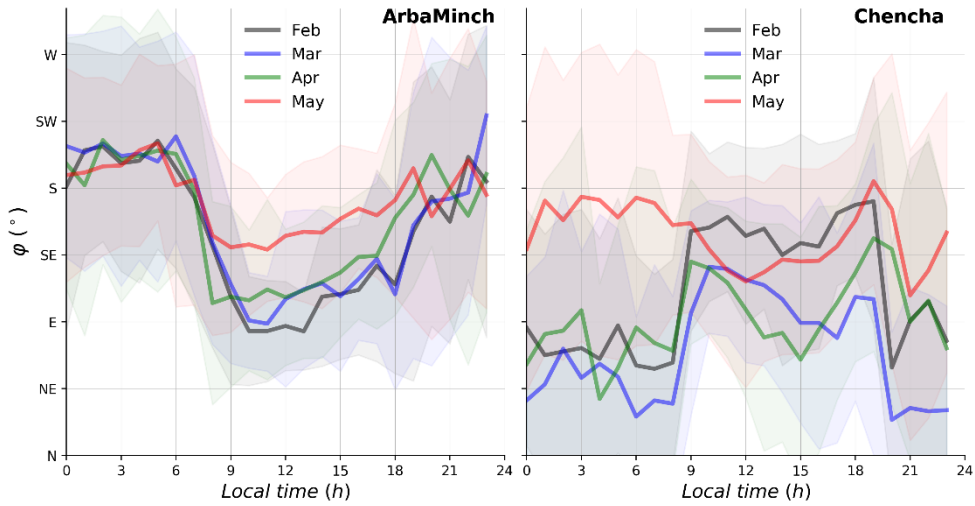
**Figure 4.4 | Diurnal evolution of monthly average wind direction (φ (°)) observed at reference (Arba Minch) and Chencha stations on the SN transect during** *belg* **2017 (Figure 4.1). The shaded regions show mean ± standard deviations. Note that the standard deviations are calculated on hourly-averaged data for each month.**

### 4.3.2 Mesoscale dynamics: The role of lake-breezes and mountain flows in the Gamo Highlands

#### 4.3.2.1 *Day–night contrast in February and May winds*

Figure 4.5 provides more detail on the diurnal variability of 2-m wind direction (φ (°)) and speed ($u$ (m·s⁻¹)). We focus on the contrasting day and night values in φ and $u$ as explained in Section 4.2.3.
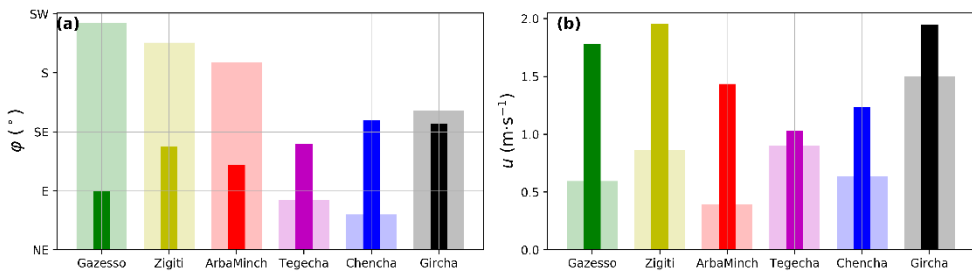


**Figure 4.5 | The dominant local wind sources in the GEMS stations network in Feb 2017 during day-time (full-colored bar plots) and nighttime (light-colored bar plots). The left and right plots show wind direction (a) and wind speed (b), respectively, as explained in Section 4.2.3.**

In February, during daytime, all the stations had nearly a southeasterly wind, except Gazesso, which is across the first mountain range in a second valley along the

EW transect (Figure 4.1 and Figure 4.5a). The $u$ ranged from 1 to 2 m·s⁻¹. It is interesting to note that, during daytime, the prevailing wind directions at all the stations were from between the southern part of Lake Abaya and the northern part of Lake Chamo and directed upward into the broad direction of the slope. The easterly wind direction in Gazesso matches with the direction of the main valley (Figure 4.1) headed from the lakes (more easterly as compared to other stations getting southeasterly flows). These directions also align with the general direction of the synoptic winds in February.

In contrast, the nighttime winds were characterised by south to southwesterly (SSW) flows along the EW transect (Zigiti and Gazesso) and by east to northeasterly (ENE) flows along the lower part of the SN transect (Tegecha and Chencha). These wind directions were not in the general (larger-scale) downslope direction. However, by looking at a detailed high-resolution topography map (see insets in Figure 4.1), we show that the nighttime wind followed small-scale topographic features. For example, in Chencha, the larger scale slope is toward the southeast, but very locally, the slope is toward a discharge valley in the west to southwest (WSW), causing ENE katabatic flows. The winds are downslope mountain flows in both transects. This is because the nighttime mountain winds form a much shallower mesoscale circulation than the daytime lake breeze and valley winds. These are typical characteristics of katabatic winds influenced by topography (Whiteman, 2000; Zardi and Whiteman, 2013).

The wind direction at Gircha was quite invariable between day and night, and also the strongest. This is because the station is located near the mountain crest and is, at night, less exposed to mountain winds from higher altitudes. As a result, the wind direction is aligned with the southeasterly background wind during day and night.

The shift in wind direction between day and night at all other stations and the alignment of the wind direction with the slopes and the direction of the lakes are clear indicators of the presence of a combined lake and valley breeze flows (Crosman and Horel, 2010). These patterns break in May. The wind direction at all stations becomes more southerly during the day and at night than in February (analysis not shown here) with minimal diurnal variations in $u$ and $\varphi$. The major difference is the direction of the synoptic-scale winds as a function of the position of the ITCZ. In February, it was directed from the southeast and, in May, from the south. The stronger influence of synoptic-scale winds in May disturbed the mesoscale dynamics, which were so prominent in February.

### 4.3.2.2   *Diurnal variability of θ and q in February along the slope*

Figure 4.6 provides a characterization of the spatial variation of the diurnal cycle of meteorological variables θ (K) and q (g·kg⁻¹) in February.
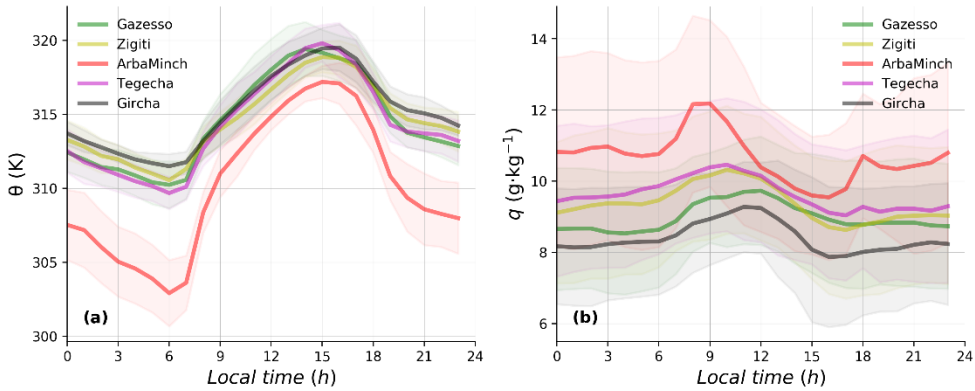
**Figure 4.6 | Diurnal evolution of potential temperature (θ) (a) and specific humidity (q) (b) in February 2017. The shaded regions show mean ± standard deviation (computed on hourly averages). Chencha is not included here for lacking SLP data (Table 4.2). Note that the standard deviation follows similar calculations to that of Figure 4.4.**

Figure 4.6a shows a distinct difference between the highland stations (Tegecha, Gircha, Zigiti and Gazesso) on the one hand and Arba Minch on the other hand. The highland stations had a very similar θ during night and at day, whereas the lowland station clearly had a 3–7 K lower θ. The difference between Arba Minch and the highland cluster is explained as follows: Arba Minch is the station nearest to Lake Abaya (Figure 4.1) and located in a relatively flat area. At night, the lowlands become cooler due to the combination of katabatic winds and the local longwave radiative cooling that creates stagnant stable boundary layer.

Figure 4.6b shows a similar distinction of the stations based on specific humidity (q): the highland stations and the lowland station displayed q with a more pronounced diurnal cycle than at the highland stations. However, the q was more variable among the highland stations than θ was (Figure 4.6a).

During the day, the lake breeze advected relatively cool and moist air toward the highlands. The nearly identical potential temperature and specific humidity at all highland stations was an indication that they were exposed to air from the same origin. The transition from mountain/land breeze to a valley/lake breeze was associated with the development of an internal boundary layer, because of more turbulent mixing over land than over the lake. This internal boundary layer was advected inland during the day. The most forward position was marked by the valley/lake wind front and was often detectable by strong changes in wind direction and speed, as well as temperature and humidity. In order to quantify the changes caused by the progression of this valley/lake breeze front, we show monthly, *i.e.* February 2017, averages of $\varphi$ and $u$ together with the tendencies (time-derivatives) of potential temperature ($\partial\theta/\partial t$) and specific humidity ($\partial q/\partial t$) (Figure 4.7).

At the Arba Minch station, the calm mountain/land breeze at night shifted to a stronger lake breeze between 0700 h and 0900 LST, as the convective boundary layer (CBL) developed and the lake breeze gained strength (Figure 4.7a,b). At the highland stations, Tegecha and Gircha, the wind speed changed almost at the same time or earlier than in Arba Minch. Since the lake breeze front needs time to travel up the mountains, the wind direction and speed change cannot be caused by the lake breeze front alone and the wind shift indicates the transition from mountain winds into valley winds.

Based on Figure 4.7c,d, we identified four stages in the temperature and humidity tendencies: (1) a stable stratification stage before sunrise, (2) an increasing stage between sunrise and 0800 LST, when the solar radiation causes heating and evaporation of dew, (3) a decreasing stage until 0900 LST, when the stronger valley wind, the arrival of the lake breeze front and associated atmospheric mixing cause the temperature and humidity to drop (remember that the $\theta$ at Arba Minch was lower than in the highlands (Figure 4.6)), and finally, (4) a nearly stable stratified stage in a well-mixed boundary layer after 0900 LST and a well-established lake breeze circulation (Figure 4.7c,d). The $\theta$ in the highlands was very comparable and q decreased predictably with elevation (Figure 4.6). The tendency in q followed a similar pattern as that of $\theta$ (Figure 4.7d), except that the maximum values occurred within an hour's time after sunrise instead of 2 h with pronounced temporal variations.
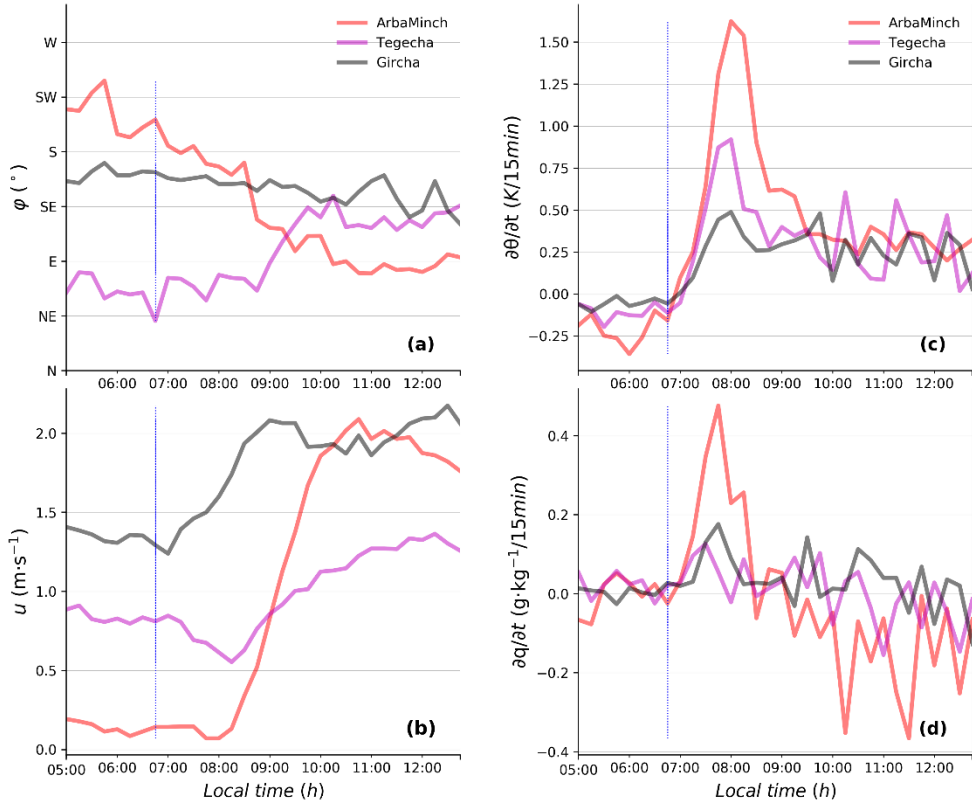
**Figure 4.7 | (a) φ (°), (b) u (m·s⁻¹), (c) ∂θ/∂t (K/15-min), and (d) ∂q/∂t (g·kg⁻¹/15-min) during the shift from stratified boundary layer to convective boundary layer in February 2017. The vertical lines show the approximate time of sunrise time in February 2017.**

Figure 4.7 shows the development of lake breezes during daytime. Changes in wind flows, θ, and q tendencies occurred after sunrise (0700 LST), marking the start of the lake breeze circulation. Similarly, relatively weaker the changes in these variables in the afternoon occurred approximately at 1630 LST, which shows the start of the mountain/valley flows (analysis not shown here) (Gebremariam, 2007). In the next section, we focus on how precipitation develops under influence of the meso- and synoptic-scale weather.

### 4.3.2.3  *Large-scale dynamics in modulating belg precipitation*

Figure 4.8 presents the diurnal variations of precipitation (mm/3h), φ (°), and SW↓ (W·m⁻²) in May for Arba Minch, Tegecha, and Chencha in the SN transect. The month of May was the wettest month of *belg* 2017.

During the complete *belg* 2017, the precipitation increased with elevation. More specifically, Arba Minch received 293 mm·*belg*⁻¹, Tegecha 459 mm·*belg*⁻¹, and Chencha 540 mm·*belg*⁻¹ (not shown here). This trend is similar to the one we found in the

WRF-modelled precipitation in Minda *et al.* (2018b). The May precipitation accounted for 40%–60% of the total *belg* precipitation in Arba Minch, Tegecha, and Chencha. The SN transect in Figure 4.8 also shows large spatial variability in precipitation. However, in the month of May alone, Tegecha received more precipitation (265 mm·month$^{-1}$) than the other stations along the SN transect. Most precipitation fell in the evening and during the night (Figure 4.8). Houze (2012) discussed that, on mountains, most nighttime precipitation happens near the base of the mountain, where the katabatic wind converges with low-level moist unstable air.

The wind regimes in May (Figure 4.8) were entirely different from those in February (Figure 4.5). Focusing on the SN transect (Figure 4.8), in May, moist, southeasterly to southerly synoptic air masses from the Indian Ocean dominate the day and night weather dynamics (Jury, 2014b; Minda *et al.*, 2018b; Viste, 2012). Furthermore, our GEMS network showed that there was nearly no significant diurnal variability in wind source and the southeasterly prevailing wind (~150–180°) (Figure 4.8), which was driven by the synoptic scale dynamics. Therefore, we explain the enhancement of late evening to nocturnal precipitation by two factors. Firstly, during the daytime, the combined effect of anabatic, valley-mountain winds, and the synoptic forcing transport moist air to higher levels, and secondly, this triggers and enhances cloud formation and intensity (shown by the decrease in SW↓ in Figure 4.8 between 1500 and 1800 LST compared to between 0600 and 0900 LST) and the subsequent precipitation during the night.



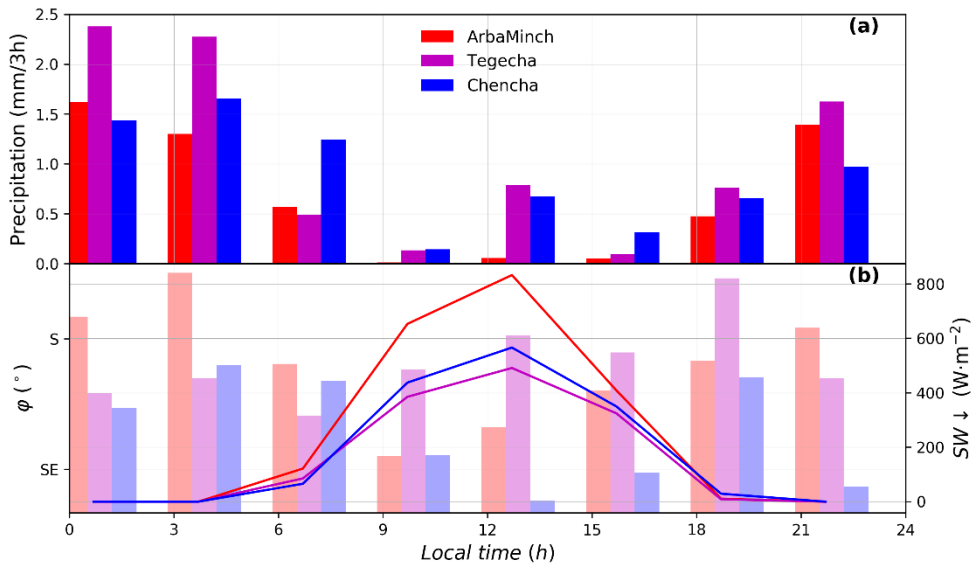**Figure 4.8 | (a) 3-h total precipitation (mm·3h$^{-1}$), (b) 3-h mean φ (°) (bar plots) and SW↓ (W·m$^{-2}$) (line plots). Data from Arba Minch, Tegecha, and Chencha GEMS network in the SN transect in May.**

### 4.3.3 Crop modelling using GEMS network meteorological data

*4.3.3.1 Simulated and modelled crop growth gradient along the SN transect*

Figure 4.9 shows a selection of the modelled potato growth variables with observed yield at experimental potato farms (Figure 4.1) located at Tegecha (2140 m), Chencha (2738 m), and Gircha (3010 m). The attainable yield and the growth variables were the LGS (*i.e.* days to crop maturity) and maximum plant height (MPH, *i.e.* plant height at maturity).

The figure shows that the observed LGS increased from 95 d in Tegecha to 120 d in Gircha. The model underestimated the observed LGS by 19% in Tegecha, represented Chencha fairly well, and overestimated it by 7% in Gircha (Figure 4.9a). The MPH increased from 72 cm to 81 cm as we went up from Tegecha to Gircha, in which the model mainly overestimated the observed MPH. The observed yield increased from 27 t·ha$^{-1}$ in Tegecha to 52 t·ha$^{-1}$ in Chencha and almost stabilised as elevation increased further. For Chencha and Gircha, the model largely underestimated the yield observations. In practice, Tegecha is a few meters above the lowest level where potato is grown; at the lower elevations, the climate is too warm and dry to support potato crop growth. Similarly, Gircha (3015 m) was around the maximum elevation where potato was grown; at higher elevations the climate was too cool and wet (Figure 4.3), with subsequent risk of diseases at extended LGS. Between these extremes, however, the conditions for growing potato were optimal (Minda *et al.*, 2018b). Figure 4.9c shows the attainable yield, which was the maximum yield attained considering soil type, climate, and cultivar, but without considering yield loss due to sub-optimal crop management and diseases, as the observed yield was. In the present case, however, the situation was quite the opposite. At higher altitudes, the attainable yield was some 35 t·ha$^{-1}$, while the observed yield was 50–55 t·ha$^{-1}$. One of the reasons for the mismatch between modelled and observed yield is that yield observations in small plots (9.0 m$^2$ of which half was considered for yield estimation) are easily overestimated as compared with large plots. Sukhatme (1947) showed that yield observations based on such small harvested areas could provide overestimations (as compared with estimates based on 50 m$^2$ plots) by more than 25%.
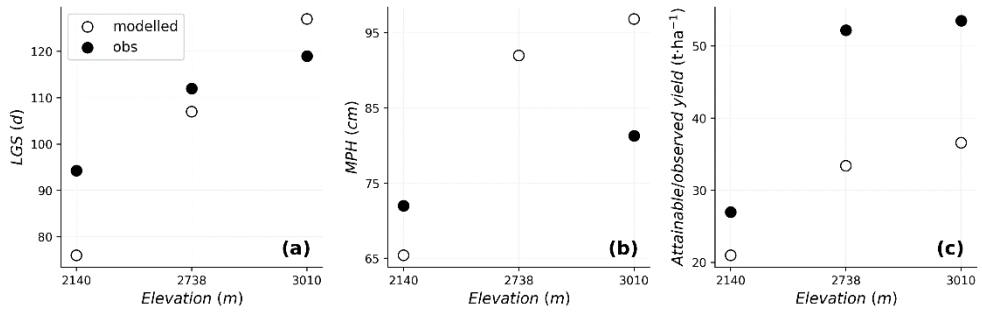
**Figure 4.9 | GECROS-modelled (open dots) and observed (closed dots) values for crop growth variables and yield for Tegecha (2140 m), Chencha (2738 m), and Gircha (3010 m) stations in the Gamo Highlands: (a) LGS (d), (b) MPH (cm), and (c) observed (attainable) crop yield (t·ha$^{-1}$). Note that MPH data for Chencha are missing.**

### 4.3.3.2 *Model sensitivity experiments*

Figure 4.10 presents the results of the sensitivity experiment as designed in Table 4.3. It shows the modelled LGS (d; a and b), MPH (cm; c and d), and yield (t·ha$^{-1}$; e and f) along the SN transect as compared to the control experiment. The left column shows the results of experiments 0–5, the right column experiments 0 and 6–8.

The variation in LGS between the experiments was larger for the elevated stations (Chencha and Gircha) compared to the lower one (Figure 4.10a). The variables causing the largest change in the crop growth dynamics were PPT followed by $T_{min}$, SW↓, and $T_{max}$ (Figure 4.10b,c). This agrees with the result found in Minda *et al.* (2018b). Of all the experiments, the one with the average distribution of precipitation ("PPT$_{avg}$") during the *belg* season resulted in the highest yield, followed by the "Normal *belg*" experiment, with the peak precipitation shifting from May to April. In these experiments, the moisture supply was improved during the crop's critical development stages (*i.e.* vegetative growth, tuber initiation, and tuber bulking stages of the crop growth) and this explains the increased yield. This indicates that the supply of moisture due to precipitation plays a key role at the developmental stages.

Focusing on the "PPT$_{avg}$" experiment, the LGS was slightly shorter (0–9 d) than in the control experiment. The MPH was much larger (~ +20 cm) for the lower station (Tegecha) but lower for both the highland stations (Chencha and Gircha), showing that an average distribution of precipitation in time results in a larger and more uniform crop growth across the highlands. The modelled yield increased by 60% in Tegecha and by 13% in Chencha and Gircha.

We found that the "Early *belg*" (experiment 6) shortened the LGS by about 10 d. The reason is that the crop starts to grow earlier as sufficient moisture was available for the crop planted only around 7 March in 2017 (Figure 4.10b), as the farmers were waiting for precipitation. The crop grows faster and taller than the control experiment (Figure 4.10d) as the weather was warmer and moister. The MPH was also

larger, but it did not result in a larger yield in Tegecha and Gircha. Similarly, the "SW↓, avg" and "Tmax avg" experiments increased MPH with a slight decrease in yield. Contrastingly, in the "Normal *belg*" experiment, the LGS and MPH were close to the control run, but the yield was larger, particularly at Tegecha and Gircha.
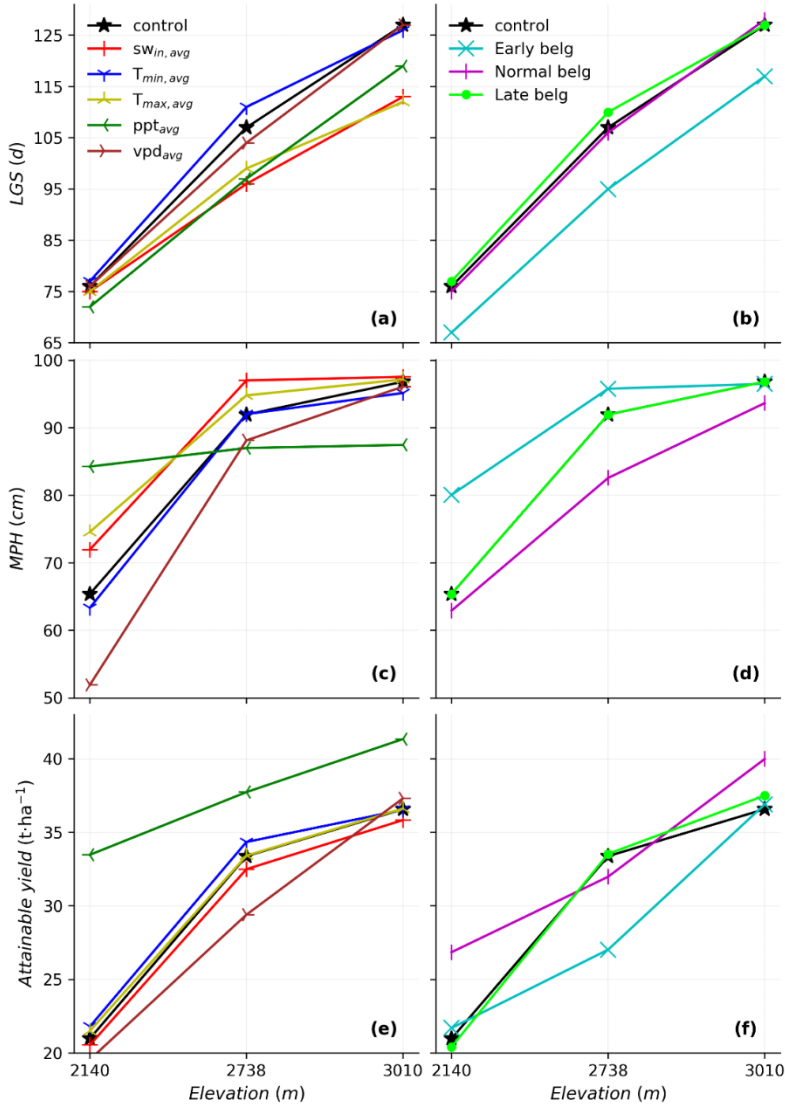


**Figure 4.10 | Model sensitivity experiments based on Table 4.3 for Tegecha (2140 m), Chencha (2738), and Gircha (3010) stations. The LGS (d) (a,b), MPH (cm) (c,d), and attainable yield (t·ha⁻¹) (e,f). The left panel shows average distribution (means of the *belg* data for each day) of experiments the major atmospheric crop drivers: SW↓, Tmin, Tmax, PPT, and VPD. The right panel shows shifting the peak precipitation in May to March ("Early *belg*"), April ("Normal *belg*"), and June ("Late *belg*") model experiments assumptions. Note that the control experiment is added in each panel for ease of comparison.**

99

Our suite of sensitivities indicates that the temporal distribution of precipitation is important for crop development and yield. Too much precipitation too early in the season was not effective, because the seed tubers could not take much moisture from the soil. Precipitation in April was the most effective; the precipitation was there when the crop needed it most, while the soil would not become dry in the later months. However, an average distribution of precipitation is most favorable for the crops in the tropical highland climate, because sufficient but not too much moisture will be available at all times. This was related to a balanced soil moisture content (because of regular precipitation supply) throughout the crop growth period as discussed below. It is interesting to see that the crop's MPH and yield were more sensitive to the temporal distribution of precipitation at the lower parts of the slope (Tegecha) than higher up in the mountains (Chencha and Gircha). This was because the high-elevated stations received some amount of precipitation in each month, whereas the lower stations had a more seasonal distribution of precipitation (Figure 4.3).

To further show the relevance of the soil moisture dynamics, Figure 4.11 presents the observed soil moisture tension (kPa), precipitation (mm·d$^{-1}$), and average precipitation (mm·d$^{-1}$) in Tegecha. The top-10-cm soil moisture tension declined from 10 kPa at the beginning of April to 200 kPa (dry soil) in mid-April. The soil saturated again after it gained more than 60 mm of precipitation. The soil moisture tension at 20 cm and below remained dry until sufficient moisture penetrated into the clay soil.
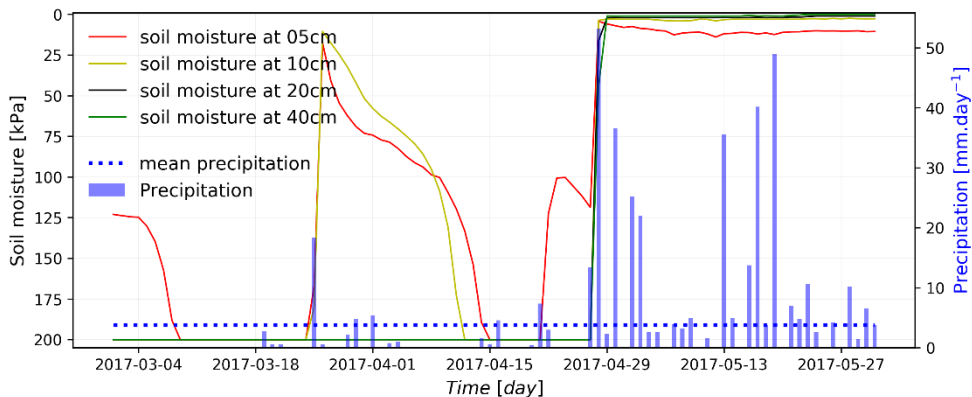


**Figure 4.11 | Observed soil moisture tension (kPa) at 5, 10, 20, and 40 cm soil depth (left y-axis) and daily precipitation (mm·d$^{-1}$; bar plot for observed and dot plot for average precipitation distribution) at the Tegecha (2140 m) station from March to May in 2017. The soil moisture tension is represented by daily averages (line plots). Note that 0 kPa means the soil is fully saturated and 200 kPa means fully dry soil.**

## 4.4 Discussion

The GEMS network enabled us to characterise the mesoscale patterns and their impact on crop growth variables. In February, preceding the potato planting, mesoscale circulations govern the diurnal weather variability within the GEMS' network domain, as the ITCZ, the main large-scale weather phenomenon, is still located in the southern hemisphere (Nicholson, 2018). WRF model output analysis (Minda *et al.*, 2018b) showed that the low-pressure system (a minimum value in SLP) was located below the Equator in January and the system marches toward northern Ethiopia in June. In February, the synoptic flow to the Gamo Highlands is northeasterly. This is a dry and warm airflow from the Arabian Peninsula (Jury, 2014b; Minda *et al.*, 2018b). The daytime mesoscale flows, in turn, were predominantly easterly to southeasterly lake and valley breezes toward and up the east facing slopes. These flows start at 0700 LST, attain climax at noontime, and start to decay after 1500 LST (Figure 4.4). During nighttime, however, weaker and more localised katabatic winds (mountain breezes) are observed (Figure 4.5) (Gebremariam, 2007). These flows start around 1630 LST. The lake/mountain breeze circulations change directions at 0800 and 1800 LST (Gebremariam, 2007).

February and May show greater differences in how the synoptic and mesoscale flows interact. In May, during day time, the moist southeasterly to southerly synoptic flows (Nicholson, 2018) coincide with the lake/valley winds. Together, they form upslope winds (Figure 4.8) (Jury, 2014b; Minda *et al.*, 2018b). Our explanation is that the high correlation between mesoscale and synoptic scales inhibits the convergence, and, as a result, it weakens the orographic lifting that results in less precipitation during daytime (Figure 4.8). This pattern is reversed during nighttime. The southerly synoptic flow dominates the weak mountain flows during nighttime. Hence, the nocturnal precipitation is enhanced by the moisture transport dominated by synoptic winds to the higher levels, local circulations, and a subsequent cooling (shown by a decreased SW↓ after 1500 LST in Figure 4.8). The combined effects occurring in the evening transition trigger cloud formation and the subsequent precipitation during the night.

We hypothesise that the precipitation regime on the other side of the mountain rim may be different, because that is where the valley and synoptic winds converge (Minda *et al.*, 2018b). This could lead to quite different growing conditions for potato. It might be convenient to strengthen the GEMS network by establishing three or more stations across the mountain ridges to obtain a better understanding of the spatial distribution of weather and crop dynamics in the Gamo Highlands.

Our findings corroborate previous results that much of the weather in East Africa is caused by the convergence between local circulation features, such as land/lake breezes and mountain/valley winds with the synoptic scale flows (Mukabana and Pielke, 1992; Pierre *et al.*, 2018). Rainfall gauges and satellite precipitation products

near Lake Tana (NE Ethiopia) showed a precipitation maximum in the evening to early morning (Haile *et al.*, 2013; Verhoef and Egea, 2014), which agrees with our findings presented in Figure 4.8. These authors also underlined that precipitation maxima are observed later in the afternoon for stations more distant from the lake, where distance to the lake is an important factor in explaining the spatial variations of the nocturnal precipitation.

Figure 4.9 shows that the LGS, MPH, and yield increase along the SN transect. This finding agrees the results found in Minda *et al.* (2018b). GECROS results showed a good agreement for the crop growth variables, LGS and MPH. These modelled variables are in the physiologically acceptable range for potato crop (FAO, 2008b; Harper, 1963). The model also captured the trend in yield along the SN transect ($r^2$ = 0.98). However, we found a large discrepancy between the modelled and the observed yield (mean bias error of −13.9 t·ha⁻¹). Using the GEMS sub-daily observations and interpolated soil data, we attempted to minimise the uncertainties in the modelled yield related to these meteorological and soil data. In consequence, we attribute the bias to (1) the crop model parameters, which are not adjusted to the to the local potato varieties in the Gamo Highlands, and (2) probable overestimation of the observed data because of small-size field trial farm. For the first case, we suggest, for future studies, recalibration of the crop parameters to the Ethiopian potato varieties and the existing farm management practices. This recalibration requires a complete observational set, which is currently not available. Although the absolute differences are large, the present model set-up is reasonable to study the sensitivity of crop growth to elevation and modifications in the GEMS network datasets. For the second case, Sukhatme (1947) suggested that a minimum of 50 m² of plot area is needed to be free from yield overestimation bias.

The weather/crop numerical experiments showed that soil moisture availability to the crop is the most important factor for crop growth. Availability of precipitation, as in the "PPT$_{avg}$" model experiment, improved the yield by 60% in Tegecha and 13% in Chencha and Gircha (Figure 4.10). The timing of the precipitation relative to the growth stage is also important. For example, the potato planting date was on 7 March 2017 in Gircha and the seed emerged at the end of the month. In the control experiment, precipitation did not occur until May 2017, which is late when compared to the climatology. In the "Normal *belg*" sensitivity experiment, the peak precipitation in May shifted to April, and hence, increased moisture was available to the crop in the critical crop development stages from emergency to tuber bulking (FAO, 2008b), which enhances the crop yield.

The larger yield in the "PPT$_{avg}$" experiment is explained by a non-linear response of crop growth to soil moisture content. In the specific representation by GECROS, photosynthesis rates depend on soil moisture. In the experiments in which the initial soil moisture content starts with mid-range values, it tends to drop to the wilting point. As a result, the photosynthesis rates may suddenly drop dramatically. This

pattern is opposite when the initial conditions are near soil moisture field capacity (Combe *et al.*, 2015). With averagely distributed precipitation during the entire season, the soil moisture content is always larger than the photosynthesis cut-off point. In this situation, the average photosynthesis rate is in between the extreme conditions of dry and wet soils (Combe *et al.*, 2015; Verhoef and Egea, 2014).

Our observations show that soil moisture, therefore, changes from moist to dry in a matter of a week and backward in a matter of days (Figure 4.11). In the model experiment with an average distribution of precipitation throughout the *belg* season, the soil water content would be constant and above the wilting point, preventing unproductive periods with soil moisture below the wilting point. This model experiment indicates that a regularly scheduled supply of water (irrigation and or precipitation) can significantly improve crop growth and yield. Simple rainfall harvesting technologies can be recommended as options to supply moisture for the crop water requirement. Note that farmers in the highlands traditionally grow crops without irrigation (Minda *et al.*, 2018b).

In situations with heavy precipitation in a short period, part of the infiltrated water will percolate to deeper soil layers and may become unavailable for plants. Runoff could also occur, but this is not taken into account in the GECROS model (Yin and van Laar, 2005). Increased precipitation beyond the moisture holding capacity of the soil facilitates nutrient loss into the deep soil layer and causes a decline in crop yield (Minda *et al.*, 2018b). These processes require further observational evidence.

## 4.5 Conclusions

The aim of this paper was to study the temporal and spatial variations in weather as a function of elevation and their impact on potato crop growth during the *belg* 2017 crop season. We used newly obtained weather and crop observations from our GEMS network. Here, we answered the following research questions:

1) *How does the topography and presence of lakes induce mesoscale circulations in the Gamo Highlands during the belg season? The observations show a southeasterly lake/valley wind pattern as predominant during the day, and opposing land/mountain winds during the night. These observed patterns are based on the lower potential temperature and a higher specific humidity originated at the lowland stations. However, the signal and pattern of these upslope winds on temperature and humidity in the highland stations were weaker. Precipitation is highly correlated to the increase in elevation.*

2) *How do the mesoscale circulations interact with the synoptic circulation driven by the ITCZ? The ITCZ, a synoptic tropical weather system, which moves northward during the belg season, is correlated with the GEMS network SLP data and causes a shift in wind direction and moisture content during its passage. An interesting finding was that the ITCZ and maximum precipitation locations did not coincide. The ITCZ passes the*

*Gamo Highlands overhead in March, but the maximum precipitation is recorded during May.*

In February, dry air masses originating at the Arabian Peninsula characterised the synoptic scale at the Gamo Highlands. Superimposed to this flows, we observed stronger E to SE lake breezes during daytime, and more localised and weaker mountain winds during nighttime. In May, and due to the northern movement of the ITCZ, the air masses originated at the SE to S reaching the Gamo Highlands are characterised by a high moisture content. Our observations show that precipitation is less often during daytime since the mesoscale winds aligned with the moist and warm SE synoptic winds. During the night, however, the interaction between the synoptic and local flows might facilitate convergence, which enhances cloud formation, and the precipitation conditions.

3) *How do the weather variations resulting from this interaction affect crop growth? The design of the GEMS network in mountain transects, with stations every few hundred meters above 2000 m and sub-hourly observations, was capable of identifying spatial and temporal variations in wind and precipitation in the potato-cropping zone.*

The observed and modelled potato growth variables such as the length of the growing season (LGS), the maximum plant height, and the yield are clear functions of elevation (Figure 4.10). Using the crop model experiments, we found that precipitation, increasing with elevation, is by far the most important meteorological variable determining crop growth and yield in the Gamo Highlands. This is probably because other meteorological variables are less limiting.

Relevant crop variables, such as the LGS, improve with the new input of the GEMS meteorological observations. The comparison of the attainable yield between the model results and the observations shows that the crop model requires a new calibration to be adjusted to the Ethiopian varieties. New observations of the attainable yield need to be done in the future to consider the field size. This future work will also address the omission of crop yield loss due to diseases higher up the mountains. There, the vegetation is more frequently wet and the growing season lasts longer due to lower temperatures.

# Responses of canopy growth and yield of potato cultivars to weather dynamics in a complex topography: *Belg* farming seasons in the Gamo Highlands, Ethiopia

*Potato is an increasingly important crop in Ethiopia. The Gamo Highlands are one of the large potential potato producing regions in Ethiopia. The growing conditions are different from those in the temperate regions, where most of the agronomical expertise on potato has been developed. The influence of environmental conditions on the crop in the Gamo Highlands is poorly understood. We conducted field trials with eight potato cultivars in six locations and during two seasons. Canopy cover (CC) and plant height (PH) were measured with high temporal resolution and tuber yields were assessed as well. The experiments were conducted near our newly installed weather stations at different elevations. CC and PH were strongly correlated with temperature sum (Tsum). Tuber yields differed among elevations and cultivars. Nevertheless, these differences were poorly explained by environmental variables. We also found no single cultivar performing best at all elevations. The number of branches was a predictor of yield, suggesting that radiation interception was limiting tuber growth. Tuber yield was optimal when the number of days to crop maturity was around 100-110 days. We conclude that Tsum is a predictor of crop growth, but environmental variables poorly explain yield variations, which calls for further investigation.*

## 5.1 Introduction

Potato (*Solanum tuberosum* L.) is an important and emerging crop in Ethiopia (Baye and Gebremedhin, 2012; Dersseh, 2017). Drought, crop failure and food insecurity have been severe, as well as other related problems in the Horn of Africa in the recent past (Haile, 2005; Philip *et al.*, 2018). For instance, the years 1972-1973, 1982-1983, 1986-1987, 1987-1988, 1997-1998, and 2015-2016 are identified as strong El Niño episodes (Philip *et al.*, 2018; Qian *et al.*, 2011; Tsidu, 2016). In Ethiopia, El Niño events are often excessively warm and dry and they often cause crop failure and famine in most part of the country (Tsidu, 2016; Viste *et al.*, 2013; Wolde-Georgis, 1997). Potato is called the hunger breaker as it has a short crop cycle as compared to cereals (Menza *et al.*, 2014; Thiele *et al.*, 2010). It therefore plays an important role in sustaining food security in difficult periods (Abebe *et al.*, 2016; Abebe *et al.*, 2013). However, because the crop is mainly grown by small farm holders with limited access to farming knowledge and technologies, the actual yield is much lower than the achievable and potential yields (Haverkort, 2018; Haverkort *et al.*, 2012; Hirpa *et al.*, 2010; Tadesse *et al.*, 2017).

Over the last decade, potato production in the western world declined significantly, mainly because of a decline in acreage. Developing countries currently produce more than developed countries and their production has more than doubled in 10 years, mainly due to increases in the area harvested and in some regions because of improvements achieved in seed technology, fertilizer use and fungicide application (Haverkort and Struik, 2015). In Eastern Africa; however, production quantity has grown exponentially since 1990 (Haverkort, 2018) primarily because of a significant increase in the acreage. The yield per hectare has hardly grown, because access to inorganic fertilizers (Mazengia *et al.*, 2015) and pesticides (Dersseh *et al.*, 2016) is limited and the farming has been conducted in nutrient depleted soils with insufficient moisture, particularly at the onset of the growing season (Dersseh, 2017; Tadele, 2017). As a result, the yield gap in the region is around 65%, which is much larger than the 35% in the western world (Haverkort, 2018; Svubure *et al.*, 2015). Note that the yield gap is the difference between the potential yield and the actual yield (Haverkort and Struik, 2015; Svubure *et al.*, 2015). Potential yield is the maximum yield attained when the crop is grown in non-limiting (*i.e.* with abundant water and nutrients) conditions, in which the abiotic and biotic stresses are controlled. The actual yield is the yield the farmer harvests.

Much of the knowledge of the relation between potato growth and environmental conditions is based on western studies in temperate climates, for example (Bodlaender, 1963; Haverkort, 2007; Hijmans, 2003; Struik, 2007; Van Dam *et al.*, 1996), where temperature is usually a limiting factor (Carter *et al.*, 1990; FAO, 2008b) during the early part of the growing season, soil moisture only becomes limiting during advanced stages of growth, and crop management is characterised by high

levels of input. The Ethiopian climate and environmental conditions are rather different, temperature is moderate (10 °C < $T_{mean}$ < 20 °C), soil moisture may be limiting, particularly during the early part of the growing season (Badr *et al.*, 2012; Minda *et al.*, 2018a; Tadele, 2017), and agronomic inputs are generally low (Baye and Gebremedhin, 2012; Tadele, 2017). Weather conditions are in fact variable too in space (Minda *et al.*, 2018b). In Ethiopia, potato can only be grown in the mid- and highlands, because the lowlands are too warm ($T_{max}$ > 25 °C, (Minda *et al.*, 2018b)). Weather conditions in the mountains change along the slope (Minda *et al.*, 2018a; Minda *et al.*, 2018b), causing potato growth and yield to also change with elevation.

There are a number of articles related to potato agronomy in Ethiopia, *e.g.* (Abdurahman *et al.*, 2017; Berihun and Wodegiorgis, 2013; Dersseh, 2017; Kirub and Asfaw, 2013). However, much less is known about the relationship between environmental conditions and potato growth in tropical regions like Ethiopia than in the temperate climates. To this end, we collected crop growth and tuber yield data in the 2017 and 2018 growing seasons along two transects in the highlands, where we also have weather stations installed (Minda *et al.*, 2018a). This study is an extension of our previous work described in (Minda *et al.*, 2018a; Minda *et al.*, 2018b). In the current paper, environmental conditions and potato growth and tuber yield relations are investigated at high temporal resolution and we identify where the growing conditions are optimal in the Gamo Highlands. Ultimately, this knowledge can help us to estimate the potential yield and select and develop varieties, which are better capable of dealing with the environmental conditions (Haverkort and Struik, 2015; Svubure *et al.*, 2015).

The Gamo Highlands, a topographically pronounced region in southern Ethiopia, is a region with a high potato production potential (Dersseh *et al.*, 2016; Minda *et al.*, 2018a; Tadesse *et al.*, 2018). The crop is best grown in a long growing season and with high incoming radiation, between ~12 and 24 MJ·m$^{-2}$·d$^{-1}$, average daily temperature between 5 and 21 °C, precipitation between 600 and 1200 mm per annum depending on the climate of a location (Bradshaw and Bonierbale, 2010; Pandey *et al.*, 2012); and in a soil with good water-holding capacity and sufficient nutrient availability (Haverkort, 2018; Tufa, 2013; Vos and Haverkort, 2007). Such environmental conditions are available in the Gamo Highlands at elevations higher than 1600 m above sea level (a.s.l.) (Minda *et al.*, 2018a; Minda *et al.*, 2018b).

The National Meteorological Agency (NMA) classified the Ethiopian climatic seasons into three: *belg* (February to May), *kirmet* (June to September), and *bega* (October to January) (Degefu, 1987; Diro *et al.*, 2008). *Kirmet* is the wettest season in most of the country, except the southern and southeastern parts of the country (Gissila *et al.*, 2004). Southern Ethiopia receives its maximum precipitation during *belg*. The other regions of the country may also receive small amounts of rain in *belg* (Diro *et al.*, 2008). *Bega* is a dry season, but potato can grow if irrigated (Haverkort *et al.*, 2012). Note that only 5% of the total arable land is irrigated in the country (Awulachew *et*

*al.*, 2010). In the Gamo Highlands, potato grows mainly during the *belg* season mainly under rainfed agriculture (Minda *et al.*, 2018a; Minda *et al.*, 2018b). Farmers prefer the *belg* season for potato cropping because of the season's meteorological and agronomic suitability for potato cropping, *i.e.* the moisture availability is optimal and disease risks are relatively low (Abdurahman *et al.*, 2017; Minda *et al.*, 2018a; Tufa, 2013). Late blight caused by *Phytophthora infestans* is the most important potato disease in Ethiopia, followed by bacterial wilt caused by *Ralstonia solanacearum* (Abdurahman *et al.*, 2017; Woldegiorgis, 2013).

The potato crop growth is traditionally explained in terms of responses to environmental variables (Haverkort, 2018; Struik, 2007). The major growth-influencing factors are temperature, photoperiod, soil moisture (in terms of precipitation and/or irrigation), the incoming shortwave radiation (SW↓), and nitrogen supply (Haverkort, 2018; Khan, 2012). These factors can explain the crop's canopy dynamics in terms of lateral or horizontal growth [*e.g.* estimated from canopy cover or Leaf Area Index (LAI) measurements and vertical growth (*e.g.* plant height)]. A summary of how meteorology influences potato growth closely related to this investigation is given below.

In a potato crop, many complex physiological processes are strongly affected by temperature (Struik, 2007). Temperature can affect canopy development, tuber bulking and growth cycle duration (Haverkort and Struik, 2015). Temperature is very different in the tropics than in temperate climates, regarding both mean and variability. A daily mean temperature of between 15-18 °C is generally considered as an optimal temperature for potato growth in the tropical highlands (Haverkort, 1990). The growth rate declines nearly linearly to zero when either the average temperature decreases to 5 °C or increases to 28 °C from this optimum. An average daily temperature ($T_{mean}$) of less than 5 °C gives low photosynthesis rate with risk of frost and diseases while a $T_{mean}$ > 28 °C causes high respiration rates with a rapid foliage development, retarded tuberization, little partitioning of dry matter to the tubers, poor starch synthesis, resulting in a large number of small tubers per plant, and low dry matter concentration (Haverkort, 1990, 2018; Van Dam *et al.*, 1996; Vos and Haverkort, 2007).

The potato crop is relatively sensitive to drought stress, which occurs regularly in the Horn of Africa (Degefu, 1987). It is only cultivated where precipitation is sufficient or where irrigation can be applied (Haverkort, 1990). Water-stressed potato plants result in yield reduction because of reduced leaf area and/or reduced photosynthesis per unit of leaf area and often produce fewer and smaller tubers (Vos and Haverkort, 2007). Of all growth stages of the crop growth period, the tuber bulking period is the most drought-sensitive stage (Van Loon, 1981).

Millard and Marshall (1986) explained that potato tuber yield is a product of four processes, namely (1) radiation interception, (2) conversion of intercepted radiation to dry matter, (3) partitioning of dry matter between tubers and other parts of the

plant, and (4) regulation of tuber dry matter contents. Sibma (1970) showed that the potato yield and the total SW↓ during the entire growing season were positively correlated. Dry matter production of a crop is linearly related with the intercepted radiation. The produced dry matter is distributed over different parts of the potato plant (Haverkort, 2007). Allen and Scott (1980) showed that the potato tuber dry weight positively and linearly correlated with the total intercepted radiation during the growing season. The Harvest Index (HI), which is a function of the amount of cumulative radiation intercepted by the crop during the growing season, is dependent on location and season and specific for a given cultivar (Haverkort, 2018).

The canopy dynamics in the potato crop is explained based on three distinct growth phases (Figure 5.1). These growth stages include the canopy buildup phase (P1), the maximum canopy cover phase (P2), and the canopy decline phase (P3) (Khan, 2012). P1 covers the time between emergence (when 50% of the plants have emerged) to the maximum canopy cover and is characterised by the appearance of stems, lateral branches and leaves, and growth of those organs. P2 is the period from the maximum canopy cover to the onset of canopy senescence; whereas the period from the onset of senescence to the end of the crop cycle is called P3 (Khan, 2012).

Crop growth at the early stages of development (emergence and initial foliar expansion) can be related and explained by the temperature sum (Tsum) rather than the number of calendar days as the crop's physiological processes depend on temperature (Haverkort, 2018; Kooman and Haverkort, 1995b). Tsum is the cumulative sum of daily average temperature above a base temperature ($T_b$) during the crop growth period. Studies considered $T_{base}$ for potato crop between 0 and 5.5 ℃ (Haverkort, 2018; Hijmans, 2003; Khan, 2012; Spitters *et al.*, 1989). Tsum is expressed in units of day-degrees (d ℃ or dd) (Haverkort, 2018). Haverkort (2018) discussed that the canopy growth during P1 can be described by a linear relation with Tsum. At the end of P1, canopy cover is at its maximum and does not change anymore with Tsum in P2, while it decreases in P3.

To our knowledge, there are only a few studies, focusing on the relationship between potato, weather and seasonal climate in Ethiopia. Haverkort *et al.* (2012) used station observations to calculate the attainable and achievable potato yield for *belg*, *meher*, and *bega* agronomic seasons. Minda *et al.*, (2018a; 2018b) conducted studies about weather variability along the slopes of the Gamo Highlands in relation to potato growth. In Minda *et al.* (2018b), potato crop growth and attainable yield are simulated using modelled weather data. The authors showed that precipitation positively influenced yield, and the minimum and maximum temperatures both negatively influenced it. Using weather observations and a potato crop model, Minda *et al.* (2018a) showed that the soil moisture is the most important variable that influenced crop yield.
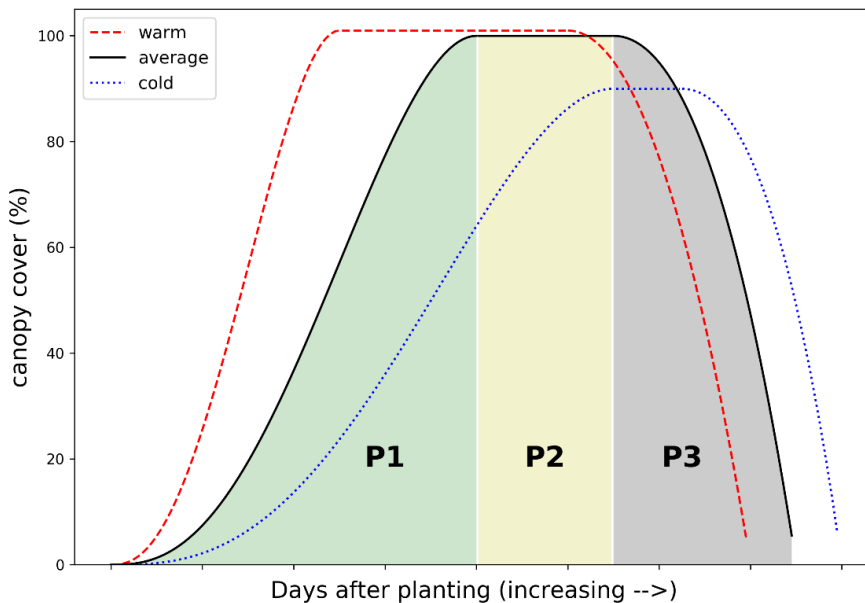
**Figure 5.1 | A hypothetical model-based representation of the canopy dynamics expressed in percent canopy cover as a function of days after planting (not scaled) based on the beta function for determinate growth for the canopy buildup phase (P1) (Khan, 2012; Yin *et al.*, 2003), maximum cover phase (P2), and canopy decline phase (P3) (Khan, 2012) as shown. Note that the break-down into these three phases indicated is only applicable to the 'average' curve shown with the solid line. We assumed canopy growth for warm, mild, and cold temperatures scenarios to mimic meteorological conditions in lowlands, midlands, and highlands of potato growing regions in the Gamo Highlands, respectively.**

The Gamo Ethiopian Meteorological Stations (GEMS) network (currently, eight automatic weather stations) is operational since April 2016. Details of the GEMS network is found in Minda *et al.* (2018a). Close to the network, we planted and monitored eight potato cultivars in the *belg*-2017 (5 locations) and *belg*-2018 (6 locations) seasons to explain crop growth and yield variations among cultivars, across elevations, and seasons as influenced by environmental conditions. Therefore, the aim of this study was to study how the potato crop growth and yield vary with variations in the environmental variables during the crop growth phases (mainly in P1) in the Gamo Highlands, southern Ethiopia. To attain our aim, we formulated the following research questions.

1)  *How does canopy growth vary with environmental variables in P1 across elevations, among potato cultivars, and between seasons? Does this growth follow similar patterns as in temperate climates?*

2)  *How does yield depend on physiological crop characteristics, such as number of tubers, number of branches, days to maturity, cultivar, and on meteorologically dependent variables, such as intercepted radiation and temperature?*

To answer these research questions, we collected high temporal resolution data (one-day or two-day intervals) on canopy cover and plant height for improved and local cultivars. We also collected data on the plant, yield and yield traits (*e.g.* branch numbers, tuber numbers and tuber weights per plant) at 5 to 6 farms (at different elevations) and for 6 improved (*Gudene, Belete, Horro, Hunde, Ararasa* and *Jalene*) and 2 local (*Suthalo* and *Kalsa*) cultivars in 2 *belg* seasons (Baye and Gebremedhin, 2012; Gebreselassie *et al.*, 2016; MOANR, 2016). From the improved cultivars, *Gudene, Belete*, and *Jalene*, and the two local cultivars are commonly cultivated in the Gamo Highlands (Tadesse *et al.*, 2016). Note that the potato crop has been cultivated in Ethiopia for more than 150 years. In the country, improved varieties started to be released since 1987 (Kolech *et al.*, 2015). In the Gamo Highlands, the crop has been cultivated for decades (Tadesse, 2013). Although this represents a significant effort, the number of possible predictor variables is large and we are facing a mathematically underdetermined system. We therefore confront the data with existing theory, which is to a large extent developed for the potato crop in a temperate climate, to test if and where these theories deviate for the mountainous tropical climate in Ethiopia.

## 5.2 Materials and methods

### 5.2.1 GEMS weather datasets during *belg*-2017 and *belg*-2018

The weather data in this study were taken from the Gamo Ethiopian Meteorological Stations (GEMS) network. The GEMS network records weather (max/min/mean temperature – $T_{max}$, $T_{min}$, $T_{mean}$, precipitation – PPT, the incoming shortwave radiation – SW↓, wind, and relative humidity), edaphic (soil moisture tension – $\psi$ and temperature – $T_{soil}$) and plant related (leaf wetness) variables with every 15-min (in *belg*-2017) or 30-min (in *belg*-2018) temporal resolution. The network is operational since April 2016. Eight automatic weather stations (AWS) have been installed in a complex topographic region in the Gamo Highlands, Southern Ethiopia. The Gamo Highlands form a heterogeneous landscape composed of complex topography extending from the narrowest portion of the Great East African Rift Valley at 1000 m a.s.l. to the summit of Mount Guge at 3600 m a.s.l., including Lake Abaya and Lake Chamo, forest, and agricultural lands. Descriptions of the study area and the GEMS network data are provided in detail in Minda *et al.* (2018a). Table 5.1 presents the locations of the experimental farm sites with mean seasonal environmental (weather and edaphic) variables and descriptions of the potato cultivars and date of planting in the *belg* seasons. *Belg*-2017 was during a La Niña phase characterised by warmer and drier season than the climatology in the Gamo Highlands (Blunden *et al.*, 2018; Minda *et al.*, 2018a; Tsidu, 2018); whereas, *belg*-2018 was relatively cool and wet (Table 5.1).

**Table 5.1 | Descriptions of the crop experimental sites with the *belg* (Feb-May) average seasonal weather (mean $T_{mean}$, mean SW↓, and *belg* total PPT); edaphic (mean soil moisture (ψ) and mean soil temperature ($T_{soil}$)); and some of the potato crop experimental descriptions in *belg*-2017 ('17) and *belg*-2018 ('18). Note that the GEMS location deviates few meters from the farm sites. The soil sensors were placed at four depths: 5, 10, 20, and 40 cm, in which averages of the four depths were reported. Note that soil moisture sensors measure from 200 (dry soil) kPa to 0 (fully saturated soil) kPa. Key: Lon – longitude, Lat – latitude, Elv – elevation.**

| Station | Lon (°) | Lat (°) | Elv (m) | Meteorology (*belg*) $T_{mean}$ (°C) '17 | '18 | SW↓ (MJ·m⁻²·d⁻¹) '17 | '18 | PPT (mm·*belg*⁻¹) '17 | '18 | Edaphic (*belg*) ψ (kPa) '17 | '18 | $T_{soil}$ (°C) '17 | '18 | No of cultivars planted '17 | '18 | Potato crop Date of planting '17 | '18 | Disease observations '17[e] | '18[e] |
|---|---|---|---|---|---|---|---|---|---|---|---|---|---|---|---|---|---|---|---|
| **Gircha** | 37.566 | 6.309 | 2985 | 13 | 12 | 17 | 16 | 444 | 476 | 61 | 44 | 16 | 14 | 8 | 2 | 07-Mar | 12-Mar | No | Yes |
| **Gazesso** | 37.333 | 6.132 | 2880 | 14 | 13 | 17 | 15 | >475[d] | 462 | 52 | 46 | 18 | 16 | 8 | 8 | 02-Mar | 03-Apr | No | Yes |
| **Chencha** [c] | 37.566 | 6.258 | 2765 | 14 | 13 | 18 | 16 | 540 | | | | | | | 2 | | 08-Mar | | Yes |
| **Zozo** [a,c] | 37.605 | 6.265 | 2695 | | | | | | | | | | | | 2 | | 12-Mar | | Yes |
| **Tegecha** [c] | 37.575 | 6.184 | 2383 | 20 | 18 | 19 | 14 | 459 | 564 | 131 | 140 | 23 | 22 | 8 | | 05-Apr | | Yes | |
| **Geresse** [b] | 37.310 | 5.929 | 2298 | | 17 | | 14 | | | | | | | 8 | 8 | 10-Apr | 05-Apr | No | Yes |
| **Derashe** [a] | 37.368 | 5.637 | 2122 | | | | | | | | | | | 8 | 8 | 01-Apr | 27-Mar | No | Yes |

[a]*Farm with no weather station nearby;* [b] *Weather data obtained from the National Meteorology Agency (NMA) manual stations, Ethiopia;* [c] *Field experiment was absent either in belg-2017 or belg-2018;* [d] *precipitation record with 2-weeks missing data;* [e] *we observed that incidence and severity levels were different among farms, but these were not quantified.*

### 5.2.2 The potato farm experiments during *belg*-2017 and *belg*-2018

The potato field experiments in this study (*belg*-2018) are follow-up field experiments (*belg*-2017) from Minda *et al.* (2018a). We planted the following six improved varieties (with their year of release): *Gudene* (2006), *Belete* (2009), *Horro* (2015), *Hunde* (2006), *Ararasa* (2006), *Jalene* (2002), and two local varieties: *Suthalo* (unknown) and *Kalsa* (unknown) (Baye and Gebremedhin, 2012; Gebreselassie *et al.*, 2016; MOANR, 2016). During *belg*-2017, the seed tubers were collected from three research centers, and the seed tubers of the local cultivars were purchased from local markets. From the *belg*-2017 harvest, we selected seed tubers from Gircha and Gazesso farms and stored them in the diffused-light storage (DLS) facility at the Gircha site (mean temperature during storage was only 11.7 $^\circ$C). The DLS facility allowed free ventilation and light diffusion; it suppressed elongation of sprouts and slowed down sprout ageing (Hirpa *et al.*, 2010). We kept the well-sprouted seed tubers stored in the cool environment for all the farms to be planted in the following *belg* season. Our planting material was of superior quality compared to the commonly planted seed material and our crops were healthier than farmers' plots in the region.

The experiments in *belg*-2017 and *belg*-2018 were done with different planting dates depending on moisture availability in the farm site (Table 5.1). A randomised complete block design – RCBD was applied with three replications (Gomez *et al.*, 1984). The plot size was 3 m × 3 m and planting pattern (between rows × between plants) was 0.75 m × 0.30 m resulting in a plant density of 4.4 plants per square meter of land. Spacing between plots and replications was 1 m and 1.5 m, respectively. Urea (144 kg·ha$^{-1}$), NPS (236 kg·ha$^{-1}$), and muriate of potash (125 kg·ha$^{-1}$) fertilizer doses were added at planting, but the urea was split into two dressings, in which the first half was applied at planting and the remaining half was added at the start of the flowering stage. Agronomic practices such as weeding, hoeing, and earthing-up were done as recommended. Data were taken from the middle two rows. This allowed us to avoid border effects (Yactayo *et al.*, 2013).

### 5.2.3 Canopy growth and crop yield observations

Plant height (cm) and canopy cover (%) data were collected to estimate the canopy growth. The distance between the soil surface (basal end of stem) to the upper most tip (shoot apex) of the main stem was considered as plant height (Deblonde and Ledent, 2001). Decreases in plant height because of increases in ridge height during hoeing and earthing-up were estimated and data were corrected. The amount of intercepted radiation can be determined using canopy cover measurements (Boyd *et al.*, 2002; Taye *et al.*, 2012). The percentage of the canopy covered with green foliage was measured with a grid with dimensions that are a multiple of the planting pattern (0.75 m, between rows × 0.30 m, between plants) divided by 100

rectangles (Haverkort, 2018; Ospina *et al.*, 2014). All rectangles at least half filled with green leaf were counted and the percentage canopy cover was determined (Boyd *et al.*, 2002; Firman and Allen, 1989; Ospina *et al.*, 2014). The center of the grid was placed on top (at center) of a selected plant, so that the shorter side (0.30 m) side of the grid was aligned with the ridge. In *belg*-2017, plant height measurements were taken six times per week for farms – Gircha and Gazesso, and for cultivars - *Gudene* and *Suthalo*. In *belg*-2018, those measurements were taken three times per week for farms – Gircha and Chencha; and for cultivars - *Gudene* and *Belete*. Canopy cover data were taken three times per week in *belg*-2017 for Gircha, and for cultivars - *Gudene* and *Suthalo*. Five randomly selected plants per plot were measured for canopy cover and plant height observations and the means of 15 plants are reported.

Boyd *et al.* (2002) provided a detailed analysis of the relation between canopy cover and LAI. They provided data that suggest that the slope of this relationship could be influenced by the way the crop was managed. These authors also showed that when the duration of ground cover was used (a parameter they coined ground cover duration), the variation in tuber yield accounted for was equally large, or even higher, than when they used leaf area duration.

The following yield and yield traits observations were systematically collected at the harvest date: total number of lateral and apical branches per plant at crop maturity (Buck-Sorlin *et al.*, 2009); number of marketable tubers per plant (80-300 g in weight and 30-60 mm in diameter); number of non-marketable tubers per plant (<80 g in weight and <30 mm in dimeter); weight of (non)-marketable tubers per plant (kg) (Abbas *et al.*, 2012). These data were taken from five randomly selected plants from the central two rows and the averages of the three plots are reported. The total yield per plot, *i.e.* the sum of the weight of marketable and non-marketable tubers, was calculated and the average of the three plots was reported. Note that in *belg*-2017, the Tegecha farm is strongly affected by diseases, mainly late blight. In the following year; however, all farms were affected by different intensities of diseases. We did not quantify or rate disease observations.

### 5.2.4 Statistical and mathematical data analysis approaches

#### 5.2.4.1 Crop growth and environmental variables relations

For studying the correlations between the environmental and crop variables, we calculated and report the average weather and crop observations to daily, or 5-daily, or sub-seasonal (*e.g.* during P1), or seasonal temporal scales. We selected the Gircha site for the following reasons. First, our weather station has been operational since April 2016 in this site. It is located in the newly established highland crops horticultural research Centre run by Arba Minch University. Second, the Gircha region is one of the best-known potato producing areas in the Gamo Highlands. Third, Gircha is the coolest amongst our farms and equipped with a DLS facility. For some data

collection or analysis, we selected *Gudene* from the improved and *Suthalo* from the local cultivars as these are the most widely improved and local cultivars cultivated in the Gamo Highlands, respectively.

For studying the temporal variation of canopy growth as a function of environmental variables, we considered P1 as the period between that time that the crop attains 10% and 90% of the maximum plant height. However, continuous measurements of plant height data are not available for some cultivars and farms. Hence, for studying the correlation between weather and tuber number per plant, P1 was best estimated from other crop datasets. In these instances, we defined P1 as the period from crop emergence (50% of the plants emerged) to a week after the date of flowering (50% of the plants flowered). We also considered average weather in P2 and P3 to study relationships between weather and tuber weight per plant. The starting date for P2 was one day after the end of P1. The end time of P3 was considered as 2 weeks after the day of crop maturity. Maturity was defined as the onset of canopy senescence (when the vines started to become yellowish) (MacKerron and Davies, 1986). We applied linear and quadratic statistical correlations to identify the relation between crop growth (plant height and canopy cover) and environmental variables.

### 5.2.4.2 *The daily crop growth and temperature sum*

Temperature sum (Tsum) explains plant development for most crops (Van de Geijn and Dijkstra, 1995). Crop growth, mainly during the early stages during emergence and initial foliage expansion, is easiest related to the Tsum, *i.e.* the cumulative daily average temperature expressed in day-degrees (d °C). Tsum is calculated using Equation ( 5.1 ).

$$\text{Tsum} \;=\; \sum_{i=1}^{i=\mathrm{n}} \left[ \frac{(T_{max} + T_{min})}{2} \right] - T_b \qquad (5.1)$$

Note that the GEMS data showed that the lowest daily average temperatures was 7 °C and the highest was 30 °C for all potato growing farms in both *belg*-2017 and *belg*-2018. As a consequence, the mean daily temperature, estimated from the minimum and maximum temperatures on that day, in the potato growing locations in the Gamo Highlands was always above $T_b$ (Haverkort, 2018; Khan, 2012; Spitters *et al.*, 1989).

### 5.2.4.3 *Estimating harvest index using the cumulative incoming shortwave radiation*

The plot of cumulative crop growth and measured canopy cover against cumulative incoming solar radiation (SW↓, cum) may be used to estimate how efficiently the intercepted solar radiation is converted into crop dry matter (Boyd *et al.*, 2002;

Haverkort, 2018; Khan, 2012). The dry matter is produced by the potato crop with a Radiation Use Efficiency (RUE) of ~ 2.0 g·MJ$^{-1}$. The RUE is the amount of dry matter (in g) produced per mega joule of global radiation intercepted. The intercepted radiation is allocated to different parts of the plant (leaves, stems, tubers, and roots), depending on the crop growth stage. The efficiency of a cultivar in allocating dry matter to the tubers can be estimated from the harvest index (HI), the ratio of tuber weight over total plant weight. We estimated total plant weight as a function of the intercepted radiation and the radiation use efficiency as shown in Equation ( 5.2 ) (Haverkort, 2018).

$$HI = \frac{Y \times DMC}{SW_{\downarrow,\text{cum}} \times RUE} \times 100 \tag{5.2}$$

here, Y is tuber fresh yield at harvest in g·m$^{-2}$; DMC is dry matter concentration (DMC = 20%); $SW_{\downarrow,\text{cum}}$ is the cumulative amount of $SW\downarrow$ intercepted by the canopy in MJ·m$^{-2}$ and RUE can be from 1.07 to 2.24 g per MJ for potato crop (Burstall and Harris, 1983; Fahem and Haverkort, 1988; Sinclair and Muchow, 1999), but here, we assumed RUE to be 2.0 g·MJ$^{-1}$. The total dry matter accumulation is directly proportional to the total amount of intercepted radiation in many crops including potato (Allen and Scott, 1980; Oliveira, 2015). For the entire crop growth period, $SW_{\downarrow,\text{cum}}$ can be calculated as (Haverkort, 2018; Ingram and McCloud, 1984; Spitters, 1987):

$$SW_{\downarrow,cum} = \int (f_t \times SW \downarrow_t)dt \tag{5.3}$$

where, $f_t$ is fraction of canopy cover observed on daily base and $SW\downarrow_t$ is the average incoming shortwave radiation in MJ·m$^{-2}$ on that day.

## 5.3 Results

### 5.3.1 The role of environmental variables on canopy growth in the canopy buildup stage

In this section, we study how the potato crop grows during the canopy buildup phase (P1, see Figure 5.1) in terms of plant height and canopy cover as a function of environmental conditions. Previous studies have shown that Tsum is a good predictor of canopy growth during P1 of the crop development stage in temperate climates (Haverkort, 2018; Kooman and Haverkort, 1995a; Mazurczyk *et al.*, 2003).

### 5.3.1.1  *Canopy cover and temperature sum*

Figure 5.1 presents a schematic overview of canopy growth in terms of calendar days for temperature regimes. Figure 5.2 presents the observed quadratic correlation between Tsum (d °C) and canopy cover (%) for the *Gudene* (a) and *Suthalo* (b) cultivars in Gircha in *belg*-2017. The linear regression between canopy cover and Tsum in P1, has an $r^2$ of 0.98 for *Gudene* and an $r^2$ of 0.96 for *Suthalo*. Haverkort (2018) also explained that canopy cover showed a linear relation with Tsum in P1. However, as Figure 5.2 shows, the relation is better described with a quadratic than linear relation, in which the $r^2$ is improved to greater than 0.99 for both cultivars. We also calculated the rate of increase in the canopy cover as function of other environmental variables, but the correlations were poor (not shown here).



**GUD Gir17**

$r^2 = 0.993$

$y = 0.0001x^2 + 0.060x + 0.614$

**SUT Gir17**

$r^2 = 0.995$

$y = 0.0002x^2 + 0.043x + 1.114$

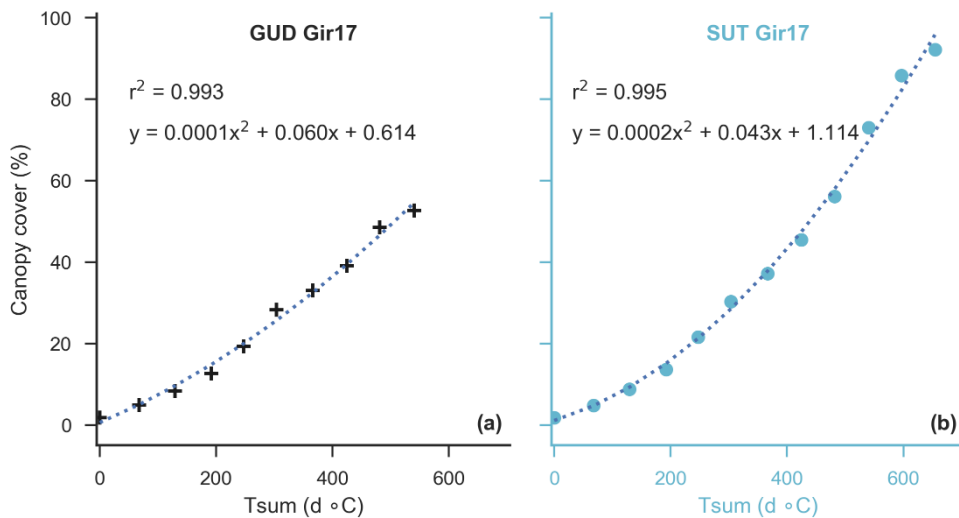**Figure 5.2 | Measured canopy cover (%) as function of Tsum (d °C) for improved cultivar Gudene (GUD) (a) and the local cultivar Suthalo (b) during *belg*-2017 in Gircha. The canopy cover – Tsum curve shows a quadratic relation. The lines in each plot show the quadratic function curve (canopy cover = slope1 × Tsum² + slope2 × Tsum + intercept) and the quadratic correlation coefficient ($r^2$) are shown.**

### 5.3.1.2   Plant height and temperature sum

In Section 5.3.1.1, we showed canopy cover described in a quadratic function of Tsum. Besides the canopy cover, Tsum also explains the plant height. Here, we will study the relationship between plant height and Tsum. Figure 5.3 shows how plant height relates to the cumulative temperatures during P1.
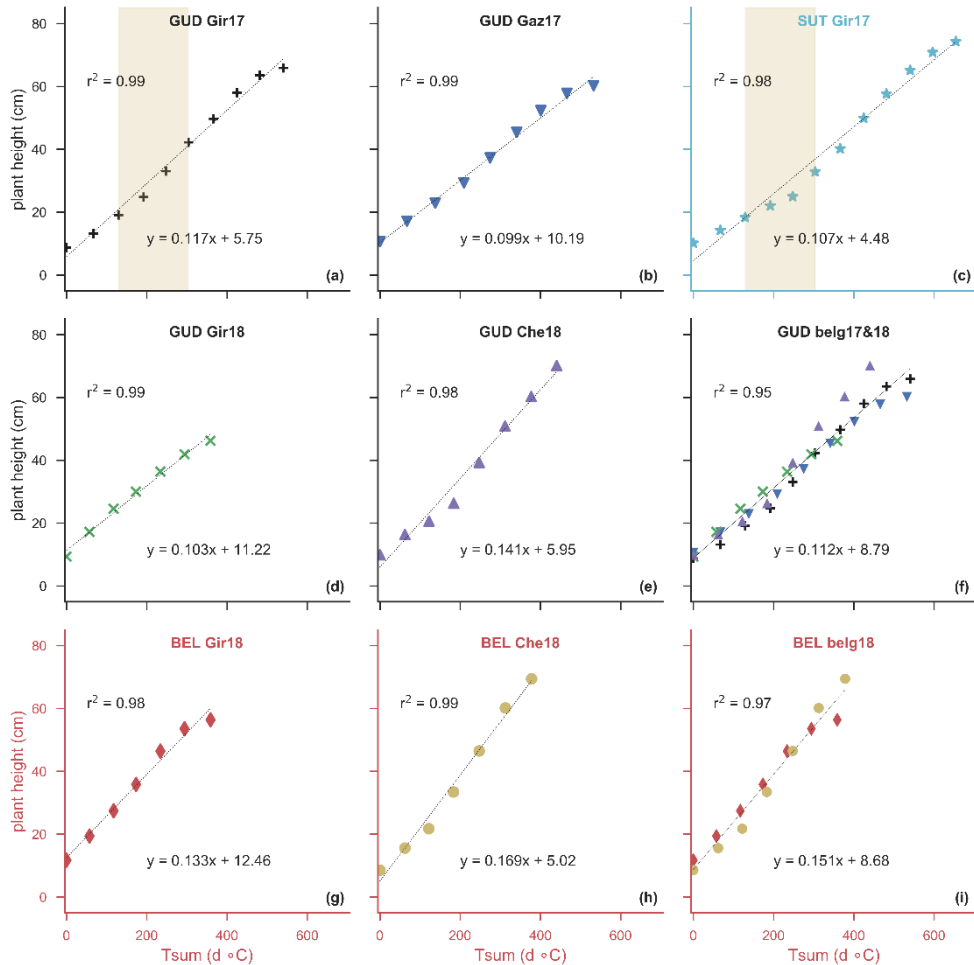


**Figure 5.3 | Measured plant height (cm) as function of Tsum (d °C) for *Gudene* (GUD) (a,b,d,e) and *Belete* (BEL) (g,h) and *Suthalo* (SUT) (c) during *belg*-2017 and *belg*-2018 represented by suffix 17, and 18, respectively. The experimental farms are Gircha (Gir), Gazesso (Gaz) and Chencha (Che). (f) and (i) show combinations (a series of data combinations for a cultivar for all sites and seasons for linear regression calculation only) of *Gudene* (black axes) and *Belete* (red axes) cultivars, respectively. The lines in each plot show the linear function line (plant height = slope × Tsum + intercept); $r^2$ shows the linear correlation coefficient; and the yellow shades (a,c) show a period with dips in the rate of increase in plant height – Tsum curves, which will be discussed in the following section.**

The plant height is strongly correlated with Tsum (Figure 5.3). The linear correlation showed an $r^2 > 0.98$ for the improved and local cultivars. The correlation was large for the medium-high (Chencha, 2765 m) and high parts of the mountains (Gazesso and Gircha > 2850 m) parts of the mountains, both in dry (*belg*-2017) and wet (*belg*-2018) seasons. The combined $r^2$ of *Gudene* in three farms and two *belg* seasons gave an $r^2$ value of 0.95 (f). Similarly, *Belete* in Gircha and Chencha showed an $r^2$ of 0.97 (i).

The slopes of the lines are in the order of 0.1 cm·(d °C)$^{-1}$ with variations of tens of percents between varieties and years. The *Belete* cultivar grew faster than the *Gudene* cultivar in Gircha in *belg*-2018. For the other cultivars and locations, the data were too sparse to explain. The high correlation coefficients between Tsum and plant height indicate that the variability in growth rates within a growing season was small. Nevertheless, there are variations, which we will study in more detail in Section 5.3.1.3.

Our results indicate that Tsum did not exclusively explain growth in plant height in P1. The Tsum – plant height curve deviated from linearity for some periods in P1 for some cultivars and environments. The periods characterised by a slowdown in the growth rate are shaded in Figure 5.3a,c. These deviations need additional environmental variables to be explained. This will be presented in detail in the following section.

### 5.3.1.3  *A further look at the plant height – temperature sum curve*

Figure 5.4b shows a day-by-day data analysis to the dip in the rate of canopy increase marked by the yellow shaded region Figure 5.3a in for the improved and Figure 5.3c for the local cultivars.
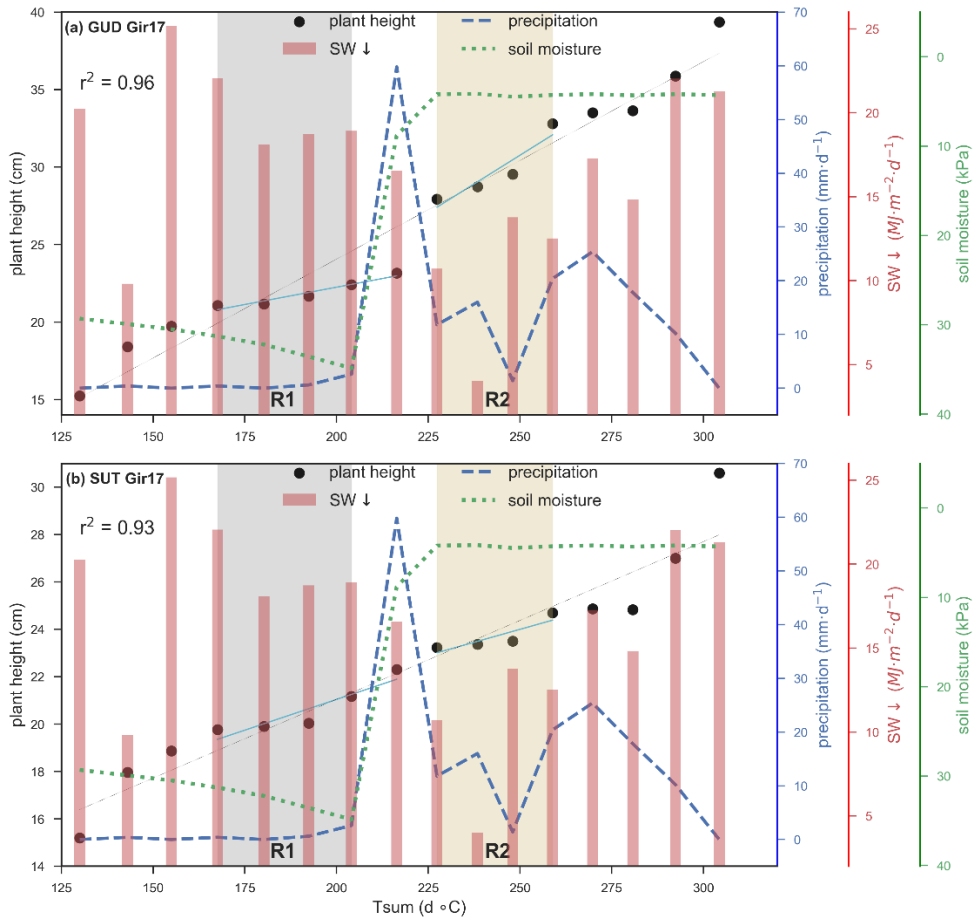
**Figure 5.4 | The correlation between Tsum (d °C) and plant height (cm) for *Gudene* (a) and *Suthalo* (b) cultivars at the Gircha farm in *belg*-2017 at the times that the dips in the rate of increase in plant height occurred (We zoom in into the highlighted spots using daily data) in Figure 5.3a and c. The daily total precipitation (mm·d⁻¹) (blue y-axis), daily total SW↓ (MJ·m⁻²·d⁻¹) (red y-axis), and soil moisture tension (ψ) (kPa) (green and inverted y-axis) are shown on the right-side y-axes. The +/bar/line plots' colors correspond to the colors of the y-axes. (R1) shows moisture limited and (R2) radiation limited regimes during this part of P1. The thin grey line shows the linear correlation line. The cyan colored lines in the shaded regions show the linear trend for the moisture and radiation limited periods during P1. The ψ is an average of four records, which are measured at four soil depths (5, 10, 20, and 40 cm) and the averages of the four sensors are reported. Note that soil moisture sensors measure from 200 kPa (dry soil) to 0 kPa (fully saturated soil).**

In Figure 5.3a and c, we showed that the $r^2$ was 0.99 for *Gudene* and 0.98 for *Suthalo* cultivars. However, for those highlighted data points in the figures, the $r^2$ was slightly decreased for *Gudene*, 0.96 and *Suthalo*, 0.93 as shown in Figure 5.4a,b. In the figures, we marked periods with contrasting environmental features: **R1** and **R2** with grey and yellow shades, respectively.

We call **R1** – moisture and **R2** – radiation limited regimes that influenced the canopy growth during P1. **R1** was a dry period without precipitation. In this period, the soil moisture tension increased from 30 to 35 kPa. We also noted that the SW↓ was high. In this circumstance, the two potato cultivars responded differently. The growth rate of the improved cultivar – *Gudene* – dropped to 20% of the overall growth rate (0.03 cm·(d °C)$^{-1}$ compared to 0.14 cm·(d °C)$^{-1}$), while the local cultivar – *Suthalo* – kept growing at 64% of the overall growth rate (0.06 cm·(d °C)$^{-1}$ compared to 0.09 cm·(d °C)$^{-1}$). Apparently, the improved cultivar was more sensitive to soil moisture than the local cultivar as explained in **R1**.

In **R2**, the soil was sufficiently moist (soil water tension decreased to 5 kPa) after having 70 mm of total precipitation. In this period; however, SW↓ declined from 20 to nearly 10 MJ·m$^{-2}$·d$^{-1}$, which indicated an increase in cloud cover. Interestingly, we found a faster growth in the plant height per degree-day for *Gudene* (0.13 cm·(d °C)$^{-1}$, *i.e.* close to overall) than for the *Suthalo* cultivar (0.01 cm·(d °C)$^{-1}$, 15% of the overall). In other words, in **R2**, the *Gudene* cultivar was more efficient in converting the limited radiation to biomass (here, in terms of vertical growth) than the local *Suthalo* cultivar. Note that the local seeds are not renewed for decades, which could influence crop growth rates. Thus, we showed that canopy growth was strongly correlated with Tsum, but other secondary factors such as moisture availability, radiation intensity and intrinsic factors related to seed quality may influence the canopy growth too.

### 5.3.2  Response of yield to variations in elevation, cultivar and environmental variables

The previous section studied how the plant height and canopy cover developed during the canopy buildup phase (P1), mainly as a function of Tsum. In this section, we will study how yield and yield traits depended on variations in weather and edaphic variables in P1, P2, and P3 as influenced by topography and cultivar.

#### 5.3.2.1  *Yield variations with topography and among cultivars*

Figure 5.5 shows how tuber yield varied across cultivars and elevations in the Gamo Highlands. The tuber yield (t·ha$^{-1}$) varied significantly among cultivars, with elevation and between *belg* seasons. In *belg*-2018, yields were nearly 50% lower than those in the previous year. *Belg*-2018 was 0.5 to 2.0 ℃ cooler, SW↓ was 1.7 to 4.6 MJ·m$^{-2}$·d$^{-1}$ lower, and precipitation was up to ~100 mm more than in *belg*-2017 depending on the location (Table 5.1). In addition, the soil was >50% moister and > 1.0 ℃ cooler than in *belg*-2017 (data not shown). Besides the inter-seasonal differences in the environmental variables, agronomical conditions were different in those years. For instance, Tegecha (2383 m a.s.l.) was the only farm affected by late blight in *belg*-2017, whereas all farms were affected by the disease in *belg*-2018, although

the level of the outbreaks differed (based on our observations, but not quantified). It is remarked that the yield variations among cultivars were larger for higher yield farms and that yield variations with elevation were larger for productive cultivars.

The figure also shows that there was a large variation in yield among cultivars and among farms at different altitudes. Particularly the elevational variation was difficult to explain and it did not show a clear pattern. This might be associated with differences in soil quality, while variation in crop management and disease intensity may conceal the effects of meteorology on crop growth. Yet, in the following sections, we will attempt to explain the variations in terms of environmental variables.
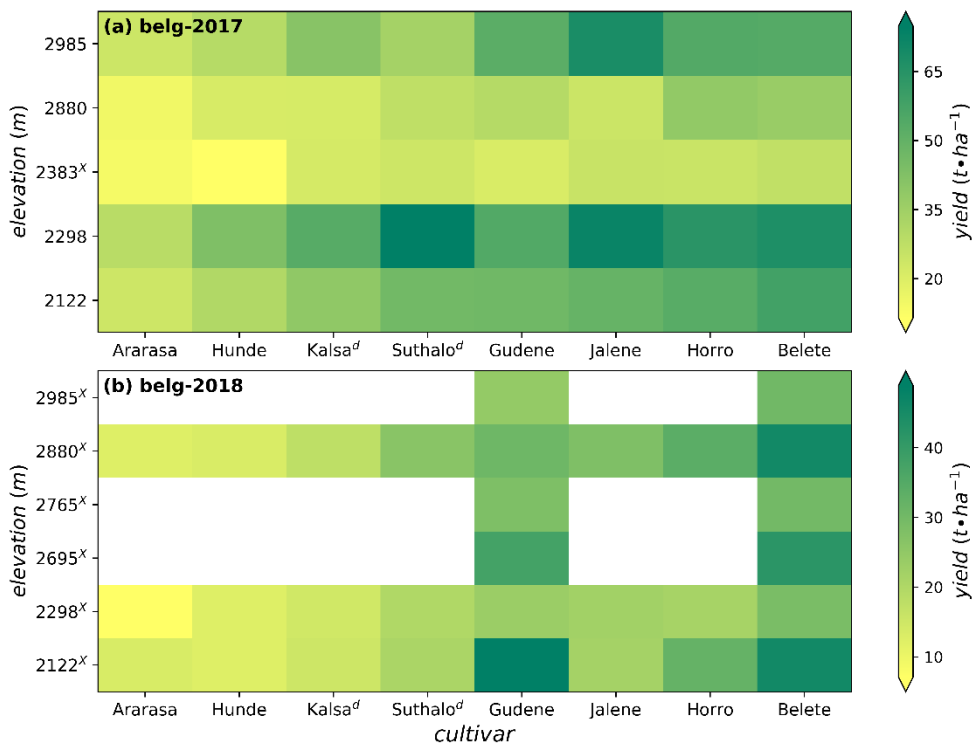


**Figure 5.5 | Yield (t·ha⁻¹) variations as a function of elevation (m) associated with the five farms in** *belg*-**2017 (a) and six farms at different elevations in** *belg*-**2018 (b) as shown in Table 5.1. The x-axis shows the eight potato cultivars planted, in order of increasing mean yield (** *belg*-**2017). The white spaces in (b) represent missing data. Note that the y-axes are not scaled and each elevation point (not continuous in space) show an experimental site mentioned in Table 5.1. Furthermore, the yields during the two** *belg* **seasons are so different that the scales of the color-bars are different. The x-axis names with a 'd' superscript are local cultivars. The 'x' superscript in the y-axis show farms affected by diseases.**

Figure 5.5 shows a substantial variation in the observed yield at 5 farms during *belg*-2017) (a) and at six farms in *belg*-2018 (b). In *belg*-2017, cultivar mean yield varied from 25 t·ha$^{-1}$ for *Ararasa* to 60 t·ha$^{-1}$ for *Belete*. However, in *belg*-2018, the yield and the variation were smaller ranging with yields from 7 t·ha$^{-1}$ for *Ararasa* and 48 t·ha$^{-1}$ for *Belete*. It is interesting to note that the relative trend in yields among cultivars in *belg*-2017 was similar as in *belg*-2018. In both years, *Belete* performed best in terms of yield in the Gamo Highlands. However, comparing yields of the cultivars at a farm level showed that *Belete* was not everywhere the best performing cultivar. For example, in the *belg*-2017, *Jalene*, *Horro*, and *Suthalo* showed the highest yield in Gircha (2985 m), Gazesso (2880 m), and Geresse (2298 m), respectively. Thus, this shows that selecting the best performing cultivar, in terms of yield, needs to be location specific. In *belg*-2018, a wetter season, we observed (not quantified) that crop diseases such as late blight affected all farms but to a variable extent.

Figure 5.6 presents the development of the canopy cover growth of the *Gudene* and *Suthalo* cultivars and the (cumulative) incoming radiation in MJ·m$^{-2}$ during *belg*-2017. The SW↓ was large during the first part of the growing season (P1), characterised by absence of thick cloud covers and precipitation. The plant uses the radiation particularly for the canopy buildup and for initializing the tubers. After canopy closure typically at the end of May, the SW↓ decreased by 50%, although the intercepted radiation was larger because the canopy cover was now at its maximum. In this phase (P2 and P3), the plant used the majority of the intercepted light for growing the tubers. In the following sections, we will study how the tuber yield depends on environmental conditions in P2 and P3 and on the choice of cultivar. We hypothesise that radiation intensity and precipitation in P1 are important predictors of tuber number, realised at the end of P1. Subsequently, harvested tuber fresh weight per plant depends on the environmental conditions in P2 and P3.
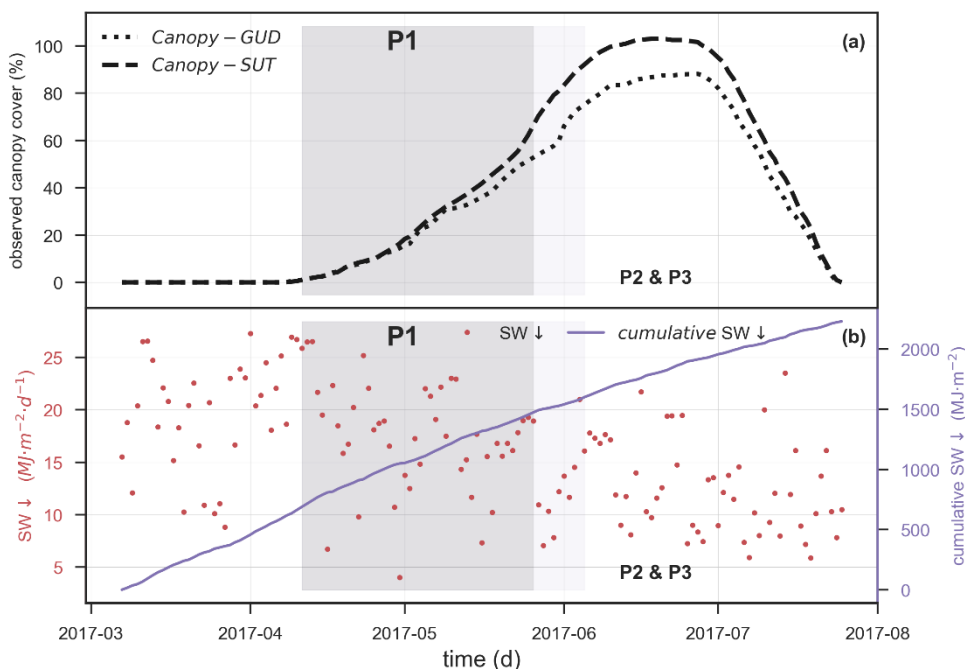
**Figure 5.6 | The observed canopy cover (%) (a) and the daily SW↓ (MJ·m⁻²·d⁻¹) (b) during the crop growth period in Gircha farm in *belg*-2017. In (b), the cumulative SW↓ (MJ·m⁻²) is shown on the right-side y-axis. The cultivars are *Gudene* (improved) and *Suthalo* (local). The crop growth phases P1-P3 are slightly different for the two cultivars.**

### 5.3.2.2   *Tuber number as a function of radiation and precipitation in P1*

Figure 5.7 shows the impact of SW↓ and precipitation in P1 on the number of tubers developed at the end of P1 for two cultivars in *belg*-2017 and *belg*-2018. For the local (*Suthalo*) cultivar, the tuber number was quite constant at around 20 tubers per plant. From our data, we were unable to find a clear relationship with radiation intensity and precipitation. With around 9 tubers per plant for the *Belete* cultivar, the number of tubers was lower than for *Suthalo*. The *Belete* tubers were 1.5 (2018) – 1.8 (2017) times heavier than the ones of other cultivars. For the *Belete* cultivar; however, the tuber number decreased from 10.0 to 7.3 per plant with increasing SW↓. The larger yield of the *Suthalo* cultivar, as compared to *Ararasa*, *Hunde* and *Kalsa*, was attributed to the larger number of tubers per plant.

The lack of a strong and physiologically expected relationship of the tuber number and radiation intensity may perhaps be explained by the high levels of radiation in the area. 10 MJ·m⁻²·d⁻¹ is the equivalent of 230 W·m⁻² or 530 μmol PAR m⁻²·s⁻¹ for 12 hours. With a light saturation point near 400 to 500 μmol PAR m⁻²·s⁻¹ (Gordon *et al.*, 1997; Pleijel *et al.*, 2002), the actual light intensity was larger than that most of the day, except during sunrise and sunset.

Tuber number per plant itself was generally poorly correlated ($r^2 = 0.11$) with yield, except for the *Suthalo* cultivar (all farms in *belg*-2017 and *belg*-2018, $r^2 > 0.84$) (not shown here).
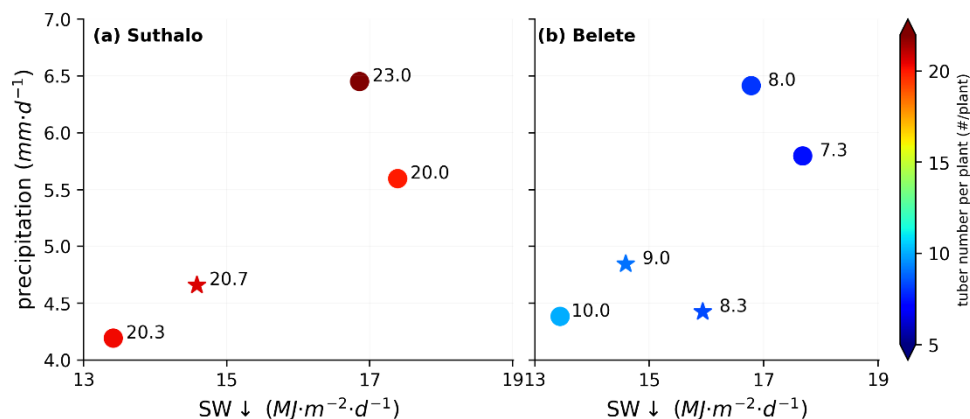


**Figure 5.7 | Tuber number per plant (color bar with values shown by the scattered points) at harvest as a function of SW↓ (MJ·m$^{-2}$·d$^{-1}$) and precipitation (mm·d$^{-1}$) for the local (a) and improved (b) cultivars during *belg*-2017 (circles) and *belg*-2018 (stars). The SW↓ and PPT are mean values in P1.**

### 5.3.2.3 *Number of branches and yield*

Figure 5.8 shows that the number of branches had quite a strong relationship with total yield, across all cultivars, at least in *belg*-2017. In *belg*-2017, the number of branches had a wider range than in *belg*-2018, as did the yield. In all experiments, the number of plants per m$^2$ was the same (Section 5.2.2). The relationship may be explained by better light interception by the plant with more branches, suggesting that the number of plants per m$^2$ could be increased. In *belg*-2018, there were a number of plots with less than 6 branches per plant, which impaired the otherwise positive relationship. Note that, in Section 5.3.2.1, we showed that the seasonal climates are significantly different in both years, which can influence the branch numbers (Table 5.1). However, number of branches might also be a reflection of physiological age of the seed tubers. The seed tubers in *belg*-2017 were from different origins whereas the seed tubers in *belg*-2018 were from the same origin.

**Figure 5.8 | Variations in the observed yield (t·ha⁻¹) for eight cultivars as function of total number of branches at maturity (#). The colors represent cultivars in four locations in *belg*-2017 (a) and six locations in *belg*-2018 (b). The linear coefficient of correlation ($r^2$) and the linear regression equation are shown in (a); and no clear correlation is observed in (b). Note that scales along x and y-axes are different for both panels.**
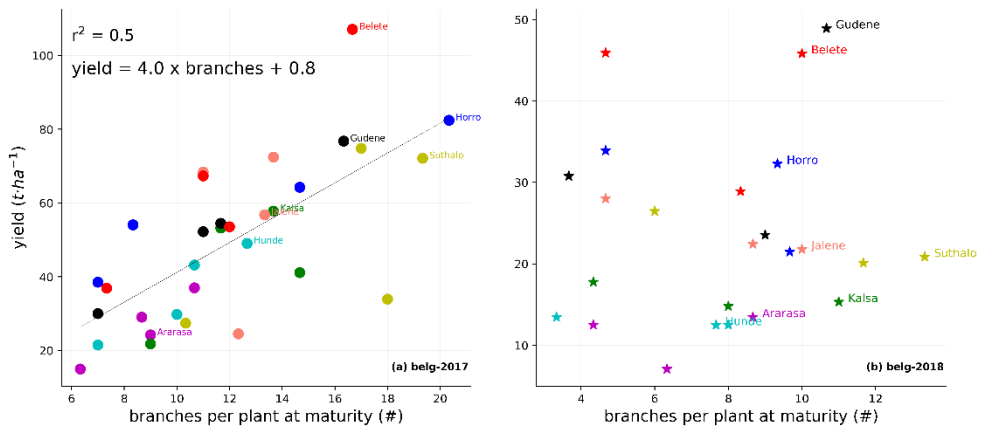
### 5.3.2.4   Days to maturity and yield

Figure 5.9 shows the yield as a function of days taken to crop maturity (Section 5.2.4.1). The figure shows a large variation in the number of days to maturity and tuber yield. In *belg*-2017 (Figure 5.9a), the results indicate an optimum yield (at around 100 days), which agrees with (Spitters, 1987). This trend was consistent for all cultivars. The highest yields were attained in the lower elevation areas (Geresse and Derashe), where the number of days to maturity was between 95 to 105 days (potato can be harvested in 90 days, and it can take up to 150 days in cooler climates such as northern Europe (FAO, 2008b)). The Tegecha site was also in this range, but yields were affected by diseases in 2017. At lower elevations, the temperature was too high and the foliage grew fast, while it did not result in bulking (Tsegaw, 2005). At higher elevations, the growth was slower, the onset of tuber formation occurred later, which eventually increases yield (Allen and Scott, 1980). In addition to the meteorology, soil moisture and nutrient availability can play key roles in determining the time to maturity and yield across farms, but we do not have these data available. In *belg*-2018 (Figure 5.9b), the yield and days to maturity data were less variable and would fit into the lower left part of Figure 5.9a. As such, the growing conditions in *belg*-2018 were much different from the ones in *belg*-2017, but the results did not contradict the results of *belg*-2017.
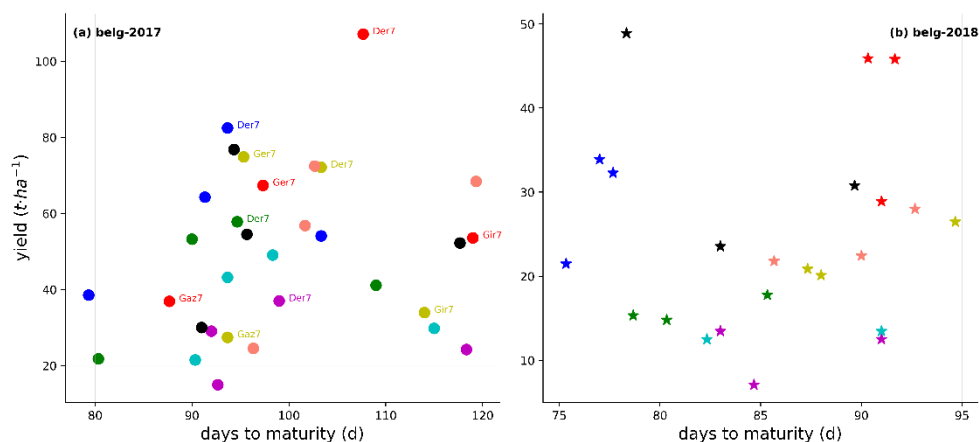
**Figure 5.9 | Variations in the observed yield (t·ha⁻¹) for eight cultivars as function of days to crop maturity (d). The colors represent cultivars in four locations (Gaz7 – Gazesso, Ger7 – Geresse, Der7 – Derashe, and Gir7 – Gircha) in *belg*-2017 (a) and six locations in *belg*-2018 (b). Note that x and y-axes ranges are different for both panels; and the colors (*e.g.* red dots and line – *Belete* and yellow dots and line – *Suthalo* cultivars) represent a cultivar in different farms.**

*5.3.2.5   Tuber fresh weight as a function of environmental variables in P2 and P3*

Figure 5.10 presents the tuber fresh weight per plant as function of SW↓, T$_{mean}$ and soil moisture tension (ψ) in *belg*-2017 and *belg*-2018. The environmental variables did not show a clear correlation with tuber fresh weight in *belg*-2018. However, in *belg*-2017, tuber fresh weight at harvest showed an increasing trend with SW↓ and ψ, and a decreasing trend with T$_{mean}$. The following explanation is about *belg*-2017.

The tuber fresh weight increased from 200 – 900 g/plant at 10.5 MJ·m⁻²·d⁻¹ in Tegecha (*belg*-2017) to 800 – 2100 g/plant at 13 MJ·m⁻²·d⁻¹ in Gircha in *belg*-2017. It is interesting to note that the variations (in terms of the standard deviations) in the tuber fresh weight per plant among cultivars increased significantly (from 500 to 1000 g/plant) as the SW↓ increased (a). However, the 2 – 4 fold increase in tuber fresh weight seems large relative to the 30% increase in radiation. Therefore, we are careful explaining the correlation as a causal relationship. The relation found may also be explained by warmer weather and decreased soil moisture in Tegecha (Minda *et al.*, 2018a). It should also be noted that Tegecha farm was affected by diseases (Figure 5.5).

127

Tuber fresh weight decreased from nearly 1400 g/plant with $T_{mean}$ of ~ 11.5 ⁰C in Gircha to 500 g/plant with $T_{mean}$ of 17 ⁰C in Tegecha in *belg*-2017. This is remarkable, because the optimal temperature for potato growth is often considered to be near 15 to 18 ⁰C (Haverkort, 1990). However, yield depends on rate and duration of growth, where temperature near the optimum mainly affects the rate of growth. Gazesso is only slightly warmer and wetter than Gircha in *belg*-2017 (Table 5.1). These are indications that SW↓ and $T_{mean}$ are probably not dominant drivers of tuber fresh weight in the Gamo Highlands and the relationships are induced by other variables.

Tegecha also shapes the soil moisture – tuber fresh weight space. At the highest soil moisture tension (the driest soil), it has the lowest tuber fresh weight. Gircha, with the highest SW↓, coolest temperature and moderate soil moisture (as compared to Tegecha and Gazesso) had the highest tuber fresh weight per plant. However, considering that soil moisture and temperature are positively correlated and both are negatively correlated with temperature, it is difficult to attribute the variations in tuber fresh weight to the environmental variables. Interestingly, the difference in tuber weight among cultivars was consistent (*Belete* and *Ararasa* were the highest and lowest, respectively in both years) among *belg* seasons.
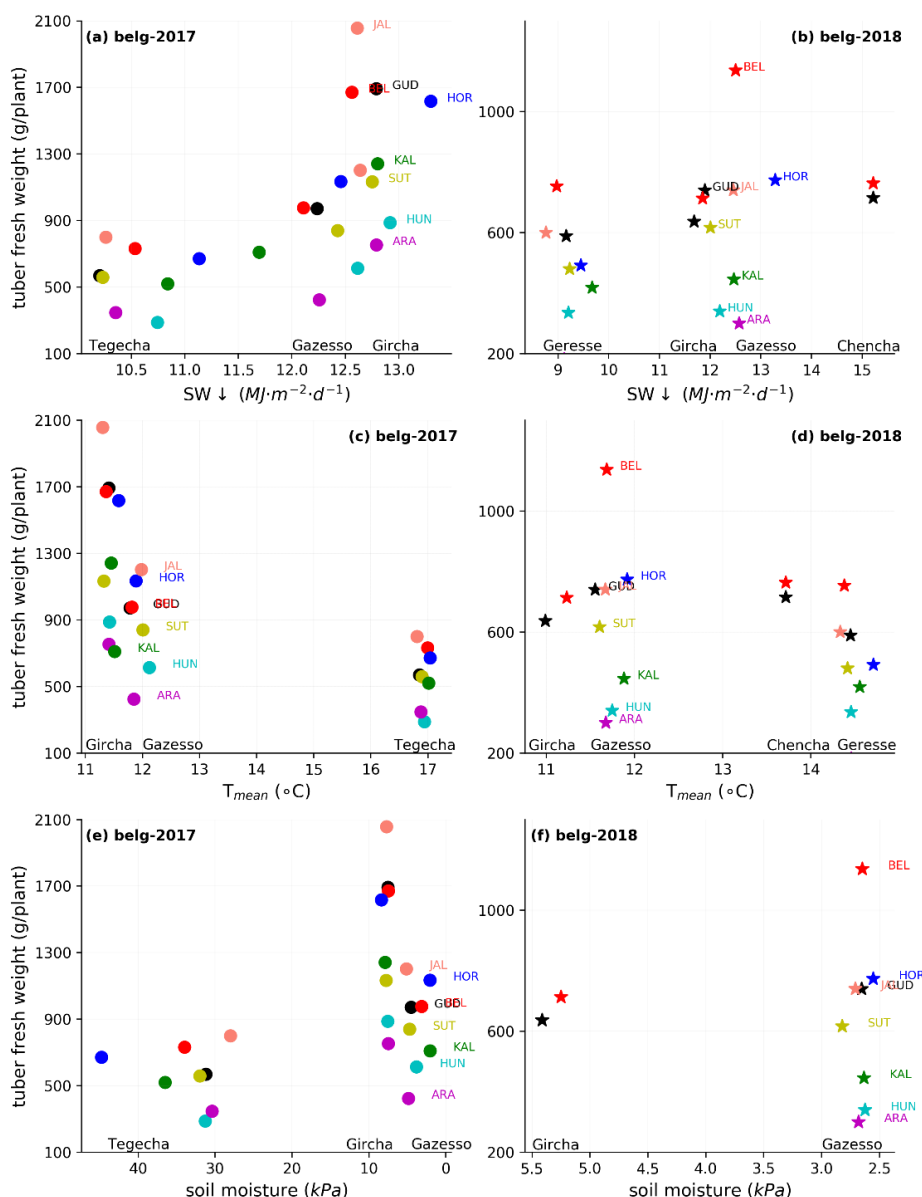
**Figure 5.10 | Tuber fresh weight gram per plant (g/plant) at harvest as a function of mean SW↓ (MJ·m$^{-2}$·d$^{-1}$) (upper row – a, b), T$_{mean}$ (°C) (middle row – c, d), and soil moisture tension (ψ) (kPa) (bottom row – e, f). The left panels show *belg*-2017 and the right panels indicate *belg*-2018. The cultivars were *Ararasa* – ARA, *Hunde* – HUN, *Suthalo* – SUT, *Kalsa* – KAL, *Horro* – HOR, *Belete* – BEL, *Gudene* – GUD, and *Jalene* – JAL as marked in colors. The weather station/farm names are indicated below the corresponding datasets shown in the scattered dots. The SW↓, T$_{mean}$ and ψ are average values in the period from P2 to P3. Note that from farms in *belg*-2017 and *belg*-2018, those farms with available SW↓, T$_{mean}$, and ψ data records are included here. Note that the mean value of ψ at four soil depths (5, 10, 20, and 40 cm) are reported; and ψ = 200kPa is a fully dry soil and ψ = 0kPa means a fully saturated soil.**

*5.3.2.6  Partitioning of dry matter over parts of the plant*

The harvest index (Section 5.2.4.3) indicates the percentage of the produced dry matter allocated to the tubers. In western countries, the HI is relatively constant at around 75% and depends on cultivar traits and growing conditions.

In our experiments, we estimate total produced dry matter from the cumulative amount of intercepted radiation. Figure 5.6 shows that the canopy cover for the local cultivar and the improved one, both grown at Gircha, developed similarly. However, the yield was significantly different for the two cultivars, resulting in a harvest index of 44% for *Suthalo* and of 80% for *Gudene*. This shows that *Gudene* invested more of its dry matter in the tubers than the *Suthalo* cultivar, and that choosing the right cultivar has an important effect on the yield.

## 5.4  Discussion

In this paper, we analysed a large number of observations of potato plant growth and yield for dependency on environmental conditions and physiological effects, aiming to find out if potato behaves similarly in Ethiopia as it does in temperate climate regions. Here, we will discuss the obtained results in relation to results from experiments in the western world, to highlight aspects that should be investigated in more detail in future experiments.

*Research question 1: How does canopy growth vary with environmental variables in P1 across elevations, among potato cultivars, and between seasons?*

Temperature sum turned out to be a strong predictor of canopy cover and plant height in the canopy buildup phase (P1, shown in Figure 5.1), with explained variances ($r^2$) > 0.90 and relatively similar slopes across cultivars and years (from Figure 5.2 to Figure 5.4). Haverkort (2018) also explained canopy cover as a linear function of Tsum during P1.

However, the growth rates appeared to also depend on cultivar and growing conditions, specifically light intensity and soil moisture (Minda *et al.*, 2018a). The local *Suthalo* cultivar appeared less sensitive to drought than the improved cultivar *Gudene* (Figure 5.4). Ethiopian farmers indeed mention that local cultivars are more drought resistant (Abebe *et al.*, 2013). Kolech *et al.* (2015) also mentioned that some of the local cultivars in Ethiopia are drought tolerant. In contrast, the canopy growth rate of *Gudene* was less sensitive to limited radiation. This suggests that the water and radiation use efficiency (RUE) of the two cultivars may be different. We cannot rule out that seed quality differed among experiments. The RUE of potato cultivars is between 1.07 and 2.24 g per MJ of intercepted radiation depending on cultivar and light intensity (Burstall and Harris, 1983; Fahem and Haverkort, 1988; Sinclair and Muchow, 1999). These findings are as expected (Kooman, 1995; Kooman and

Haverkort, 1995a) and we do not recommend further research in the field of response of canopy cover and plant height to meteorological conditions. However, we do recommend further research into the performance of different cultivars under meteorologically or nutrient-limiting conditions with experiments under field conditions or in controlled chambers, and with controlled seed quality. It is also worthwhile to investigate the RUE of the local and improved cultivars for better understanding of the Tsum and canopy growth relations.

*Research question 2: How does yield depend on physiological crop characteristics, such as number of tubers, number of branches, days to maturity, cultivar, and on meteorologically dependent variables, such as intercepted radiation and temperature?*

Yield and yield traits showed significant variations among farms, cultivars and *belg* seasons. There were consistent differences (factor 2) between the average yields at farms located at different elevations. Elevation itself; however, did not seem a strong predictor (Figure 5.5). We anticipate that soil fertility, management or climate may explain the differences between farms.

Cultivar was an important predictor of yield variation (factor 3) across all farms and years. Even though some farms and cultivars had higher overall yield, there was no single farm that performed best with all cultivars and there was no single cultivar, which performed best at all farms. Apparently, a cultivar's performance is specific for the conditions at a farm.

The number of tubers per plant did not vary logically with radiation intensity and precipitation (Figure 5.7). However, the range of those variables was small and the variables were probably not limiting plant growth. The average number of tubers per plant across all farms and cultivars was 14 in *belg*-2017 and 10 in *belg*-2018. Most cultivars had tuber numbers close to the average, except *Ararasa* and *Hunde* in *belg*-2018 (about half) and *Suthalo* (about double in both years). Tuber number was not a predictor of yield for most cultivars, because the weight of individual tubers varied among cultivars. Consequently, the number of tubers per plant does not seem to be a variable of interest for further research. Similarly, Onder *et al.* (2005) showed that tuber number per plant was not affected by irrigation, but the mean tuber weight and tuber yield increased quite strongly with irrigation level. Haverkort *et al.* (1990) found that tuber number per plant increased from 9 to 21 per plant when precipitation increased from 0.5 to 3 mm·d$^{-1}$ during the first 40 days after planting. The authors also showed that a further increase in precipitation did not lead to an additional increase in the number of tubers per plant. As the lower range of precipitation in our study was 4.0 mm·d$^{-1}$ (Figure 5.7), it appears that our results are in line with those of Haverkort *et al.* (1990).

The number of branches per plant appeared to be a medium strong predictor of tuber yield ($r^2 = 0.5$), while the plant density was identical in all experiments (Figure 5.8a). In irrigation experiments, Yuan *et al.* (2003) showed that increases in irrigation

are associated with a larger number of branches ($r^2 > 0.8$) and ultimately increased tuber yield. Taye *et al.* (2012) also found that the number of branches positively affected light absorption; and tuber yield for a tuber crop (*Plectranthus edulis*, a crop comparable to potato, *Solanum tuberosum* L.) in Ethiopia. The result suggests that radiation interception was an important constraint and that light interception was not maximal yet in the conditions during the experiment.

In *belg*-2017, the yield was optimal at around 100 days to maturity of the plant (Figure 5.9) (FAO, 2008b). This occurred predominantly at the somewhat lower farms (~2,200 m a.s.l.). The highest yields in Derashe can be associated with early tuberization, resulting in an extended period of tuber growth and/or increased rate of tuber bulking (Borah *et al.*, 1960). At higher elevation (*e.g.* at Gircha), the growth was slower. This can be related to a delay in the onset of tuber formation, which extended the crop maturation period, but decreased yield (Allen and Scott, 1980). The more humid conditions also make the crop susceptible to diseases (Tufa, 2013). At farms at even lower elevations, the temperatures were so high that the crop grew very fast, but with decreased tuberization rate (Tsegaw, 2005). These results are very similar to the ones we found in Minda *et al.* (2018b), where we explained the optimum yield at mid-levels in terms of radiation and soil moisture. With increasing elevation, the temperature becomes closer to the optimum temperature for potato, and the soil becomes moister. The lower temperatures and moister conditions increase the duration of leaf wetness, which is an important predictor for the occurrence of diseases like late blight. At mid-levels, the potato crop finds an optimum between those effects. It is interesting to note that cultivars have different responses to radiation and soil moisture limitations in P1 (Section 5.3.1.3). Although this may be an interesting explanation, we need to be careful being too resolute, since the physiological age and size of the seed tubers may also cause differences in growth and yield. We also observed that the optimal number of days to maturity was different for each cultivar. We do not have detailed, cultivar-specific data about the growth of the tubers during P2 and P3, but this would definitely be worth further research.

Additionally, we may have found evidence that an increase in radiation intensity from 10 to 13 MJ·m$^{-2}$·d$^{-1}$ in P2 and P3 increased yield from ~500 to ~1300 g/plant (Figure 5.10). However, these data were sparse and the range in radiation intensity was small. The suggestion that radiation interception was not saturated is remarkable, because Figure 5.6 shows that the canopy cover was near 100% at the end of P1. However, the radiation intensities are strong enough in this tropical environment for lower leaf levels to still intercept significant amounts of radiation. This suggests that LAI may be a better variable to express radiation interception and photosynthesis rates. Allen and Scott (1980) also showed that tuber dry weight increased nearly linearly from ~500 to 1000 g/plant as the total intercepted radiation increased from

500 to 1500 MJ·m$^{-2}$·season$^{-1}$. In their experiment, the total radiation interception depended on the canopy cover or the LAI (Allen and Scott, 1980). Figure 5.10 also showed that tuber weight per plant increased with soil moisture tension.

Curiously, we found that yield decreases with temperature from 11 to 18 °C, which is often mentioned as the optimal temperature for potato growth. Haverkort (2018) explained that the optimal daily T$_{mean}$ for tuber production is 18 °C and that tuber fresh weight decreases nearly linearly below and above that temperature. Van Dam *et al.* (1996) found that tuber dry weight was the highest at 15 °C for both Spunta and Désirée cultivars. Timlin *et al.* (2006) explained that tuber dry weight and temperature showed a quadratic relation, in which the optimal tuber weight is attained at different temperatures (17-22 °C), depending on the number of harvest days taken. Figure 5.10 shows that in our situation, fresh tuber weight (g/plant) was the highest when T$_{mean}$ < 14 °C and SW↓ > 16 MJ·m$^{-2}$·d$^{-1}$ as opposed to Van Dam *et al.* (1996) and Timlin *et al.* (2006). This contrasting result gives us the impression that temperature is not the real limiting factor determining the tuber fresh weight in our experiments. This underlines the importance of explaining the results carefully and designing a new field campaign, which enables us to disentangle soil, potato physiology, and meteorological factors.

With the available data, we could quantify the harvest index for two cultivars at Gircha. They appeared to be very different, 44 and 80%. This again shows that cultivars can behave very differently even though exposed to the same environmental and management conditions.

We did not find evidence that potato is behaving differently in Ethiopia than in the temperate climates. However, temperature is rather constant in time and relatively close to the optimal temperature. Close to the equator and in the *belg* season, radiation intensities are large and probably only limiting early in the morning and late in the afternoon. LAI, however, may affect the radiation absorption.

We have collected abundant potato growth data, distributed over farms and cultivars. Only plant height and canopy cover were monitored during the growing season. Yield, tuber number and tuber weight were only measured at the end of the growing season. Thus, during P2 and P3, we had more predictor variables than response variables. In the future, we advise to use a simpler experimental structure, to better control seed quality, but to increase the frequency of the measurements during P2 and P3, particularly with respect to the below ground growth variables. Furthermore, we recommend to investigate the sensitivities of each cultivar to radiation, soil moisture and temperature and these variables should be monitored in detail during the entire growing season and different climatological years. Above/below ground yield traits (total dry matter, tuber number and tuber weight) should be measured frequently during the growing season. Because these require a large effort, the number of cultivars used should be reduced in favour of the number of replications.

**5**

## 5.5 Conclusions

Based on the analysis of field trials with eight potato cultivars in six locations and during two seasons, our conclusions on the relationships of environmental variables and potato dynamics at different phases are the following.

During the canopy buildup phase (P1), temperature sum is a strong predictor of plant height and canopy cover of potato in Ethiopia. There are only small variations in growth rate among cultivars, but cultivars appear to have diverging sensitivities to soil moisture and radiation limitations.

Tuber yield is largely determined by growing conditions in the maximum cover phase (P2), and the canopy decline phase (P3), because tuber number (initiated in P1) is not a predictor of total yield. Yield is quite variable between farms at different elevations and between cultivars. The number of branches and radiation intensity appear to positively affect the yield, but the underlying processes remain to be quantified and understood. Possibly, light interception and photosynthesis rates are enhanced in plants with more branches. Leaf Area Index may be an important constraint and it should be measured in future experiments.

The choice of cultivar has a large effect on yield. Still no single cultivar had the largest yield at all farms. This suggests that cultivars have different sensitivities to environmental conditions. It may follow that cultivars have a specific optimal elevation zone to grow in.

# 6
# General discussion

The overarching aim of this PhD thesis has been to provide quantitative insights into the role played by meteorology and elevation on the dynamics of crop growth, more specifically the potato. The study area was located in the Gamo Highlands, a region in southwest Ethiopia with a complex topography and a high degree of land heterogeneity. The weather in this region is mainly driven by large-scale dynamics such as the intertropical convergence zone (ITCZ), and is also modulated by local meteorological flows such as the lake-mountain breezes. This region is also of interest since potato, a crop which is sensitive to environmental cues, has been widely grown and plays a key role in ensuring food security in the region. These considerations have opened an opportunity to investigate the role played by environmental conditions, *i.e.* meteorological and edaphic variables, on the growth and yield of potato.

The study of weather and crop dynamics in this complex terrain requires an approach that combines the disciplines of meteorology and crop physiology. From a methodological viewpoint, a strategy that combined both observations and models is followed in the thesis. The approach and strategy implemented could help us to obtain deeper insights into weather-crop relationships. To this end, a high-resolution state-of-the-art weather model was adopted. Meteorological variables were simulated using the weather model and supplied to an advanced process-based crop model. The modelling design was also complemented by field crop experiments conducted near our network of automatic weather stations, installed at different elevations. This chapter puts the most relevant findings of the thesis in perspective and suggests potential ways to continue our research efforts to improve our understanding of Ethiopian weather-crop dynamics.

## 6.1  The model perspective

### 6.1.1  Meteorology at fine grid spacing

Analysis of the results of the fine resolution (2 km × 2 km) of the Weather Research and Forecasting model (WRF) (Skamarock *et al.*, 2005) revealed significant spatial and temporal variations in the major meteorological crop drivers: minimum and maximum temperatures ($T_{min}$ and $T_{max}$) and precipitation (PPT). The results are reported and discussed in Chapter 3. They showed a satisfactory performance of the WRF model compared with the observations. A specific finding was that the bimodal precipitation trend (*i.e.* precipitation maxima in April and October) in the region of interest is well simulated as compared to the data recorded at two elevations. This has been shown by Diro *et al.* (2008) and Korecha (2013). These observations were representative of the lowland (*e.g.* Arba Minch station) and highland (*e.g.* Chencha station) altitudes.

However, there were some mismatches between the simulated and observed data. We suppose that the causes for these mismatches can be related to a number of cases, as mentioned by Tariku and Gan (2018). Here, we discuss two such cases: (1) uncertainty related to observations and (2) uncertainty related to the weather model. For the first case, both the number and quality of weather stations in Africa are limited (Dinku *et al.*, 2014). Van Vooren *et al.* (2018) discussed uncertainties related to gauged-based weather stations, such as instrument failures, systematic measurement biases, losses due to evaporation and wetting, transmission, digitisation and storage errors. The authors also showed that gauged stations are installed in basins in mountainous areas, where they tend to underreport the actual areal mean precipitation. With regard to the second case, the following issues can be raised: the model's representation of topography, the parameterization schemes employed, the land use/land cover (LULC) implemented and the soil moisture and soil temperature initialisation values.

On the spatial scale, the modelled elevations were 62 m and 100 m above the actual elevations of Arba Minch and Chencha, respectively. Due to this mismatch in elevation, biases were observed in $T_{min}$, with Mean Bias Error – MBE of -0.5 °C and $T_{max}$, MBE of -3.5 °C, for the Arba Minch weather station. It has also been reported that the WRF model driven by the ERA-Interim reanalysis (Dee *et al.*, 2011) underestimated the observed temperature in the Ethiopian Highlands (Abdelwares *et al.*, 2018; Van Vooren *et al.*, 2018).

Where the model's temperature bias due to elevation representation is concerned, it is possible to correct the simulated temperature using environmental lapse-rate calculated from the GEMS observed datasets following the recommendations of Kunz *et al.* (2007). However, there is no simple method to correct biases related to important meteorological crop drivers such as PPT and the incoming

shortwave radiation (SW↓). In this regard, one option would be to increase the spat ial resolution, for example, from 54 km to 2 km horizontal resolution. First, we showed that the stations' elevations are much better represented in the fine resolution (*e.g.* the location of the Chencha station is smoothed and is shown as 1100 m lower than true elevation in coarse resolution as compared to 100 m above the true elevation in fine resolution). Second, the potato-growing zone, *i.e.* 1500 m to 3200 m a.s.l. as presented in Tufa (2013), is well represented in the fine resolution (51% and 8% of the grids cells in the fine and coarse resolution respectively fall within the potato-growing zone). Third, the spatial details of weather in the highlands are bet- ter represented in the fine resolution than in the coarse resolution. Fourth, the mod- elled yield with the fine resolution is reasonable in terms of crop growth variables such as length of the growing season (LGS) and Leaf Area Index (LAI), while these measures lie within an unacceptable range in the coarse resolution (FAO, 2008b; Harper, 1963). In agreement with the benefits obtained by the use of the fine resolu- tion model, Torma *et al.* (2015) also discussed the added values of nested Regional Climate Models (RCMs) in a complex topographic region in the Alpine region. The authors, for a fine resolution (0.11° as compared to 0.44° and 1.32°) RCM, showed improvement in modelled precipitation (with spatial correlation [$r^2$] of 0.52-0.58 for 0.11°, 0.30-0.45 for 0.44°, and 0.09-0.25 for 1.32° resolution model).

For these reasons, moving to a finer spatial scale, for example 1 km × 1 km, could better represent the topography and explicitly resolve the sub-grid weather pro- cesses such as cumulus clouds and its transition to deep convection (Hijmans *et al.*, 2005; Stensrud, 2007; Zhao *et al.*, 2015). In particular, cloud onset, formation and in- tensity could be improved from the high-resolution model study (Abdelwares *et al.*, 2018). Weather prediction based on a finer scale can also improve downscaling of the meteorological outputs to the field-plot scale. Doing so offers yield predictions (Headey *et al.*, 2014) on rural farmer scale can help smallholders make farm-level decisions (Gibbons and Ramsden, 2008). The finer resolution model, in our case, has significantly improved simulated temperatures (explained in terms of MBE and RMSE) and annual total precipitation. We also want to raise our concern for simu- lated precipitation on daily basis as compared to the observations. For precipitation, the coarse resolution showed improvements, as discussed in Chapter 3.

Our result showed that WRF is dry-biased (with an MBE of -1.3 mm·d⁻¹ for the Arba Minch station) around Lake Abaya and Lake Chamo and wet-biased for ele- vated areas (with an MBE of +3.7 mm·d⁻¹ for the Chencha station). In agreement with our findings, for the low elevation areas around the Lake Victoria basin in eastern Africa, Argent *et al.* (2015) showed that the WRF model underestimated the observed precipitation, with a Root Mean Square Error (RMSE) of 139 to 199 mm·year⁻¹. On the other hand, Abdelwares *et al.* (2018) showed a moist bias (RMSE of between 2 to 3 mm·d⁻¹) over elevated areas in Ethiopia using the WRF model driven by the ERA-

Interim reanalysis. See Willmott (1982) for model-observations statistical comparisons.

Several authors have mentioned that the WRF model is sensitive to the model's physics parameterization scheme options (Abdelwares *et al.*, 2018; Tariku and Gan, 2018). They recommended selecting the best-performing schemes from the set of parameterization options given in the WRF model namelist input file (*e.g.* six cumulus scheme options are provided). Pohl *et al.* (2011) and Tariku and Gan (2018) recommended a selection of suitable parameterization schemes (*e.g.* cumulus convection, microphysics, and short- and longwave radiation) and model settings to improve forecasting performance. It is important to underline that suitable parameterization schemes may be different for different regions. Hence, the schemes should be selected at regional level (Abdelwares *et al.*, 2018; Argent *et al.*, 2015; Tariku and Gan, 2018) as shown in Table 6.1. Following these suggestions, we recommend selection of best-fitting parameterization schemes to the Gamo Highlands before longer-period modelling is carried out.

**Table 6.1 | Recommended WRF model settings for the Lake Victoria Basin in East Africa; Ethiopian Highlands (Eastern Nile River Basin); Ethiopian Highlands (Nile River Basin), and this study.**

| WRF Model descriptions | Source | | | |
|---|---|---|---|---|
| | Argent *et al.* (2015) | Abdelwares *et al.* (2018) | Tariku and Gan (2018) | This study |
| Region | Lake Victoria Basin | Eastern Nile Basin (Ethiopian Highlands) | Nile River Basin | Gamo Highlands |
| Model version | 3.3 | 3.5 | 3.6.1 | 3.4.1 |
| Horizontal res. | 10 km | 10 km | 12 km | 2 km |
| GCM forcing | NCEP FNL | ERA-Interim | ERA-Interim | ERA-Interim |
| Sea Surface Temp (SST) forcing | Optimum interpolation SST data | ERA-Interim | ERA-Interim | ERA-Interim |
| Validation datasets | Satellite-obs. merged (TRMM 3B42) | Gridded datasets (PPT – GPCC, Temp – UDEL) | Satellite (TRMM), Gauged (GPCC), Reanalysis (CFSR) | Station observations |
| Study period | 1198-1999 (Oct-Dec) | 1998-1999 (Jun-Sep, Dec-Mar) | 1999-2001 | 2001-2010 |
| Variables analysed | PPT/Temp | PPT/Temp | PPT/Temp | PPT/Temp/ SW↓ |
| Cumulus convection | Betts-Miller-Janjic | Betts-Miller-Janjic | Kain-Fritsch | Explicit |
| Planetary Boundary Layer (PBL) | ACM2 (Pleim) scheme | Mellor-Yamada-Janjic (MYJ) | MYJ | Yonsei University (YSU) |
| Shortwave radiation | Dudhia | CAM | Dudhia | Dudhia |
| Longwave radiation | Rapid Radiative Transfer Model (RTTM) | CAM | RRTM | RRTM |
| Microphysics | Eta | WRF Single-Moment (WSM) 6-class | WSM 3-class | WSM 6-class |
| Land Surface Model | Noah | Noah | Noah | Thermal diffusion |

Regarding the temporal integration of our results, our weather and crop modelling covered a sub-climatology period from 2001 to 2010. Feeding a significantly growing population (currently, the Ethiopian population is estimated to be 110 million (FAO, 2019) with an annual growth rate of 3% (CSA, 2013)) in a changing climate needs understanding of both the future climate and its impact on food security. In this regard, future climate projections (*e.g.* 2001 to 2019 base period and projections from 2020 to 2037, 2050, and 2100) with a range of assumptions (*e.g.* Representative Concentration Pathways – RCP2.6 to RCP8.5) could have a number of benefits. First, these datasets can be used to investigate how the future climate in the Anthropocene epoch will influence mesoscale and synoptic scale flows in the Gamo Highlands, as discussed by (Ashok and Yamagata, 2009; Marchant *et al.*, 2007; Shongwe *et al.*, 2011). Second, such long-term datasets can be employed in the study of regional climate change (*e.g.* to analyse trends in precipitation and temperature) and climate variability (*e.g.* to estimate the probability of extreme weather events such as droughts and heat-waves). Third, the data can be used as crop model input to predict crop yields (Sheffield *et al.*, 2006); for example, to estimate future crop growth, diseases, and yields in the warming climate with elevated $CO_2$ levels, in order to assist decision-making at local level (Haverkort and Struik, 2015; Hijmans, 2003; Schleussner *et al.*, 2018) to anticipate changes in food security.

Downscaling future climate data from global circulation models such as EC-Earth Hazeleger *et al.*, (2010; 2012) to study regional impacts and even further down to local scales could have enormous benefits. From such studies, climate change adaptation decisions, for example decreasing the yield gap, can be recommended as a means of improving food security in sub-Saharan Africa (Hall *et al.*, 2017; Newbery *et al.*, 2016). Finally, the EC-Earth model can be used as an input for initial and lateral boundary conditions of the WRF model to study future climate scenarios at regional to local levels. This could help to explore the response of meteorological and potato crop variables influenced by elevation under future climate conditions.

Fine horizontal resolution LULC maps, soil moisture and temperature model initializations have a significant impact on improving meteorological forecast performance (Kurkowski *et al.*, 2003). However, there is still room for improvement regarding an update of the land properties. Hong *et al.* (2009) utilised the Moderate Resolution Imaging Spectroradiometer (MODIS) satellite datasets to drive the WRF vegetation fraction and to compare surface energy fluxes with the default WRF vegetation fraction. The authors showed that the model was highly sensitive to changes in the vegetation fractions employed. The modified vegetation fraction from the MODIS data improved energy flux simulations (*e.g.* for sensible heat flux, RMSE of 63 W·m$^{-2}$ and $r^2$ of 0.81 as compared with 78 W·m$^{-2}$ and $r^2$ of 0.67 as were calculated for Texas in the USA). Wen *et al.* (2012) used LULC data obtained from the Earth Observing System from the MODIS satellite and initialised the WRF model with ob-

served soil moisture and temperature observations. Their analysis using the implemented model settings showed improved agreement in surface temperature (bias = 0.9 °C and RMSE = 2.0 °C as compared to bias = 1.6 °C and RMSE = 2.7 °C), Relative Humidity – RH (bias = -7.8% and RMSE = 14.1% as compared to bias = -14.9% and RMSE = 19.1%), wind direction, and heat fluxes as compared with *in situ* observations. Using soil moisture (satellite and ground observations merged) and soil texture (field surveys) data in the WRF model improved simulated soil moisture values (Lin and Cheng, 2016). The use of remotely sensed LULC maps, soil moisture and temperature data in WRF models can be a key strategy to improve model performance in the Gamo Highlands.

### 6.1.2 Crop model

The process-based crop model, GECROS (Yin and van Laar, 2005), was employed and compared with the observations described in Chapter 4. Although the model reasonably predicted the yield trend with elevation, it underestimated the yield observations. The main reason for the model-observation mismatch is that we set up GECROS based on data obtained from the literature; for example (Khan, 2012; Yin and van Laar, 2005) for genotypic characteristics model inputs as we lacked the detailed field observations needed to calibrate the model. This task needs detailed experiments to quantify model constants and parameters. We suggest a new alternative approach to potato crop modelling and forward a remark for crop modellers, which we explain as follows.

1) *GECROS is more versatile than most crop models; however, it is also complex in that the model requires several detailed input parameters (Haverkort and Struik, 2015; Ingwersen et al., 2018). Besides, most of the potato crop models are designed to function in the temperate region (De Wit et al., 2019; Haverkort and Harris, 1987). We learned that calibrating the model to the tropical mountainous environment and Ethiopian potato cultivars is a challenge, as sufficient data are not available to do so. It may therefore be reasonable to use simple but robust models such as LINTUL-POTATO (Kooman and Haverkort, 1995a; Spitters, 1990) and WOFOST (Boogaard et al., 1998; De Wit et al., 2019; Van Diepen et al., 1989). The LINTUL-POTATO model, for example, is based on model descriptions of accumulated dry matter as a function of intercepted solar radiation and light use efficiency, and the model uses fewer model inputs than GECROS (Haverkort et al., 2015; Shibu et al., 2010; Van Keulen and Stol, 1995). The LINTUL model is also widely used for potato modelling at global scale (Fleisher et al., 2017; Haverkort et al., 2004; Hijmans, 2003; Van Keulen and Stol, 1995), in the tropical environments (Fleisher et al., 2017; Pereira and Nova, 2008; Pereira et al., 2008), and in Ethiopia (Haverkort et al., 2012; Quiroz et al., 2014).*

2) *For crop modelers, we make the following point. A yield estimate, which can be compared with observed crop yield, can be simulated for the wrong reason. We modelled an attainable yield of ~20 t·ha⁻¹ with weather data using coarse resolution data, which was nearly equal to the fine resolution model data, both datasets being with in the estimated yield range. However, the LAI and LGS were < 1.0 m⁻²·m⁻² and 2 months, respectively, in the coarse model domain. These values are not acceptable for a potato crop (FAO, 2008b; Harper, 1963; Haverkort, 2018). Hence, we recommend that crop modelers focus on not only simulated yield but also check the acceptability of model outputs such as the LAI and LGS.*

## 6.2  The observational perspective

In order to improve model performance, it is essential to have independent observation datasets at different elevations and on sub-daily temporal scales, as described in Chapter 3. This chapter presents the strategy for setting up an appropriate weather network of observations that enables better evaluation of the model results. Weather data for the Arba Minch (1200 m a.s.l.) and Chencha (2700 m a.s.l.) stations were obtained from the Ethiopian National Meteorological Agency (NMA). However, station data in sub-Saharan Africa are known to have limitations: (1) poor data quality (*e.g.* large gaps in the data, and errors in the manually recorded data); (2) poor station spatial network density (*e.g.* stations are installed near main roads in urban areas and their numbers are limited in rural areas); and (3) accessing data is often a challenge (Dinku *et al.*, 2014; Funk *et al.*, 2015a). To overcome weather information limitations in the Gamo Highlands, the Gamo Ethiopian Meteorological Stations (GEMS) network was established, as described in Chapter 4.

The GEMS is a network of eight automatic weather stations (AWS), that has been operational since April 2016. Data generated by the GEMS were used to study both the local scale weather (*e.g.* lake-mountain breeze flows) and global weather phenomena (*e.g.* tracking the ITCZ – Intertropical Convergence Zone to predict wet periods) and was deployed as crop model input as discussed in Chapter 4. Chapter 5 discussed how these data were utilised to study the relationships between environmental factors and crop growth. In 2017, in Ethiopia, there are only 22 first class/class-I (synoptic) stations, nearly 150 principal/indicative/class-II stations and nearly 155 AWS stations (NMA, 2018). The GEMS is a dense network (a station covers an area of about 18 km × 18 km) compared to the national network of stations (where a station covers ~60 km × 60 km). However, our network does not sufficiently cover the heterogeneous landscapes of the Gamo Highlands (*e.g.* Lake Abaya and Lake Chamo, and landmass east of the lakes). Our estimation is that three additional AWS's and one radiosounding observation station would strengthen the characterization of the meteorological state variables and their relationship to the formation of the thermally driven mesoscale flows on the slopes facing south-east (SE). One

AWS (additional sensors including lake temperature profiling) and two AWS's should be installed on the other side of the lakes, so that the role of the lakes in modulating the weather dynamics in the Gamo Highlands can be effectively investigated. Adding an upper-air observation (radiosounding) setup to the existing Arba Minch station would aid the study of the upper air profile (temperature, wind RH, and pressure) and evaluate the performance of the weather models in three dimensions (Banks *et al.*, 2016).

The GEMS network is operational on the slopes facing SE on the Gamo Highlands. On these slopes, south-easterly to southerly winds occur during *belg* precipitation during May in *belg*-2017 as discussed in Chapter 4. The meteorology in the northwest (NW) facing slopes can be quite different. For instance, if the mountain-valley winds converge on the SE slopes during precipitation on the NW slopes, divergence can be expected. It would therefore be of interest to study the meteorological dynamics using an additional GEMS network (three AWS's: somewhere on the lower part of the slope, on the middle heights and at an elevated location on the NW slope) combined with remotely sensed data.

Furthermore, blending the GEMS data with remotely sensed meteorological (precipitation, temperature and shortwave radiation) and soil moisture and temperature could help to improve the spatial resolution (to the same or higher resolution than the weather model). An example could be the cloud physical properties product derived from visible light observations on board MSG (Meteosat Second Generation), which are available at a resolution of 3 km (http://msgcpp.knmi.nl). However, because most precipitation in the region develops during the afternoon and at night, the visible light observations are unfortunately of limited use. Previously, merged satellite and station observation datasets have been produced in Ethiopia and these improved the spatial extent and data quality of the observed data (Dinku *et al.*, 2014; Funk *et al.*, 2015b). High-resolution weather data in the complex topographic region can be used for weather model validation (spatially) and input for crop models for yield mapping. Similarly, the soil moisture (observed and remotely sensed merged data) data can be deployed to initialise soil models as inputs to crop models.

Another important impact of meteorology on crop dynamics and storage is related to diseases. Crop diseases are observed in field experiments conducted during *belg*-2017 and *belg*-2018 as discussed in depth in Chapter 5. Potato crop diseases such as late blight – caused by *Phytophthora infestans*, and bacterial wilt – caused by *Ralstonia solanacearum*, are among the major threats to the Ethiopian potato agronomy sector (Abdurahman *et al.*, 2017; Damtew *et al.*, 2018). Here, we need to stress the major differences in both seasonal weather and crop disease observations among the six farms and eight cultivars studied in Chapter 5. In *belg*-2017, only the Tegecha farm, at 2383 m a.s.l., was affected mainly by late blight and we observed that most potato plants at more elevated locations in the Gamo Highlands were healthy. In the following *belg* season, however, all our farms were infected (although there were

differences in infection levels among farms and cultivars) by late blight, although crops on the experimental farms were much better than the farmers' crops in terms of severity and incidence. The major difference between the two *belg* seasons was the weather, in that *belg*-2017 was warmer and drier while the following year was cooler and moister. The high late-blight pressure during the *belg*-2018 season may be associated with the more humid atmosphere in that season (Johnson *et al.*, 1996). The GEMS network's leaf-wetness and meteorological data such as temperature, PPT, and RH data can be used to simulate crop disease conditions and to identify differences in disease pressure between the two *belg* seasons (Cao *et al.*, 1997; Hartill *et al.*, 1990).

There are some important observational strategies that we consider could improve potato field experiments. They are (1) plot size design for robust yield estimates; (2) preparation of planting material for realistic studies of the relationship between environment and potato crop; and (3) time-series monitoring of harvest index to understand the role of elevation on potato growth and yield. These points are discussed in the following paragraphs:

1) *The plot size design of our field crop trials was 3.0 m × 3.0 m with four rows, following the Randomized Complete Block Design (RCBD) in triplicates (Gomez et al., 1984). Data were collected from the central two rows (1.5 m × 3.0 m) and the average of the three plots is reported. However, Sukhatme (1947) showed that yield assessments with such small plot size lead to overestimation, which could be one of the potential reasons for the large divergence between modelled and observed yields described in Chapter 4. The author also suggested a larger plot design (~7.0 m × 7.0 m) in order to reduce bias. We recommend this design and select few cultivars for our future field trials.*

2) *Disease-free planting material of well-defined physiological age is crucial to study the role of environment on potato crop growth and yield, especially when different cultivars are being compared (FAO, 2008b; Struik and Wiersema, 1999) as described in Chapter 5. Advanced seed multiplication methods such as tissue culture, minituber production using aeroponics or hydroponics, but also true potato seeds, can be useful in this connection (Chindi et al., 2013), because they can provide disease-free material and standardized physiological status. However, these methods are not only expensive for developing nations but also cause new limitations in that the crops developed from these kinds of propagation materials behave differently from those from normal seed tubers (Muthoni et al., 2013). We recommend adopting a simple approach to multiply potato seeds in a controlled way before experiments are carried out. The approach is to collect seed from several cultivars from different sources (i.e. agricultural research centres in Ethiopia) and conduct the multiplications in cool environments such as research fields at high altitudes, such as the Gircha Horticultural research centre in the Gamo Highlands. This approach was followed during belg-2018 in our experiments, as explained in Chapter 5.*

3)  As Chapter 5 quantifies and discusses, it was difficult to find a clear pattern and relationship between observed yield and environmental variables and elevation. For future studies, based on our findings, we recommend applying the RBCD plot size suggested by Sukhatme (1947) and planting material prepared as explained in ( 1) above. Following the experimental designs, the field experiments also need to be carried out systematically to study the relationship between weather and crop growth in regions of complex topography. In the first belg year, we ought to test the performance of cultivars in a location such as Gircha. In the following belg season, we should analyzed the role of meteorology and elevation on a cultivar (e.g. at Gudene) at different elevations. With this experimental plan, continuous monitoring (for example, on a weekly basis) of above-/below-ground biomass is needed. Such a measurement plan would give us a deeper understanding of the role of weather and elevation on potato cultivars and yields, which we found in our modelling experiment, described in Chapter 3. In the third belg season, we should repeat the same experiment as in the previous year, but now with several cultivars. Our study focused on the belg season's potato agronomy because there is sufficient moisture to farm potato, and crop diseases are less prevalent during that season. However, farmers in Ethiopia also grow potato during the meher season. Hence, it would be of interest to repeat the same experimental design for comparative study among the two seasons (e.g. specifically crop disease pressure among seasons).

To conclude, in this thesis we adopted a combined approach of modelling and observations to study weather and the interplay between weather and crop dynamics in a complex topographic region in the Gamo Highlands in southwest Ethiopia. The region is of interest because weather varies on small spatiotemporal scales and the potato crop plays a key role in improving food security in the region. The findings indicate that there are still gaps in both modelling and observations that can be improved. With respect to modelling, there are two potential areas for improvement.

- *Increasing the horizontal resolution of the weather model to 1 km. This can better resolve topography and fine scale weather processes. The improved resolution would enable us to simulate crop yield to nearly plot-scales.*

- *Using less complex crop models such as LINTUL-POTATO.*

With respect to observations, there are three areas in which improvements can be implemented.

- *Intensifying the GEMS network to improve our understanding of weather and crop dynamics in the Gamo Highlands.*

- *Merging the GEMS datasets with remotely-sensed products for a better understanding of spatial variations in weather.*

- *Adopting systematic strategies such as studying a range of different cultivars at a single location and a single cultivar at different elevations, and comparing disease prevalence during the belg and meher seasons in field crop experiments.*

**6**

# 7
# Conclusions

The aim of this PhD project was to provide quantitative insights into the role played by meteorology in the dynamics of the potato crop in a tropical highland environment. To this end, our research strategy and approach combined fine-resolution numerical modelling with a dense network of meteorological stations. The resulting meteorological datasets were used to drive a crop growth model whose output was compared with data from field trials at various altitudes and in different seasons. The region under study was the Gamo Highlands in southwest Ethiopia, which plays an important role in the national potato production of Ethiopia. However, little attention has been paid to how different spatiotemporal weather scales influence the different stages of crop growth and yield. In this thesis, I have attempted to repair the gap in our knowledge of this area. The thesis is based on three research questions presented below. Here, I provide a summary of my main findings.

---

Research question 1: *How do complex topography and heterogeneous landscapes affect weather and crop dynamics on different spatiotemporal scales?*

---

Steep orographic gradients and heterogeneous landscapes significantly influence weather in mountainous regions, so weather models require fine resolution to adequately describe topographic details and to resolve the associated atmospheric processes. Currently, a typical General Circulation Model (GCM) employs a horizontal resolution of approximately 50 km. Simulated meteorological products of such a global scale model give rise to large biases in weather outputs as compared with observations. This is because the coarse resolution models smooth out topographic variations and thus cannot explicitly describe the true effect of topography on meteorology. Since the outputs of these models are used as inputs for crop growth models, the simulated crop yield and variables related to crop dynamics are likely to be

of poor quality. My aim in this first question was therefore to study how a fine res-
olution model with a 2 km horizontal resolution can improve our understanding of
the weather and crop dynamics in a region with complex terrain and land-use vari-
ability – the Gamo Highlands. I focussed primarily on the major meteorological crop
drivers such as precipitation (PPT), temperature ($T_{max}$ and $T_{min}$) and the incoming
shortwave radiation (SW↓). Spatial and temporal variations in the weather elements
significantly influence key crop growth variables such as plant height, the Length of
the Growing Season (LGS), Leaf Area Index (LAI), dry matter distributed between
above- and below-ground plant biomass, yield and yield components. As a core
strategy, I coupled (one-way) to the Weather Research and Forecasting (WRF) model
output with the Genotype-by-Environment interaction on CROp growth Simulator
(GECROS) model; the crop growth variables (LGS and LAI) were carefully investi-
gated.

To this end, I employed the WRF model for weather simulations, studying a 10-
year period to represent a sub-climatological duration and determine the interan-
nual weather variabilities. I also selected the *belg* (February to May) season, as this
is the most important cropping season for potato cultivation in Ethiopia, because soil
moisture is fed by important rainfalls. Furthermore, I identified climatologically nor-
mal (2006) and anomalous (2008 and 2010) years drawn from the 10-year datasets.
The model's boundary and initial conditions were prescribed by the ERA-Interim
reanalysis data. The model was run in four domains centred on the Gamo High-
lands, in which the outer coarse (52 grid-points and each grid with 54 km × 54 km
model resolution) and the inner, nested fine resolution (42 grid-points each with 2
km × 2 km model resolution) domains were chosen for further analysis. The coarse-
and fine-resolution domains were run with temporal resolutions of three-hourly and
hourly periods, respectively. Weather observations at representative elevations
(Arba Minch in the lowlands, at 1200 m above sea level (a.s.l.) and Chencha in the
highlands, at 2700 m a.s.l.) were used to evaluate the performance of the WRF model.
The meteorological outputs and soil variables accessed from the ISRIC soil database
were used as input to the GECROS crop model.

The analysis showed that the WRF model's performance was reasonable in rep-
resenting the trends in the annual cycles of the weather elements as compared to the
stations' observations, with an $r^2 > 0.89$ for precipitation for the fine-resolution do-
main. On daily averages; however, there was a large model bias. In short, the fine
resolution output tends to a cool bias (mean bias error [MBE] of -3.2 °C for $T_{max}$),
underestimated precipitation in the lowlands (*e.g.* Arba Minch, MBE of -1.3 mm·d$^{-1}$),
but overestimated it in the highlands (*e.g.* Chencha, MBE of 3.7 mm·d$^{-1}$). Temporally,
the model analysis showed a clear interannual variability. The simulated PPT from
2001 to 2010, for instance, showed that 2006 (1162 mm·*belg*$^{-1}$), 2008 (740 mm·*belg*$^{-1}$)
and 2010 (1755 mm·*belg*$^{-1}$) were the climatologically normal, driest, and wettest *belg*
seasons, respectively. The model findings also revealed significant spatial variations

in the highlands. To mention, the temperature is dropped aloft in agreement with the environmental lapse rate of ~6 °C/km. The 10-years *belg* averaged $T_{min}$ and $T_{max}$ fell from around 20 °C and 30 °C in the valley around Lake Abaya and Chamo to around 5 °C and 15 °C at the summit of Mount Guge, respectively. PPT increased almost exponentially from about 200 mm·$belg^{-1}$ in the lowlands to 1200 mm·$belg^{-1}$ in the highlands, while SW↓ also significantly fell by about 150 W·$m^{-2}$ in the Gamo Highlands.

An analysis of the crop model datasets identified three different potato yield zones in the highlands. The classification is based on the representative potato crop variables: LGS and LAI. The three yield zones were: a zone with linearly increasing yield – **Zone-I** (1100 to 1500 m a.s.l.); a zone with constant yield – **Zone-II** (1600 to 2650 m a.s.l) and another zone with linearly increasing yield – **Zone-III** (> 2950 m a.s.l). While the elevation is increasing, the modelled crop yield maintained nearly constant in yield Zone-II. I explained this unexpected result based on findings of model sensitivity experiments. This is related to the contrasting roles of precipitation and temperature in explaining yield. First, yield decreased as precipitation increased with altitude due to increased soil nutrient leaching. Second, yield increased when the temperature was becoming cooler due to larger LGS. These opposing roles of precipitation and temperature regimes in yield simulations resulted in a compensating effect on yield.

Attainable yield simulations driven by the coarse and fine resolutions WRF model outputs yielded similar results (~22 t·$ha^{-1}$). However, the LAI based on the coarse resolution grid was too low (~ 1.0 vs 3.0 $m^2$·$m^{-2}$), and moreover, the crop completed the growth cycle too early (~60 vs 140 days), which are physically not acceptable for the potato crop. These unacceptable model outputs are obtained because of the warmer and drier weather simulated by the coarse resolution model. I attributed these to the smoothed topography of the model (*e.g.* in the coarse resolution domain Arba Minch and Chencha elevations deviated by -400 and +1100 m respectively from the observed measurements), causing the weather to resemble that in the valleys throughout the domain. I emphasise that it must be kept in mind that a comparable yield with observed data may be obtained whilst growth variables such as the LGS and LAI are unsuitable for the crop involved. For this reason, agrometeorological modellers need to investigate not only yields but also reasonable crop growth variables of the model outputs.

From this study, I learned the need for accurate observations of weather and crop growth in space and time. In studying the impact of weather on potato growth, it is essential to employ an adequate network of stations to quantify the role of local to synoptic weather scales in complex terrain. However, observations on sub-hourly to hourly temporal scales with reasonable spatial coverage are seldom available in sub-Saharan Africa. In my follow-up investigation, I therefore deployed a relatively dense network of automatic weather stations capable of providing weather/edaphic

**7**

variables records in sub-hourly temporal scales. The spatiotemporal variations in weather were studied as a function of altitude, and their impact on potato crop growth during *belg* season of 2017 was analysed. With this new weather-crop observational datasets, I formulated the following question:

Research question 2: *What can we learn from a dense network of meteorological-soil observations with respect to the crop growth variables (e.g. length of growing season and attainable yield)?*

For high-quality and sub-hourly interval weather records, my two co-authors and I installed the Gamo Ethiopian Meteorological Stations (GEMS) network in the three yield zones specified in Chapter 3. The GEMS network consists of six (currently eight) automatic weather stations that have been operational since April 2016. The stations are systematically distributed and installed in the three yield zones, and cover a 30-km radius. The stations are installed as follows: in yield **Zone-I**: Arba Minch (1200 m a.s.l); in **Zone-II**: Tegecha (2091 m a.s.l), Zigiti (2414 m a.s.l), Chencha (2753 m a.s.l) and Gazesso (2847 m a.s.l); and in **Zone-III**: Gircha (3015 m a.s.l). This network of stations enabled me, for the first time in Ethiopia, to quantitatively investigate meteorological crop drivers in a complex and relatively large topographic region. Meteorological variables such as air temperature, PPT, SW↓, relative humidity, sea-level pressure [SLP], wind, etc.; soil moisture and soil temperature (at 5, 10, 20, and 40 cm soil depths); and leaf-wetness (two sensors to the east and west of each station) data were recorded at 15-min temporal resolution. This high-frequency datasets enabled me to obtain a quantification of meteorological and edaphic factors on a sub-hourly scale and at a reasonable level of spatial detail.

Close to the GEMS network, I commenced potato crop field trials (five locations and eight cultivars) on smallholder farmers' lands in *belg*-2017. The field experimental setup is discussed in detail below. To answer this question, the GEMS network datasets were used as input to the GECROS model, which calculates crop growth and yield at several elevations in the Gamo Highlands. The same GECROS model setup was deployed as for the previous question. I compared the attainable crop yield and crop growth variables such as the LGS and maximum plant height (MPH) with the observed datasets from the field trials, and performed model sensitivity analyses to test the crop model's sensitivity to variations (in elevations and the systematically manipulated GEMS datasets) in the meteorological observations.

The GEMS observations and GECROS model outputs produced the following findings. The *belg* season's mesoscale and synoptic weather phenomena showed large temporal (diurnal to intraseasonal) and spatial variations in the Gamo Highlands. At the mesoscale level, strong daytime flows could be observed. The day

flows are combinations of lake breezes – driven by the lake-land temperature difference; anabatic flows – updrafts developed due to differentially heated mountain slopes and are cross-valley flows; and valley winds – along-valley flows. At night, however, local and weaker flows as compared to the daytime were observed. These flows can be mountain breezes – again driven by the mountain-lake temperature difference; katabatic flows – thermally driven and cross-valley flows; and mountain winds – along-valley flows. The observed SLP and wind observations and reanalysis data displayed a strong dependence of synoptic flows (*e.g.* the Intertropical Convergence Zone [ITCZ]) on a monthly basis. February (dry) is more mesoscale dominated, while May (wet) was a synoptic-scale weather system influenced month during *belg*-2017. In February, lakes and mountains played major roles, while in May, large-scale features such as the ITCZ played a prominent role. Subsequently, the day-night weather contrast (*e.g.* temperature and wind flow) were much larger in February than in May. An interesting finding was that the ITCZ overhead the Gamo Highlands (in mid-March) whereas, the main wet period was during May in *belg*-2017. This shows that the ITCZ and precipitation belt did not coincide. Moreover, precipitation seldom occurred during the day, mostly falling in the late afternoon to night period. These weather phenomena could be associated with moisture convergence between south-easterly to southerly synoptic winds, with local flows triggered by afternoon solar heating and complex terrain.

Data from the potato field trials and model experiment revealed wide variations in the LGS and MPH and attainable yield at different elevations in the Gamo Highlands. The GECROS crop model was sensitive and reproduced well the trends in the observed growth variables and yield across elevations. However, the model greatly underestimated the observed yield, which revealed the need to calibrate the model specifically for Ethiopian cultivars in the tropical mountainous environment. Furthermore, model sensitivity experiments based on fixing a weather variable to be constant (setting the seasonal average value for all the days of the growing season) while maintaining the others as observed, showed that precipitation was the most important meteorological factor (mainly in drier and warmer seasons such as *belg*-2017) in determining yields.

The earlier studies discussed in Chapters 3 and 4 revealed significant spatial (lowlands, midlands and highlands) and temporal (diurnal to interannual scales) variations in weather in the Gamo Highlands. Ultimately, these variations caused large differences in crop growth (*e.g.* variations in LGS and LAI as a function of elevation) and yield (*e.g.* dry-matter distribution in the plant parts and three yield zones explained in Chapter 3) up in the Gamo mountains. These findings triggered and led me to design the environment-crop correlational study as presented below.

**7**

My third study thus had the following motivation: much of our knowledge regarding environmental factors and crop growth relationships has been gained in the temperate climate majorly in the developed world. Nevertheless, potato cultivation is expanding, and its production has shown an increasing trend in the developing world, while it is beginning to show a declining trend in developed countries. This shows that potato has become an important crop in food security in developing countries, among them specifically Ethiopia. This study therefore attempted to analyse the relationship between environmental conditions and potato growth at different altitudes. I further explored how the growth and yield of the potato crop vary as a function of environmental conditions in different potato cultivars and stages of crop growth. Therefore, this study for the first time linked variations in environmental variables in several spatial and temporal scales to potato crop dynamics in Ethiopia. To realise this objective, I asked the following research question:

Research question 3: *How do variations in the observed environmental variables correlate with crop growth and yield on sub-seasonal, seasonal, and interseasonal scales in the Gamo Highlands? Can we identify periods in which the meteorological crop drivers have a different influence on potato growth characteristics?*

In order to answer the question, I designed potato crop field trials in 2017 and 2018, which turned out to become two climatologically contrasting (drier and wetter vs warmer and cooler) *belg* seasons. These trials were planned in such a way that they would complement the GEMS network as described in the previous question. Data from the GEMS network were used for the environment – crop growth variables correlation study. I planted six improved (*Belete, Gudene, Jalene, Ararasa, Horro,* and *Hunde*) and two local (*Suthalo* and *Kalsa*) cultivars at five farms in 2017 and six farms in 2018 in the Gamo Highlands. The Randomised Complete Block Design setup was implemented in triplicates. The plot size was $3 \times 3$ m$^2$ with a plant density of 4.4 plants·m$^{-2}$. Fertiliser rates and farm management practices were identical at all farms in both *belg* seasons and according to recommendations. Representative crop growth data (*e.g.* plant height and canopy cover), yield and yield traits (*e.g.* tuber number and weight per plant) were collected either on a daily basis (*e.g.* plant height), at crop maturity (*e.g.* branch number per plant) or at the end of the season (*e.g.* number of tubers per plant). For the sake of robust statistics, five plants from the middle two rows were continuously monitored, and averages of 15 plants (from three plots) are reported. These crop data were correlated with environmental (meteorological and edaphic) data calculated on daily, sub-seasonal, seasonal, and interseasonal temporal scales during the two years of the study.

I made this set of observations in three important phases of potato growth: canopy buildup (P1), maximum canopy (P2) and canopy decline (P3). In P1, canopy growth (*i.e.* plant height and canopy cover) and number of tubers per plant were associated with environmental variables observed during the growth phase. To explain further, I calculated temperature sum (Tsum) and correlated it with the canopy growth observation during P1. Tsum can be defined as the sum of the daily mean temperatures ($T_{mean}$) less the base temperature ($T_{base}$: if $0\ ^{\circ}C \leq T_{mean} \leq 5.5\ ^{\circ}C$). Tuber weight per plant was correlated with environmental factors during P2 and P3. The total dry matter stored in each plant was calculated as a function of intercepted radiation throughout the growing season.

Analysis of the data showed that Tsum was a strong predictor ($r^2 > 0.95$) of canopy growth during P1. This is observed irrespective of cultivar type in a given farm, farms at different altitudes and during both seasons. However, there are some periods during which Tsum explained crop growth to a slightly lesser extent. Those variations in Tsum and the crop growth curve were further explained in terms of precipitation, SW↓, soil moisture and cultivar type (*i.e.* either an improved or a local cultivar). As such, the local cultivar – *Suthalo* performed better under drought conditions, whereas the improved cultivar – *Gudene* was more efficient under reduced-radiation regimes. These explanations are based on increases in plant height per degree-day. The results also showed that below-ground traits such as tuber number and weight and tuber yield are poorly explained by weather and edaphic variables. Among the crop-related variables, the number of branches per plant (data collected at crop maturity) well correlated with tuber yield at the end of the season. The poor correlations between environmental conditions and yield traits demonstrate the need for further investigation and continuous monitoring of above- and below-ground biomass at different elevations for both improved and existing local cultivars. Furthermore, I recommend tuber seed multiplication of all the available cultivars in the same environment (*i.e.* in an elevated and cooler place, *e.g.* Gircha Horticultural research centre in the Gamo Highlands) before field trials. This strategy can help us to improve seed quality with a defined standardised physiological status.

# Summary

**Motivation**: Ethiopia is one of the Sub-Saharan countries that are strongly influenced by climate fluctuations. These meteorological changes directly affect agriculture and consequently cause disturbances on the regional and local economy. To pinpoint a few crucial issues: (1) the agricultural sector in Ethiopia accounts for 80% of the employment and contributes 45% of the GDP. A relevant factor in relation to this PhD thesis is that the country's agriculture is by 95% rainfed agronomy. (2) The Ethiopian landscape is composed of complex terrains of the East African mountain system – the Ethiopian Highlands (40% of the Ethiopia's landmass is elevated more than 1500 m above sea level). This complex orography modulates weather and climate at scales ranging from local to regional. In the region, weather dynamics are mainly driven by both synoptic (*e.g.* Intertropical Convergence Zone – ITCZ) and mesoscale flows (*e.g.* lake and mountain breezes). These weather scales ultimately influence the way crops grow. The aim of this study was to evaluate how weather and crop growth vary in a complex terrain and heterogeneous landscape. I focus on the Gamo Highlands, south-west Ethiopia, a mountainous region with two large Rift-Valley lakes in Ethiopia. The crop of interest was potato – a crop that has become popular in Ethiopia, significantly contributing to food security and income, but sensitive to climatic variations. As a research method, I deployed a high-resolution weather and crop modelling approach to describe how the growth and yield of the potato crop depend on the variations in weather. For observation-based studies and for testing the models' performance, six automatic weather stations were installed and field crop experiments were conducted near the stations. More specifically, this thesis addresses the role of meteorological crop drivers (*e.g.* the incoming shortwave radiation (SW↓), maximum temperature ($T_{max}$), minimum temperature ($T_{min}$) and precipitation (PPT)) and edaphic variables (soil moisture and soil temperature) on the yield and growth of the Ethiopian potato cultivars.

**Research methods and findings**: In Chapter 1, I reviewed the contemporary global environmental challenge, the Anthropocene geologic era, in relation to the food system in perspective. In this chapter, I cascaded the problem from the global to the local scale. The chapter argued that the global weather models need to be downscaled to the local scales in order to study weather and climate impacts on crop dynamics in complex topographic landscapes such as Ethiopia.

In Chapters 2 and 3, I presented the model-observation combined research strategy implemented in this thesis. The temporal and spatial variations in weather and crop dynamics are analysed using data from 2001 to 2010. To this end, the Weather Research and Forecasting (WRF) model is used to simulate weather at coarse ($54 \times 54$ km$^2$) and fine ($2 \times 2$ km$^2$) resolutions during the 10-years. The model is validated with *in situ* data. The meteorological crop growth drivers (SW$\downarrow$, T$_{max}$, T$_{min}$, PPT, vapour pressure deficit and wind speed) and soil data from the ISRIC soil database are supplied as inputs to a process-based crop model called GECROS. The 10-year *belg* seasons WRF model analysis is showed large temporal and spatial variabilities in SW$\downarrow$, T$_{max}$, T$_{min}$ and PPT in the Gamo Highlands. For example, T$_{max}$ ranged from 10 °C on the summit of mount Guge to 30 °C in the valley around Lake Abaya and Lake Chamo. Temporally, the *belg* season of 2006 is identified as climatologically normal whilst the 2008 (driest) and 2010 (wettest) *belg* seasons are categorized as anomalous years. The temporal variations in simulated attainable potato yield showed a high yield (~20 to 30 t·ha$^{-1}$) during the normal *belg* season whereas the yield was lower (5 to 10 t·ha$^{-1}$ less than in the normal year) for the anomalous *belg* seasons (Chapter 2). As compared to the coarse resolution domain, the fine resolution domain is better represented topography and weather variations. Because of the improved representation of topography and weather in the fine resolution domain, the leaf area index (LAI) and the length of the growing season (LGS) simulated by the GECROS model were in the recommended range for potato (LAI of 3 m$^2$·m$^{-2}$ and LGS of 120 days are simulated). For comparison, modelled values were unacceptably low in the coarse resolution domain (LAI of 1.0 m$^2$·m$^{-2}$ and LGS of 60 days). It is also interesting to see that temperature and precipitation played opposing roles in the modelled yield, a phenomenon I called a *compensating effect*. To explain the term, moving up the mountains, the temperature decreases – with a positive effect on yield, and precipitation increases with a negative effect on yield. The lower temperature at higher elevation increases the LGS; as a result, more carbon is allocated to the tubers than in a shorter growing season. The higher precipitation at higher elevation may give rise to soil nutrient loss caused by leaching. Aloft the highlands, temperature and PPT are showed opposite trends, but their effects are balanced out in the ultimate yield (Chapter 3).

Chapter 4 presented the Gamo Highlands Meteorological Stations (GEMS) – a network of six automatic weather stations, which were operational since April 2016 in two transects of the highlands. Near to the GEMS network, potato field trials are conducted. I used the GEMS data to study both the mesoscale and synoptic weather scales influencing the Gamo Highlands. Furthermore, I deployed the *in situ* data to the GECROS crop model. The GEMS data are analysed for *belg*-2017 showed major differences between the start (February) and the end (May) of the *belg* season. February and May are more mesoscale and synoptic scale weather system dominated months, respectively. During February, the day-night wind sources showed strong variation. Strong south to south-easterly lake breezes are observed during daytime; whereas, weak and more localised mountain winds are identified during the night-time. In May, the day-night flow contrast was small and the dominant flows were southerly. The location of ITCZ calculated by the NOAA (National Oceanic and Atmospheric Administration) and the GEMS observed sea-level-pressure (SLP) data showed strong correlation. My analysis showed that the low-pressure system (ITCZ) and the rainbelt are not coincided in the Gamo Highlands. The maximum PPT is received in May where the ITCZ is located on average nearly 6° (north) away from Gamo Highlands. During the maximum PPT in May 2017, the southerly moist air masses from the moisture sources (*e.g.* Indian Ocean) may move to the low-pressure system located to the north of the study area. During the daytime, PPT is less probable as cloud formation was less likely due to the enhanced solar radiation. However, during night-time, the southerly moisture can be trapped in the highlands and orographic PPT can be triggered. This PPT is locally modulated due to the presence of the Gamo Highlands and presence of the lakes. The moisture is crucial for potato agronomy during the *belg* season. The GECROS model sensitivity analysis, using the GEMS data, showed that model input of constant PPT (*belg*-averaged) gave the highest crop yield due to improved soil moisture throughout the growing season.

Chapter 5 dealt with investigating the role of environmental factors on potato yield and growth in the Gamo Highlands. Here, the GEMS weather and edaphic data are correlated with crop growth variables such as plant height, canopy cover, yield and yield traits. The GEMS and crop observation datasets showed that plant height and canopy cover are strongly correlated with temperature sum (Tsum) with an $r^2 > 0.95$ during the canopy buildup phase (P1). Tsum (d °C) is defined as the sum of the daily average temperatures during the growing season. The crop growth - Tsum correlation is further explained in terms of SW↓ and soil moisture, in which an improved (*Gudene*) and a local (*Suthalo*) cultivar showed different responses to SW↓ and soil moisture regimes. Data also showed that tuber yield is poorly explained by meteorological and edaphic data, suggesting further research activity in this regard. When the number of days to crop maturity was between 100-110 days, an optimal tuber yield is obtained.

Chapter 6 presented the main findings of the thesis in perspective. Finally, Chapter 7 discussed the key findings in-line with the research questions stated in Chapter 1.

**Conclusions and perspectives**: In complex terrain, weather/climate varies over short distances affecting crop growth. To describe crop growth and yield in the region, a high-resolution weather model, coupled to a crop model is needed. The weather model outputs can be used as input to the crop model. A dense station network installed in a complex topographic region can give us insights on mesoscale flows (*e.g.* lake-mountain flows), synoptic systems (*e.g.* south-north movement of the ITCZ) and crop growth (*e.g.* LGS and LAI). Additional weather stations (*e.g.* on the lee-side of the Gamo Highlands and east of the Lakes Abaya and Chamo) can give us improved understanding of weather scales and crop growth. Tsum during the P1 is found to be a good predictor of plant height and canopy cover for the Ethiopian potato cultivars. The poor correlation between environmental variables and yield and yield traits suggests more dedicated field experiments should be designed. One of the suggested field experiments is continuous monitoring of the partitioning of dry matter to the tubers to study how crop yield varies as a function of elevation and meteorology.

**Keywords**: canopy buildup phase, complex topography, local and global weather scales, potato, weather and crop modelling.

# Samenvatting

**Motivatie:** Ethiopië is een van de landen in Sub-Sahara-Afrika die sterk worden beïnvloed door klimaatschommelingen. Deze meteorologische veranderingen zijn rechtstreeks van invloed op de landbouw en veroorzaken verstoringen in de regionale en lokale economie. Enkele belangrijke zaken zijn: (1) de landbouwsector in Ethiopië zorgt voor 80% van de werkgelegenheid en omvat 45% van het BNP. Een relevante factor voor dit proefschrift is dat de landbouw van het land voor 95% regenafhankelijk is. (2) Het Ethiopische landschap bestaat uit complexe terreinen van het Oost-Afrikaanse gebergte - de Ethiopische hooglanden (40% van Ethiopië ligt meer dan 1500 m boven de zeespiegel). Deze complexe orografie moduleert weer en klimaat op schalen variërend van lokaal tot regionaal. In de regio wordt de weersdynamiek voornamelijk bepaald door zowel synoptische (*bijv.* Intertropical Convergence Zone - ITCZ) als mesoschaalstromen (*bijv.* meer- en bergwinden). Deze meteorologische omstandigheden beïnvloeden de manier waarop gewassen groeien. Het doel van deze studie was om te evalueren hoe weer en gewasgroei variëren in een complex terrein en heterogeen landschap. Ik concentreer me op de Gamo Highlands, Zuidwest-Ethiopië, een bergachtig gebied met twee grote Riftvallei-meren. Het gewas dat onderzocht is, is de aardappel. De aardappel is populair geworden in Ethiopië en draagt aanzienlijk bij aan voedselzekerheid en inkomen, maar het is gevoelig voor klimatologische variaties. Als onderzoeksmethode heb ik een methode voor weer- en gewasmodellering met hoge resolutie gebruikt om te beschrijven hoe de groei en de opbrengst van het aardappelgewas afhangen van de variaties in het weer. Voor het doen van observaties en voor het testen van de prestaties van de modellen werden zes automatische weerstations geïnstalleerd. Experimenten met veldgewassen werden uitgevoerd in de buurt van de weerstations. Dit proefschrift gaat in op de rol van meteorologisch bepalende factoren voor gewasgroei (*bijv.* de inkomende kortegolfstraling (SW↓), maximum temperatuur ($T_{max}$), minimum temperatuur ($T_{min}$) en neerslag (PPT)) en edafische variabelen (bodemvocht en bodemtemperatuur) op de opbrengst en groei van de aardappel in Ethiopia.

**Methoden en resultaten:** In hoofdstuk 1 besprak ik de hedendaagse mondiale uitdaging voor het milieu, het Antropoceen, in relatie tot het betreffende voedselsysteem. In dit hoofdstuk heb ik het probleem van de mondiale naar de lokale schaal vertaald. Het hoofdstuk beargumenteerde dat de mondiale weermodellen moeten worden teruggeschaald naar een lokaal niveau om de weers- en klimaateffecten op de gewasdynamiek in complexe topografische landschappen, zoals Ethiopië, te bestuderen.

In Hoofdstukken 2 en 3 presenteerde ik de in dit proefschrift gehanteerde gecombineerde onderzoeksstrategie van modelleren en observeren. De temporele en ruimtelijke variaties in weer- en gewasdynamiek werden geanalyseerd met behulp van gegevens van 2001 tot 2010. Het Weather Research and Forecasting (WRF) model werd gebruikt om het weer bij een grove (54 × 54 km²) en fijne (2 × 2 km²) resolutie gedurende de 10 jaar te simuleren. Het model werd gevalideerd met gegevens ter plaatse. De meteorologische gewasgroeifactoren (SW↓, $T_{max}$, $T_{min}$, PPT, dampdruk verschil en windsnelheid) en bodemdata van de ISRIC-bodemdatabase werden benut als input voor het gewasmodel GECROS. De WRF-modelanalyse voor de 10 *belg*-seizoenen toonde grote temporele en ruimtelijke variabiliteit in SW↓, $T_{max}$, $T_{min}$ en PPT in de Gamo hoogvlaktes. $T_{max}$ varieerde bijvoorbeeld van 10 °C op de top van de berg Guge tot 30°C in de vallei rond de meren Abaya en Chamo. Betreffende de temporele variatie werd het *belg*-seizoen in 2006 geïdentificeerd als klimatologisch normaal, terwijl de *belg*-seizoenen 2008 (droogste jaar) en 2010 (natste jaar) als afwijkend werden gecategoriseerd. De temporele variaties in de gesimuleerde haalbare aardappelopbrengst vertoonden een hoge opbrengst (~20 tot 30 t·ha⁻¹) tijdens het normale *belg*-seizoen, terwijl de opbrengst lager was (5 tot 10 t·ha⁻¹ minder dan in het normale jaar) voor de afwijkende *belg*-seizoenen (hoofdstuk 2). In vergelijking met de grove resolutie werd bij fijne resolutie de variatie in topografie en meteorologie beter weergegeven. Vanwege de verbeterde weergave van topografie en het weer bij fijne resolutie, lagen de bebladeringsindex (LAI) en de lengte van het groeiseizoen (LGS) gesimuleerd door het GECROS-model in het aanbevolen bereik voor aardappel (een gesimuleerde LAI van 3 m²·m⁻² en een LGS van 120 dagen). Ter vergelijking: de waarden bij grove resolutie waren onaanvaardbaar laag (LAI van 1,0 m²·m⁻² en LGS van 60 dagen). Het is ook interessant om te zien dat temperatuur en neerslag een tegenovergestelde rol speelden in de gemodelleerde opbrengst, een fenomeen dat ik het 'compenserend effect' noemde. Om de term uit te leggen: tegen de bergen op neemt de temperatuur af, met een positief effect op opbrengst, terwijl de neerslag toeneemt, met een negatief effect op opbrengst. De lagere temperatuur op grotere hoogte verhoogt de LGS; als gevolg hiervan is meer koolstof beschikbaar voor de knollen dan in een korter groeiseizoen. De hogere neerslag op grotere hoogte kan aanleiding geven tot verlies van voedingsstoffen in de bodem veroorzaakt door uitloging. In de hooglanden zijn temperatuur en PPT tegengestelde

trends, maar hun effecten worden gecompenseerd in de uiteindelijke opbrengst (Hoofdstuk 3).

Hoofdstuk 4 presenteerde de Gamo Highlands Meteorological Stations (GEMS) - een netwerk van zes automatische weerstations, die sinds april 2016 operationeel waren in twee doorsnedes van de hooglanden. In de buurt van het GEMS-netwerk werden veldproeven met aardappelen uitgevoerd. Ik heb de GEMS-gegevens gebruikt om zowel de mesoschaal als de synoptische weerschalen te bestuderen die de Gamo Highlands beïnvloeden. Verder heb ik de in-situ gegevens ingezet voor het GECROS-gewasmodel. De GEMS-gegevens geanalyseerd voor *belg*-2017 toonden grote verschillen tussen de start (februari) en het einde (mei) van het *belg*-seizoen. Februari en mei zijn maanden gedomineerd door weer op respectievelijk een meer meso- of synoptische schaal. In februari vertoonde de herkomst van wind overdag of 's nachts sterke variatie. Overdag wordt er sterke zuidelijke tot zuidoostelijke wind vanuit de meren waargenomen, terwijl er gedurende de nacht sprake is van een zwakke en meer plaatselijke wind. In mei was het contrast tussen dag en nacht klein, en de dominante windrichting zuidelijk. De locatie van ITCZ berekend door de NOAA (National Oceanic and Atmospheric Administration) en de door GEMS waargenomen druk op zeeniveau (SLP) vertoonden een sterke correlatie. Mijn analyse toonde aan dat het lagedruksysteem (ITCZ) en de regenzone niet samenvallen in de Gamo hooglanden. De maximale PPT wordt bereikt in mei, wanneer de ITCZ gemiddeld bijna 6 ° (noord) van de Gamo Highlands verwijderd is. Tijdens de maximale PPT in mei 2017 kan de zuidelijke vochtige lucht (vanuit bijvoorbeeld de Indische Oceaan) naar het lagedruksysteem ten noorden van het studiegebied bewegen. Overdag is PPT minder waarschijnlijk omdat wolkvorming minder waarschijnlijk is vanwege de toegenomen zoninstraling. 's Nachts kan echter het zuidelijke vocht in de hooglanden opgesloten raken, wat kan leiden tot orografische PPT. Deze PPT wordt plaatselijk bepaald door de aanwezigheid van de Gamo hooglanden en de aanwezigheid van de meren. Het vocht is cruciaal voor de aardappelteelt tijdens het *belg*-seizoen. De gevoeligheidsanalyse van het GECROS-model, met behulp van de GEMS-gegevens, toonde aan dat een stabiel PPT (*belg*-gemiddelde) de hoogste opbrengst gaf, als gevolg van een verbeterde bodemvochtigheid gedurende het groeiseizoen.

S

Hoofdstuk 5 ging over het onderzoeken van de rol van omgevingsfactoren op de aardappelopbrengst en -groei in de Gamo hooglanden. In dit hoofdstuk zijn de GEMS meteorologische en edafische gegevens gecorreleerd met variabelen voor gewasgroei, zoals planthoogte, bebladeringsindex, opbrengst en opbrengstkarakteristieken. Uit de GEMS en gewaswaarnemingsdatasets bleek dat planthoogte en bebladeringsindex sterk samenhangen met de temperatuursom (Tsum), r²> 0.95, tijdens de loofopbouwfase (P1). Tsum (d°C) wordt gedefinieerd als de som van de dagelijkse gemiddelde temperaturen tijdens het groeiseizoen. De correlatie tussen gewasgroei en Tsum wordt verder uitgelegd in termen van SW↓ en bodemvocht, waarbij een verbeterd (*Gudene*) en een lokaal (*Suthalo*) aardappelras verschillende reacties toonden op SW↓ en bodemvochtregimes. Gegevens toonden ook aan dat de knolopbrengst slecht wordt verklaard door meteorologische en edafische gegevens, hetgeen duidt op de noodzaak voor aanvullend onderzoek. Wanneer het aantal dagen tot volle wasdom 100-110 dagen bedroeg, was de knolopbrengst optimaal.

Hoofdstuk 6 plaatste de belangrijkste bevindingen van het proefschrift in perspectief. Ten slotte besprak Hoofdstuk 7 de belangrijkste bevindingen in antwoord op de onderzoeksvragen in hoofdstuk 1.

**Conclusies en perspectieven:** Op complex terrein varieert het weer en klimaat over korte afstanden, wat de groei van gewassen beïnvloedt. Om de gewasgroei en -opbrengst in de regio te beschrijven, is een weermodel met hoge resolutie, gekoppeld aan een gewasmodel, nodig. De resultaten van het weermodel kunnen worden gebruikt als invoer voor het gewasmodel. Een fijnmazig netwerk van meetstations dat in een complexe topografische regio is geïnstalleerd, kan ons inzicht verschaffen in de luchtstromen op mesoschaal (*bijv.* meer – berg stromen), synoptische systemen (*bijv.* zuid-noordbeweging van de ITCZ) en gewasgroei (*bijv.* LGS en LAI). Extra weerstations (*bijv.* aan de lijzijde van de Gamo hooglanden en ten oosten van de meren Abaya en Chamo) kunnen ons een beter begrip geven van weerschalen en groei van gewassen. Tsum tijdens de P1 blijkt een goede voorspeller te zijn van planthoogte en bebladeringsindex voor de aardappelrassen in Ethiopia. De zwakke correlatie tussen omgevingsvariabelen en opbrengst en opbrengstkenmerken suggereert dat er meer specifieke veldexperimenten moeten worden ontworpen. Een van de voorgestelde veldexperimenten is het continu monitoren van de opslag van droge stof naar de knollen om te bestuderen hoe de gewasopbrengst varieert als een functie van hoogte en meteorologie.

**Trefwoorden:** loofontwikkeling, complexe topografie, plaatselijke en mondiale weerschalen, aardappel, weermodellering, gewasmodellering.

# References

Abbas, G., Hafiz, I., Abbasi, N. and Hussain, A., 2012. Determination of processing and nutritional quality attributes of potato genotypes in Pakistan. Pak J Bot, 44: 201-208.

Abdelwares, M., Haggag, M., Wagdy, A. and Lelieveld, J., 2018. Customized framework of the WRF model for regional climate simulation over the Eastern NILE basin. Theoretical and applied climatology, 134(3-4): 1135-1151, doi: 10.1007/s00704-017-2331-2.

Abdurahman, A., Griffin, D., Elphinstone, J., Struik, P.C., Schulz, S., Schulte-Geldermann, E. and Sharma, K., 2017. Molecular characterization of Ralstonia solanacearum strains from Ethiopia and tracing potential source of bacterial wilt disease outbreak in seed potatoes. Plant Pathology, 66(5): 826-834, doi: 10.1111/ppa.12661.

Abebe, G., Bijman, J., Pascucci, S., Omta, S. and Tsegaye, A., 2016. Diverging quality preferences along the supply chain: implications for variety choice by potato growers in Ethiopia, Quality and innovation in food chains: Lessons and insights from Africa. Wageningen Academic Publishers, pp. 89-102, doi: 10.3920/978-90-8686-825-4_6.

Abebe, G.K., Bijman, J., Pascucci, S. and Omta, O., 2013. Adoption of improved potato varieties in Ethiopia: The role of agricultural knowledge and innovation system and smallholder farmers' quality assessment. Agricultural Systems, 122: 22-32, doi: 10.1016/j.agsy.2013.07.008.

Abrahamsen, P. and Hansen, S., 2000. Daisy: an open soil-crop-atmosphere system model. Environmental Modelling & Software, 15(3): 313-330, doi: 10.1016/S1364-8152(00)00003-7.

ACMAD, 2017. African Center of Meteorological Application for Development: ITD and ITCZ positions.

Adam, M., 2010. A framework to introduce flexibility in crop modelling: from conceptual modelling to software engineering and back, PhD thesis, Wageningen University and Research, Wageningen, The Netherlands.

Adger, W.N., Huq, S., Brown, K., Conway, D. and Hulme, M., 2003. Adaptation to climate change in the developing world. Progress in Development Studies, 3(3): 179-195, doi: 10.1191/1464993403ps060oa.

Allen, E.J. and Scott, R.K., 1980. An Analysis of Growth of the Potato Crop. J Agr Sci, 94(03): 583-606, doi: Doi 10.1017/S0021859600028598.

Araya, N.S., 2011. Weather insurance for farmers: experience from Ethiopia, Paper presented at the IFAD Conference on New Directions for Smallholder Agriculture, pp. 25.

Argent, R., Sun, X., Semazzi, F., Xie, L. and Liu, B., 2015. The Development of a Customization Framework for the WRF Model over the Lake Victoria Basin, Eastern Africa on Seasonal Timescales. Advances in Meteorology, 2015: 15, doi: 10.1155/2015/653473.

Ash, A., McIntosh, P., Cullen, B., Carberry, P. and Smith, M.S., 2007. Constraints and opportunities in applying seasonal climate forecasts in agriculture. Australian Journal of Agricultural Research, 58(10): 952-965, doi: 10.1071/AR06188.

Ashok, K. and Yamagata, T., 2009. The El Niño with a difference. Nature, 461: 481, doi: 10.1038/461481a.

Assefa, E. and Bork, H.-R., 2014. Dynamics and driving forces of agricultural landscapes in Southern Ethiopia–a case study of the Chencha and Arbaminch areas. Journal of Land Use Science(ahead-of-print): 1-16, doi: 10.1080/1747423X.2014.940613.

Assembly, G., 2015. Resolution adopted by the General Assembly on 10 September 2015.

Awulachew, S.B., Erkossa, T. and Namara, R.E., 2010. Irrigation potential in Ethiopia. Constraints and opportunities for enhancing the system, International water Management Institute contributions, Addis Ababa.

Ayana, M., 2011. Deficit irrigation practices as alternative means of improving water use efficiencies in irrigated agriculture: case study of maize crop at Arba Minch, Ethiopia. African Journal of Agricultural Research, 6(2): 226-235.

Badr, M., El-Tohamy, W. and Zaghloul, A., 2012. Yield and water use efficiency of potato grown under different irrigation and nitrogen levels in an arid region. Agricultural Water Management, 110: 9-15, doi: 10.1016/j.agwat.2012.03.008.

Banks, R.F., Tiana-Alsina, J., Baldasano, J.M., Rocadenbosch, F., Papayannis, A., Solomos, S. and Tzanis, C.G., 2016. Sensitivity of boundary-layer variables to PBL schemes in the WRF model based on surface meteorological observations, lidar, and radiosondes during the HygrA-CD campaign. Atmospheric Research, 176-177: 185-201, doi: 10.1016/j.atmosres.2016.02.024.

Barry, R.G. and Chorley, R.J., 2009. Atmosphere, weather and climate. Routledge.

Baye, B. and Gebremedhin, W., 2012. Potato research and development in Ethiopia achievements and trends, Seed Potato Tuber Production and Dissemination: Experiences, Challenges and Prospects. Proceedings of the National Workshop on Seed Potato Tuber Production and Dissemination. Ethiopian Institute of Agricultural Research (EIAR)/Amhara Regional Agricultural Research Institute (ARARI)/International Potato Center (CIP), Addis Ababa, Ethiopia; Bahir Dar, Ethiopia; Lima, Peru, pp. 12-14.

Bazzaz, F.A., 1990. The Response of Natural Ecosystems to the Rising Global CO2 Levels. Annual Review of Ecology and Systematics, 21(1): 167-196, doi: 10.1146/annurev.es.21.110190.001123.

Bell, S., Cornford, D. and Bastin, L., 2015. How good are citizen weather stations? Addressing a biased opinion. Weather, 70(3): 75-84.

Berhane, F. and Zaitchik, B., 2014. Modulation of Daily Precipitation over East Africa by the Madden–Julian Oscillation. Journal of Climate, 27(15): 6016-6034, doi: 10.1175/jcli-d-13-00693.1.

Berihun, B. and Wodegiorgis, G., 2013. Potato Research and Development in Ethiopia: achievements and trends. In: G. Woldegiorgis, S. Schulz and B. Berihun (Editors), Tuber production and dissemination expreiences, challenges and prospects. Proceedings of the National Workshop on Seed Potato Tuber Production and Dissemination, 12-14 March 2012, Bahir Dar, Ethiopia. Ethiopian Institute of Agricultural Research (EIAR) and Amahara Regional Agricultural Research Institute (ARARI) Bahir Dar, pp. 35-44.

Blunden, J. and Arndt, D.S., 2016. State of the Climate in 2015. Bull. Am. Meteorol. Soc., 97(8): Si-S275, doi: 10.1175/2016BAMSStateoftheClimate.1.

Blunden, J., Arndt, D.S. and Hartfield, G., 2018. State of the Climate in 2017. Bull. Am. Meteorol. Soc., 99(8): Si-S332, doi: 10.1175/2018BAMSStateoftheClimate.1.

Bodlaender, K.B.A., 1963. Influence of temperature, radiation and photoperiod on development and yield. In: J.D. Ivins, E.L. Milthorpe and Butterworths (Editors), In The Growth of the Potato, London, UK, pp. 199-210.

Boogaard, H., Eerens, H., Supit, I., van Diepen, C., Piccard, I. and Kempeneers, P., 2002. Description of the MARS crop yield forecasting system (MCYFS). Joint Research Centre, Study contract (19226-2002): 02-F1FED.

Boogaard, H., van Diepen, C., Rotter, R., Cabrera, J. and van Laar, H., 1998. WOFOST 7.1; user's guide for the WOFOST 7.1 crop growth simulation model and WOFOST Control Center 1.5. 0927-4499, SC-DLO.

Borah, M., Burt, R., Headford, D., Milthorpe, F. and Sadler, E.M., 1960. Growth of the potato plant. Annals of Applied Biology, 48(2): 433-434.

Bouman, B.A.M., van Keulen, H., van Laar, H.H. and Rabbinge, R., 1996. The 'School of de Wit' crop growth simulation models: A pedigree and historical overview. Agricultural Systems, 52(2): 171-198, doi: 10.1016/0308-521X(96)00011-X.

Boyd, N., Gordon, R. and Martin, R., 2002. Relationship between leaf area index and ground cover in potato under different management conditions. Potato research, 45(2-4): 117-129.

Bradshaw, J.E. and Bonierbale, M., 2010. Potatoes, In Root and tuber crops. Springer, pp. 1-52.

Brönnimann, S., 2018. Global Warming (1970–Present). In: S. White, C. Pfister and F. Mauelshagen (Editors), The Palgrave Handbook of Climate History. Palgrave Macmillan UK, London, pp. 321-328, doi: 10.1057/978-1-137-43020-5_26.

Brown, H.E., Huth, N. and Holzworth, D., 2011. A potato model built using the APSIM Plant.NET Framework, 19th International Congress on Modelling and Simulation, pp. 961-967.

Buck-Sorlin, G.H., Evers, J.B., Vos, J., Andrieu, B., Chelle, M. and de Visser, P.H.B., 2009. Functional–structural plant modelling: a new versatile tool in crop science. Journal of Experimental Botany, 61(8): 2101-2115, doi: 10.1093/jxb/erp345.

Burstall, L. and Harris, P., 1983. The estimation of percentage light interception from leaf area index and percentage ground cover in potatoes. The Journal of Agricultural Science, 100(1): 241-244, doi: 10.1017/S0021859600032676.

Camberlin, P., 2009. Nile Basin Climates. In: H.J. Dumont (Editor), The Nile: Origin, Environments, Limnology and Human Use. Springer Netherlands, Dordrecht, pp. 307-333, doi: 10.1007/978-1-4020-9726-3_16.

Cane, M.A., Eshel, G. and Buckland, R.W., 1994. Forecasting Zimbabwean maize yield using eastern equatorial Pacific sea surface temperature. Nature, 370: 204, doi: 10.1038/370204a0.

Cao, K., Ruckstuhl, M. and Forrer, H., 1997. Crucial weather conditions for Phytophthora infestans. PAGV-Special Report no 1 January 1997: 85.

Carbone, G.J., 1993. Considerations of meteorological time series in estimating regional-scale crop yield. Journal of Climate, 6(8): 1607-1615, doi: 10.1175/1520-0442(1993)006<1607:Comtsi>2.0.Co;2.

**R**

## References

Carter, T., Parry, M., Porter, J. and Goudriaan, J., 1990. Climate change and future crop suitability in Europe. The greenhouse effect and primary productivity in European agro-ecosystems: 3-6.

Cattani, E., Merino, A. and Levizzani, V., 2016. Evaluation of monthly satellite-derived precipitation products over East Africa. Journal of Hydrometeorology, 17(10): 2555-2573, doi: 10.1175/jhm-d-15-0042.1.

Ceglar, A., Toreti, A., Lecerf, R., van der Velde, M. and Dentener, F., 2016. Impact of meteorological drivers on regional inter-annual crop yield variability in France. Agricultural and Forest Meteorology, 216: 58-67, doi: 10.1016/j.agrformet.2015.10.004.

Chindi, A., Woldegiorgis, G., Solomon, A., Tesema, L., Negash, K., Lemaga, B. and Schulz, S., 2013. Enhancing potato seed production using rapid multiplication techniques, In Roots, Tubers and Bananas. International Potato Center (CIP).

Collins, M., An, S.-I., Cai, W., Ganachaud, A., Guilyardi, E., Jin, F.-F., Jochum, M., Lengaigne, M., Power, S., Timmermann, A., Vecchi, G. and Wittenberg, A., 2010. The impact of global warming on the tropical Pacific Ocean and El Niño. Nature Geoscience, 3: 391, doi: 10.1038/ngeo868.

Combe, M., Vilà-Guerau de Arellano, J., Ouwersloot, H.G., Jacobs, C.M.J. and Peters, W., 2015. Two perspectives on the coupled carbon, water and energy exchange in the planetary boundary layer. Biogeosciences, 12(1): 103-123, doi: 10.5194/bg-12-103-2015.

Cramer, W., Bondeau, A., Woodward, F.I., Prentice, I.C., Betts, R.A., Brovkin, V., Cox, P.M., Fisher, V., Foley, J.A., Friend, A.D., Kucharik, C., Lomas, M.R., Ramankutty, N., Sitch, S., Smith, B., White, A. and Young-Molling, C., 2001. Global response of terrestrial ecosystem structure and function to CO2 and climate change: results from six dynamic global vegetation models. Glob Change Biol, 7(4): 357-373, doi: 10.1046/j.1365-2486.2001.00383.x.

Crosman, E.T. and Horel, J.D., 2010. Sea and Lake Breezes: A Review of Numerical Studies. Boundary-Layer Meteorology, 137(1): 1-29, doi: 10.1007/s10546-010-9517-9.

Crutzen, P.J., 2006. The "Anthropocene". In: E. Ehlers and T. Krafft (Editors), Earth system science in the Anthropocene. Springer Berlin Heidelberg, Berlin, Heidelberg, pp. 13-18, doi: 10.1007/3-540-26590-2_3.

CSA, 2002. Agricultural Sample Enumeration 2001-2002 (1994 E.C), Area and Production - National, Addis Ababa, Ethiopia.

CSA, 2013. Population projections for Ethiopia 2007-2037, Addis Ababa, Ethiopia.

CSA, 2014. Report on Area, Production and Farm Management Practice of Belg Crops for Private Peasan Holdings, Addis Ababa, Ethiopia.

Cunningham, A., German, L., Paumgarten, F., Chikakula, M., Barr, C., Obidzinski, K., van Noordwjik, M., de Koning, R., Purnomo, H. and Yatich, T., 2008. Sustainable trade and management of forest products and services in the COMESA region: an issue paper.

Damtew, E., Tafesse, S., Lie, R., van Mierlo, B., Lemaga, B., Sharma, K., Struik, P.C. and Leeuwis, C., 2018. Diagnosis of management of bacterial wilt and late blight in potato in Ethiopia: A systems thinking perspective. NJAS - Wageningen Journal of Life Sciences, 86-87: 12-24, doi: 10.1016/j.njas.2018.03.003.

Davis-Instruments, 2018. Davis Instruments Support.

Daye, D.D. and Healey, J.R., 2015. Impacts of land-use change on sacred forests at the landscape scale. Global Ecology and Conservation, 3: 349-358, doi: 10.1016/j.gecco.2014.12.009.

De Wit, A., Baruth, B., Boogaard, H., van Diepen, K., van Kraalingen, D., Micale, F., te Roller, J., Supit, I. and van den Wijngaart, R., 2010. Using ERA-INTERIM for regional crop yield forecasting in Europe. Climate Research, 44(1): 41-53, doi: 10.3354/cr00872.

De Wit, A., Boogaard, H., Fumagalli, D., Janssen, S., Knapen, R., van Kraalingen, D., Supit, I., van der Wijngaart, R. and van Diepen, K., 2019. 25 years of the WOFOST cropping systems model. Agricultural Systems, 168: 154-167, doi: 10.1016/j.agsy.2018.06.018.

Deblonde, P.M.K. and Ledent, J.F., 2001. Effects of moderate drought conditions on green leaf number, stem height, leaf length and tuber yield of potato cultivars. European Journal of Agronomy, 14(1): 31-41, doi: 10.1016/S1161-0301(00)00081-2.

Dee, Dick, Fasullo, John, Shea, Dennis, Walsh and (Eds), J.N.-S., 2016. The Climate Data Guide: Atmospheric Reanalysis: Overview & Comparison Tables.

Dee, D.P., Uppala, S.M., Simmons, A.J., Berrisford, P., Poli, P., Kobayashi, S., Andrae, U., Balmaseda, M.A., Balsamo, G., Bauer, P., Bechtold, P., Beljaars, A.C.M., van de Berg, L., Bidlot, J., Bormann, N., Delsol, C., Dragani, R., Fuentes, M., Geer, A.J., Haimberger, L., Healy, S.B., Hersbach, H., Hólm, E.V., Isaksen, L., Kållberg, P., Köhler, M., Matricardi, M., McNally, A.P., Monge-Sanz, B.M., Morcrette, J.J., Park, B.K., Peubey, C., de Rosnay, P., Tavolato, C., Thépaut, J.N. and Vitart, F., 2011. The ERA-Interim reanalysis: configuration and performance of the data assimilation system. Quarterly Journal of the Royal Meteorological Society, 137(656): 553-597, doi: 10.1002/qj.828.

DeFauw, S.L., He, Z., Larkin, R.P. and Mansour, S.A., 2012. Sustainable Potato Production and Global Food Security. In: Z. He, R. Larkin and W. Honeycutt (Editors), Sustainable Potato Production: Global Case Studies. Springer Netherlands, Dordrecht, pp. 3-19, doi: 10.1007/978-94-007-4104-1_1.

Degefu, W., 1987. Some aspects of meteorological drought in Ethiopia. Cambridge University Press.

Dersseh, W.M., 2017. Agronomic and socioeconomic sustainability of farming systems: a case in Chencha, South Ethiopia, PhD thesis, Wageningen University and Research, Wageningen, The Netherlands, doi: 10.18174/422284.

Dersseh, W.M., Gebresilase, Y.T., Schulte, R.P.O. and Struik, P.C., 2016. The Analysis of Potato Farming Systems in Chencha, Ethiopia: Input, Output and Constraints. American Journal of Potato Research: 1-12, doi: 10.1007/s12230-016-9521-9.

Devaux, A., Kromann, P. and Ortiz, O., 2014. Potatoes for sustainable global food security. Potato Research, 57(3-4): 185-199, doi: 10.1007/s11540-014-9265-1.

Dinku, T., Ceccato, P. and Connor, S.J., 2011. Challenges of satellite rainfall estimation over mountainous and arid parts of east Africa. International journal of remote sensing, 32(21): 5965-5979, doi: 10.1080/01431161.2010.499381.

Dinku, T., Hailemariam, K., Maidment, R., Tarnavsky, E. and Connor, S., 2014. Combined use of satellite estimates and rain gauge observations to generate high-quality historical rainfall time series over Ethiopia. International Journal of Climatology, 34(7): 2489-2504, doi: 10.1002/joc.3855.

Diro, G.T., Black, E. and Grimes, D., 2008. Seasonal forecasting of Ethiopian spring rains. Meteorological Applications, 15(1): 73-83, doi: 10.1002/met.63.

Diro, G.T., Grimes, D. and Black, E., 2011a. Large scale features affecting Ethiopian rainfall, African Climate and Climate Change. Springer, pp. 13-50, doi: 10.1007/978-90-481-3842-5_2.

Diro, G.T., Grimes, D., Black, E., O'Neill, A. and Pardo-Iguzquiza, E., 2009. Evaluation of reanalysis rainfall estimates over Ethiopia. International Journal of Climatology, 29(1): 67-78, doi: 10.1002/joc.1699.

**R**

Diro, G.T., Toniazzo, T. and Shaffrey, L., 2011b. Ethiopian rainfall in climate models, African climate and climate change. Springer, pp. 51-69, doi: 10.1007/978-90-481-3842-5_3.

Dutra, E., Giuseppe, F.D., Wetterhall, F. and Pappenberger, F., 2013. Seasonal forecasts of droughts in African basins using the Standardized Precipitation Index. Hydrology and Earth System Sciences, 17(6): 2359-2373, doi: 10.5194/hess-17-2359-2013.

Elliott, J., Müller, C., Deryng, D., Chryssanthacopoulos, J., Boote, K., Büchner, M., Foster, I., Glotter, M., Heinke, J. and Iizumi, T., 2015. The global gridded crop model intercomparison: data and modeling protocols for phase 1 (v1. 0). Geoscientific Model Development, 8(2): 261-277, doi: 10.5194/gmd-8-261-2015.

Elsen, P.R. and Tingley, M.W., 2015. Global mountain topography and the fate of montane species under climate change. Nature Climate Change, 5: 772, doi: 10.1038/nclimate2656.

Ewing, E., 1981. Heat stress and the tuberization stimulus. American Potato Journal, 58(1): 31-49.

Fahem, M. and Haverkort, A.J., 1988. Comparison of the growth of potato crops grown in autumn and spring in North Africa. Potato Research, 31(4): 557-568, doi: 10.1007/bf02361845.

FAO, 2008a. Climate change and food security: a framework document. Food and Agriculture Organization of the United Nations Rome.

FAO, 2008b. International year of the potato 2008. Food and Agriculture Organization (FAO).

FAO, 2016. The State of Food and Agriculture–Climate Change, Agriculture and Food Security. Food and Agriculture Organization of the United Nations Rome.

FAO, 2019. FAO statistical databases FAOSTAT.

Firman, D. and Allen, E., 1989. Relationship between light interception, ground cover and leaf area index in potatoes. The Journal of Agricultural Science, 113(3): 355-359, doi: 10.1017/S0021859600070040.

Fleisher, D.H., Condori, B., Quiroz, R., Alva, A., Asseng, S., Barreda, C., Bindi, M., Boote, K.J., Ferrise, R., Franke, A.C., Govindakrishnan, P.M., Harahagazwe, D., Hoogenboom, G., Naresh Kumar, S., Merante, P., Nendel, C., Olesen, J.E., Parker, P.S., Raes, D., Raymundo, R., Ruane, A.C., Stockle, C., Supit, I., Vanuytrecht, E., Wolf, J. and Woli, P., 2017. A potato model intercomparison across varying climates and productivity levels. Glob Change Biol, 23(3): 1258-1281, doi: 10.1111/gcb.13411.

Fraedrich, K., 1972. A simple climatological model of the dynamics and energetics of the nocturnal circulation at Lake Victoria. Quarterly Journal of the Royal Meteorological Society, 98(416): 322-335, doi: 10.1002/qj.49709841606.

Freeman, D., 2002. From warrior to wife: Cultural transformation in the Gamo Highlands of Ethiopia. Journal of the Royal Anthropological Institute, 8(1): 23-44.

Frisvold, G.B. and Murugesan, A., 2013. Use of Weather Information for Agricultural Decision Making. Weather, Climate, and Society, 5(1): 55-69, doi: 10.1175/wcas-d-12-00022.1.

Funk, C., Nicholson, S.E., Landsfeld, M., Klotter, D., Peterson, P. and Harrison, L., 2015a. The Centennial Trends Greater Horn of Africa precipitation dataset. Scientific Data, 2: 150050, doi: 10.1038/sdata.2015.50.

Funk, C., Peterson, P., Landsfeld, M., Pedreros, D., Verdin, J., Shukla, S., Husak, G., Rowland, J., Harrison, L., Hoell, A. and Michaelsen, J., 2015b. The climate hazards infrared precipitation with stations—a new environmental record for monitoring extremes. Scientific Data, 2: 150066, doi: 10.1038/sdata.2015.66.

Garbrecht, J.D. and Schneider, J.M., 2007. Climate forecast and prediction product dissemination for agriculture in the United States. Australian Journal of Agricultural Research, 58(10): 966-974, doi: 10.1071/AR06191.

Garg, H.P. and Garg, S.N., 1983. Prediction of global solar radiation from bright sunshine hours and other meteorological data. Energy Conversion and Management, 23(2): 113-118, doi: 10.1016/0196-8904(83)90070-5.

Gayler, S., Wang, E., Priesack, E., Schaaf, T. and Maidl, F.X., 2002. Modeling biomass growth, N-uptake and phenological development of potato crop. Geoderma, 105(3): 367-383, doi: 10.1016/S0016-7061(01)00113-6.

Gebremariam, B., 2007. Basin scale sedimentary and water quality responses to external forcing in Lake Abaya, southern Ethiopian Rift Valley, PhD thesis, Freie Universität Berlin, Germany.

Gebreselassie, H., Mohamed, W. and Shimelis, B., 2016. Evaluation of Potato (Solanum tuberosum L.) Varieties for Yield and Yield Components in Eastern Ethiopia. Journal of Biology, Agriculture and Healthcare, 6(5): 146-154.

Geerts, B. and Dejene, T., 2005. Regional and diurnal variability of the vertical structure of precipitation systems in Africa based on spaceborne radar data. Journal of Climate, 18(7): 893-916, doi: 10.1175/jcli-3316.1.

George, T.S., Taylor, M.A., Dodd, I.C. and White, P.J., 2018. Climate change and consequences for potato production: A review of tolerance to emerging abiotic stress. Potato Research: 1-30.

Gibbons, J.M. and Ramsden, S.J., 2008. Integrated modelling of farm adaptation to climate change in East Anglia, UK: Scaling and farmer decision making. Agriculture, Ecosystems & Environment, 127(1): 126-134, doi: 10.1016/j.agee.2008.03.010.

Gissila, T., Black, E., Grimes, D. and Slingo, J., 2004. Seasonal forecasting of the Ethiopian summer rains. International Journal of Climatology, 24(11): 1345-1358.

Gleixner, S., Keenlyside, N., Viste, E. and Korecha, D., 2017. The El Niño effect on Ethiopian summer rainfall. Climate Dynamics, 49(5): 1865-1883, doi: 10.1007/s00382-016-3421-z.

Godfray, H.C.J., Beddington, J.R., Crute, I.R., Haddad, L., Lawrence, D., Muir, J.F., Pretty, J., Robinson, S., Thomas, S.M. and Toulmin, C., 2010a. Food Security: The Challenge of Feeding 9 Billion People. Science, 327(5967): 812-818, doi: 10.1126/science.1185383.

Godfray, H.C.J., Crute, I.R., Haddad, L., Lawrence, D., Muir, J.F., Nisbett, N., Pretty, J., Robinson, S., Toulmin, C. and Whiteley, R., 2010b. The future of the global food system. Philosophical Transactions of the Royal Society B: Biological Sciences, 365(1554): 2769-2777, doi: 10.1098/rstb.2010.0180.

Gomez, K.A., Gomez, K.A. and Gomez, A.A., 1984. Statistical procedures for agricultural research. John Wiley & Sons.

Gordon, R., Brown, D. and Dixon, M., 1997. Stomatal resistance of three potato cultivars as influenced by soil water status, humidity and irradiance. Potato Research, 40(1): 47-57.

Gregory, P.J., Ingram, J.S.I. and Brklacich, M., 2005. Climate change and food security. Philosophical Transactions of the Royal Society B: Biological Sciences, 360(1463): 2139-2148, doi: 10.1098/rstb.2005.1745.

Griggs, D., Stafford-Smith, M., Gaffney, O., Rockström, J., Öhman, M.C., Shyamsundar, P., Steffen, W., Glaser, G., Kanie, N. and Noble, I., 2013. Policy: Sustainable development goals for people and planet. Nature, 495(7441): 305.

**R**

Gu, J., Yin, X., Zhang, C., Wang, H. and Struik, P.C., 2014. Linking ecophysiological modelling with quantitative genetics to support marker-assisted crop design for improved yields of rice (Oryza sativa) under drought stress. Annals of Botany, 114(3): 499-511, doi: 10.1093/aob/mcu127.

Haile, A.T., Habib, E., Elsaadani, M. and Rientjes, T., 2013. Inter-comparison of satellite rainfall products for representing rainfall diurnal cycle over the Nile basin. International Journal of Applied Earth Observation and Geoinformation, 21: 230-240, doi: 10.1016/j.jag.2012.08.012.

Haile, A.T., Rientjes, T., Gieske, A. and Gebremichael, M., 2009. Rainfall variability over mountainous and adjacent lake areas: the case of Lake Tana basin at the source of the Blue Nile River. Journal of Applied Meteorology and Climatology, 48(8): 1696-1717, doi: 10.1175/2009jamc2092.1.

Haile, M., 2005. Weather patterns, food security and humanitarian response in sub-Saharan Africa. Philosophical Transactions of the Royal Society B: Biological Sciences, 360(1463): 2169-2182.

Hall, C., Dawson, T.P., Macdiarmid, J.I., Matthews, R.B. and Smith, P., 2017. The impact of population growth and climate change on food security in Africa: looking ahead to 2050. International Journal of Agricultural Sustainability, 15(2): 124-135, doi: 10.1080/14735903.2017.1293929.

Hammes, P. and De Jager, J., 1990. Net photosynthetic rate of potato at high temperatures. Potato Research, 33(4): 515-520.

Hansen, J., Sato, M., Ruedy, R., Lo, K., Lea, D.W. and Medina-Elizade, M., 2006. Global temperature change. Proceedings of the National Academy of Sciences, 103(39): 14288-14293, doi: 10.1073/pnas.0606291103.

Harper, P., 1963. Optimum leaf area index in the potato crop. Nature, 197(4870): 917-918, doi: 10.1038/197917b0.

Hartill, W.F.T., Young, K., Allan, D.J. and Henshall, W.R., 1990. Effects of temperature and leaf wetness on the potato late blight. New Zealand Journal of Crop and Horticultural Science, 18(4): 181-184, doi: 10.1080/01140671.1990.10428093.

Haverkort, A., Verhagen, A., Grashoff, A. and Uithol, P., 2004. Potato-zoning: a decision support system on expanding the potato industry through agro-ecological zoning using the LINTUL simulation approach. Decision support systems in potato production: bringing models to practice. Wageningen Academic, Wageningen: 29-44.

Haverkort, A.J., 1986. Yield levels of potato crops in Central Africa. Agricultural Systems, 21(3): 227-235, doi: 10.1016/0308-521X(86)90041-7.

Haverkort, A.J., 1990. Ecology of potato cropping systems in relation to latitude and altitude. Agricultural Systems, 32(3): 251-272, doi: 10.1016/0308-521X(90)90004-A.

Haverkort, A.J., 2007. Chapter 17 - Potato crop response to radiation and daylength. In: D. Vreugdenhil et al. (Editors), In Potato Biology and Biotechnology. Elsevier Science B.V., Amsterdam, pp. 353-365, doi: 10.1016/B978-044451018-1/50059-2.

Haverkort, A.J., 2018. Potato handbook: crop of the future. Potato World Magazine, 2018, The Hague.

Haverkort, A.J., de Ruijter, F.J., van Evert, F.K., Conijn, J.G. and Rutgers, B., 2013. Worldwide sustainability hotspots in potato cultivation. 1. Identification and mapping. Potato Research, 56(4): 343-353, doi: 10.1007/s11540-013-9247-8.

Haverkort, A.J., Franke, A.C., Steyn, J.M., Pronk, A.A., Caldiz, D.O. and Kooman, P.L., 2015. A Robust Potato Model: LINTUL-POTATO-DSS. Potato Research, 58(4): 313-327, doi: 10.1007/s11540-015-9303-7.

Haverkort, A.J. and Harris, P.M., 1986. Conversion coefficients between intercepted solar radiation and tuber yields of potato crops under tropical highland conditions. Potato Research, 29(4): 529-533, doi: 10.1007/bf02357918.

Haverkort, A.J. and Harris, P.M., 1987. A model for potato growth and yield under tropical highland conditions. Agricultural and Forest Meteorology, 39(4): 271-282, doi: 10.1016/0168-1923(87)90020-7.

Haverkort, A.J. and Struik, P.C., 2015. Yield levels of potato crops: Recent achievements and future prospects. Field Crops Research, 182: 76-85, doi: 10.1016/j.fcr.2015.06.002.

Haverkort, A.J., Van De Waart, M. and Bodlaender, K.B.A., 1990. The effect of early drought stress on numbers of tubers and stolons of potato in controlled and field conditions. Potato Research, 33(1): 89-96, doi: 10.1007/bf02358133.

Haverkort, A.J., van Koesveld, F., Schepers, H., Wijnands, J., Wustman, R. and Zhang, X., 2012. Potato prospects for Ethiopia: on the road to value addition. Praktijkonderzoek Plant & Omgeving.

Haverkort, A.J. and Verhagen, A., 2008. Climate change and its repercussions for the potato supply chain. Potato Research, 51(3): 223, doi: 10.1007/s11540-008-9107-0.

Hazeleger, W., Severijns, C., Semmler, T., Stefanescu, S., Yang, S., Wang, X., Wyser, K., Dutra, E., Baldasano, J.M. and Bintanja, R., 2010. EC-Earth: a seamless earth-system prediction approach in action. Bulletin of the American Meteorological Society, 91(10): 1357-1363, doi: 10.1175/2010BAMS2877.1.

Hazeleger, W., Wang, X., Severijns, C., Ştefănescu, S., Bintanja, R., Sterl, A., Wyser, K., Semmler, T., Yang, S., van den Hurk, B., van Noije, T., van der Linden, E. and van der Wiel, K., 2012. EC-Earth V2.2: description and validation of a new seamless earth system prediction model. Climate Dynamics, 39(11): 2611-2629, doi: 10.1007/s00382-011-1228-5.

Headey, D., Dereje, M. and Taffesse, A.S., 2014. Land constraints and agricultural intensification in Ethiopia: A village-level analysis of high-potential areas. Food Policy, 48: 129-141, doi: 10.1016/j.foodpol.2014.01.008.

Heidmann, T., Tofteng, C., Abrahamsen, P., Plauborg, F., Hansen, S., Battilani, A., Coutinho, J., Doležal, F., Mazurczyk, W. and Ruiz, J., 2008. Calibration procedure for a potato crop growth model using information from across Europe. ecological modelling, 211(1-2): 209-223, doi: 10.1016/j.ecolmodel.2007.09.008.

Hijmans, R.J., 2003. The effect of climate change on global potato production. American Journal of Potato Research, 80(4): 271-279, doi: 10.1007/BF02855363.

Hijmans, R.J., Cameron, S.E., Parra, J.L., Jones, P.G. and Jarvis, A., 2005. Very high resolution interpolated climate surfaces for global land areas. International Journal of Climatology, 25(15): 1965-1978, doi: 10.1002/joc.1276.

Hirpa, A., Meuwissen, M.P., Tesfaye, A., Lommen, W.J.M., Lansink, A.O., Tsegaye, A. and Struik, P.C., 2010. Analysis of seed potato systems in Ethiopia. American Journal of Potato Research, 87(6): 537-552, doi: 10.1007/s12230-010-9164-1.

Hirpa, A., Meuwissen, M.P., van der Lans, I.A., Lommen, W.J., Oude Lansink, A.G., Tsegaye, A. and Struik, P.C., 2012. Farmers' opinion on seed potato management attributes in Ethiopia: A conjoint analysis. Agronomy Journal, 104(5): 1413-1424.

Hoegh-Guldberg, O., Jacob, D., Taylor, M., Bindi, M., Brown, S., Camilloni, I., Diedhiou, A., R. Djalante, Ebi, K., Engelbrecht, F., Guiot, J., Hijioka, Y., Mehrotra, S., Payne, A., Seneviratne, S.I., Thomas, A., Warren, R. and Zhou, G., 2018. Impacts of 1.5°C Global Warming on Natural and Human Systems. In: Global warming of 1.5°C. An IPCC Special Report on the impacts of global warming of 1.5°C above

**R**

pre-industrial levels and related global greenhouse gas emission pathways, in the context of strengthening the global response to the threat of climate change, sustainable development, and efforts to eradicate poverty [V. Masson-Delmotte, P. Zhai, H. O. Pörtner, D. Roberts, J. Skea, P.R. Shukla, A. Pirani, W. Moufouma-Okia, C. Péan, R. Pidcock, S. Connors, J. B. R. Matthews, Y. Chen, X. Zhou, M. I. Gomis, E. Lonnoy, T. Maycock, M. Tignor, T. Waterfield (eds.)]. In Press., World Meteorological Organization, Geneva, Switzerland.

Holden, S. and Yohannes, H., 2002. Land redistribution, tenure insecurity, and intensity of production: A study of farm households in Southern Ethiopia. Land Economics, 78(4): 573-590, doi: 10.2307/3146854.

Hong, S., Lakshmi, V., Small, E.E., Chen, F., Tewari, M. and Manning, K.W., 2009. Effects of vegetation and soil moisture on the simulated land surface processes from the coupled WRF/Noah model. Journal of Geophysical Research: Atmospheres, 114(D18), doi: 10.1029/2008JD011249.

Hoogenboom, G., 2000. Contribution of agrometeorology to the simulation of crop production and its applications. Agricultural and Forest Meteorology, 103(1): 137-157, doi: 10.1016/S0168-1923(00)00108-8.

Houze, R.A., 2012. Orographic effects on precipitating clouds. Reviews of Geophysics, 50(1).

Huddleston, B., Ataman, E. and d'Ostiani, L.F., 2003. Towards a GIS based analysis of mountain environment and population. FAO Rome.

Hunink, J.E., Immerzeel, W.W. and Droogers, P., 2014. A High-resolution Precipitation 2-step mapping procedure (HiP2P): Development and application to a tropical mountainous area. Remote Sensing of Environment, 140: 179-188, doi: 10.1016/j.rse.2013.08.036.

Ingram, J. and Brklacich, M., 2006. Global Environmental Change and Food Systems GECAFS: A new interdisciplinary research project, Earth System Science in the Anthropocene. Springer, pp. 217-228.

Ingram, K.T. and McCloud, D.E., 1984. Simulation of Potato Crop Growth and Development1. Crop Science, 24: 21-27, doi: 10.2135/cropsci1984.0011183X002400010006x.

Ingwersen, J., Högy, P., Wizemann, H.D., Warrach-Sagi, K. and Streck, T., 2018. Coupling the land surface model Noah-MP with the generic crop growth model Gecros: Model description, calibration and validation. Agricultural and Forest Meteorology, 262: 322-339, doi: 10.1016/j.agrformet.2018.06.023.

Instruments, D., 2006a. Derived variables in Davis weather products. Support documents for: Wireless Vantage Pro2™ Plus with.

Instruments, D., 2006b. Vantage Pro2™ Console Manual. Davis Instruments Corp. Hayward.

IPC, 2009. International Potato Center: World Potato Atlas - Ethiopia. In: K. Theisen (Editor).

IPCC, 2018a. Annex I: Glossary [R. Matthews (ed.)]. In: Global warming of 1.5°C. An IPCC Special Report on the impacts of global warming of 1.5°C above pre-industrial levels and related global greenhouse gas emission pathways, in the context of strengthening the global response to the threat of climate change, sustainable development, and efforts to eradicate poverty [V. Masson-Delmotte, P. Zhai, H. O. Pörtner, D. Roberts, J. Skea, P.R. Shukla, A. Pirani, W. Moufouma-Okia, C. Péan, R. Pidcock, S. Connors, J. B. R. Matthews, Y. Chen, X. Zhou, M. I. Gomis, E. Lonnoy, T. Maycock, M. Tignor, T. Waterfield (eds.)]. In Press.

IPCC, 2018b. Summary for Policymakers. In: Global warming of 1.5°C. An IPCC Special Report on the impacts of global warming of 1.5°C above pre-industrial levels and related global greenhouse gas emission pathways, in the context of strengthening the global response to the threat of climate change, sustainable development, and efforts to eradicate poverty [V. Masson-Delmotte, P. Zhai, H. O. Pörtner, D. Roberts, J. Skea, P. R. Shukla, A. Pirani, W. Moufouma-Okia, C. Péan, R. Pidcock, S.

Connors, J. B. R. Matthews, Y. Chen, X. Zhou, M. I. Gomis, E. Lonnoy, T. Maycock, M. Tignor, T. Waterfield (eds.)]. In press, World Meteorological Organization, Geneva, Switzerland.

James, R. and Washington, R., 2013. Changes in African temperature and precipitation associated with degrees of global warming. Climatic Change, 117(4): 859-872, doi: 10.1007/s10584-012-0581-7.

Jayne, T.S., Chamberlin, J. and Headey, D.D., 2014. Land pressures, the evolution of farming systems, and development strategies in Africa: A synthesis. Food Policy, 48: 1-17, doi: 10.1016/j.foodpol.2014.05.014.

Jiménez, P.A., Dudhia, J. and Navarro, J., 2011a. On the surface wind speed probability density function over complex terrain. Geophysical Research Letters, 38(22), doi: 10.1029/2011GL049669.

Jiménez, P.A., González-Rouco, J.F., García-Bustamante, E., Navarro, J., Montávez, J.P., Vilà-Guerau de Arellano, J., Dudhia, J. and Muñoz-Roldan, A., 2010. Surface wind regionalization over complex terrain: Evaluation and analysis of a high-resolution WRF simulation. Journal of Applied Meteorology and Climatology, 49(2): 268-287, doi: 0.1175/2009JAMC2175.1.

Jiménez, P.A., González-Rouco, J.F., Montávez, J.P., García-Bustamante, E., Navarro, J. and Dudhia, J., 2013. Analysis of the long-term surface wind variability over complex terrain using a high spatial resolution WRF simulation. Climate Dynamics, 40(7): 1643-1656, doi: 10.1007/s00382-012-1326-z.

Jiménez, P.A., Vilà-Guerau de Arellano, J., Dudhia, J. and Bosveld, F.C., 2016. Role of synoptic- and meso-scales on the evolution of the boundary-layer wind profile over a coastal region: the near-coast diurnal acceleration. Meteorology and Atmospheric Physics, 128(1): 39-56, doi: 10.1007/s00703-015-0400-6.

Jiménez, P.A., Vilà-Guerau de Arellano, J., González-Rouco, J.F., Navarro, J., Montávez, J.P., García-Bustamante, E. and Dudhia, J., 2011b. The Effect of Heat Waves and Drought on Surface Wind Circulations in the Northeast of the Iberian Peninsula during the Summer of 2003. Journal of Climate, 24(20): 5416-5422, doi: 10.1175/2011JCLI4061.1.

Jin, X., Kumar, L., Li, Z., Feng, H., Xu, X., Yang, G. and Wang, J., 2018. A review of data assimilation of remote sensing and crop models. European Journal of Agronomy, 92: 141-152, doi: 10.1016/j.eja.2017.11.002.

Johnson, D.A., Alldredge, J.R. and Vakoch, D.L., 1996. Potato late blight forecasting models for the semiarid environment of south-central Washington. Phytopathology, 86(5): 480-484.

Jones, J.W., Hoogenboom, G., Porter, C.H., Boote, K.J., Batchelor, W.D., Hunt, L., Wilkens, P.W., Singh, U., Gijsman, A.J. and Ritchie, J.T., 2003. The DSSAT cropping system model. European Journal of Agronomy, 18(3-4): 235-265.

Jovanovic, N., Musvoto, C., De Clercq, W., Pienaar, C., Petja, B., Zairi, A., Hanafi, S., Ajmi, T., Mailhol, J.C., Cheviron, B., Albasha, R., Habtu, S., Yazew, E., Kifle, M., Fissahaye, D., Aregay, G., Habtegebreal, K., Gebrekiros, A., Woldu, Y. and Froebrich, J., 2018. A Comparative analysis of yield gaps and water productivity on smallholder farms in Ethiopia, South Africa and Tunisia. Irrigation and Drainage, doi: 10.1002/ird.2238.

Jury, M.R., 2012. Ethiopian highlands crop-climate prediction: 1979–2009. Journal of Applied Meteorology and Climatology, 52(5): 1116-1126, doi: 10.1175/JAMC-D-12-0139.1.

Jury, M.R., 2014a. Evaluation of coupled model forecasts of Ethiopian highlands summer climate. Advances in Meteorology, 2014, doi: 10.1155/2014/894318.

Jury, M.R., 2014b. Southern Ethiopia Rift Valley lake fluctuations and climate. Scientific Research and Essays, 9(18): 794-805, doi: 10.5897/SRE2014.6062.

**R**

Jury, M.R., 2019. Diurnal climate of the Abyssinia highlands during summer 2015 (A paper in review).

Kanamaru, H., 2009. Food security under a changing climate. World Meteorological Organization (WMO) Bulletin, 58(3): 205.

Karl, T.R. and Trenberth, K.E., 2003. Modern global climate change. Science, 302(5651): 1719-1723, doi: 10.1126/science.1090228.

Kassie, B.T., 2014. Climate variability and change in Ethiopia: Exploring impacts and adaptation options for cereal production, PhD thesis, Wageningen University and Research, Wageningen, The Netherlands.

Kates, R.W., 2018. What is sustainable development? Environment, 47(3): 9-21.

Kates, R.W., Parris, T.M. and Leiserowitz, A.A., 2005. What is sustainable development? Goals, indicators, values, and practice. Environment(Washington DC), 47(3): 8-21.

Keating, B.A., Carberry, P.S., Hammer, G.L., Probert, M.E., Robertson, M.J., Holzworth, D., Huth, N.I., Hargreaves, J.N.G., Meinke, H., Hochman, Z., McLean, G., Verburg, K., Snow, V., Dimes, J.P., Silburn, M., Wang, E., Brown, S., Bristow, K.L., Asseng, S., Chapman, S., McCown, R.L., Freebairn, D.M. and Smith, C.J., 2003. An overview of APSIM, a model designed for farming systems simulation. European Journal of Agronomy, 18(3): 267-288, doi: 10.1016/S1161-0301(02)00108-9.

Keeble, B.R., 1988. The Brundtland report: 'Our common future'. Medicine and War, 4(1): 17-25, doi: 10.1080/07488008808408783.

Kendon, E.J., Roberts, N.M., Senior, C.A. and Roberts, M.J., 2012. Realism of Rainfall in a Very High-Resolution Regional Climate Model. Journal of Climate, 25(17): 5791-5806, doi: 10.1175/jcli-d-11-00562.1.

Kerandi, N., Arnault, J., Laux, P., Wagner, S., Kitheka, J. and Kunstmann, H., 2018. Joint atmospheric-terrestrial water balances for East Africa: a WRF-Hydro case study for the upper Tana River basin. Theoretical and Applied Climatology, 131(3): 1337-1355, doi: 10.1007/s00704-017-2050-8.

Khan, M., 2012. Assessing genetic variation in growth and development of potato, PhD thesis, Wageningen University and Research, Wageningen, The Netherlands.

Khan, M., Yin, X., van der Putten, P.E.L. and Struik, P.C., 2014. An ecophysiological model analysis of yield differences within a set of contrasting cultivars and an F1 segregating population of potato (Solanum tuberosum L.) grown under diverse environments. Ecological Modelling, 290: 146-154, doi: 10.1016/j.ecolmodel.2013.11.015.

Khan, M.S., van Eck, H.J. and Struik, P.C., 2013. Model-based evaluation of maturity type of potato using a diverse set of standard cultivars and a segregating diploid population. Potato Research, 56(2): 127-146, doi: 10.1007/s11540-013-9235-z.

Kiniry, J.R., Landivar, J.A., Witt, M., Gerik, T.J., Cavero, J. and Wade, L.J., 1998. Radiation-use efficiency response to vapor pressure deficit for maize and sorghum. Field Crops Research, 56(3): 265-270, doi: 10.1016/S0378-4290(97)00092-0.

Kirub, A. and Asfaw, F., 2013. Seed Potato Tuber Production and Dissemination, In Proceedings of the National Workshop on Seed Potato Tuber Production and Dissemination, Bahir Dar, Ethiopia.

Klemm, T. and McPherson, R.A., 2017. The development of seasonal climate forecasting for agricultural producers. Agricultural and Forest Meteorology, 232: 384-399, doi: 10.1016/j.agrformet.2016.09.005.

Kolech, S.A., Halseth, D., De Jong, W., Perry, K., Wolfe, D., Tiruneh, F.M. and Schulz, S., 2015. Potato Variety Diversity, Determinants and Implications for Potato Breeding Strategy in Ethiopia. American Journal of Potato Research, 92(5): 551-566, doi: 10.1007/s12230-015-9467-3.

Kooman, P.L., 1995. Yielding ability of potato crops as influenced by temperature and daylength, PhD thesis, Wageningen University and Research, Wageningen, The Netherlands.

Kooman, P.L. and Haverkort, A.J., 1995a. Modelling development and growth of the potato crop influenced by temperature and daylength: LINTUL-POTATO. In: A.J. Haverkort and D.K.L. MacKerron (Editors), Potato Ecology And modelling of crops under conditions limiting growth: Proceedings of the Second International Potato Modeling Conference, held in Wageningen 17–19 May, 1994. Springer Netherlands, Dordrecht, pp. 41-60, doi: 10.1007/978-94-011-0051-9_3.

Kooman, P.L. and Haverkort, A.J., 1995b. Modelling development and growth of the potato crop influenced by temperature and daylength: LINTUL-POTATO. In: A.J. Haverkort and D.K.L. MacKerron (Editors), Potato Ecology And modelling of crops under conditions limiting growth: Proceedings of the Second International Potato Modeling Conference, held in Wageningen 17–19 May, 1994. Springer Netherlands, Dordrecht, pp. 41-59, doi: 10.1007/978-94-011-0051-9_3.

Korecha, D., 2013. Characterizing the Predictability of Seasonal Climate in Ethiopia, PhD thesis, University of Bergen, Norway.

Korecha, D. and Barnston, A.G., 2007. predictability of June-September rainfall in Ethiopia. Monthly weather review, 135(2): 628-650, doi: 10.1175/MWR3304.1.

Korecha, D. and Sorteberg, A., 2013. Validation of operational seasonal rainfall forecast in Ethiopia. Water Resources Research, 49(11): 7681-7697, doi: 10.1002/2013WR013760, 2013.

Kunz, H., Scherrer, S.C., Liniger, M.A. and Appenzeller, C., 2007. The evolution of ERA-40 surface temperatures and total ozone compared to observed Swiss time series. Meteorologische Zeitschrift, 16(2): 171-181, doi: 10.1127/0941-2948/2007/0183.

Kurkowski, N.P., Stensrud, D.J. and Baldwin, M.E., 2003. Assessment of Implementing Satellite-Derived Land Cover Data in the Eta Model. Weather and Forecasting, 18(3): 404-416, doi: 10.1175/1520-0434(2003)18<404:Aoisdl>2.0.Co;2.

Lagouvardos, K., Kotroni, V., Bezes, A., Koletsis, I., Kopania, T., Lykoudis, S., Mazarakis, N., Papagiannaki, K. and Vougioukas, S., 2017. The automatic weather stations NOANN network of the National Observatory of Athens: operation and database. Geosci. Data J., 4(1): 4-16, doi: 10.1002/gdj3.44.

Leenaars, J.G.B., van Oostrum, A.J.M. and M. Ruiperez, G., 2014. Africa soil profiles database, Version 1.2. ISRIC Report 2014/01, ISRIC, Wageningen, The Netherlands.

Lehner, M. and Rotach, M.W., 2018. Current challenges in understanding and predicting transport and exchange in the atmosphere over mountainous terrain. Atmosphere, 9(7): 276, doi: 10.3390/atmos9070276.

Lesk, C., Rowhani, P. and Ramankutty, N., 2016. Influence of extreme weather disasters on global crop production. Nature, 529: 84, doi: 10.1038/nature16467.

Lewis, K., 2017. Understanding climate as a driver of food insecurity in Ethiopia. Climatic Change, 144(2): 317-328, doi: 10.1007/s10584-017-2036-7.

Lin, T.-S. and Cheng, F.-Y., 2016. Impact of Soil Moisture Initialization and Soil Texture on Simulated Land–Atmosphere Interaction in Taiwan. Journal of Hydrometeorology, 17(5): 1337-1355, doi: 10.1175/jhm-d-15-0024.1.

Liu, J., Williams, J.R., Zehnder, A.J.B. and Yang, H., 2007. GEPIC – modelling wheat yield and crop water productivity with high resolution on a global scale. Agricultural Systems, 94(2): 478-493, doi: 10.1016/j.agsy.2006.11.019.

**R**

Lobell, D.B. and Field, C.B., 2007. Global scale climate–crop yield relationships and the impacts of recent warming. Environmental Research Letters, 2(1): 014002, doi: 10.1088/1748-9326/2/1/014002.

Lobell, D.B. and Gourdji, S.M., 2012. The influence of climate change on global crop productivity. Plant Physiology, 160(4): 1686, doi: 10.1104/pp.112.208298.

Long, S.P., Ainsworth, E.A., Leakey, A.D.B., Nösberger, J. and Ort, D.R., 2006. Food for Thought: Lower-Than-Expected Crop Yield Stimulation with Rising CO&lt;sub&gt;2&lt;/sub&gt; Concentrations. Science, 312(5782): 1918, doi: 10.1126/science.1114722.

Long, S.P., Marshall-Colon, A. and Zhu, X.G., 2015. Meeting the global food demand of the future by engineering crop photosynthesis and yield potential. Cell, 161(1): 56-66, doi: 10.1016/j.cell.2015.03.019.

Lorenz, E.N., 1963. Deterministic Nonperiodic Flow. Journal of the Atmospheric Sciences, 20(2): 130-141, doi: 10.1175/1520-0469(1963)020<0130:dnf>2.0.co;2.

Luck, J., Spackman, M., Freeman, A., Tre̦bicki, P., Griffiths, W., Finlay, K. and Chakraborty, S., 2011. Climate change and diseases of food crops. Plant Pathology, 60(1): 113-121, doi: 10.1111/j.1365-3059.2010.02414.x.

Lunde, T.M., Bayoh, M.N. and Lindtjørn, B., 2013. How malaria models relate temperature to malaria transmission. Parasit Vectors, 6, doi: 10.1186/1756-3305-6-20.

Lutaladio, N. and Castaldi, L., 2009. Potato: The hidden treasure. Journal of Food Composition and Analysis, 22(6): 491-493, doi: 10.1016/j.jfca.2009.05.002.

Ma, G., Huang, J., Wu, W., Fan, J., Zou, J. and Wu, S., 2013. Assimilation of MODIS-LAI into the WOFOST model for forecasting regional winter wheat yield. Mathematical and Computer Modelling, 58(3): 634-643, doi: 10.1016/j.mcm.2011.10.038.

MacKerron, D. and Davies, H., 1986. Markers for maturity and senescence in the potato crop. Potato Research, 29(4): 427-436.

MacKerron, D.K.L., 2007. Chapter 35 - Mathematical models of plant growth and development. In: D. Vreugdenhil et al. (Editors), Potato Biology and Biotechnology. Elsevier Science B.V., Amsterdam, pp. 753-776, doi: 10.1016/B978-044451018-1/50077-4.

Maracchi, G., Sirotenko, O. and Bindi, M., 2005. Impacts of present and future climate variability on agriculture and forestry in the temperate regions: Europe. Climatic Change, 70(1): 117-135, doi: 10.1007/s10584-005-5939-7.

Marchant, R., Mumbi, C., Behera, S. and Yamagata, T., 2007. The Indian Ocean dipole–the unsung driver of climatic variability in East Africa. African Journal of Ecology, 45(1): 4-16, doi: 10.1111/j.1365-2028.2006.00707.x.

Marletto, V., Ventura, F., Fontana, G. and Tomei, F., 2007. Wheat growth simulation and yield prediction with seasonal forecasts and a numerical model. Agricultural and Forest Meteorology, 147(1): 71-79, doi: 10.1016/j.agrformet.2007.07.003.

Mass, C.F., Ovens, D., Westrick, K. and Colle, B.A., 2002. Does increasing horizontal resolution produce more skillful forecasts? The results of two years of real-time numerical weather prediction over the Pacific Northwest. Bulletin of the American Meteorological Society, 83(3): 407-430, doi: 10.1175/1520-0477(2002)083<0407:Dihrpm>2.3.Co;2.

May, J., 2018. Keystones affecting sub-Saharan Africa's prospects for achieving food security through balanced diets. Food Research International, 104: 4-13, doi: 10.1016/j.foodres.2017.06.062.

Mazengia, W., Schulte, R., Tadese, Y., Griffin, D., Schulz, S. and Struik, P.C., 2015. The Farming Systems of Potential Potato Production Areas of Chencha, Southern Ethiopia. Chapter 37. In: J. Low, M.

Nyongesa, S. Quinn & M Parker (eds), Potato and Sweetpotato in Africa: Transforming the Value Chains for Food and Nutrition Security. CABI, Cambridge, UK: 382-396.

Mazurczyk, W., Lutomirska, B. and Wierzbicka, A., 2003. Relation between air temperature and length of vegetation period of potato crops. Agricultural and Forest Meteorology, 118(3): 169-172, doi: 10.1016/S0168-1923(03)00113-8.

McCown, R.L., Hammer, G.L., Hargreaves, J.N.G., Holzworth, D.P. and Freebairn, D.M., 1996. APSIM: a novel software system for model development, model testing and simulation in agricultural systems research. Agricultural Systems, 50(3): 255-271, doi: 10.1016/0308-521X(94)00055-V.

Meinshausen, M., Smith, S.J., Calvin, K., Daniel, J.S., Kainuma, M.L.T., Lamarque, J.-F., Matsumoto, K., Montzka, S.A., Raper, S.C.B., Riahi, K., Thomson, A., Velders, G.J.M. and van Vuuren, D.P.P., 2011. The RCP greenhouse gas concentrations and their extensions from 1765 to 2300. Climatic Change, 109(1): 213-241, doi: 10.1007/s10584-011-0156-z.

Menne, M.J., Durre, I., Vose, R.S., Gleason, B.E. and Houston, T.G., 2012. An Overview of the Global Historical Climatology Network-Daily Database. Journal of Atmospheric and Oceanic Technology, 29(7): 897-910, doi: 10.1175/jtech-d-11-00103.1.

Menza, M., Girmay, G. and Woldeyes, F., 2014. Enhancing Household Food Security through Irish Potato Production in Gamo Highlands of Southern Ethiopia. Scholarly Journal of Agricultural Science, 4(7): 410-419.

Met-Office, 2015. Food insecurity and climate change technical report (Met office, Hadley Centre), UK.

Meyers, M.P. and Steenburgh, W.J., 2013. Mountain weather prediction: phenomenological challenges and forecast methodology, Mountain Weather Research and Forecasting. Springer, pp. 1-34, doi: 10.1007/978-94-007-4098-3_1.

Millard, P. and Marshall, B., 1986. Growth, nitrogen uptake and partitioning within the potato (Solanum tuberosum L.) crop, in relation to nitrogen application. The Journal of Agricultural Science, 107(2): 421-429, doi: 10.1017/S0021859600087220.

Minda, T.T., van der Molen, M.K., Heusinkveld, B.G., Struik, P.C. and Vilà-Guerau de Arellano, J., 2018a. Observational Characterization of the Synoptic and Mesoscale Circulations in Relation to Crop Dynamics: Belg 2017 in the Gamo Highlands, Ethiopia. Atmosphere, 9(10): 398, doi: 10.3390/atmos9100398.

Minda, T.T., van der Molen, M.K., Struik, P.C., Combe, M., Jiménez, P.A., Khan, M.S. and Vilà-Guerau de Arellano, J., 2018b. The combined effect of elevation and meteorology on potato crop dynamics: a 10-year study in the Gamo Highlands, Ethiopia. Agricultural and Forest Meteorology, 262: 166-177, doi: 10.1016/j.agrformet.2018.07.009.

MOANR, 2016. Crop variety register Issue No. 18. Ministry of Agriculture and Natural Resources (MOANR), Ethiopia, Addis Ababa, Ethiopia.

Motha, R.P., 2007. Implications of climate change on long-lead forecasting and global agriculture. Australian Journal of Agricultural Research, 58(10): 939-944, doi: 10.1071/AR06104.

Mukabana, J.R. and Pielke, R.A., 1992. Numerical simulation of the influence of the large-scale monsoon flow on the diurnal weather patterns over Kenya. Atmospheric science paper; no. 542.

Muthoni, J., Shimelis, H. and Melis, R., 2013. Alleviating potato seed tuber shortage in developing countries: Potential of true potato seeds. Australian Journal of Crop Science, 7(12): 1946.

Myhre, Shindell, G.D., Bréon, F.M., Collins, W., Fuglestvedt, J., Huang, J., Koch, D., Lamarque, J.F., Lee, D., Mendoza, B., Nakajima, T., Robock, A., Stephens, G., Takemura, T. and Zhang, H., 2013.

**R**

Anthropogenic and Natural Radiative Forcing. In: Climate Change 2013: The Physical Science Basis. Contribution of Working Group I to the Fifth Assessment Report of the Intergovernmental Panel on Climate Change [Stocker, T.F., D. Qin, G.-K. Plattner, M. Tignor, S.K. Allen, J. Boschung, A. Nauels, Y. Xia, V. Bex and P.M. Midgley (eds.)]. Cambridge University Press, Cambridge, UK and New York, NY, USA.

Newbery, F., Qi, A. and Fitt, B.D.L., 2016. Modelling impacts of climate change on arable crop diseases: progress, challenges and applications. Current Opinion in Plant Biology, 32: 101-109, doi: 10.1016/j.pbi.2016.07.002.

Ngetich, K., Mucheru-Muna, M., Mugwe, J., Shisanya, C., Diels, J. and Mugendi, D., 2014. Length of growing season, rainfall temporal distribution, onset and cessation dates in the Kenyan highlands. Agricultural and Forest Meteorology, 188: 24-32, doi: 10.1016/j.agrformet.2013.12.011.

Niang, I., Ruppel, O.C., Abdrabo, M.A., Essel, A., Lennard, C., Padgham, J. and Urquhart, P., 2014. Africa. In: Climate Change 2014: Impacts, Adaptation, and Vulnerability. Part B: Regional Aspects. Contribution of Working Group II to the Fifth Assessment Report of the Intergovernmental Panel on Climate Change [Barros, V.R., C.B. Field, D.J. Dokken, M.D. Mastrandrea, K.J. Mach, T.E. Bilir, M. Chatterjee, K.L. Ebi, Y.O. Estrada, R.C. Genova, B. Girma, E.S. Kissel, A.N. Levy, S. acCracken, P.R. Mastrandrea, and L.L. White (eds.)]. Cambridge University Press, Cambridge, UK and New York NY, USA.

Nicholson, S.E., 1996. A review of climate dynamics and climate variability in Eastern Africa. The limnology, climatology and paleoclimatology of the East African lakes: 25-56.

Nicholson, S.E., 2009. A revised picture of the structure of the "monsoon" and land ITCZ over West Africa. Climate Dynamics, 32(7): 1155-1171, doi: 10.1007/s00382-008-0514-3.

Nicholson, S.E., 2011. Dryland climatology. Cambridge University Press.

Nicholson, S.E., 2018. The ITCZ and the Seasonal Cycle over Equatorial Africa. Bulletin of the American Meteorological Society, 99(2): 337-348.

NMA, 2018. Regional Meteorological Station Information. National Meteoroloical Agency, Ethiopia.

NOAA, 2017. NOAA - Climate prediction Center: Africa InterTropical Front (ITF). NOAA.

Oerke, E.C. and Dehne, H.W., 2004. Safeguarding production—losses in major crops and the role of crop protection. Crop Protection, 23(4): 275-285, doi: 10.1016/j.cropro.2003.10.001.

Oliveira, J., 2015. Growth and development of potato (Solanum tuberosum L.) crops after different cool season storage, PhD thesis, Lincoln University Digital Thesis, New Zealand.

Onder, S., Caliskan, M.E., Onder, D. and Caliskan, S., 2005. Different irrigation methods and water stress effects on potato yield and yield components. Agricultural Water Management, 73(1): 73-86, doi: 10.1016/j.agwat.2004.09.023.

Oren, R., Ellsworth, D.S., Johnsen, K.H., Phillips, N., Ewers, B.E., Maier, C., Schäfer, K.V., McCarthy, H., Hendrey, G. and McNulty, S.G., 2001. Soil fertility limits carbon sequestration by forest ecosystems in a CO2-enriched atmosphere. Nature, 411(6836): 469-472, doi: 10.1038/35078064.

Ospina, C.A., Lammerts van Bueren, E.T., Allefs, J.J.H.M., Engel, B., van der Putten, P.E.L., van der Linden, C.G. and Struik, P.C., 2014. Diversity of crop development traits and nitrogen use efficiency among potato cultivars grown under contrasting nitrogen regimes. Euphytica, 199(1): 13-29, doi: 10.1007/s10681-014-1203-4.

Otieno, G., Mutemi, J., Opijah, F., Ogallo, L. and Omondi, H., 2018. The impact of cumulus parameterization on rainfall simulations over East Africa. Atmospheric and Climate Sciences, 8(03): 355, doi: 10.4236/acs.2018.83024.

Pandey, A., Ostrowski, M. and Pandey, R.P., 2012. Simulation and optimization for irrigation and crop planning. Irrigation and Drainage, 61(2): 178-188, doi: 10.1002/ird.633.

Parry, M., Parry, M.L., Canziani, O., Palutikof, J., van der Linden, P. and Hanson, C., 2007. Climate change 2007-impacts, adaptation and vulnerability: Working group II contribution to the fourth assessment report of the IPCC, 4. Cambridge University Press.

Pasteris, P.A., Puterbaugh, T. and Motha, R., 2004. Climate services - A USDA perspective. 14th Conf. on Applied Climatology, Seattle, WA, Amer. Meteor. Soc., 6.8.

Peiris, D., Crawford, J., Grashoff, C., Jefferies, R., Porter, J. and Marshall, B., 1996. A simulation study of crop growth and development under climate change. Agricultural and Forest Meteorology, 79(4): 271-287.

Pereira, A. and Nova, N.V., 2008. Potato Maximum Yield as Affected by Crop Parameters and Climatic Factors in Brazil. 43(5): 1611, doi: 10.21273/hortsci.43.5.1611.

Pereira, A.B., Nova, V., Augusto, N., Ramos, V.J. and Pereira, A.R., 2008. Potato potential yield based on climatic elements and cultivar characteristics. Bragantia, 67(2): 327-334, doi: 10.1590/S0006-87052008000200008.

Pérombelon, M., 2002. Potato diseases caused by soft rot erwinias: an overview of pathogenesis. Plant Pathology, 51(1): 1-12.

Philip, S., Kew, S.F., Oldenborgh, G.J.v., Otto, F., O'Keefe, S., Haustein, K., King, A., Zegeye, A., Eshetu, Z., Hailemariam, K., Singh, R., Jjemba, E., Funk, C. and Cullen, H., 2018. Attribution Analysis of the Ethiopian Drought of 2015. Journal of Climate, 31(6): 2465-2486, doi: 10.1175/jcli-d-17-0274.1.

Pierre, C., Wilson, G., Olivier, P., Vincent, D., M., F.B. and Nathalie, P., 2018. Major role of water bodies on diurnal precipitation regimes in Eastern Africa. International Journal of Climatology, 38(2): 613-629, doi: 10.1002/joc.5197.

Pleijel, H., Danielsson, H., Vandermeiren, K., Blum, C., Colls, J. and Ojanperä, K., 2002. Stomatal conductance and ozone exposure in relation to potato tuber yield—results from the European CHIP programme. European Journal of Agronomy, 17(4): 303-317, doi: 10.1016/S1161-0301(02)00068-0.

Pohl, B., Crétat, J. and Camberlin, P., 2011. Testing WRF capability in simulating the atmospheric water cycle over Equatorial East Africa. Climate Dynamics, 37(7): 1357-1379, doi: 10.1007/s00382-011-1024-2.

Portmann, F.T., Siebert, S. and Döll, P., 2010. MIRCA2000—Global monthly irrigated and rainfed crop areas around the year 2000: A new high-resolution data set for agricultural and hydrological modeling. Global Biogeochemical Cycles, 24(1), doi: 10.1029/2008GB003435.

Qian, C., Wu, Z., Fu, C. and Wang, D., 2011. On Changing El Niño: A View from Time-Varying Annual Cycle, Interannual Variability, and Mean State. Journal of Climate, 24(24): 6486-6500, doi: 10.1175/jcli-d-10-05012.1.

Quiroz, R., Harahagazwe, D., Condori, B., Barreda, C., de Mendiburu, F., Amele, A., Anthony, E.A., Bararyenya, A., Byarugaba, A. and Demo, P., 2014. Potato yield gap analysis in SSA through participatory modeling: Optimizing the value of historical breeding trial data.

**R**

Raes, D., Steduto, P., Hsiao, T.C. and Fereres, E., 2009. AquaCrop—The FAO crop model to simulate yield response to water: II. Main algorithms and software description. Agronomy Journal, 101(3): 438-447, doi: 10.2134/agronj2008.0140s.

Raja, R., Nayak, A.K., Panda, B.B., Lal, B., Tripathi, R., Shahid, M., Kumar, A., Mohanty, S., Samal, P., Gautam, P. and Rao, K.S., 2014. Monitoring of meteorological drought and its impact on rice (Oryza sativa L.) productivity in Odisha using standardized precipitation index. Archives of Agronomy and Soil Science: 1-15, doi: 10.1080/03650340.2014.912033.

Ramapriyan, H.K. and Murphy, K., 2017. Collaborations and Partnerships in NASA's Earth Science Data Systems. Data Science Journal, 16.

Raposo, R., Wilks, D. and Fry, W., 1993. Evaluation of potato late blight forecasts modified to include weather forecasts: a simulation analysis. Phytopathology, 83(1): 103-108.

Ray, D.K., Mueller, N.D., West, P.C. and Foley, J.A., 2013. Yield trends are insufficient to double global crop production by 2050. PloS one, 8(6): e66428.

Raymundo, R., Asseng, S., Cammarano, D. and Quiroz, R., 2014. Potato, sweet potato, and yam models for climate change: A review. Field Crops Research, 166: 173-185, doi: 10.1016/j.fcr.2014.06.017.

Resop, J.P., Fleisher, D.H., Timlin, D.J. and Reddy, V., 2014. Biophysical constraints to potential production capacity of potato across the US eastern seaboard region. Agronomy Journal, 106(1): 43-56, doi: 10.2134/agronj2013.0277.

Rhein, M., S.R.R., S. Aoki, E.C., D. Chambers, R.A. Feely, S. Gulev, G.C. Johnson, S.A. Josey, A. Kostianoy, C. Mauritzen, D. Roemmich, Talley, L.D. and Wang, F., 2013. Observations: Ocean. In: Climate Change 2013: The Physical Science Basis. Contribution of Working Group I to the Fifth Assessment Report of the Intergovernmental Panel on Climate Change [Stocker, T.F., D. Qin, G.-K. Plattner, M. Tignor, S.K. Allen, J. Boschung, A. Nauels, Y. Xia, V. Bex and P.M. Midgley (eds.)] (Cambridge University Press, New York).

Riddle, E.E. and Cook, K.H., 2008. Abrupt rainfall transitions over the Greater Horn of Africa: Observations and regional model simulations. Journal of Geophysical Research: Atmospheres, 113(D15), doi: 10.1029/2007JD009202.

Rieck, M., Nuijens, L. and Stevens, B., 2012. Marine boundary layer cloud feedbacks in a constant relative humidity atmosphere. Journal of the Atmospheric Sciences, 69(8): 2538-2550, doi: 10.1175/jas-d-11-0203.1.

Rientjes, T., Haile, A.T. and Fenta, A.A., 2013. Diurnal rainfall variability over the Upper Blue Nile Basin: A remote sensing based approach. International Journal of Applied Earth Observation and Geoinformation, 21: 311-325, doi: 10.1016/j.jag.2012.07.009.

Rogelj, J., den Elzen, M., Höhne, N., Fransen, T., Fekete, H., Winkler, H., Schaeffer, R., Sha, F., Riahi, K. and Meinshausen, M., 2016. Paris agreement climate proposals need a boost to keep warming well below 2 °C. Nature, 534: 631, doi: 10.1038/nature18307.

Rosenzweig, C., Elliott, J., Deryng, D., Ruane, A.C., Müller, C., Arneth, A., Boote, K.J., Folberth, C., Glotter, M., Khabarov, N., Neumann, K., Piontek, F., Pugh, T.A.M., Schmid, E., Stehfest, E., Yang, H. and Jones, J.W., 2014. Assessing agricultural risks of climate change in the 21st century in a global gridded crop model intercomparison. Proceedings of the National Academy of Sciences, 111(9): 3268-3273, doi: 10.1073/pnas.1222463110.

Rosenzweig, C. and Parry, M.L., 1994. Potential impact of climate change on world food supply. Nature, 367(6459): 133-138, doi: 10.1038/367133a0.

Rowell, D.P., Booth, B.B.B., Nicholson, S.E. and Good, P., 2015. Reconciling past and future rainfall trends over East Africa. Journal of Climate, 28(24): 9768-9788, doi: 10.1175/jcli-d-15-0140.1.

Salathé, E.P., Steed, R., Mass, C.F. and Zahn, P.H., 2008. A High-Resolution Climate Model for the U.S. Pacific Northwest: Mesoscale Feedbacks and Local Responses to Climate Change. Journal of Climate, 21(21): 5708-5726, doi: 10.1175/2008jcli2090.1.

Samberg, L.H., Shennan, C. and Zavaleta, E.S., 2010. Human and environmental factors affect patterns of crop diversity in an Ethiopian highland agroecosystem. The Professional Geographer, 62(3): 395-408.

Sánchez-Lugo, A., Morice, C., Berrisford, P. and Argüez, A., 2018. Temperature: Global surface temperatures [in "State of the Climate in 2017"]. Bulletin of the American Meteorological Society, 99(8): S11-S13, doi: 10.1175/2018BAMSStateoftheClimate.1.

Schlenker, W. and Roberts, M.J., 2009. Nonlinear temperature effects indicate severe damages to U.S. crop yields under climate change. Proceedings of the National Academy of Sciences, 106(37): 15594-15598, doi: 10.1073/pnas.0906865106.

Schleussner, C.-F., Deryng, D., Müller, C., Elliott, J., Saeed, F., Folberth, C., Liu, W., Wang, X., Pugh, T.A.M., Thiery, W., Seneviratne, S.I. and Rogelj, J., 2018. Crop productivity changes in 1.5 °C and 2 °C worlds under climate sensitivity uncertainty. Environmental Research Letters, 13(6): 064007, doi: 10.1088/1748-9326/aab63b.

Schulte-Geldermann, E., 2013. Tackling Low Potato Yields in Eastern Africa: an overview of constraints and potential strategies. In: G. Woldegiorgis, S. Schulz and B. Berihun (Editors), Tuber production and dissemination expreiences, challenges and prospects. Proceedings of the National Workshop on Seed Potato Tuber Production and Dissemination, 12-14 March 2012, Bahir Dar, Ethiopia. Ethiopian Institute of Agricutural Research (EIAR) and Amahara Regional Research Institute (ARARI) Bahir Dar pp. 72-80.

Scott, G.J., Rosegrant, M.W. and Ringler, C., 2000. Global projections for root and tuber crops to the year 2020. Food Policy, 25(5): 561-597, doi: 10.1016/S0306-9192(99)00087-1.

Segele, Z.T. and Lamb, P.J., 2005. Characterization and variability of Kiremt rainy season over Ethiopia. Meteorology and Atmospheric Physics, 89(1-4): 153-180.

Segele, Z.T., Leslie, L.M. and Tarhule, A.A., 2015. Sensitivity of Horn of Africa rainfall to regional sea surface temperature forcing. Climate, 3(2): 365, doi: 10.3390/cli3020365.

Seligman, N., 1987. Simulation of water use, nitrogen nutrition and growth of a spring wheat crop. Simulation Monographs, Pudoc, Wageningen, The Netherlands.

Serafin, S., Adler, B., Cuxart, J., De Wekker, S.F., Gohm, A., Grisogono, B., Kalthoff, N., Kirshbaum, D.J., Rotach, M.W. and Schmidli, J., 2018. Exchange Processes in the Atmospheric Boundary Layer Over Mountainous Terrain. Atmosphere, 9(3): 102, doi: 10.3390/atmos9030102.

Sheffield, J., Goteti, G. and Wood, E.F., 2006. Development of a 50-Year High-Resolution Global Dataset of Meteorological Forcings for Land Surface Modeling. Journal of Climate, 19(13): 3088-3111, doi: 10.1175/jcli3790.1.

Shibu, M.E., Leffelaar, P.A., van Keulen, H. and Aggarwal, P.K., 2010. LINTUL3, a simulation model for nitrogen-limited situations: Application to rice. European Journal of Agronomy, 32(4): 255-271, doi: 10.1016/j.eja.2010.01.003.

Shongwe, M.E., Oldenborgh, G.J.v., Hurk, B.v.d. and Aalst, M.v., 2011. Projected Changes in Mean and Extreme Precipitation in Africa under Global Warming. Part II: East Africa. Journal of Climate, 24(14): 3718-3733, doi: 10.1175/2010jcli2883.1.

**R**

Sibma, L., 1970. Relation between total radiation and yield of some field crops in the Netherlands. Netherlands Journal of Agricultural Science, 18(2): 125-31.

Sinclair, T.R. and Muchow, R.C., 1999. Radiation Use Efficiency. In: D.L. Sparks (Editor), Advances in Agronomy. Academic Press, pp. 215-265, doi: 10.1016/S0065-2113(08)60914-1.

Skamarock, W.C., Klemp, J.B., Dudhia, J., Gill, D.O., Barker, D.M., Wang, W. and Powers, J.G., 2005. A description of the advanced research WRF version 2, National Center For Atmospheric Research Boulder Co Mesoscale and Microscale Meteorology Div.

Spitters, C., Van Keulen, H. and Van Kraalingen, D., 1989. A simple and universal crop growth simulator: SUCROS87, Simulation and systems management in crop protection. Pudoc, Wageningen, The Netherlands, pp. 147-181.

Spitters, C.J.T., 1987. An analysis of variation in yield among potato cultivars in terms of light absorption, light utilization and dry matter partitioning. Acta Horticulturae: 71-84.

Spitters, C.J.T., 1990. Crop growth models: Their usefulness and limitations. International Society for Horticultural Science (ISHS), Leuven, Belgium, pp. 349-368, doi: 10.17660/ActaHortic.1990.267.42.

Steduto, P., Hsiao, T.C., Raes, D. and Fereres, E., 2009. AquaCrop—The FAO crop model to simulate yield response to water: I. Concepts and underlying principles. Agronomy Journal, 101(3): 426-437, doi: 10.2134/agronj2008.0139s.

Steeneveld, G.J., Koopmans, S., Heusinkveld, B.G. and Theeuwes, N.E., 2014. Refreshing the role of open water surfaces on mitigating the maximum urban heat island effect. Landscape and Urban Planning, 121: 92-96, doi: 10.1016/j.landurbplan.2013.09.001.

Steeneveld, G.J., Mauritsen, T., Bruijn, E.I.F.d., Arellano, J.V.-G.d., Svensson, G. and Holtslag, A.A.M., 2008. Evaluation of limited-area models for the representation of the diurnal cycle and contrasting nights in CASES-99. Journal of Applied Meteorology and Climatology, 47(3): 869-887, doi: 10.1175/2007jamc1702.1.

Steffen, W., Grinevald, J., Crutzen, P. and McNeill, J., 2011. The Anthropocene: conceptual and historical perspectives. Philosophical Transactions of the Royal Society A: Mathematical, Physical and Engineering Sciences, 369(1938): 842, doi: 10.1098/rsta.2010.0327.

Stensrud, D., 2007. Parameterization Schemes: Keys to Understanding Numerical Weather Prediction Models, doi: 10.1017/cbo9780511812590.

Stocker, T.F., Qin, D., Plattner, G.-K., Tignor, M., Allen, S.K., Boschung, J., Nauels, A., Xia, Y., Bex, V. and Midgley, P.M., 2013. Climate change 2013: The physical science basis. Intergovernmental Panel on Climate Change, Working Group I Contribution to the IPCC Fifth Assessment Report (AR5) (Cambridge University Press, New York).

Streck, N.A., de Paula, F.L.M., Bisognin, D.A., Heldwein, A.B. and Dellai, J., 2007. Simulating the development of field grown potato (Solanum tuberosum L.). Agricultural and Forest Meteorology, 142(1): 1-11, doi: 10.1016/j.agrformet.2006.09.012.

Struik, P.C., 2007. Chapter 18 - Responses of the Potato Plant to Temperature. In: D. Vreugdenhil et al. (Editors), Potato Biology and Biotechnology. Elsevier Science B.V., Amsterdam, pp. 367-393, doi: 10.1016/B978-044451018-1/50060-9.

Struik, P.C., Abdurahman, A., Dersseh, W., Gebresilase, Y., Griffin, D., Weakliam, J., Woldegiorgis, G., Schulz, S., Almekinders, C. and Schulte, R., 2014. Improving seed-to-ware, ware and knowledge chains in potato cultivation in eastern Africa.

Struik, P.C. and Wiersema, S.G., 1999. Seed potato technology. Wageningen Academic Pub.

Stull, R., 2000. Meteorology for scientists and engineers. Brooks/Cole.

Sukhatme, P.V., 1947. The Problem of Plot Size in Large-Scale Yield Surveys. Journal of the American Statistical Association, 42(238): 297-310, doi: 10.1080/01621459.1947.10501928.

Svubure, O., Struik, P.C., Haverkort, A.J. and Steyn, J.M., 2015. Yield gap analysis and resource footprints of Irish potato production systems in Zimbabwe. Field Crops Research, 178: 77-90, doi: 10.1016/j.fcr.2015.04.002.

Tadele, Z., 2017. Raising crop productivity in Africa through intensification. Agronomy, 7(1): 22, doi: 10.3390/agronomy7010022.

Tadesse, T., 2013. Experiences, Challenges, and Opportunities in Participatory Quality Potato Seed Production: the Case of Southern Region [in Seed Potato Tuber Production and Dissemination]. In: W. Gebremedhin, S. Steffen and B. Baye (Editors). Ethiopian Institute of Agricultural Research and Amhara Agricultural ResearchInstitute, Bahir Dar, Ethiopia.

Tadesse, Y., Almekinders, C.J., Schulte, R.P.O. and Struik, P.C., 2017. Understanding farmers' potato production practices and use of improved varieties in Chencha, Ethiopia. Journal of Crop Improvement, 31(5): 673-688, doi: 10.1080/15427528.2017.1345817.

Tadesse, Y., Almekinders, C.J.M., Schulte, R.P.O. and Struik, P.C., 2016. Tracing the seed: Seed diffusion of improved potato varieties through farmers' networks in Chencha, Ethiopia Exp. Agric., 53(4): 481-496, doi: 10.1017/s001447971600051x.

Tadesse, Y., Almekinders, C.J.M., Schulte, R.P.O. and Struik, P.C., 2018. Potatoes and livelihoods in Chencha, southern Ethiopia. NJAS - Wageningen Journal of Life Sciences, doi: 10.1016/j.njas.2018.05.005.

Tafesse, S., Damtew, E., van Mierlo, B., Lie, R., Lemaga, B., Sharma, K., Leeuwis, C. and Struik, P.C., 2018. Farmers' knowledge and practices of potato disease management in Ethiopia. NJAS - Wageningen Journal of Life Sciences, 86-87: 25-38, doi: 10.1016/j.njas.2018.03.004.

Takle, E.S., Anderson, C.J., Andresen, J., Angel, J., Elmore, R.W., Gramig, B.M., Guinan, P., Hilberg, S., Kluck, D., Massey, R., Niyogi, D., Schneider, J.M., Shulski, M.D., Todey, D. and Widhalm, M., 2014. Climate Forecasts for Corn Producer Decision Making. Earth Interactions, 18(5): 1-8, doi: 10.1175/2013ei000541.1.

Tans, P. and Keeling, R., 2014. Trends in atmospheric carbon dioxide. National Oceanic & Atmospheric Administration, Earth System Research Laboratory of Global Monitoring Division. Retrieved.

Tariku, T.B. and Gan, T.Y., 2018. Sensitivity of the weather research and forecasting model to parameterization schemes for regional climate of Nile River Basin. Climate dynamics, 50(11-12): 4231-4247, doi: 10.1007/s00382-017-3870-z.

Taye, M., Lommen, W.J.M. and Struik, P.C., 2012. Effects of shoot tipping on development and yield of the tuber crop Plectranthus edulis. The Journal of Agricultural Science, 150(4): 484-494, doi: 10.1017/S002185961100075X.

Thiele, G., Theisen, K., Bonierbale, M. and Walker, T., 2010. Targeting the poor and hungry with potato science. Potato J, 37(3-4): 75-86.

Tilman, D., Fargione, J., Wolff, B., D'Antonio, C., Dobson, A., Howarth, R., Schindler, D., Schlesinger, W.H., Simberloff, D. and Swackhamer, D., 2001. Forecasting agriculturally driven global environmental change. Science, 292(5515): 281-284, doi: 10.1126/science.1057544.

**R**

## References

Timlin, D., Lutfor Rahman, S.M., Baker, J., Reddy, V.R., Fleisher, D. and Quebedeaux, B., 2006. Whole Plant Photosynthesis, Development, and Carbon Partitioning in Potato as a Function of Temperature. Agronomy Journal, 98(5): 1195-1203, doi: 10.2134/agronj2005.0260.

Torma, C., Giorgi, F. and Coppola, E., 2015. Added value of regional climate modeling over areas characterized by complex terrain—Precipitation over the Alps. Journal of Geophysical Research: Atmospheres, 120(9): 3957-3972, doi: 10.1002/2014JD022781.

Tsegaw, T., 2005. Response of potato to paclobutrazol and manipulation of reproductive growth under tropical conditions, PhD thesis, University of Pretoria, Pretoria, South Africa.

Tsidu, G.M., 2012. High-resolution monthly rainfall database for Ethiopia: homogenization, reconstruction, and gridding. Journal of Climate, 25(24): 8422-8443, doi: 10.1175/JCLI-D-12-00027.1.

Tsidu, G.M., 2016. Southern Africa [in "State of the Climate in 2015"]. Bull. Am. Meteorol. Soc., 97(8): S189-S192, doi: 10.1175/2016BAMSStateoftheClimate.1.

Tsidu, G.M., 2018. Eastern Africa [in "State of the Climate in 2017"]. Bull. Am. Meteorol. Soc., 99(8): S216-S217, doi: 10.1175/2018BAMSStateoftheClimate.1.

Tubiello, F., Rosenzweig, C., Goldberg, R., Jagtap, S. and Jones, J., 2002. Effects of climate change on US crop production: simulation results using two different GCM scenarios. Part I: Wheat, potato, maize, and citrus. Climate Research, 20(3): 259-270.

Tufa, A.H., 2013. Economic and agronomic analysis of the seed potato supply chain in Ethiopia, PhD thesis, Wageningen University and Research, Wageningen, The Netherlands.

UNDP, 2018. Goal 2: Zero hunger. UNDP - United Nations Development Programme.

Van Dam, J., Kooman, P. and Struik, P.C., 1996. Effects of temperature and photoperiod on early growth and final number of tubers in potato (Solanum tuberosum L.). Potato Research, 39(1): 51-62.

Van de Geijn, S.C. and Dijkstra, P., 1995. Physiological effects of changes in atmospheric carbon dioxide concentration and temperature on growth and water relations of crop plants. In: A.J. Haverkort and D.K.L. MacKerron (Editors), Potato ecology and modelling of crops under conditions limiting growth: Proceedings of the Second International Potato Modeling Conference, held in Wageningen 17–19 May, 1994. Springer Netherlands, Dordrecht, pp. 89-99, doi: 10.1007/978-94-011-0051-9_6.

Van Diepen, C.A., Wolf, J., van Keulen, H. and Rappoldt, C., 1989. WOFOST: a simulation model of crop production. Soil Use and Management, 5(1): 16-24, doi: 10.1111/j.1475-2743.1989.tb00755.x.

Van Evert, F.K., de Ruijter, F.J., Conijn, J.G., Rutgers, B. and Haverkort, A.J., 2013. Worldwide sustainability hotspots in potato cultivation. 2. Areas with improvement opportunities. Potato Research, 56(4): 355-368, doi: 10.1007/s11540-013-9248-7.

Van Ittersum, M. and Donatelli, M., 2003. Modelling cropping systems-highlights of the symposium and preface to the special issues. European Journal of Agronomy, 3(18): 187-197.

Van Ittersum, M.K., Leffelaar, P.A., van Keulen, H., Kropff, M.J., Bastiaans, L. and Goudriaan, J., 2003. On approaches and applications of the Wageningen crop models. European Journal of Agronomy, 18(3-4): 201-234, doi: 10.1016/S1161-0301(02)00106-5.

Van Keulen, H. and Stol, W., 1995. Agro-ecological zonation for potato production. In: A.J. Haverkort and D.K.L. MacKerron (Editors), Potato Ecology And modelling of crops under conditions limiting growth: Proceedings of the Second International Potato Modeling Conference, held in Wageningen 17–19 May, 1994. Springer Netherlands, Dordrecht, pp. 357-371, doi: 10.1007/978-94-011-0051-9_23.

Van Laar, H., Goudriaan, J. and van Keulen, H., 1992. Simulation of crop growth for potential and water-limited production situations: as applied to spring wheat, CABO-DLO.

Van Loon, C.D., 1981. The effect of water stress on potato growth, development, and yield. American Potato Journal, 58(1): 51-69, doi: 10.1007/bf02855380.

Van Oldenborgh, G.J., Collins, M., Arblaster, J., Christensen, J.H., Marotzke, J., Power, S.B., Rummukainen, M., Zhou, T., Stocker, T.F. and Qin, D., 2013. Annex I: Atlas of global and regional climate projections.

Van Vooren, S., van Schaeybroeck, B., Nyssen, J., van Ginderachter, M. and Termonia, P., 2018. Evaluation of CORDEX rainfall in northwest Ethiopia: Sensitivity to the model representation of the orography. International Journal of Climatology, doi: 10.1002/joc.5971.

Verhoef, A. and Egea, G., 2014. Modeling plant transpiration under limited soil water: Comparison of different plant and soil hydraulic parameterizations and preliminary implications for their use in land surface models. Agricultural and Forest Meteorology, 191: 22-32, doi: 10.1016/j.agrformet.2014.02.009.

Viste, E., Korecha, D. and Sorteberg, A., 2013. Recent drought and precipitation tendencies in Ethiopia. Theoretical and Applied Climatology, 112(3-4): 535-551, doi: 10.1007/s00704-012-0746-3.

Viste, E.M., 2012. Moisture transport and precipitation in Ethiopia, PhD Thesis, University of Bergen, Norway.

Viviroli, D., Weingartner, R. and Messerli, B., 2003. Assessing the hydrological significance of the world's mountains. Mountain research and Development, 23(1): 32-41, doi: 10.1659/0276-4741(2003)023[0032:ATHSOT]2.0.CO;2.

Von Grebmer, K., Bernstein, J., de Waal, A., Prasai, N., Yin, S. and Yohannes, Y., 2015. 2015 Global hunger index: armed conflict and the challenge of hunger. Intl Food Policy Res Inst.

Vos, J. and Haverkort, A.J., 2007. Chapter 16 - Water Availability and Potato Crop Performance. In: D. Vreugdenhil et al. (Editors), Potato Biology and Biotechnology. Elsevier Science B.V., Amsterdam, pp. 333-351, doi: 10.1016/B978-044451018-1/50058-0.

Waddell, J., Gupta, S., Moncrief, J., Rosen, C. and Steele, D., 2000. Irrigation-and nitrogen-management impacts on nitrate leaching under potato. Journal of Environmental Quality, 29(1): 251-261.

Wang, C.-l., Shen, S.-h., Zhang, S.-y., Li, Q.-z. and Yao, Y.-b., 2015. Adaptation of potato production to climate change by optimizing sowing date in the Loess Plateau of central Gansu, China. Journal of Integrative Agriculture, 14(2): 398-409, doi: 10.1016/S2095-3119(14)60783-8.

Wen, X., Lu, S. and Jin, J., 2012. Integrating Remote Sensing Data with WRF for Improved Simulations of Oasis Effects on Local Weather Processes over an Arid Region in Northwestern China. Journal of Hydrometeorology, 13(2): 573-587, doi: 10.1175/jhm-d-10-05001.1.

Wheeler, T. and von Braun, J., 2013. Climate change impacts on global food security. Science, 341(6145): 508-513, doi: 10.1126/science.1239402.

Whiteman, C.D., 2000. Mountain meteorology: fundamentals and applications. Oxford University Press.

Willmott, C.J., 1982. Some comments on the evaluation of model performance. Bulletin of the American Meteorological Society, 63(11): 1309-1313, doi: 10.1175/1520-0477(1982)063<1309:SCOTEO>2.0.CO;2.

WMO, 2016. WMO statement on the state of the global climate in 2015.

WMO, 2018. WMO statement on the state of the global climate in 2017.

Wolde-Georgis, T., 1997. El Niño and drought early warning in Ethiopia (March 1, 1997). Intern. J. African Studies, 2: 1-10.

**R**

## References

Woldegiorgis, G., 2013. Potato variety development strategies and methodologies in Ethiopia. In: W. Gebremedhin, S. Steffen and B. Baye (Editors), In seed potato tuber production and dissemination: experiences, challenges and prospects. Ethiopian Institute of Agricultural Research and Amhara Regional Agricultural Research Institute, Bahir Dar, Ethiopia.

Yactayo, W., Ramírez, D.A., Gutiérrez, R., Mares, V., Posadas, A. and Quiroz, R., 2013. Effect of partial root-zone drying irrigation timing on potato tuber yield and water use efficiency. Agricultural Water Management, 123: 65-70, doi: 10.1016/j.agwat.2013.03.009.

Yarleque, C., Vuille, M., Hardy, D.R., Posadas, A. and Quiroz, R.C.J.D., 2016. Multiscale assessment of spatial precipitation variability over complex mountain terrain using a high-resolution spatiotemporal wavelet reconstruction method. Journal of Geophysical Research: Atmospheres, 121(20): 12,198-12,216, doi: 10.1002/2016jd025647.

Yin, X., Goudriaan, J., Lantinga, E.A., Vos, J. and Spiertz, H.J., 2003. A Flexible Sigmoid Function of Determinate Growth. Annals of Botany, 91(3): 361-371, doi: 10.1093/aob/mcg029.

Yin, X. and Struik, P.C., 2010. Modelling the crop: from system dynamics to systems biology. Journal of Experimental Botany, 61(8): 2171-2183, doi: 10.1093/jxb/erp375.

Yin, X. and van Laar, H., 2005. Crop systems dynamics: an ecophysiological simulation model for genotype-by-environment interactions. Wageningen Academic Publishers, Wageningen

Yuan, B.-Z., Nishiyama, S. and Kang, Y., 2003. Effects of different irrigation regimes on the growth and yield of drip-irrigated potato. Agricultural Water Management, 63(3): 153-167, doi: 10.1016/S0378-3774(03)00174-4.

Zardi, D. and Whiteman, C.D., 2013. Diurnal Mountain Wind Systems. In: F.K. Chow, S.F.J. De Wekker and B.J. Snyder (Editors), Mountain Weather Research and Forecasting: Recent Progress and Current Challenges. Springer Netherlands, Dordrecht, pp. 35-119, doi: 10.1007/978-94-007-4098-3_2.

Zhao, G., Siebert, S., Enders, A., Rezaei, E.E., Yan, C. and Ewert, F., 2015. Demand for multi-scale weather data for regional crop modeling. Agricultural and Forest Meteorology, 200: 156-171, doi: 10.1016/j.agrformet.2014.09.026.

# Acknowledgments

A PhD project is like social work in Ethiopia. In the project, several actors are involved to reach the success of a person. Here, I would like to forward my sincere appreciations and thanks to my promotors, co-authors, people who assisted me in the fieldwork, persons who commented on the papers, front and back page designers, people who shared and contributed to the data, individuals who contributed resources, my MAQ colleagues, encouraging and motivating people, caring and supporting friends, supporting people in prayers, friends from the Netherlands, my family and the funding organization for this PhD project.

Among the lead actors in my study, (co)-promotors come at the front-line! I stayed only a quarter of my study period in Wageningen. It has to be understood that supervision of my sandwich PhD is much more challenging than other PhD categories. It's reasonable to start my sincere acknowledgment with my first promotor – Jordi. You played the largest role in maintaining the high quality and timely accomplishment of this thesis! Your depth of scientific understanding, timely planning and your skill in making things happen deserve to be mentioned. You showed me the perfect scientific path, in which I can follow your footsteps. You taught me to see things from a broad perspective, which you called a 'helicopter-view'; how atmospheric crop drivers interact within themselves and influence crop growth; developing sound research questions; you are a skilful and knowledgeable person in designing and engineering a paper and a thesis; how to write a high-standard article; you show how to extract facts in terms of refined numbers, plots and tables; responding to referees' queries, etcetera. Importantly, our relationship in all the years was so positive. This was also a key to my success! You understand me and respond to my questions promptly. In our relationships since 2013, I've learned a number of principles from you: (1) initialising a small project to create a larger one; (2) efficiently working in interdisciplinary projects: working on the interface between meteorology and other disciplines (crop science, chemistry, forestry, water management, etc.); (3) talented in changing science into projects, especially PhD projects; (4) building knowledge – most of your PhD's are your MSc's; (5) high organizational and managerial skill; (6) an open and pure in heart personality. Overall, thank you dear Jordi! Gracias Jordi!! አጅግ በጣም አመሰግናለሁ ፕሮፌሰር ጆርዲ!!

It's not fair to say you are solely a meteorologist and someone in related fields! Michiel, you are also an advanced computer scientist! We have been together since 2013 as you were supervising my major MSc thesis. It's like watching a science movie while sitting with you when you are scripting! Matlab, FORTRAN, Python and any other computer-related topic in atmospheric sciences. The data automation and beautiful plots in my thesis are impacted by you! It's enough for me to grow towards your level in these regards – and I can! You are so systematic and wise. In the beginning, you work in small pieces. In the end, you couple models. You are so critical and work in details of something. I was so amazed how you redesigned a rejected paper (my 1st paper) to be 'great again'! Oh, thank you Michiel! You also showed me how to write a 'response to reviewers'. I say your responses are so substantial that they highly satisfy reviewers! I see I'm becoming a critical reviewer for authors. Working with you after completing a paper with Jordi seems a nice finishing work. You add beauty to the paper: put numbers, re-arrange plots, re-plot tables, re-arrange sections, paragraphs, sentences, etcetera! Off course, I benefitted to work with both of you! Jordi – Michiel combination is amazing! I'm lucky to have you! Dank u wel Michiel. እጅግ በጣም አመሰግናለሁ ዶ/ር ሚኪል!!

In my fieldwork, I had many challenges! Nevertheless, I never spent a night in the field, except once. That night I was with you, Bert and my field assistants in Gazesso! Cold and rainy weather in the Gamo Highlands at 3000 m above sea level. A night in the middle of rats! This was not a challenge to you, rather an adventure and a good opportunity! Thank you! You invited me to your place for a nice dinner with your lovely daughters: Lotte, Romyio and Fierre! Thank you so much – Michiel! In addition, I'm happy you saw the beautiful town of Arba Minch – a view from the Paradise Lodge to Lake Abaya, Lake Chamo, Nech Sar national park and the mountains! You had the taste of Arba Minch coffee in my place – with my wife and talking to my kids. Bert was amazed by the delicious fish dish in Arba Minch. It was hard for him to believe the fish hotel owners gain profit! Yet, they are rich guys! Bert, I learned that a meteorologist needs to be a technician as well. Your field training helped me to have quality data and to have long-lasting sensors! Now, I also became weather sensor specialist – installing several automatic weather stations since then. Thank you, Bert!

It was you who told us that my MSc small thesis can grow to a PhD project! At the start of my PhD project, you were an advisor in the PhD study. In the middle of the project, you were a supervisor. In the end, you were a promotor! It's like the morning sun slowly becoming radiant and powerful at noon. A few minutes talking with you can grow to a nice paper! It was a great opportunity to work with you – Paul! Without you, the crop part of the thesis could be nonsense. As a person from atmospheric sciences, it would be not simple to write an agronomy oriented paper to be published in a journal in the field! Nevertheless, sitting near to you, with unlimited access to your office, I've managed to finish my final paper. You have made

I would like to thank Mathias Rotach, University of Innsbruck, Austria. Mathias, you shared knowledge related to mountain meteorology and commented on Chapter 3, Chapter 4 and the front cover. Thank you! The beautiful front and back covers were designed by architect Tekalign T. Minda. Tekalign, I'm proud of having you, my younger brother! You are so smart! The following people commented on the front cover: architect Hagos Aman, architect Tonja (my younger brother), Bisrat Elias, Tewodros Addisu and Thomas Lemma (contribution). This acknowledgment is edited by Tesfaye Habtemariam from AMU.

Field assistants (Admasu Adiyo, Zelalem Aniley, Tonja Torora, Yared Godenie, Alemayehu Wodajo, Metadel, Zeleke, Tekalign Torora and Habtamu Hailemariam). Encouragement, motivation, and support during field work (Guchie Gulie, Agena Tanga, Abiyot Tsegaye, Fassil Eshetu, Sabura Shara, Addisu Fekadu, Yechale Kebede, Simon Shibiru, Teklu Wogayehu, Beshah Mogossie, Samuel Dagalo, Bisrat Elias, Tewodros Addisu and Kedir Mehommed). Supporting and caring friends (Admasu Tassew, Bereket Tessema, Zuria Sumale, Tewodros Adissu and Bisrat Elias). Prayer and Spiritual support: Esayas Emene, Dawit Tadesse, Abraham Lakew, Wageingen Amanuel congregation brothers (Bereket, Araya, Solomon, Tilahun, Behailu and Adam) and sisters (Hebste, Saba, Wossen, Terefech, Ferewoyni, Addis, Mahlet, Meti, Bilissie, Birikti & Mekides), my beloved mom – Garafie and my mother-in-low – Aster. I would like to thank Meron & Wondie and Elisa & Gert-Jan.

I have a caring and beloved brother in Holland. I do not have words to explain to you! Your councils are awesome! We had wonderful prayer times; you shared your life; you helped me in difficult times. Much thanks – my brother, Dawit Tadesse. I have also a lovely Dutch family: Jan-Dirk and Geertje! Thank you for several dinner invitations to Rotterdam – to your place. Your assistance in shopping positively influenced my economy! Thank you! I'm so happy that you make Arba Minch your home place! We are colleagues at Arba Minch University and best friends in Arba Minch city!

Last, but not least – my family! I couldn't give you enough time. Working in office and field during daytime and again working at home during the night. You have also taken all the home responsibility in my absence. Thank you, my beloved – Ewnet Zeleke. All the privileges of the PhD are primarily ours! I know how much we enjoy being together! You missed the lovely times while I was abroad. I was feeling as if I punished you when I departed. It's done! And love you my sons – Asaph and Christian! You are always concerned of my family! You also shared my burdens. Thank you dad (Torora), mom (Garafie), brothers (Tekuash, Tonja, Tekalign & Yonas), sisters (Fanaye & Tewabech)!

\*\*\*

## Dedication

As there is diamond-ship in nature, there exists diamond-ship in humanity. You are an Ethiopian black diamond – my model for strength, purity, determination and academic excellence! This thesis is dedicated to your legacy – the late **Anto Arkato. Anto Arkato** completed his PhD in the University of Twente and was an assistant professor at Arba Minch University, Ethiopia.

\*\*\*

# About the author

Thomas Torora Minda was born on 1st January 1981 in a small village (called Limat or *ye Sar Sefer* – meaning cottage houses area) near the main campus of Arba Minch University (AMU), Arba Minch, Ethiopia. He is currently an assistant professor in the faculty of meteorology and hydrology, Arba Minch Water Technology Institute, AMU. Thomas attended preschool to primary school in Limat. From junior secondary to high school, he attended in Arba Minch town, walking 5 km away from Limat.

After successfully passing the Ethiopian School Leaving Certificate Examination – ESLCE, he joined department of Chemistry, Addis Ababa University. His B.Sc in Chemistry study concluded in July 2005. Following his completion, he joined Arba Minch College of Teachers Education as a graduate assistant. He thought Chemistry and Environmental Science courses for 7-years. While teaching in the college, he also attended his M.Sc in Meteorology Science in his current faculty, AMU. For his M.Sc thesis, he conducted research on rainwater chemistry and local source identification. The thesis was supervised by Dr. Ababu Teklemariam (currently a senior lecturer in University of Swaziland) and Dr. Kinfe Kassa (AMU). He got a scholarship to present his thesis in a workshop organized by the International Center for Theoretical Physics – ICTP, Trieste, Italy in May 2012. In relation to his B.Sc and M.Sc study, he had interest to study atmospheric chemistry. He obtained admission to M.Sc, Climate Studies from Wageningen University and Research (WUR) and he got the Netherlands Fellowship Programme – NFP-nuffic fellowship.

In M.Sc Climate Studies, he followed a research track called air quality and atmospheric chemistry. His major thesis focused measuring and modelling ambient air-quality in Arba Minch. He made measurement of black carbon and nitrogen dioxide concentrations in Arba Minch town. He used these data to validate WRF-Chem – a meteorology-chemistry based atmospheric transport model. He conducted his major thesis work under the supervision of Dr Michiel van der Molen and Prof. Maarten Krol in the Meteorology and Air Quality (MAQ) chair group, WUR. He had interest to peruse a PhD study in WUR. Following his interest, he conducted a minor thesis related to his current PhD project – agricultural meteorology. He found this field of study as critically demanding for his country to attain food security (has interest in air quality too). This 4-months thesis work has been conducted under the supervision of Prof. Jordi Vilà and Dr. Michiel van der Molen. Meanwhile, Prof. Paul

Struik was optimistic about the project and showed willingness to be part of the supervision team. Thomas successfully completed the M.Sc programme. Soon after the completion, he got an admission to a PhD programme in WUR from the three supervisors. He also joined the faculty of Meteorology and Hydrology, AMU in lecturer rank. Shortly after joining AMU, his PhD project concept note submitted to NFP-nuffic has been selected for funding. This four-year thesis is the outcome of the project.

Thomas future interest is to teach and continue his research work. His teaching and future research directions are in the area of agricultural meteorology, air quality and meteorology. He wants to be intensively engaged in crop and atmospheric variables measurements as observations are limited in Ethiopia. He also wants to integrate these data with modelling and satellite products related to agriculture, meteorology and air-quality. He enjoys his teaching profession. Thomas also teacher of the Bible in the public.

Sharing something good he has to others makes him happy. Besides, he motivates people (mainly the youths in Ethiopia) in the struggles to realise their dreams (mainly in the academia). Thomas is from illiterate father and mother. He was from the low economy category in Ethiopia and is the first born among seven children. In his school years, he had needed to support his school related costs, clothing and to contribute to the livelihood of his family. He was a shoe polisher, grass/wood collector from the Gamo Highlands and seller in Arba Minch town, livestock herder, bicycle (someone's property) renter, daily labourer in Arba Minch state farm and Arba Minch University. These jobs are not only least paid but also not considered in job list in Ethiopia. He had done the works for half a day (government schools in Ethiopia are half-a-day shift based) during school and full day during summer time. In his B.Sc study in Addis Ababa University, he was employed as tutorial teacher (during the evenings and weekend) to earn money. Today, Mr Torora family can be categorised as one the most educated families in Ethiopia (a PhD in science, 3 MSc in architecture and civil engineering, 2 BSc in ICT and 1 diploma in technic). Torora has contributed 3 lecturers and 2 librarians to AMU. The family income has been transformed to a middle income in Ethiopia, which is exclusively academic based economic growth. Thomas has impacted not only his family but also several youths in Limat and some of his students. He will have huge opportunity to transform a helpless person to be a man.

Thomas' hobbies are reading the Bible and historical books. He enjoys visiting natural environments with his family and friends.

# List of publications

1. **Minda, T. T**., van der Molen, M. K., Struik, P. C., Combe, M., Jiménez, P. A., Khan, M. S., & Vilà-Guerau de Arellano, J. The combined effect of elevation and meteorology on potato crop dynamics: A 10-year study in the Gamo Highlands, Ethiopia. *Agricultural and forest meteorology*, **2018**, 262, 166-177, doi: 10.1016/j.agrformet.2018.07.009.

2. **Minda, T.T**.; Molen, M.K.; Heusinkveld, B.G.; Struik, P.C.; Vilà-Guerau de Arellano, J. Observational Characterization of the Synoptic and Mesoscale Circulations in Relation to Crop Dynamics: *Belg* 2017 in the Gamo Highlands, Ethiopia. *Atmosphere*, **2018**, 9, 398, doi: 10.3390/atmos9100398.

3. **Minda, T.T.**; van der Molen, M.K.; Vilà-Guerau de Arellano, J.; Chulda, K.C.; Struik, P.C. Responses of Canopy Growth and Yield of Potato Cultivars to Weather Dynamics in a Complex Topography: *Belg* Farming Seasons in the Gamo Highlands, Ethiopia. *Agronomy*, **2019**, 9, 163, doi: 10.3390/agronomy9040163.

**Netherlands Research School for the**
**Socio-Economic and Natural Sciences of the Environment**

# D I P L O M A

## For specialised PhD training

The Netherlands Research School for the
Socio-Economic and Natural Sciences of the Environment
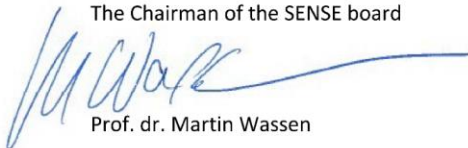(SENSE) declares that

# *Thomas Torora Minda*

born on 1 January 1981,  Arba Minch, Ethiopia

has successfully fulfilled all requirements of the
Educational Programme of SENSE.

Wageningen, 30 October 2019

The Chairman of the SENSE board

Prof. dr. Martin Wassen

the SENSE Director of Education

Dr. Ad van Dommelen

*The SENSE Research School has been accredited by the Royal Netherlands Academy of Arts and Sciences (KNAW)*

K O N I N K L I J K E   N E D E R L A N D S E
A K A D E M I E   V A N   W E T E N S C H A P P E N

The SENSE Research School declares that **Thomas Torora Minda** has successfully fulfilled all requirements of the Educational PhD Programme of SENSE with a work load of 37.0 EC, including the following activities:

**SENSE PhD Courses**

o   Environmental research in context (2016)
     Research in context activity: 'Initiating and organizing expert and stakeholder workshop on 'Advancing weather-crop forecasting science in the Gamo highlands, Ethiopia (2016)'

**Other PhD and Advanced MSc Courses**

o   Essentials of scientific writing and presenting , Wageningen Graduate Schools (2016)
o   Reviewing a scientific paper, Wageningen Graduate Schools (2016)

**External training at a foreign research institute**

o   *In-situ* training on automatic weather and soil moisture stations: site selection based on WMO standards, installation, and data management, Gam highlands, Ethiopia (2016)
o   Automatic weather and soil moisture instrument stations: site selection based on WMO standards, installation, and data processing, Arba Minch University, Ethiopia (2018)

**Management and Didactic Skills Training**

o   Teaching in the MSc course 'Weather Prediction and Climate Modelling', Arba Minch University, Ethiopia (2019)

**Selection of Oral Presentations**

o   *Modelling potato productivity in complex terrain: 10-years study based on a high-spatial resolution weather-crop model.* BBOS Autumn Symposium, 28-30 October 2015, Renesse, the Netherlands
o   *Modelling potato productivity in complex terrain: 10-years study based on high-spatial resolution weather-crop model.* International Agro-meteorological Conference, 3-4 July 2017, Addis Ababa, Ethiopia
o   *Combined effect of meteorology and elevation on potato production in the Gamo highlands, Ethiopia.* Potato production in Africa: Challenges and opportunities, 17 October 2017, Wageningen, The Netherlands
o   *The combined effect of meteorology and elevation on potato dynamics: a 10-year study in the Gamo Highlands, Ethiopia.* 18th international symposium on sustainable water resources development symposium, 8-9 June 2018, Arba Minch, Ethiopia

SENSE Coordinator PhD Education

Dr. ir. Peter Vermeulen

# Propositions

1. High-resolution weather data are crucial to study crop dynamics in a complex terrain.
   (this thesis)
2. The synoptic and mesoscale weather systems have specific yet integrated roles during the belg season in the Gamo Highlands of Ethiopia.
   (this thesis)
3. The advancements in computational capabilities will improve weather forecast in complex terrain, but those benefits might not be realized in sub-Saharan Africa due to economic constraints.
4. Food security, weather and climate need to be integrated to design and implement agricultural programmes and policies in Ethiopia.
5. Complex problems in sub-Saharan Africa do not necessarily require complex solutions.
6. Maternal and paternal roles are not in-born in humanity but inculcated from caring mothers and fathers.
7. Life is more about generality than specialty.

Propositions belonging to the thesis, entitled
Weather and crop dynamics in a complex terrain, the Gamo Highlands - Ethiopia: Towards a high-resolution and model-observation based approach

Thomas Torora Minda
Wageningen, 30 October 2019